An Integrated Study of the Early Cretaceous (Valanginian) Reservoir from the Gamtoos Basin, Offshore South Africa with Special Reference to Seismic Facies, Formation Evaluation and Static Reservoir Modeling

By

AYODELE OLUWATOYIN LASISI

(Student No: 3217090)

B.Sc. Hons (Ado-Ekiti), B.Sc. Hons (Western Cape), M.Sc. (Western Cape)

UNIVERSITY *of the* WESTERN CAPE

A Research Thesis Submitted to the University of the Western Cape, South Africa

Faculty of Natural Sciences Department of Earth Sciences

for the award of the Degree of

Doctor of Philosophy

In

Applied Geology

Supervisor: Prof. Tapas K. Chatterjee
Co-Supervisor: Prof. J. V. Bever Donker

DECLARATION

I declare that "*An Integrated Study of the Early Cretaceous (Valanginian) Reservoir from the Gamtoos Basin, Offshore South Africa with Special Reference to Seismic Facies, Formation Evaluation and Static Reservoir Modeling"* is my own work, it has not been submitted before for any degree or examination in any other University, and that all sources I have used or quoted have been indicated and acknowledged by means of complete references.

Oluwatoyin L. Ayodele. **May, 2019.**

…….

Signature

DEDICATION

This project is gratefully dedicated

to ***the God Almighty***

and

My parents (Mother and Father): Mrs. Stella Ayodele and Late Mr. Ayodele Olupona.

ACKNOWLEDGEMENTS

The work was carried out in the Department of Earth Sciences, University of the Western Cape, Cape Town South Africa. I would like to express my gratitude and thanks to my Supervisor and Co-supervisor Prof. Tapas K Chatterjee and Prof. J.V.Bever Donker respectively for their guidance and constructive comments during the course of the entire work. I'm indeed grateful to Inkaba yeAfrica and National Research Foundation (NRF), South Africa, for theirs financial support towards completion of this research. The Geophysical data, well completion reports and samples for biostratigraphic analysis were provided by the Petroleum Agency of South Africa (PASA), Cape Town office.

I express sincere thanks to Prof. Charles Okujeni (former Chairperson), Dr. M. Opuwari, Sr. Lecturer, Departmental Secretary Mrs Wasielah Davids and Mrs Yafah Williams for all support extended during the course of this work. I express sincere thanks to Dr. Chris Shamakinde for his approachable manners and open-mind discussion during the course of this study.

Thanks to my fellow post graduates students in the Petroleum lab; Monica Oghenekome , Moses Magoba, Oluseyi Abegunde, Friz Agbor, Eric Saffou, Adrian Williams , Pascal Amachi, Joseph Mayala Nsingi, Tosin Aina, and Ayodeji Egunlusi for creating conducive environments for the success of this studies. The discussion with Moses Magoba has been very helpful for my research. This page will not be completed without mention Leah Hoosain (Schlumberger Corporation) for her assistance and special training in uses of Petrel software, she was not only a great teacher for my research but also a good mentor, thanks for your time, always ready to assist.

I also acknowledge Dr. Segun Akinyemi for discovering the potential in me and bringing me to the academia world, I say big thank you for making this journey possible. I would like to express my sincere gratitude to Dr. Fadipe Oluwaseun (a friend and colleague) of Schlumberger Corporation for advice in structuring the thesis.

My deepest thanks to my mother Stella Ayodele for her prayers, my siblings; Ayoko Yetunde and others for believing in me. Thanks to my Brother-in-law, Mr. Taiwo Ayoko for his moral support and to my ladies friends Buhle Nshele, Mary Boka for their support in bad and good time, without theirs love, I would not have achieved this.

Lastly, unmeasured thanks to my God, the creator of my life for his amazing grace and mercy, wisdom and understanding, strength given me to complete my studies —Glory be to God (Amen!!!).

BRIEF INFORMATION ON RESEACH OUTPUT AND SKILLS.
PERSONAL INFORMATION.
NAME: Oluwatoyin Lasisi Ayodele

RESEARCH OUTPUTS:

Petrophysical Evaluation of Sandstone Reservoir of F-O2 gas field, Central Bredasdorp Basin, Offshore South Africa. Conference paper at the Cape-Karoo Imbizo Conference in Port-Elizabeth, Eastern Cape South Africa. 2014.

Pore pressure prediction of some selected wells from the Southern Pletmos Basin, Offshore South Africa. Presentation at the Cape-Karoo Imbizo Conference in Port-Elizabeth, Eastern Cape South Africa. 2015.

Pore pressure prediction of some selected wells from the Southern Pletmos Basin, Offshore South Africa. Article published in the Journal, Geological Society of South Africa Special Issue, 2016. Volume 119, 1, 203- 214.

Ayodele, O.L, Chatterjee, T.K, van Bever Donker, J.M., (2018). Seismic Sequence and Seismic Facies Analysis of the Early Cretaceous (Valanginian) depositional sequence Gamtoos Basin, offshore South Africa. Presentation at National Association of Black Geoscientist (NABG), 37th Annual Conference, Houston, Texas, USA, September, 2018.

Ayodele, O.L, Chatterjee, T.K, van Bever Donker, J.M., (2018). Static Reservoir Modeling of the Valanginian Depositional Sequence of Gamtoos Basin, offshore South Africa. AAPG International Conference and Exhibition, Cape Town, South Africa, November, 2018. Publish; Search and Discovery Article #11180, January 14 (2019) ** AAPG Data pages, Inc. http://www.searchanddiscovery.com/pdfz/documents/2019/11180ayodele/ndx_ayodele.pdf.html

AWARDS AND SCHOLARSHIPS RECEIVED.

Golden Key International Honour Society Merit Award 2013, South Africa.
Inkaba yeAfrica Scholarship for MSc. Research in Geology 2013-2014.

National Research Foundation (NRF) and Innovation Doctoral Scholarship (PhD), South Africa 2015-2017.

SHORT COURSE CETIFICATES ATTENDED.

Attendees training and workshop: On field development, drilling techniques, procedure and reservoir engineering by Total Professors associate (TPA) 2012

Shell International training Attendees: on seismic interpretations 2013.

Deep Water Seismic interpretation: Next Professional Training Course, Schlumberger oil Company, 2013.

Introduction to drilling: Next Professional Training Course, Schlumberger oil Company, 2014.

Halliburton training Attendees: Petrophysics and Geomechanics 2014.
Attendee: On application of Sequence Stratigraphy in Petroleum Exploration; AAPG Africa Region Lecture, 2014.

Petrel Fundamentals Training Course, Schlumberger oil Company 2015.
Petrel Geophysics Training Course, Schlumberger oil Company 2015.
Short course on; From Rocks to Model: Geological reservoir characterization and modelling AAPG Houston, Texas 2017.

ELECTRONIC DATA PROCESSING KNOWLEDGE (EDP)

Windows based geological and geophysical software including; Petrel 2014 and 2015®, Techlog 2017®, Interactive Petrophysics (IP) 2012®, Kingdom Suite (SMT) and CorelDraw Graphic Suite.

Table of Contents:

Contents

List of Figures

List of Tables:

EXTENDED ABSTRACT

Introduction

Integrated approaches in the study of petroleum exploration are increasingly becoming significant in recent times and have yielded much better result as oil exploration is a combination of different related topics. The production capacity in hydrocarbon exploration has been the major concern for oil and gas industries. In the present work an integrated approach was made with seismic, well logs and biostratigraphy for predicting the depositional environment and to understand the heterogeneity within the reservoirs belonging to Valanginian (Early Cretaceous) age of Gamtoos Basin, Offshore South Africa.

Objectively, the integrated work was mainly based on seismic stratigraphy (seismic sequence and seismic facie analysis) for interpretation of the depositional environments with combination of microfossil biostratigraphic inputs. The biostratigraphic study provides evidences of paleo depth from benthic foraminifera and information about bottom condition within the sedimentary basin, changing of depositional depth during gradual basinal fill during the Valanginian time.

The petrophysical characterization of the reservoir succession was based on formation evaluation studies using well logs to investigate the hydrocarbon potential of the reservoir across Valanginian depositional sequence. Further, the static modeling from 2D-seismic data interpreted to a geological map to 3D-numerical modeling by stochastic model to quantify the evaluation of uncertainty for accurate characterisation of the reservoir sandstones and to provide better understanding of the spatial distribution of the discrete and continuous Petrophysical properties within the study area.

Materials and Methods

The data used for the present research include 2D-(SEG-Y) Seismic lines (45), digitals wireline logs (LAS format), drilling cutting samples and well reports include: geological, geophysical, and engineering reports of the six exploratory wells from the study area. The quality control (QC) which includes log-editing, log splicing and environmental corrections was performed on the log data when loaded in Interactive Petrophysics software (IP®). The hydrocarbon bearing reservoirs intervals was identified both qualitatively and quantitatively by reconsidering the well log data. The well log data used for this work are Gamma Ray, Resistivity logs (LLD and MSFL), Neutron and Density logs, Sonic log and Clipper log. The qualitative analysis was done by examined through the well log signatures. The gamma-ray

log with horizontal scale from: 0 to 150 or from 0 to 200 maximum were considered for some wells depending on availability and then were calibrated in Standard America Petroleum Institute (API) unit. A shale baseline of 65 and 80 API respectively was used to discriminate between the sands and shale; these were identified by gamma-ray log (GR) based on deflection of gamma-ray log motif to lower and higher concentrations region of radioactive materials, thus, indicating sands and shale respectively. The quantitative analysis involves the calculation of parameters such as, Clay/shale volume, effective porosity, water saturation and permeability. Water saturation value is calculated here by considering the shaly nature of the Valanginian sequence. For this, Sw Indonesian (SwInd) model was chosen to estimate water saturation. The values such; (tortuosity factor), a=1, (water saturation exponent) n= 2 and (cementation exponents) m= varies from 1.94 to 1.98 were used to develop the model. Cut-off values were also determined for the porosity, permeability, water saturation and volume of clay from various cross-plots in the study.

The 2D-seismic lines were loaded in Petrel 2014® software and subjected to merging with their respective navigation files to make sure accurate positioning within the study block. Seismic–well tie was performed to ensure the amplitude match between seismic and wells and to generate synthetic to enable proper mapping of different horizons sequences on the seismic sections. The Valanginian horizon sequences on the seismic sections were mapped and Two-Way-Time (TWT) maps were generated. Consequently, velocity modelling was performed and time depth maps generated which was later converted to depth map and used to estimate thickness in time and depth respectively. A structural model was created using different faults interpretations, mapped and converted to depth maps to generate stratigraphic framework.

Lithological sequences were defined based on python script (Gamma Ray (GR 1) <80, 0, If (GR1 >80 GR 1 <102, 1, 2)), where 0 represents sandstone, 1 represent siltstone and 2 represents shale. The GR values less than 80 API are classified 0, (Sandstone), GR values between 80 – 102 API classified as Siltstone, while GR value greater 102 API are classified under Shale. Facies logs was generated and upscaled for the wells and facies modeling was performed by means of stochastic method using the Sequential Indicator Simulator (SIS) algorithm. The Petrophysical properties includes porosity, permeability and water saturation were also upscaled along the wells to populate on grid cells. The Stochastic simulation algorithm method by means of Sequential Gaussian Simulation (SGS) was geostatistically applied in assigning the properties on Petrel 2014®.

Seismic stratigraphy analyses were performed based on seismic sequence and seismic facies analysis using comprehensive classification characteristic of seismic reflection termination patterns such as onlap, downlap, toplap, erosional truncation and configuration of the seismic reflections such as, amplitude, continuity, frequency and the external geometry reflection on depositional sequence interpretation approached model identified on a seismic section outlined by (Mitchum Jr, *et al.*, 1977) and (Vail, *et al.*, 1977) respectively. This was also calibrated with well log (Gamma-ray; GR) for detailed geologic description of the environment and lithofacies distribution based on GR log motif. 3D-lithofacies surface map attributes depth thickness model was also constructed for the Valanginian section to correlate with the lithostratigraphic interpretations to deduce depositional environment of the study area. The biostratigraphic analysis was carried out using well cuttings for two representative wells following conventional methods and using the microfossil group foraminifera as a tool.

Results

The seismic sequence and the seismic facies analyses based on classification characteristic and configuration of the seismic reflection terminations pattern indicate that the depositional environment of the Valanginian section across the drilled wells in the northern part was under deep marine regime and that comprises of submarine fan, basin floor fan and abyssal environment with an indication of periods of erosional surfaces and non-deposition of sediments. Also within this area a low energy facies extending from continental shelf to marine slope was identified. This suggests shallow marine to deep marine depositional environment prevailed in the northern part of the study area. On the other hand, the southern part of the study area revealed the evidence of mass flooding within marine-shelf to further deeper oceanic area possible presence of a submarine canyon with a canyon fill deposit and sub marine fan lobe. Therefore, it was concluded that the deposition in the present study area was under marine shelf to deep marine environment.

The calibrated gamma-ray log signatures revealed an aggradation stacking parasequence predominantly of sand and silt of cylindrical-blocky and serrated pattern of sand-stone to siltstone indicating channel-fill, submarine canyon–fill, storm dominated shelf and distal deep marine slope environments in the northern area. While the southern part of the study area indicate similar aggradation stacking parasequence (cylindrical or blocky shape) built-up of thick uniformly graded medium-to-fine-to-coarse grained-silt-shale- sandstone association that were deposited in a wide range of environments from deep tidal channel-fill, shallow

marine, submarine channel to deep marine environments similar to the northern part suggesting a transgressive system tract.

The 3D-lithofacies surface depth attribute facies map indicates a mass flooding characterised by thick bedded siltstone lobe (siltstone facies) with intercalated fine mud-rock (Shale facies) and minor sandstone in low energy turbidite channel depositional environment in the south-western part of the study area. The northern part indicates a diachronous deposition dominated by sandstone, intercalated with minor siltstone and shale, probably deposited in a high energy turbidite channel, followed by low energy settling of the siltstones and shale before the next pulse of high energy sandstones were deposited. The north-east to the south-east of the Valanginian sequence suggests that high energy turbidites might be encoutered, the marine deposits dominated by sandstone intercalated with siltstone and minor shale that are characterized by erosional surfaces due to tectonic processes as a result of uplift that created a sediment hiatus in the section .

The foraminiferal biostratigraphic studies carried out in two representative wells indicate a close similarity in faunal assemblage, suggesting the two intervals are homotaxial. Comparison of the microfaunal assemblage with known Valanginian sections in different localities confirm the geological age. The study further indicates that deposition took place in a marine slope under uppermost bathyal to upper bathyal condition.

The Petrophysical formation evaluation from the well log data reveal that out of the total eleven, only seven sand intervals are hydrocarbons producing within the studied Valanginian section. This is based on the data analysed from the five exploratory wells (Ha-B2, Ha-G1, Ha-K1, Ha-A1, and Ha-I1) from the north to the south of the study area. Cut-off parameters were applied to distinguish between the pay and non-pay intervals. Porosity, permeability, water saturation and volume of clay were calculated within the pay sand intervals. The estimated average effective porosity for the pay sand intervals of the wells ranged from 12.5% to 16.2%, the average water saturation ranged from 35.9% to 50.2%, the average volume of clay ranged from 10.0% to 20.6%. The calculated permeability obtained for the reservoir intervals is less than 1mD, ranges from 0.08mD to 0.1mD indicating that the Valanginian section is poorly permeable, has no ability to transmit fluids and lower water saturation reservoirs. This suggests that the sandstone reservoirs within the Valanginian sequence is a hydrocarbon bearing gas reservoir where the effective porosity is varying from

fair-to-good in the northern part and poor-to-fair in the south and characterised by poor permeability in the entire region.

The stochastic modeling reveals that the facies and the spatial distribution of the discrete and continuous Petrophysical properties (porosity, permeability and water saturation) for the studied Valanginian section. The model indicates that the section is hydrocarbon bearing with a dominant shale facies distributed across the section without any substantial reservoir sand. The model revealed variation in effective porosity from poor to good from the southern to the north with overall poor permeability values throughout the entire section. The northern part of the area showing fair-to-good effective porosity and the southern part indicates poor to fair effective porosity with lower water saturation and poor permeability across the entire section respectively i.e. a section with no significant pore spaces capable to accommodate fluids and poor connectivity to transmit fluids. The model revealed the highest and lowest porosity values of 19% and 0.08% respectively, permeability values of 0.1mD (< 1.0 mD) and highest and lowest water saturation values of 0.30 to 0.45 (30% to 45%) across the Valanginian section of the study area.

Conclusions

Based on the integrating method applied, the present research able to resolve that the reservoir sediments in the study area were deposited during Valanginian stage (Early Cretaceous) under marine set up within a set of environments that ranges from deeper shelf to deep marine (slope) under a fluctuating bathymetry of ~ 500m. This resulted in deposition of a series of sedimentary succession from deep marine to storm dominated shelf and distal deep marine slope environments. Within this succession sands were deposited as channel fill, basin floor fan lobe or as canyon fill deposits which are likely to be a working carrier beds (stratigraphic control) for the hydrocarbon bearing reservoirs .

The heterogeneity within the sandstone reservoirs prone to be hydrocarbon bearing with lower water saturation and the porosity varies widely from poor to fair to good as observed from the Southern part towards the Northern area within the Valanginian section. The permeability is poor throughout the section and thus do not have the ability to transmit fluids. This is due to the shale facies dominantly distributed across the succession.

CHAPTER ONE

1. Scientific Background and State-of-the-Art

1.1 Introduction and Background Information

The Gamtoos Basin is among the five en-echelons sub-basin on the south-eastern margin of the Outeniqua Basin, offshore South Africa. It is an extension of a line of basins that developed westwards from the Oudtshoorn sub-basin and is bordered in the north by the Gamtoos Fault. The basin attains a throw of 12km in the distal offshore, is a complex rift type basin that exists both in onshore and offshore. It is a structurally complex basin and severely faulted as a result of Agulhas-Falkland Fracture Zone (AFFZ) (Andreoli, *et al.*, 1996; Broad, 1990; Bate & Malan, 1992). This basin consists of relatively simple half grabens bounded by a major fault to the northeast and containing comparable thicknesses of sediments.

The offshore and onshore parts of the Gamtoos Basin cover about 5,038 sq. km, while the offshore seismic line covers about 4,272 km. The Gamtoos Basin has been found to be the smallest among the five en-echelon sub-basins namely: Bredasdorp, Pletmos, Algoa and Southern Outeniqua in the Outeniqua Basin, South Africa. The Gamtoos and Algoa basins are considered as twins basins as both contain half grabens that are separated by Paleozoic basement arches (Malan, *et al.*, 1990). After high intensity exploration for hydrocarbon prospects in the Gamtoos Basin, it has been discovered to be containing sedimentary source rocks of good-oil, wet-gas-to-oil prone and dry-gas-to-oil prone prospects. The early and late rift subsidence related deposits of these half grabens consist of thick sediments containing Kimmeridgian-to- Portlandian-to- Hauterivian (D to 6At1) wet-gas-to-oil-prone shales with sandstones of reservoir potential in the Valanginian. In addition, the late rift subsidence during the Hauterivian also resulted in thick sedimentary packages of organic-rich shale rock for petroleum generation (Malan, *et al.*, 1990; McMillan, *et al.*, 1997).

However, detailed understanding of this basin remains unsolved in terms of petrophysical characterization qualities of its Valanginian reservoir sandstone and the depositional environment that made up this sequence of sediments. The seismic stratigraphy in terms of seismic sequence and seismic facies analysis has not yet been examined for clarification of the depositional environment. No significant work on depositional environment of the Valanginian sediments from sedimentological or biostratigraphic aspects were carried out so far in the Gamtoos Basin.

The present work involves an integrated approach which includes interpretation of the seismic stratigraphy in terms of seismic sequence and seismic facies analysis, integrated with the microfossil biostratigraphy to arrive at an understanding of the depositional environment of the sedimentary rock sequence. Petrophysical analysis and static modeling was carried out to describe the heterogeneity of the reservoir quality within the Valanginian section of the basin. This was based on an evaluation of the volume of clay, porosity, permeability and water saturation potential of the reservoir rock of the formation, deduced from core analyses and well logs.

An understanding of seismic facies, Petrophysical characterization of well logs as well as the interpretation of both cores and biostratigraphy are vital tools in exploration and exploitation of hydrocarbons in the oil industries. The seismic facies analysis aids the information on depositional environment particularly in an area where there are no well controls. The importance of seismic facies analysis is well known in hydrocarbon exploration and different seismic parameters are used for the purpose of extracting the necessary structural and stratigraphic information. As stated above, seismic facies analysis based on seismic reflection characteristics is useful in determining depositional environments. It also helps to understand the lithology, fluid content, porosity and relative age. Petrophysical characterization parameters enhance the information on reservoir quality assessment and its production capacities. These parameters such as porosity, permeability, and clay volume and water saturation serve as a determining factor for the hydrocarbon potential of any basin.

Biostratigraphy is the study of stratigraphy based on fossil occurrence. The applications of microfossil biostratigraphy in oil industries play a key part on reservoir scale in all phases from exploration through appraisal, development and ultimately in structuring the geologic model for hydrocarbon exploration, drilling operations and production phase. This study further helps in fixing the geological age and also demarcation of hiatus and estimation of the paleo depth.

1.2 Problem Statement

Previous exploration reports by South Africa Oil Exploration Corporation (SOEKOR), (1971) and Roux, (1997) only outline the potential of the Gamtoos Basin, in a superficial manner. The early Cretaceous sedimentation of Berriasian and Valanginian age turbidity channel and fan sands, is the primary target in the Gamtoos Basin which locally dominated the early rift deposition (Broad, 1989; Broad, 1990).These sequences consist of thick source rocks and good reservoir sands which are of great significance in the hydrocarbon exploration, particularly the Valanginian sequence which consists of highly significant reservoir sands across the Outeniqua sub-basins, offshore South Africa (Broad & Mills, 1993) classified this basin as a synrift succession which contains thick organic-rich marine shales, with sandstones deposited in the Early Cretaceous of the Valanginian sequence that has economic significance as petroleum source rocks and good reservoirs respectively.

McLachlan & McMillan, (1979), focused mainly on microfauna studies in the study area in sediments of the Cretaceous drift succession of Early Barremian to Late Maastrichtian age. However, the studies did not provide detailed account of the geological age and depositional environments of older group of sediments belonging to Valanginian age. The nature of heterogeneity and the quality of the sandstone reservoirs were also not studied. The only reference available for the Valanginian succession is from a brief geological history they described in their work. Some reference of this succession is available also in the Well Completion Report.

In the present work an integrated approach using seismic stratigraphy based on seismic sequence and seismic facies analysis and formation evaluation by means of Petrophysical analysis from well logs and Static modeling studies have been selected as the method to study the depositional sequence of sediments belonging to the Valanginian age. The depositional set up of the sediments belonging to Valanginian age was studied in this work is mainly based on lithology and biostratigraphy. This integrated work will further improve the understanding and provide comprehensive output on:

- The heterogeneities of the sandstone reservoir qualities of the hydrocarbon potential in the basin,
- The geological age and the depositional environment of the sedimentary succession from the biostratigraphic studies.

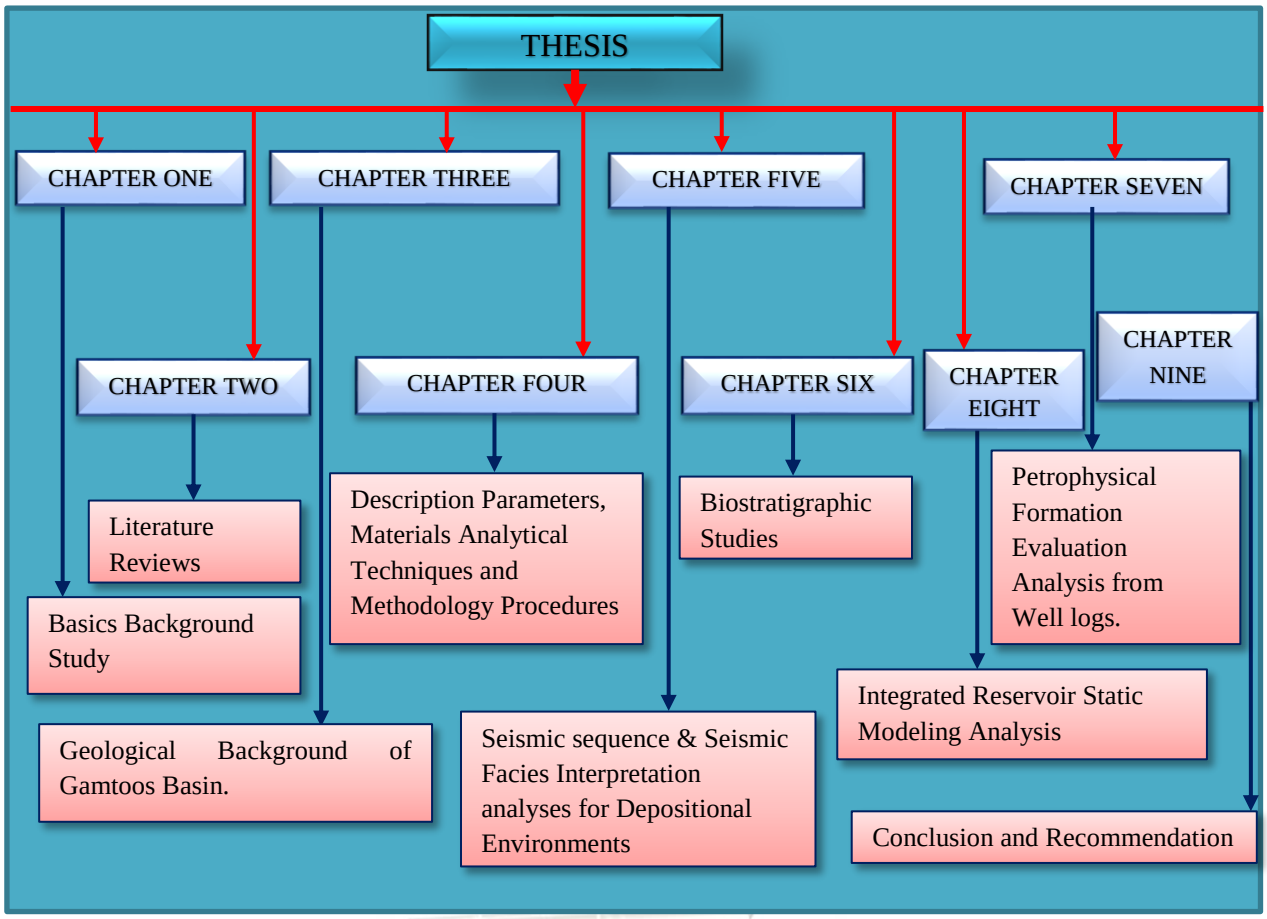

Figure 1. 1: Framework diagram of the thesis.

1.3 Location of Study Area

The Gamtoos sub-basin of the Outeniqua Basin, offshore South Africa is the extension of a line of basins that extended eastwards from the onshore Oudtshoorn sub-basin located north of Mossel Bay and bounded in the north by the Gamtoos Fault. The latter attains a throw to the South of 12km in the distal offshore. The Gamtoos Basin is located on the south-east margin of South Africa and extends from onshore areas to the offshore region, covers about 5,038 km^2. Along the Southern coastline of the Western Cape and Eastern Cape Provinces on the Eastern edge of the continental shelf, is the Agulhas bank with water depths of less than 200 m increasing rapidly beyond 500 m in the south at the present day shelf edge, due to the erosion caused by the Agulhas current flowing along the south-westward in the shelf edge. The Gamtoos Basin is considered as a twin basin to the Algoa Basin on the Eastern edge of the continental shelf located on the south-eastern margin of the shelf and existing both onshore and offshore. The Algoa Basin covers about 8,193 sq. km including both onshore and offshore. These basins are a product of rift and drift activity during the Gondwanaland break up (Brown, *et al.*, 1995).

The rift basins are overlain by Aptian to Early Albian fill of the Gamtoos and Algoa canyons. The canyons are more pronounced and larger in the Algoa Basin than in the Gamtoos Basin, regionally about 10 to 30 km wide, close to 2km deep and extending 60 km in south easterly direction across the Algoa Basin, containing channel sandstones with reservoir potential in both basins. Basement, the half grabens and canyon fill are overlain by Albian sediments (Malan, *et al.*, 2009). Nevertheless, the focused area of the present work is the Ha-gas field of block 13C. This is located along South-east to the North of the Gamtoos Basin is about 250 km north east of the proven field developments in the Bredasdorp sub-basin, which produces mostly gas with some oil, from Berriasian to Valanginian Syn-Rift sediments which till date supplies the PetroSA Gas-to-Liquids (GTL) plant situated in Mosel Bay via the F-A field platform (Mudaly, *et al.*, 2009).

The study area is bounded in the west and east by geographical co-ordinates as follows: Ha-A1, (Lat: 34°21'24.013"S, Long: 25°40'23.868") Ha-B2, (Lat: 34°24'21.17"S, Log: 25°36'32.86"E.). Ha-K1, (Lat; 34°18'30.33".S Long: 25°41'48.75"E). Ha-I1, (Lat: 34°15'21.9"S, Long: 25°42'31.7"E). Ha-N1, (Lat: 34°13'38.70"S, Long: 25°40'50.50"E). Ha-G1, (Lat: 34°18'30.33"S, Long: 25°41'48.75"E).

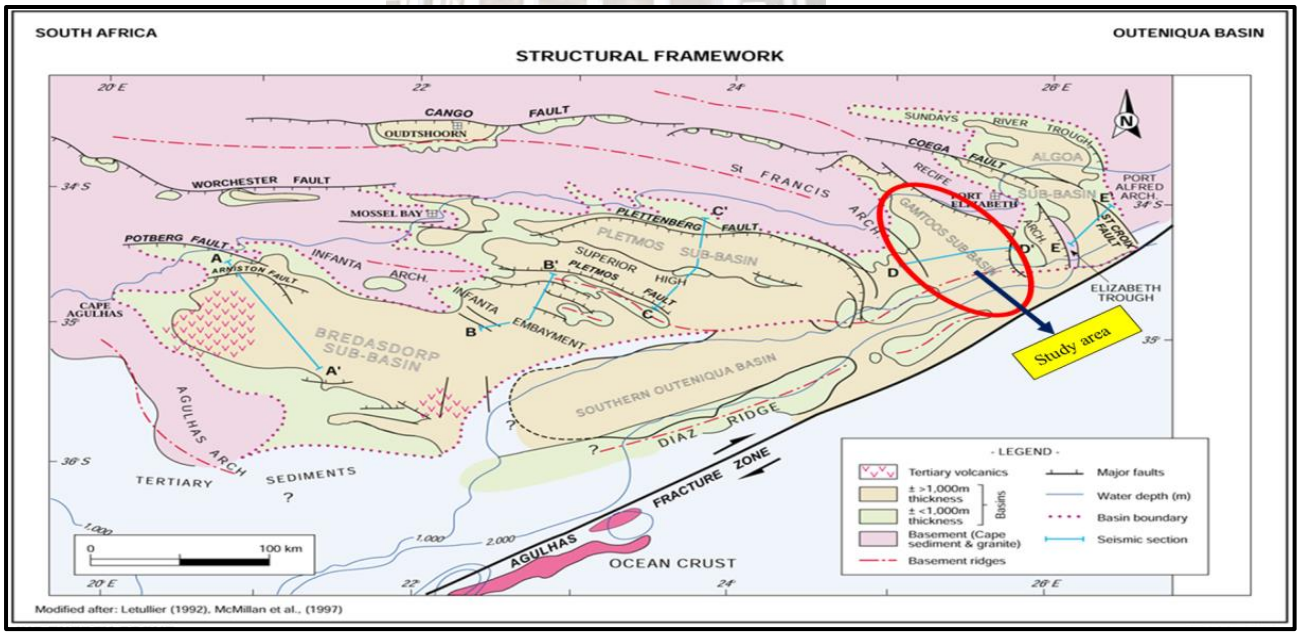

Figure 1. 2: Location of the study area, onshore and offshore for oil and gas wells within Block 13C, Gamtoos Basin. (Modified after: Letullier (1992), McMillian et al., (1997).

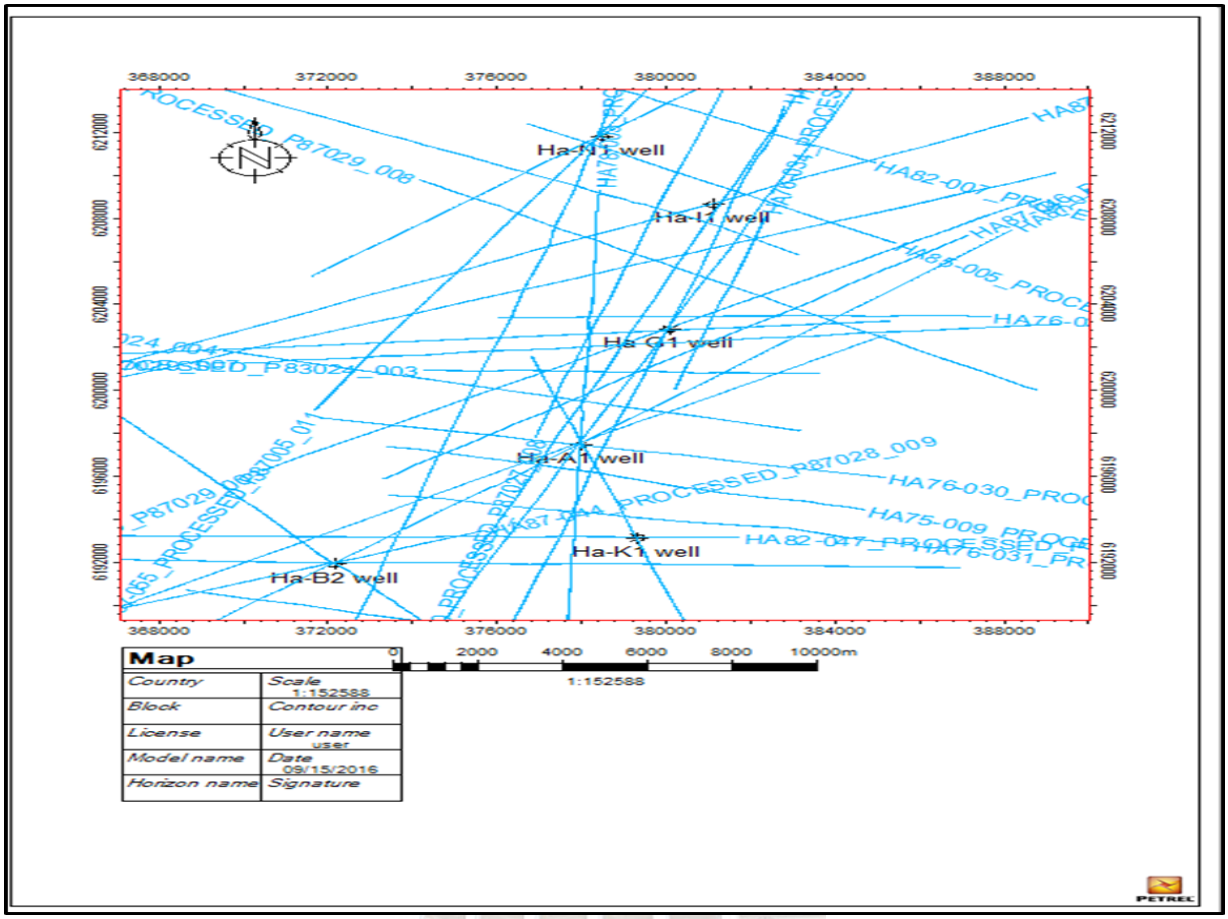

Figure 1. 3: Base map of well locations and 2-DSeismic lines in the Gamtoos Basin.

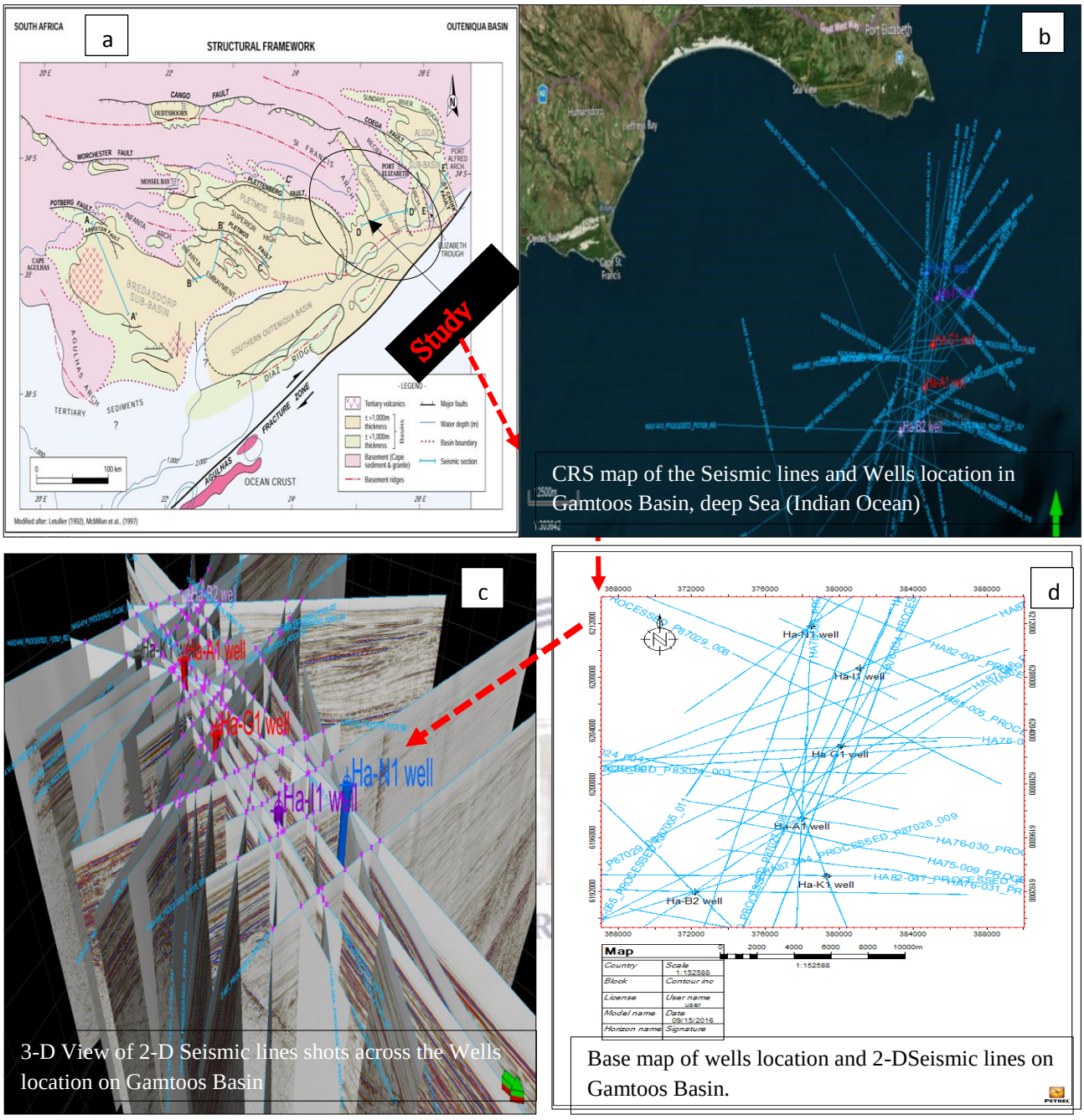

Figure 1. 4: Combined maps showing the Basin location study (a), Coordinate Reference System (CRS) (b) 2-D Seismic lines, wells location in deep Sea (c), and the Base map and 2-D Seismic lines reflections of Gamtoos Basin (d).

1.4 Research Aims and Objectives

The study is based on the integration of seismic stratigraphy, built on seismic sequence and seismic facies and tied-in with the biostratigraphy studies. Furthermore, the petrophysical analysis of the reservoir and static modeling will contribute to a better understanding of the hydrocarbon potential of the Valanginian age rock sequence of Gamtoos Basin.

The study aims to understand the depositional environment from the assessment of geologic time and age based on microfossils. Integrated analysis of seismic stratigraphy and biostratigraphy studies provide in-depth understanding of the heterogeneity complexity of the sandstone reservoir rock potential for the hydrocarbon exploration of the Valanginian age in Gamtoos Basin. This is achieved by integrating Seismic sequence and Seismic Facies analysis tied-in with biostratigraphy, Petrophysical well log analysis and static modeling application. This approach will provide in-depth understanding of the depositional environments using various microfaunal fossil groups and reservoir quality of the hydrocarbon potential of the basin.

1.4.1 The Research Approach

The physical rock characteristics such as lithology, fluid type, and hydrocarbon bearing zones were qualitatively defined while parameters such as porosity, permeability, resistivity of formation water, water saturation and hydrocarbon saturation where possible were estimated using Interactive Petrophysics (IP)® software for selected reservoir intervals of the wells. Petrophysical wireline log data was further used to identify the potential production reservoir zones from the study's wells to determine depth, thickness of zones, and also distinguish between oil, gas or water in the reservoir. The static model would be built from the seismic horizon and shall be used to populate and distribute the Petrophysical parameters of the formation sequence. The seismic facies combined with wireline log response analysis gives more information on depositional environment, particularly in an area of very limited well information.

1.5 Specific Research Objectives

The specific objectives to study the sandstone reservoir sediments of Valanginian sequence are:

- To characterize and evaluate the Petrophysical parameters of the potential sandstone reservoir of the sequence by means of well logs.
- To construct a static reservoir model based on Petrophysical properties and litho-facies variation for understanding the qualities of the reservoir potential.
- To populate and distribute the Petrophysical and facies parameters within the model for clear understanding of the formation reservoir potential.
- To study, identify and interpret the seismic sequence and seismic facies reflection pattern of the sediments from seismic data to understand the depositional environment of the succession.
- To interpret the depositional environment of the reservoir succession during the Valanginian time using the microfossil group 'foraminifera' and to understand the depth of deposition using benthic microfossils.

1.6 General Review of Work on the Gamtoos Basin

The Gamtoos Basin is one of the five sub-basins found in the Southern Outeniqua Basin off the south coast of South Africa. However, while some studies have been carried out on this basin, there are very few available literatures that deal with general geology, stratigraphy, paleo-geography, sedimentological, structural features and hydrocarbon potential of the reservoir and source rocks, as all are internal reports not accessible to the general public. Due to the nature of this research, this section began with the broad overview of the previous work that has been done in the Gamtoos Basin. The available literature indicates that deposition initiated in Gamtoos Basin under deep marine condition. The sedimentary processes that involve bulk emplacement such as, Slumps: (sediment transport by mass with little deformation or folding of layers), Slurries: (debris flows and mud flows- destroying any previous bedding or layering), and turbidite currents (the rapid movement of large slurries down slope) that made up its sequence and reservoir geometry. The land-derived sediments (terrigenous sediments) on the continental slope and continental rise are transported into deep sea by slurries or turbidity currents down slope. Turbidity currents are driven by gravity which enhanced movement of debris far into the sea. Sediment transport is accelerated during

low stand conditions, when sea level falls during which the coast is at the shelf break creating rivers to deposit their sediment load directly on the slope.

The early sedimentation in the Gamtoos Basin indicates substantial lateral variation in depositional environments. The Late Jurassic (Portlandian, Kimmeridgian) to Early Cretaceous (Berriasian and Valanginian) turbidity channel and fan sands are considered as the primary target for exploration in the Gamtoos Basin and locally dominated the early rift deposition. The Kimmeridgian sedimentation on the flanks of the St. Francis Arch is characterized by a basal non-marine conglomeratic and red-bed interval, which is overlain by shallow–marine interbedded sandstones and siltstones (Broad, 1989; Broad, 1990). However, to the east near the Gamtoos fault and the Gamtoos Basin depocentres, the upper slope black claystones with minor turbiditic sandstones are accumulated during this time under low-oxygen conditions. The microfauna are sparse with mostly agglutinated foraminifera and radiolaria which are always present and sometimes occurring in floods. Several intervals indicated organic enrichments with a good potential as a source rocks, though they were buried at around 4000m depths (McMillan, 1990). There are indications of minor gas shows while drilling the thin sandstone in the sequence (Broad, 1989; Broad, 1990).

Southern oil exploration corporation (now PetroSA), through a broad sequence stratigraphic approach, based on seismic mapping of multiple unconformities, established the stratigraphic specification procedures for South African offshore sedimentary successions and various structural elements such as, structural highs and faults within the drift successions, basins and sub-basins. The drift succession denoted as a sub-set of the stratigraphic units, the deposition of which has been referenced to the initial and later period of the gradual west-southwest ward extending plates off the southern coast of Africa. These arrangements brought about the creation of Outeniqua sub-basins which are named as Bredasdorp, Pletmos, Gamtoos and Algoa basins from West to East. The boundary of the Pre-drift successions is marked by the drift-onset unconformity (1At1), which occurred in the late Valanginian. Post drift successions refer to stratigraphic units which are related to the development of true passive margin after the termination of transitional rift-drift in the mid Albian (Petroleum Agency of South Africa, 2004/2005). McLachlan & McMillan, (1979), comment on the substantial change in sedimentary and tectonic style seen at the unconformity associated with seismic horizon D to 6At1 which show the rapid subsidence and sedimentation during the pre-Kimmeridgian to Hauterivian period. But the sediments later are much thinner compared with

the equivalent interval previously at Pletmos and Bredasdorp Basin except the 13At1 to 15At1 canyon fill. Frewin, *et al.,* (2000) debated the geologic characterization of a deep-marine channel lobe system. The Ga-A gas field is part of the oil fields discovered by Soekor both having hydrocarbon accumulation within the turbidite structure in the Cretaceous drift succession of the Pletmos Basin that extended to Gamtoos Basin. Based on the seismic lines that showed numerous unconformities within the drift successions, stratigraphic naming reflects a sequence stratigraphy approach. Turner, *et al.,* (2000) recognize the individual sea level falls through early Aptian and mid-Albian resulting in materials being eroded from pre-existing Highstand shelf sandstones and transported into the central basin by turbidity currents from the west-southwest. However, Turner, *et al.,(*2000) were able to extrapolate sandstone reservoirs into the Gamtoos Basin from the Pletmos Basin which consist of a stack of merged channels and lobes. The fan lobes consisting of coarsening-upward while channelized reservoirs are fining upward.

According to Brown, *et al.,* (1995) sequences defined by significant unconformities shown on seismic sections were given numbers (1-22) while unconformities were labelled by the sequence overlying them (1A 4B, etc.) an example would be: Type 1 = At1.

1.7 Exploration and Prospecting History of the Gamtoos Basin (BLOCK 13 C).

Exploration of hydrocarbon accumulation in South African coastal basins started several years back, the first oil and gas exploration commences in year 1960s by Soekor (the former State Oil Company of South Africa which became PetroSA). In 1965, a small accumulation of oil of non-commercial quantity was discovered onshore in the Western Cape Province location of the Southern Outeniqua Basin. The hydrocarbon exploration in the Gamtoos Basin and its onshore blocks which cover a large area of 5,038 sq. km began in 1968 with drilling of (Petroleum Agency of South Africa, 2004/2005) the Swartkops borehole east of Port Elizabeth in the onshore part of the Uitenhage trough in the Late Jurassic (Portlandian) which consist of a lateral variation in lithologies through the D' to 1At1 sequence (McMillan, 1990). The drilling in the onshore portion of the trough revealed that horizon D' attains a maximum depth of about 1800 m. This revealed a basal non-marine red sandstone and conglomerate, overlain by fluvial sandstone (Swartkops Member). The offshore drilling in the Uitenhage Trough occurred only in the southern half, away from the onshore well, on basement horizon D' which attains a maximum of 4 seconds two-way-time (TWT) approximately 8000 m in the most distal part. However, no commercial production of oil or

gas has been achieved despite encouraging hydrocarbon shows (Malan , 1993). A drill stem test (DST) has produced "36 gravity oil" at an insignificant flow rate. Oil shows and log evaluation showed the presence of reservoir oil in a closed borehole, but drill stem testing was ineffective. The subsequent drilling of adjacent wells was unsuccessful to confirm any hydrocarbon reservoir therefore concluded that the oil might have been trapped in the local fracture.

However, offshore, hydrocarbon shows were encountered in the borehole drilled in the Port Elizabeth and Uitenhage troughs and in the Gamtoos Basin (McMillan, *et al.*, 1997). But drill stem tests were not performed offshore, although the reservoir shows have been sufficiently encouraging for hydrocarbon exploration to continue. Also, an encouraging hydrocarbon show is the 630 km^2 wet-gas-to-oil sniffer anomaly noted in Algoa bay; this anomaly was centred in the overlying area of the northern extension of the Algoa canyon and the St Croix fault. Thus, the distribution of the reservoirs and source rocks suggests that the best hydrocarbon potential may be accumulated in poorly explored southern parts of the Gamtoos Basin and the undrilled southern Port- Elizabeth and southern Uitenhage troughs (McLachlan & Wickens, 1990).

Exciting opportunities for these complex basins can be concluded based on:

- The combination of an abundance of reservoir quality sandstones in the northern Uitenhage trough with the presence of the sniffer hydrocarbon anomaly upgrade in Gamtoos and Algoa basins.
- Encouraging hydrocarbon shows present in Albian sandstone beneath the Algoa and Gamtoos canyon, with similar untested stratigraphic traps present in the south.
- An onshore data set of 22 borehole and offshore data sets of 19 boreholes, with comprehensive multichannel seismic coverage.

Moreover, there are numbers of identified prospects in these basins and one advantage is that the water less than 300 m deep. The Gamtoos and Algoa basins are semi-explored and have known reservoir units, numerous petroleum charges, regional top-seal as well as several traps. Thus, the good temporal relationships between these factors have indicated good potential for undiscovered petroleum accumulations in the basins (Malan , 1993).

CHAPTER TWO

2. *Literature Review*

2.1 Introduction

The topics included in this review focus on seismic sequence, seismic facies, geophysical well logs, biostratigraphy (focussing mainly on the microfossil group 'Foraminifera'). The discussion on seismic sequences and seismic facies analysis focuses on using seismic parameters' attributes to understand the structural information of the sediment, mainly the depositional processes and the environment of deposition. The description is based on the integration of the core data and well logs, with the aim to improve the formation evaluation in terms of the reservoir qualities, identify the microfossil groups present and interpretation of overall depositional environment and the possible related source of errors that may arise during the analysis. These were thoroughly reviewed, because the geologist uses this information to draw a map that can guide in establishing the next location for drilling for oil. Also the data can be used to correlate the age between wells and to determine the depositional environment based on paleo water depth. Many of the benthic foraminifera live in a specified depth interval and their preservation in the sediments are useful to understand the Paleobathymetry.

2. 2 Seismic Stratigraphy

Seismic stratigraphy is the method used to extract stratigraphic information from seismic data, by means of interpreting seismic reflection within the geological frame work and was introduced by Vail, *et al.*, (1977). The application of Seismic stratigraphy to extract information from seismic data is divided into three parts namely:

1. Seismic sequence stratigraphy analysis (which deals with separating time depositional units according to unconformities),
2. Seismic facies analysis (used to determine depositional environments) and the reflection characteristic analysis which is the aspect that is used to study the lateral variation of individual reflection events, or sequence of events, in order to
3. Locate the occurrence of the stratigraphic change by means of identifying their nature such as DHI (direct hydrocarbon indicator), which is the major tool for this by modelling both synthetic seismograms and seismic logs to detect hydrocarbon, mostly gas.

The seismic stratigraphy is based on the properties of primary reflections that are generated through velocity and density contrasts on physical surfaces of the rocks consisting mainly of strata surfaces and unconformities. The interpreted result from the seismic section can be recorded in Chronostratigraphic depositional and structural patterns. However, the main concept of seismic stratigraphy is the identification of stratigraphic units comprised of fairly conformable successions of genetically related strata, known as a depositional sequence (Figure 2.1). These are both bounded at the top (B) and base (A) by an unconformity.

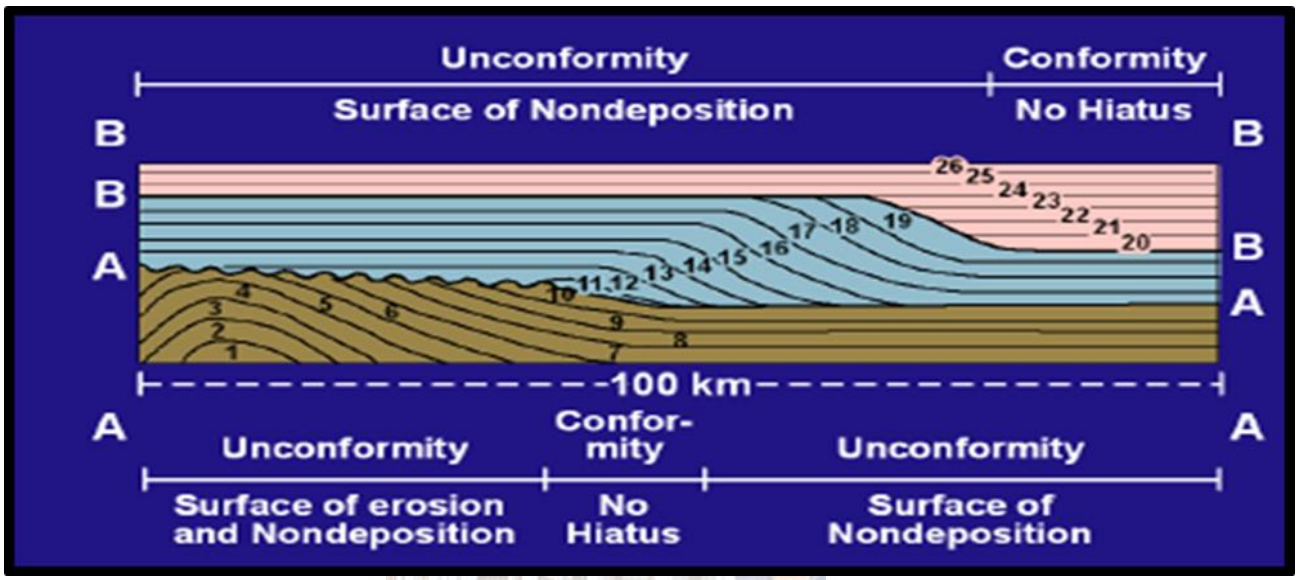

Figure 2. 1: Schematics of a depositional sequence (Modified by Vail et al., 1977).

2.2.1. Seismic Sequence Analysis Concepts

Seismic sequence analysis is one of the concepts used to interpret sequence stratigraphy from seismic data by means of seismic reflection. It is the process of identifying unconformities and correlative conformities on reflection seismic sections in order to separate the packages of the sequence with different depositional time unit. The discontinuities or unconformities and the depositional boundaries can be recognized by interpreting the seismic reflection termination such as onlap, downlap, and toplap as well as truncation orderly displayed by a discontinuity surface. The depositional sequence boundaries can be identified by the termination reflection that is caused by lateral termination of the strata known as discordant surfaces. The three major types of discordance at upper and lower boundaries can be recognized and are described below. The concordance can be referred to as the continuous sedimentation. The sediment lying on top of one another have the same strike and dip (Figure 2.2). According to Catuneanu, *et al.*, (2009) in seismic stratigraphy, there are four strata

terminations that can be used to identify sequence stratigraphic surfaces. Two are found at upper surfaces and are called onlap and downlap, while the other two occur at lower surfaces and are called truncation and toplap (Figure 2.3). In addition, offlap strata termination is a major strata stacking pattern that indicates the recognition of force regression and describes the subaerial unconformities and their correlative conformities. Such lapouts are useful to interpretation of depositional trend as well as system tracts. The strata geometries and strata terminations can be used to define surfaces and system tracts, and understand accommodation conditions during the deposition (Catuneanu, *et al.*, 2009).

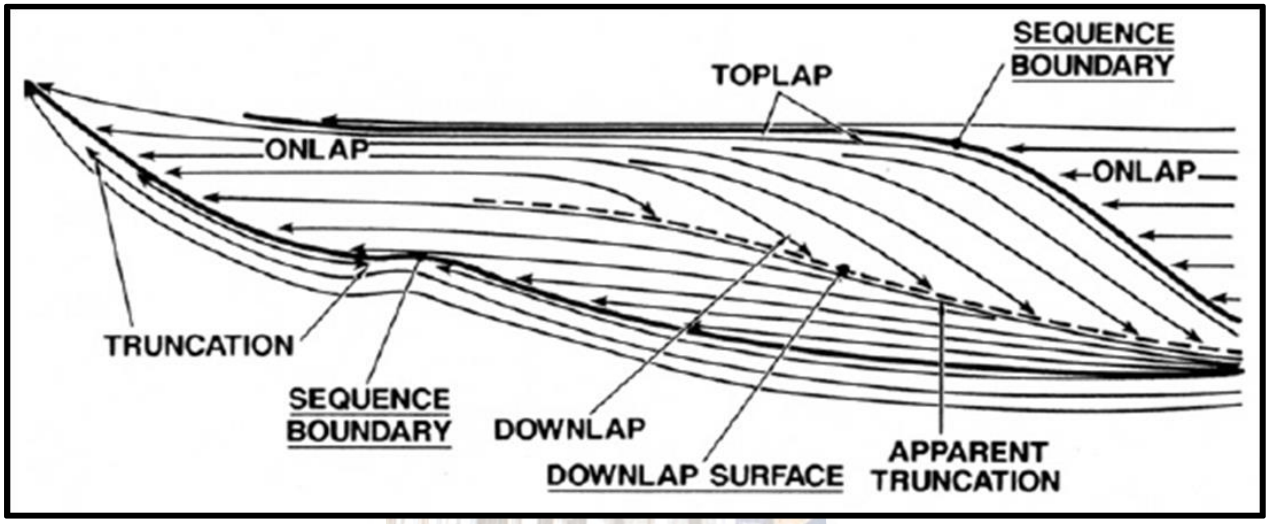

Figure 2. 2: Reflection termination and types of discontinuity (the discontinuity names are underlined) after Vail, 1987.

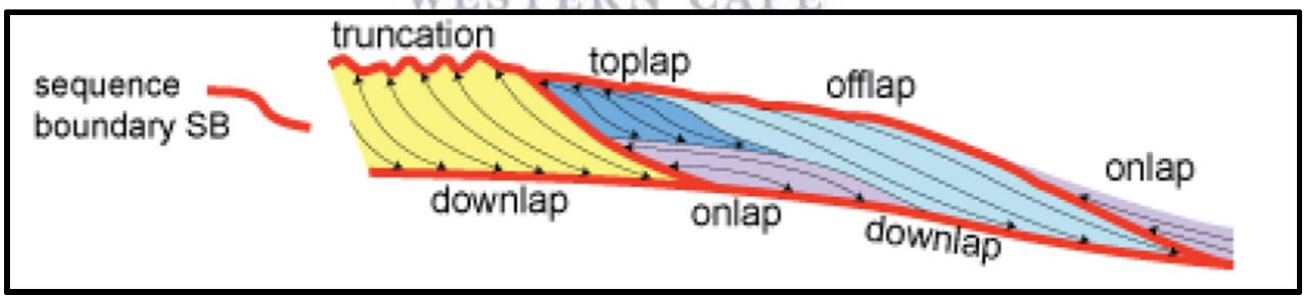

Figure 2. 3: Schematic of seismic strata termination (After Catuneanu, 2002).

2.2.1.1 Lower Boundary

Onlap:

An onlap is a base-discordancy in which the initial strata terminate updip against an initially inclined surface, or it is an initially inclined surface that terminates against strata of greater inclination (Figure 2.4). Onlap can also be referred to as lapout, and indicate the lateral

termination of sedimentary units at its depositional limit. An onlap type of termination can develop in marine, coastal and non-marine environments, such as:

Marine onlap: This developed on continental slopes during transgressions (slope aprons, (Galloway, 1989);

Healing-phase deposits, (Allen & Posamentier, 1993), occur when there is deep-water transgressive strata onlap on the maximum regressive surface.

Costal onlap: This is also known as transgressive coastal to shallow-water strata onlapping on the transgressive (tidal, wave) revilement surface.

Fluvial onlap: referred to as landward shift of the upstream end of the aggradation area in a fluvial system during the base level rise (normal regression and transgression) when fluvial strata onlap on the subaerial unconformities.

Downlap

Downlap is also a base-discordancy in which the initially strata terminate downdip progressively against an initially horizontal or differently inclined surface (Figure 2.4). It is also known as baselap, and indicates the base of a sedimentary section at its depositional limits. The downlap strata termination is usually observed at the base of prograding clinoforms either in shallow or deep marine environments. It is uncommonly found in non-marine settings, except in lacustrine environments. Thus, downlap represents a change from marine (or lacustrine) slope deposition to marine (or lacustrine) non-deposition. However, base-concordance refers to the strata of the sequence which do not terminate against the lower boundary.

2.2.1.2 Upper Boundary

Toplap

This is the termination of strata (clinoforms) against an overlying lower angle (updip), surface (upper boundary) primarily due to non-deposition or as a result of bypassing sediment with possible minor erosion (Figure 2.4). The strata lapout (lateral termination of a reflection at its deposition section) follows landward direction at the top of the section, but the successive termination rests progressively seaward. Thus, toplap surface signify the proximal depositional limit of the sedimentary section. In seismic stratigraphy, the topset of a deltaic system (delta plain deposits) can be too thin or weak to be recognised on a seismic section

profile as separate units (thickness below the seismic resolution). In events of this, the topset may be mistaken for toplap (apparent toplap).

Erosional truncation

Erosional truncation is the termination of strata against the upper boundary of a sequence due to erosion. These commonly occur where strata are tilted as a result of structural movements (Figure 2.4). Top concordance refers to the strata at the top of the sequence that do not terminate against an upper boundary.

Structural truncation: This is the lateral termination of a stratum by structural disruption that is generated by faulting, gravity sliding, and igneous intrusion or salt flowage.

Apparent truncation: Is the termination of relatively low-angle seismic reflections beneath a dipping seismic surface, where that surface represents marine compression (Figure 2.4a). However, other types of strata termination include:

Offlap: Is the progressive offshore shift of the updip termination of the sedimentary sections in a conformable succession of rocks in which an individual successively younger section exposed a portion of the older section on which it lies. Thus, offlap is the outcome of base level fall; therefore it is an indicative for forced regression. **Lapout** is the lateral termination of a reflection (generally a bedding plane) at its depositional section.

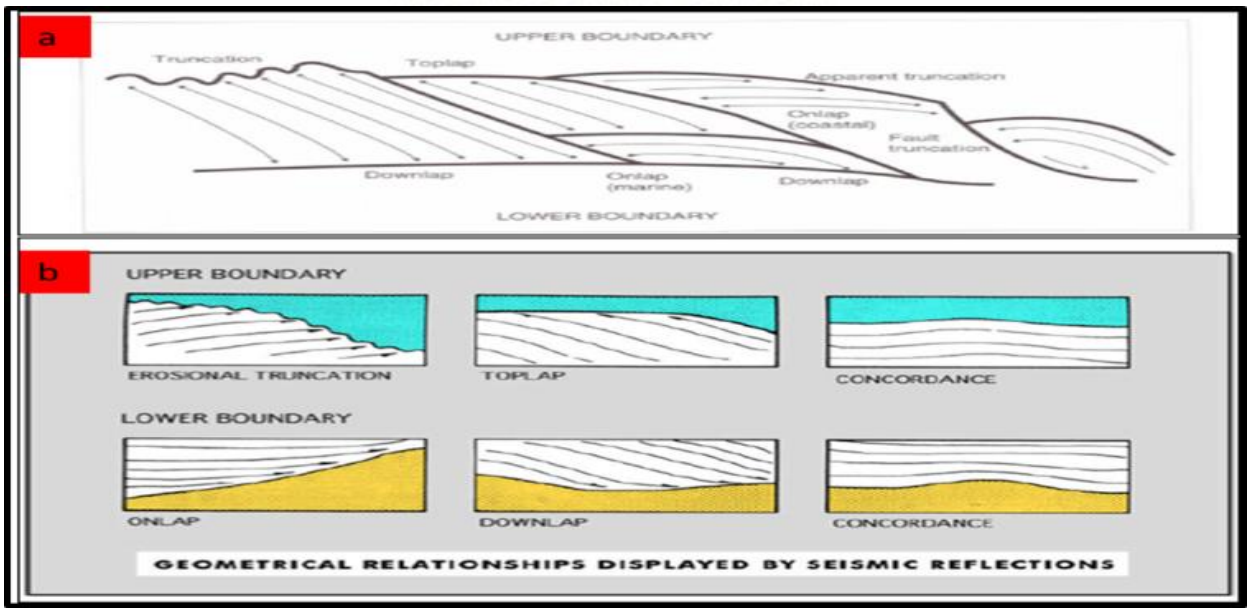

Figure 2.4: Schematic reflection discordance (Emery & Myers , 1996). (b) Types of unconformable relationships displayed by reflection geometries on seismic section, (Veeken, 2007).

2.2.1.3 Seismic Facies Analysis Concepts

Seismic facies concepts were introduced in exploration geophysics only a few years ago, but the concept has not been widely used. Though, seismic facies analysis has been subsequently used in interpretation of seismic stratigraphy for hydrocarbon exploration from seismic data. However, in this study the focus shall be on seismic facies analysis in addition to seismic sequence analysis. Seismic facies analysis makes use of different seismic parameters for the purpose of getting other than structural information. The procedures are usually applied in oil exploration. A seismic facies unit is defined as a sedimentary unit which is different from the adjacent units in the seismic facies characteristic (Roksandic, 1978). Seismic facies may sometimes correspond to geological facies, however, in some case it doesn't correspond due to different factors such as:

(a) Resolution from the seismic method is much less than that of the geology methods.
(b) Seismic data do not include all information necessary for the definition of a geological facies.
(c) Some seismic parameters are influenced by secondary processes which are not strictly connected with a geological facies. For instance, the presence of gas may change the seismic signature.

Besides, the characteristic of seismic signature of some geological bodies essentially composed of one geological facies can be caused by features originating from the post-depositional processes. Such is the case with diapir cores (core from dome strata or rocks).

The objective of using seismic facies analysis is to enable the correlation of reflection attributes with the stratigraphic characteristics of the identified sequence. It can also provide a correlation frame work between seismic and well data. These reflection characteristics are thought to correspond to the unique geological and depositional history of the sequence (Mitchum Jr, *et al.*, 1977). However, several previous studies have shown a direct correlation between seismic facies type and lithology. Nevertheless, calibration between the two is still a basin specific; therefore, an independent analysis must be carried out for the basin of interest.

Seismic facies analysis aids in interpreting lithofacies distribution, determining the depositional environment and energy sources from seismic data reflection characteristics (Mitchum Jr, *et al.*, 1977), such as: amplitude, continuity, configuration and interval velocity that distinguish them from neighbouring sets. Sangree & Widmier, (1974) and Sheriff , (1975) directed that the following seismic data or seismic facies elements such as: reflection

amplitude, dominant frequency, interval velocity, reflection configuration, reflection continuity, external form of seismic facies units i.e. the geometry of the seismic facies units, should be considered in seismic facies analysis (Figure 2.5 and 2.6). Thus, interpretation of lithofacies and depositional environments using seismic facies analysis involved the following internal and external key seismic parameter units:

Internal key seismic parameter units include:

- The reflection termination (reflection discordance) such as: (onlap, downlap, erosional truncation, and toplap) found at the upper and lower boundary in a seismic sequence (Figure 2.4).
- The geometry reflection such as: reflection amplitude: low, high and variable. Continuity: high, low, and variable. Frequency: thickness of each layer (Figure 2.5)
- The reflection configuration includes: parallel, divergent, chaotic, prograding, such as: sigmoid, oblique, shingled, and hummocky (Figures 2.6, 2.7 & 2.8).

External key seismic parameter units include:

- Three dimensional forms such as: Sheet, Sheet drape, Wedge, Bank, Lens, Mound and Fills, (Figure 2.8).

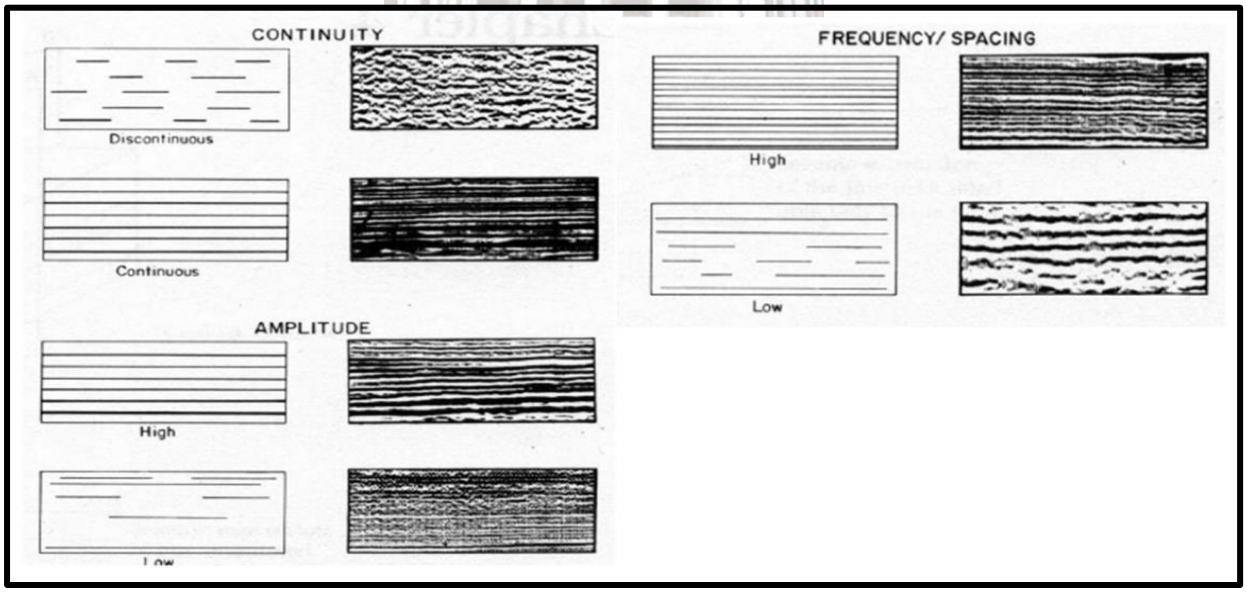

Figure 2.5: Geometry reflection attributes: continuity, amplitude and frequency/spacing (modified by (Badley, 1985)

Nevertheless, there are two ways of interpreting seismic facies data such as direct and indirect interpretation. The direct interpretation of seismic facies analysis is aimed at finding out geological causes responsible for the seismic signature of seismic facies units, such as

predicting the lithology, fluid content, porosity, relative age, overpressure shale, type of stratification, geometry of the geological body corresponding to the seismic facies unit and its geological setting. While the indirect interpretation tends to reach conclusions on depositional processes and environment, sediment transports direction, and some aspect of geological evolution (transgression, regression, subsidence, uplift and erosion). The result of the seismic facies analysis can be shown on seismic facies cross-sections and seismic facies map, depending on the availability of seismic data and geological conditions of the area under consideration. The seismic facies map can be of different types such as a general seismic facies map indicating distribution of different seismic facies units, sand-shale ratio map, and direction of cross-bedding and paleo-transport maps etc.

2.2.1.4. Important Notes in Seismic Facie Analysis

(Sangree & Widmier, 1979), recognised the following key factors in using seismic facies analysis.

1) An understanding of the impacts of lithology and bed spacing on reflection parameters such as: amplitude, frequency and the continuity of reflections (Figure 2.5).

Table 2. 1: The features of reflections and Geological interpretation of amplitude, frequency and continuity of reflection (Sangree & Widmier, 1979).

Features of reflections	**Geological interpretation**
Amplitude	Fluid content, impedance (Velocity-density) contrasts, layer spacing (cause constructive and destructive interference).
Frequency	Fluid content and bed spacing.
Continuity of reflections	Depositional processes and bedding or layer continuity.

2) Parallel and sub-parallel: This formed by strata which were possibly deposited under stable basin conditions or at uniform rates on a uniformly subsiding shelf, (Figure 2.6).

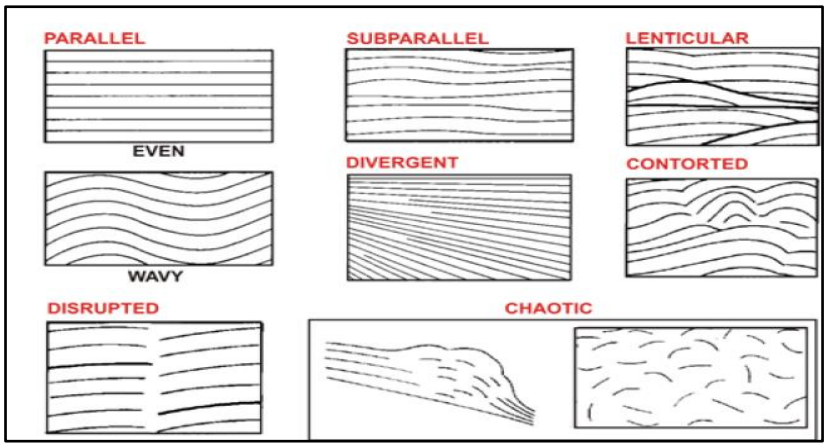

Figure 2. 6: Internal structures (parallel and sub-parallel) reflection patterns on seismic section (Mitchum Jr, et al., 1977a).

a) Divergent: The divergent reflection configurations are characterised by a wedge shape unit where lateral thickness of the whole unit is as a result of thickening individual reflection sub-units in the main units (Figure 2.6). This configuration is interpreted to indicate lateral variations according to rate of deposition or progessive tilting of the sedimentary surface in deposition.

b) Prograding: The prograding reflection configuration created by sediments that are horizontally out-building sediments deposited earlier or sediments deposited in a progradation pattern forming a gently sloping depositional surface known as clinoforms. However, prograding reflection configuration shapes are sigmoidal (superposed S-shaped reflector) and oblique, complex sigmoid-oblique, shingled and hummocky, (Figure 2.7).

c) Chaotic: Chaotic reflection configuration patterns (Figure 2.6), occurred as a result of penecontemporaneous, soft-sediment deformation or possibly deposition of sediments in a variable high-energy environment e.g (basement environment), thereby interpreted to signify a disordered arrangement of reflection surfaces.

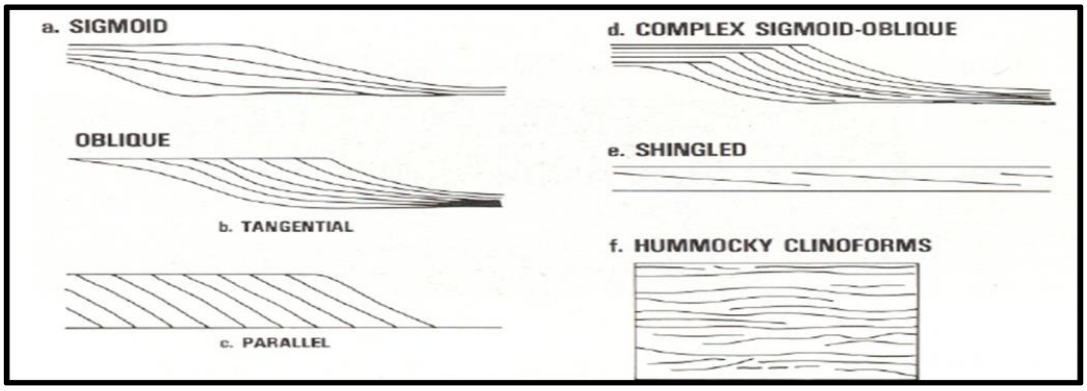

Figure 2. 7: Seismic reflection configurations patterns interpreted as prograding clinoforms. (Mitchum Jr, et al., 1977).

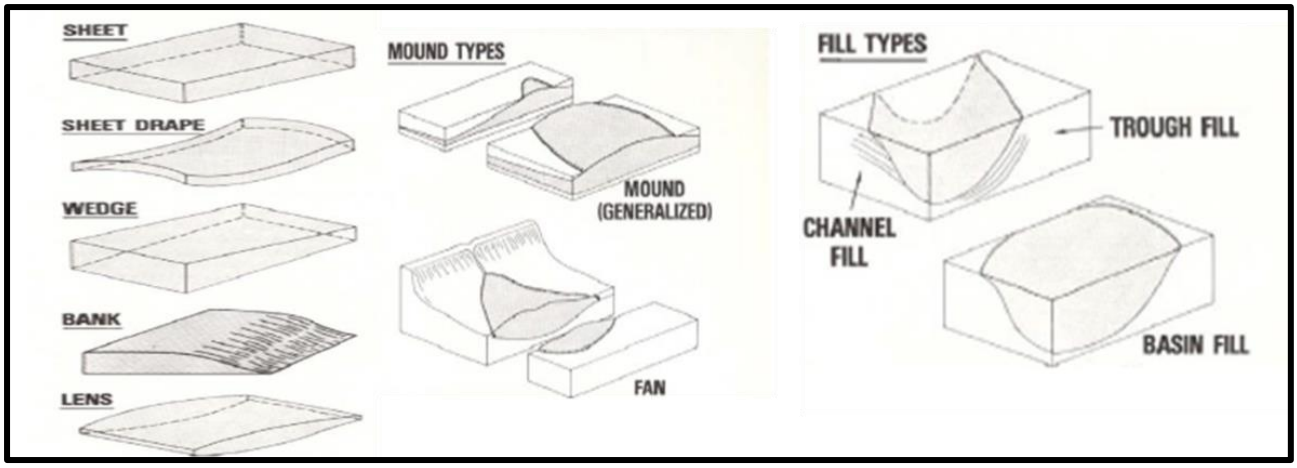

Figure 2. 8: Seismic reflection configurations of external seismic facies units in three dimensional patterns (Mitchum Jr, et al., 1977).

2.3 Parasequences

The parasequence is the fundamental unit of sequence which is defined as the relatively conformable succession of beds or bedsets that are both bounded at the base and top by marine flooding surfaces or their correlative surfaces (Van Wagoner, *et al.*, 1990). Generally, parasequences are irregular shallowing-upward sedimentary cycles and the lower section of the parasequence consists of deeper water facies and its upper section shallower water facies. However, in a typical siliciclastic wave dominated shoreline setting, particular sets of facies occur in order: the parasequence that traversed these facies begins with bioturbated offshore mudstone, overlain by either the storm beds of the transition zone or the lower shore face. This in turn is followed by the cross bedding of the shore face environment and ultimately passing upward into the seaward-inclined laminae of the foreshore. The sequence is typically topped by coastal plain coal beds (Figure 2.9).

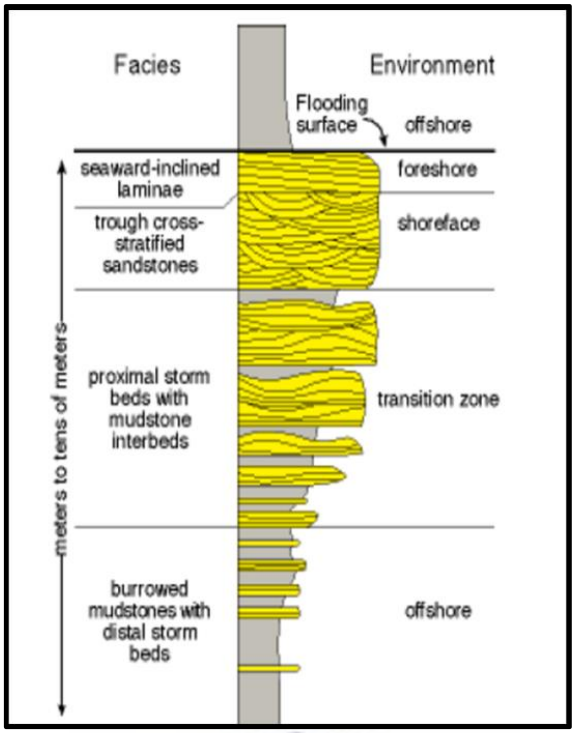

Figure 2. 9: Typical wave dominated parasequence (Van Wagoner, et al., 1990).

Parasequences are commonly used to describe individual prograding sediments bodies in coastal to shallow-water systems. They have correlative surfaces both on the coastal plains, which can be an erosive surface, root horizon, and as local erosion surface, and basinward as an upward succession of facies which suggests of deepening depositional surfaces. However, a parasequence which developed on a muddy siliciclastic shoreline exhibits a different set of facies, which arrayed vertically in a shallowing upward order; such parasequence begins with cross-bedded, subtidal sands, followed by inter-bedded bioturbated mudstone and rippled sands of intertidal environment, overlain by mudstones of the supratidal zone and swamp coal (Figure 2.10). A flooding surface is the surface across which there is an abrupt change of facies that can either indicate an increase in water depth or a decrease in sediment supply (Van Wagoner, *et al.*, 1988). Flooding surfaces occur over a paleosol, offshore transition, open marine limestone, or any depositional facies. Flooding surfaces may reach maximum landward position called maximum transgression. The horizon of the maximum transgression within the sequence is called maximum flooding surface (MFS) (Van Wagoner, *et al.*, 1990)

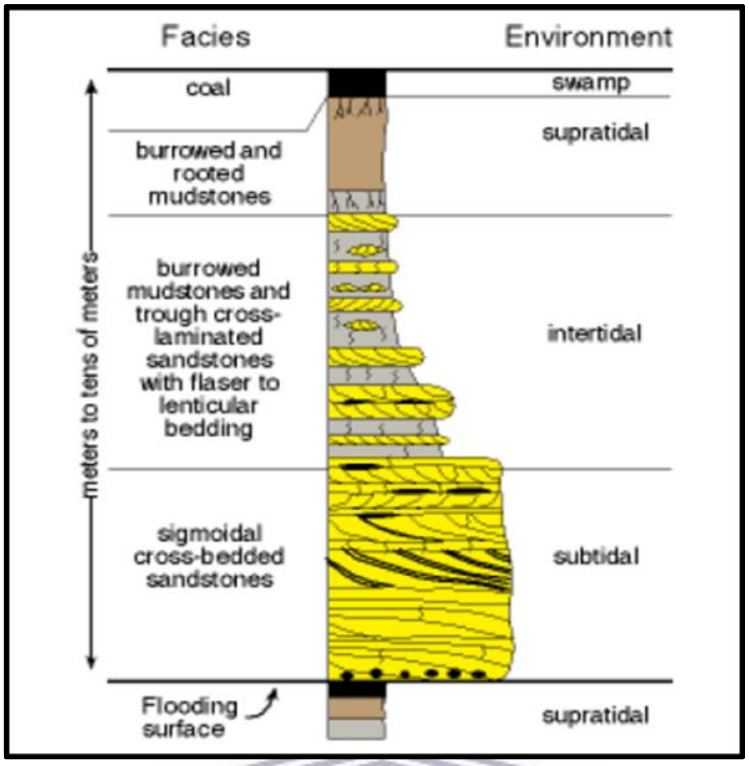

Figure 2 10: Typical tidal-parasequence (Van Wagoner, et al., 1990)

2.3.1 Parasequence Sets and Stacking Patterns

Furthermore, stacking patterns respond to interplay of changes in the rate of sedimentation and base level, and reflect a combination of depositional trend such as progradation, aggradation and down cutting. Each stratum stacking pattern describes particular genetic types of deposits such as transgressive, normal regressive and force regressive (Hunt & Tucker, 1992). However, due to predictive strata stacking patterns in a sequence, parasequences are classified into parasequence sets. Thus, parasequence sets are basically a succession of genetically related parasequences which form distinctive stacking patterns typically bounded by major marine flooding surface and their correlative surfaces. These sets of successive parasequences can exhibit consistence in thickness and facies composition depending on sediment supply and accommodation which can be progradational, (coarsening upward), aggradational (representing relatively constant water depth) and retrogradational (can dip upward–backstepping) (Figure 2.11). All these correspond to different forms of system tract.

2.3.2 Progradational Stacking

This is the lateral outbuilding, or progradation, of strata towards the seaward direction. This is the parasequence set or stacking in which successively younger parasequences deposited

farther basinward, implying that the overall rate of depositing sediments is greater than the rate of development of accommodation space (Figure 2.11). It also creates an overall shallowing-upward trend within the parasequence set, and can be recognised by the progressive appearance of shallower-water facies upward in the parasequence set, as well as the progressive loss of deeper-water facies upward in the parasequence set. It is bounded by a flooding surface (Hunt & Tucker, 1992).

2.3.3 Aggradational Stacking

This is the vertical build-up of a sedimentary sequence, which generally occurs when there is a relative sea level rise caused by subsidence or eustatic sea-level rise, thereby enhancing the rate of sediment influx to the extent that it is sufficient to match the formation of the depositional surface and can form near the sea level (i.e. when carbonates or clastics sustain in HST). This occurs when the sediment rate is equal to the sea level rise, thus producing aggradational stacking in a parasequence when the patterns of the facies at the top of the each parasequence are essentially the same (facies of shoreline stays in the same position) (Figure 2.11).

2.3.4 Retrogradational Stacking

This is the movement of the coastline landward as a result of transgression. This occurs when the sea-level rises with low sediments influx. A retrogradational parasequence set is a parasequence set in which successive younger parasequences are deposited farther landward in a backstepping form. For instance, the contact between the shoreline sands and the coastal plain facies at the top of each parasequence will appear to move farther landward in each successive parasequence. Thus, the overall rate of deposition or sediments deposited is less than the rate of accommodation space (Figure 2.11). Therefore, accommodation space is created more rapidly than it is filled, water depth develops deeper, and facies gradually move farther landward. Although each parasequence is shallowing-upward, the amount of deepening at the flooding surface surpasses the amount of shallowing in the next parasequence, creating a net overall deepening in the parasequence set.

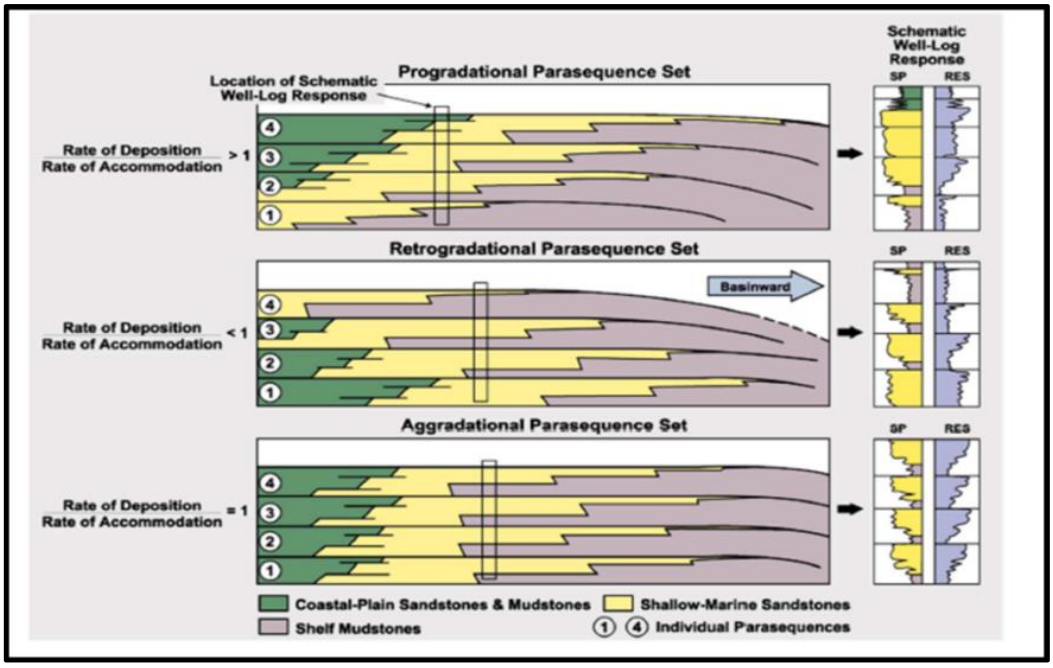

Figure 2. 11: Typical stacking of parasequence sets (Van Wagoner, et al., 1990)

2.4 Core Description

Core analysis is the preliminary fundamental point of geologic and engineering studies for reservoir characterisation. It is the only tool used in the reservoir assessment that measures the formation properties. Core and well cuttings are the subsurface rock materials. Therefore, convectional cores enable us to visualize subsurface formation properties which can help in reducing uncertainty that is associated with the reservoir, seal distribution and –quality. The analysis may aim to determine formation properties such as

- porosity (storage capacity for reservoir fluid),
- permeability (reservoir flow capacity),
- saturation (fluid type and content), and,
- sedimentary structures,
- lithology (grain size distribution, grain density, and mineral composition),
- fossil and trace fossil association and
- flow characteristics of the fluid (Bateman , 1985). As well as
- the effect of an overburden stress,

All these provide useful information to geologists and engineers whether a wellbore will be economic or not, also to understand the depositional environments, reservoir geometry and quality. Laboratory core analyses usually provide accurate measurements, however, error in

conducting laboratory test procedures in analysis of core sampling preparation may cause damage to the core if not correctly performed (Sinclair & Duguid, 1990). Damaging processes, such a plugging can cause partial disintegration of a formation and thereby extensively affect the results of the petrophysical property measurement. Thus, partial disintegration of core due to the plugging process has been observed as the source of overly optimistic permeability measurements (Hurst,1987b). The excessive breakage of the core during the transportation, and removal from the barrel, as well as laying them out in the laboratory may also cause damaging of the cores. Laboratory procure during the drying samples can extract the water content in the clay particles (Sinclair & Duguid, 1990).This could result in misidentification of minerals on the petrophysical properties.

Jahaz, (1990), describes the analysis of using core obtained from qualitative geological description by the use of complex analytical tools, including x-ray diffraction (XRD), and Scanning electron microscopy (SEM). Today there are however no calibration standards or uniformly accepted experimental procedures. Consequently, there are a lot of substantial inconsistencies in the analyses of a major reservoir by different laboratories thereby enhancing the reality that validation of the result can only be done only within the arranged procedures based on singular laboratory. For instance, measuring porosity in the dried core plug by means of humidity controlled approaches has been observed to be constantly lower compared to those measured from oven-dried core plugs (Penney & Looi, 1996). Thus, analysis of related groups of core samples by different laboratories based on their individual techniques can result in significant differences in the evaluation of potential reservoir sequences. The method of drying core samples, for instance has been known to be vital in conserving the in-situ morphology of some minerals (illite) as well as understanding the difference in permeability measurements obtained from core analysis and well test data (Pallat, *et al.*, 1984). In addition, related observation was noted by McHardy, *et al.*, (1982) in comparing the morphology of illite contained in samples that have gone through different drying processes. Therefore, as a result of deficiency in the measurement, the rock properties validated based on the evaluation of particular core analysis methods may not always be counted, as the extent of the errors in assessment that could arise during the analysis is not acceptable. The major consequence is that, core analysis results can be completely different from the geophysical data. In that case, the predictions based on the geophysical log are occasionally doubtful without a reflection of the laboratory analytical procedures. Nevertheless, another coring method such as sidewall coring may be carried out when

supplementary rock samples are needed after the drilling of the well prior to casing. Sidewall cores are acquired with a wire tool by means of firing a hollow cylindrical bullet by pulling the wires connecting the barrel to the gun, into the formation and subsequently recovering it after the formation wall has been affected by these cylindrical bullets, (Figure 2.12). Core barrels are designed for penetrating formations of different hardness; the types of barrels and the size of the charge are varied to enhance recovery of different formations. However, the major problem with coring is due to the susceptibility of the formation sample toward the physical changes on its journey from the well foot to the surface. Several high-tech coring mechanisms that can conserve the orientation, pressure and the original fluid saturations of core samples have been established.

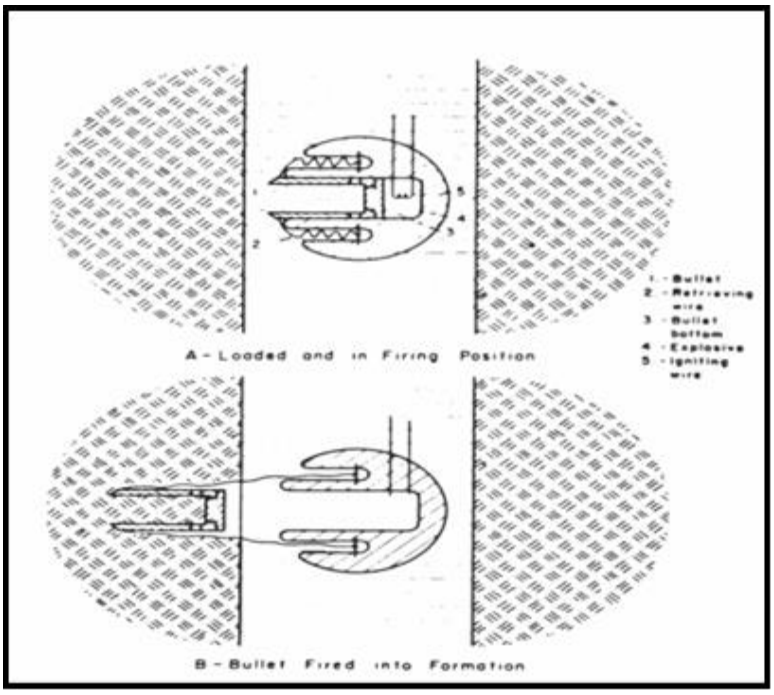

Figure 2. 12: Sidewall-Coring Scheme (Schlumberger, 1972).

2.5 Petrophysical Well logs or Wireline logs

Petrophysical well logging or wireline logging is the act performed by engineers and geologists to extract subsurface information on physical properties of rocks which are exposed during the drilling of an oil well. This is obtained by means of measuring equipment called logging tools (sonde) lowered on a cable (wireline) into the well. These measurements of the different rock properties are transmitted through the cable which contains several conductors to the surface components (computer unit) where the readings are noted. The recording of this information on paper or film establishes the well-log. This process is

sometimes referred to as geophysical well log technique which was introduced by Conrad Schlumberger and Henri Doll (brothers) in Alsace, France, 1927. In addition, geophysical well logging has become essential in hydrocarbon exploration as to the geological sampling (cutting samplings) during the drilling shows an inaccurate record of formations encountered. Mechanical coring methods are more expensive and slower but their results are explicit. However, logging is more precise, but it requires the attention of an experienced geologist or Petrophysics for the interpretation. Logging, when it's well calibrated, corrects the anomalous gap between the cutting and cores thereby providing detailed subsurface information. The circumstances which entail core and log measurements differ extensively. Well logs measure in-situ parameters and they are not usually assigned to geological factors. The logging tools are also affected by the environmental factors, including temperature, overburden pressure, casing and other factors (Rider, 1996).

However, as stated above, wireline loggings differ from drilling logs. Reason being that they are performed after the termination or an interruption of drilling the well, by means of lowering instruments into the hole; this process is known as Logging While Drilling (LWD) (Schlumberger, 2000), Visual examination of samples brought to surface is done by means of geological logs including: cuttings logs, core-loggings or petrophysical loggings as recognised tools, (Ofwona, 2010). The drilling logs are performed during the drilling and record factors such as such as drilling-rate, torque and mud-loss which comprises drilling mud salinity, PH and mud weight, etc. These are ways of obtaining petrophysical information about the rock formations as the bit penetrates through the formation and produces a primitive lithological log. They main objective of well logging is to acquire petrophysical properties of reservoirs such as porosity, permeability and hydrocarbon saturation etc. For the hydrocarbon exploration, logs also enhanced subsurface information regarding to the fluids in the pores of the reservoir rocks. The petrophysical parameters such as effective porosity ($\emptyset$), water saturation (Sw), formation resistivity(Rw), hydrocarbon saturation (So) and true resistivity (Rt) are all evaluated by means of using well log data.

Thus, Petrophysical well log analysis and interpretation are very important tasks to distinguish the reservoir Petrophysical parameters like porosity, water saturation, and thickness of hydrocarbon bearing zone (Schlumber, 1974; E1-Gawad, 2007). The well logging application is principally directed towards determining the lithological and Petrophysical components by means of relevant techniques combining various logging data.

Well logs have been effectively used as part of drilling practise in exploration and development wells, to offer more information and greater accuracy of reservoir evaluation (Connolly , 1965; Brown, 1967). They are also utilised to identify depositional environment (Serra & Abbott, 1982; Serra, 1985; Rider, 1996; Rider , 1990), and the depth and thickness of productive zones. Additionally, they are also used to differentiate between oil, gas and water in reservoirs to assist in estimation of hydrocarbon reserves (Asquith, *et al.*, 2004).

2.5.1 Classification of Geophysical Wireline Logs

The geophysical wireline logs are classified either based on their mode of operation of the logging tools or mode of their usage which involves measuring physical parameters and the conclusions that can be obtained from them.

2.5.2 Classification of Geophysical Well logs Based on Mode of Operational Principle includes

- Electrical logs: Spontaneous Potential (SP) log and Resistivity logs.
- Nuclear or Radioactive logs: Gamma ray (GR), Density and Neutron logs.
- Acoustics log: Sonic logs.

2.5.3 Classification based on their usage mode includes

- Resistivity logs by: Induction, Lateral log and Deep-resistivity
- Lithology logs by: Gamma ray and Spontaneous potential.
- Porosity logs by: Sonic, Density and Neutron logs.
- Auxiliary logs by: Calliper, Dip meter, Bit size logs etc.

2.5.4 Characteristics of Selected Wireline Logs.

2.5.4.1 Radioactive Log

Radioactive logs entail the use of radioactivity to identify the lithologies of the formation and to determine their porosity and density; this is done mostly in a cased hole. Radioactive logs can be classified into two groups such as: Gamma ray that passively measures the natural gamma ray radioactivity of the formation and the gamma ray that measures induced radioactivity from the strong radioactive sources in the Sonde. However, the first group of an element that uses a natural radioactive phenomenon is due to the presence of potassium, thorium and uranium in lithologies. Based on the effect of radioactivity on lithology, we know that shale commonly has the highest radioactive value, while sands are intermediately

radioactive, and dolomite, limestone and quartz generally show a low radioactivity (Bassiouni, 1994). Sometimes elements, such as ash bands, potash beds, and radioactive ores with higher levels of radioactivity than shales, may be encountered. Due to high radioactivity of shale sediments, most of the radioactive elements tend to concentrate on shale and other fine sediments, the clay particles which are chemically active absorb radioactive minerals. Also, some heavy metals selectively precipitate and entrain fine sediments (Bassiouni, 1994), but potassium is the major contributor to shale radioactivity. Common shale log tools may be used to identify them. Having said that though, radioactive log tools must be carefully interpreted, because not all shale formations are radioactive, and conversely, not all the radioactive formations are shale.

However, Shale-free sandstones and carbonate confines with very minute radioactive minerals as a result of chemical environment that existed during their deposition are not favourable to accommodation of radioactive minerals. Gamma ray activity varies from region to region but may be constant in a specific field. The spectral gamma ray is the borehole equivalent of the gamma ray spectrometer. This measures the numbers of gamma rays and their energy spectrums. It allows determination of specific concentrations of potassium (K^{40}), thorium, and uranium. These measurements enable the emission of uranium content to obtain a superior evaluation of shale contents. It's different from the simple gamma ray log which measures the radioactivity of the three elements (potassium (K^{40}), thorium, and uranium) that can be used to represent the depositional environment of formations. Uranium-radium series, the thorium series and potassium-40 (K^{40}) are the most abundant in sedimentary rocks. Uranium-radium series are mostly concentrated in marine sediments while the thorium is found mostly in terrestrial sediments; they exhibit a certain level of natural radioactivity. There are two types of these radioactivity logs, namely:

(i) The Gamma ray or formation density log that deals with densities.
(ii) The neutron or porosity logs.

2.5.4.2 Gamma ray Log

The gamma ray log is the result of measuring the total gamma ray intensity in the wellbore. The gamma radiation in the wellbore reflects the radio-active activity of the different formations which surround the well. This log can be used to identify different formations as well as to determine their depths and thickness (Bassiouni, 1994), also, they aid in distinguishing between potential hydrocarbon formations (sands, carbonate) and shales. All

rocks have some radioactivity. However, the radioactive material initially occurs in igneous rock and is later dispersed unequally throughout sedimentary formations during the erosion, transportation, and deposition processes. In sedimentary formations, most of the radioactive elements tend to concentrate in clay minerals, which in turn concentrate in shales (Bassiouni, 1994). In general, sandstones, limestones and dolomites have very little radioactive content. Black shale and marine shale display the highest level of radioactivity. Radioactivity is related to lithology but not directly or rigorously so. It can be used to distinguish shale and non-shale formation and also enables the estimation of the shale content of shaly formations. A high level of radioactivity is however not always associated with the presence of clay minerals, hence the use of natural radioactivity in lithology differentiation requires good knowledge of the local lithology (Bassiouni, 1994) e.g. a high gamma ray may not suggest shaliness but rather reflect the presence of radioactive sands such as potassium rich feldspar, glauconitic or micaceous sandstones. Clean formations usually have a very low amount of radioactivity due to low or non- concentration of radioactive elements, unless radioactive contaminants such as volcanic ash or granite wash are present or if the formation contains dissolved radioactive salts prevailing during the depositional period.

The simple gamma ray tool (Figure 2.13) is a very sensitive gamma ray detector and consists of a scintillation counter of sodium iodide crystals and a photo-multiplier tube. When the crystal is hit by gamma radiation, it emits ultra violet or blue-light photons. These photons strike anodes placed at successively higher potentials. The scintillation counter is the most suitable instrument for radiation detection. It is characterized by fast reaction and high detection efficiency (50% to 60%). These characteristics allow it to detect thin beds. The standard unit of measurement is API. The gamma ray log can be recorded in a cased well, which enables the formation of correlation curves in completion and workover operation. It is frequently used as a substitute or to complement SP log curves in wells drilled with salt mud, air, or oil-based muds. It is also useful for location of shaly and non-shaly formations and most importantly, for general correlation.

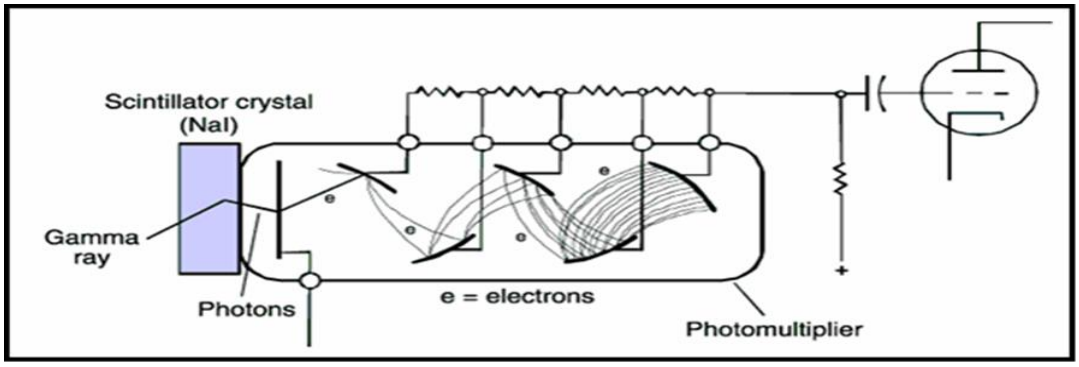

Figure 2. 13: Gamma ray tool (Serra, 1984).

2.5.4.3 Neutron Log

The neutron log is a porosity log that measures mainly the hydrogen ion concentration in a formation. Other porosity logs include; density logs and sonic logs, these tools' responses are all affected by the formation's porosity, fluids, and matrix and these characteristics can thus be determined. The tools' responses are related to porosity and are therefore referred to as a porosity log (Rider, 1996). Neutron logs are primarily used for delineating a porous formation and determination of their porosity. Hence, in clean formations whose pores are filled with water or oil, the neutron logs indicate the amount of liquid filling the pore spaces and hence the porosity. Qualitatively, in a gas zone, it is an excellent discriminator between gas and oil (Rider, 1996) when comparing the neutron log with another porosity log (such as a density log or a sonic log) or with core analysis. The combination of neutron log with one or more porosity logs reveals more accurate porosity values and identification of gross lithology, evaporates, hydrated minerals and volcanic rocks, and even an evaluation of shale content. It is therefore one of the best subsurface lithology indicators available (Rider, 1996).

In the neutron log, there is a radioactive source where formations are bombarded with radioactive elements (fast neutrons rather than gamma rays); this created inelastic scattering, elastic scattering and absorption phenomenon occurrences in the formation. These neutrons travelling through formations only slow down drastically when they collide with atoms of similar mass i.e. Hydrogen atoms. Once they have been slowed by recurrent collisions, they are absorbed (inelastic scattering) into the nuclei of heavier atoms present, and cause emission of gamma rays recorded by counter. The number of neutrons that strike the detector (neutron count) is affected by a number of factors in the borehole environment, such as hole size, mud weight and casing size (Bateman , 1985).

An example of neutron tools invented to compensate environmental effects is illustrated in (figure 2.14 A and B). The neutron tools commonly comprise of a fast neutron source and two detectors, near and far. Thus, by bombarding the formation with neutrons, the detectors measure the energy loss as they are passing through it. The tool's sources are mainly chemical, such as plutonium-beryllium (PuBe) or americium-beryllium (AmBe), and usually produce fast neutrons with high energy levels around 4Mev. The far detector is affected by both borehole and formation, while the near detector records signals from the borehole directly. The ratio of the counting rates from the two detectors gives only information about the formation, which is used to produce a record of the neutron porosity index. However, the rapid rates at which the neutron slows down, the nearer to the counter the gamma rays are produced, thereby resulting in a stronger signal. Since hydrogen is an important component of both water and oil, the neutron log measures liquid-filled porosity in clean formations, whose pores are filled with water or oil,.

Consequently, for any gas zone or pores that are filled with gas rather than oil or water, the neutron logs usually indicate low reading values. This is due to the lower concentration of hydrogen in gas as compared to oil or water. But, the neutron reading is usually high in pores containing oil and water. The lowering of neutron porosity by gas is known as the Gas effect. As the two tools, gamma-gamma and neutron react to permeability and fluid in a similar way to respectively SP (spontaneous potential) and resistivity, it can be used to replace the latter methods in cased holes. Clay minerals in the formation also affect the neutron tool. The bound lattice water presence in the clay minerals can enhance high porosity to be indicated by the neutron log, but the effective porosity in such rocks might be zero owing to the presence of fine clay particles in the pore spaces.

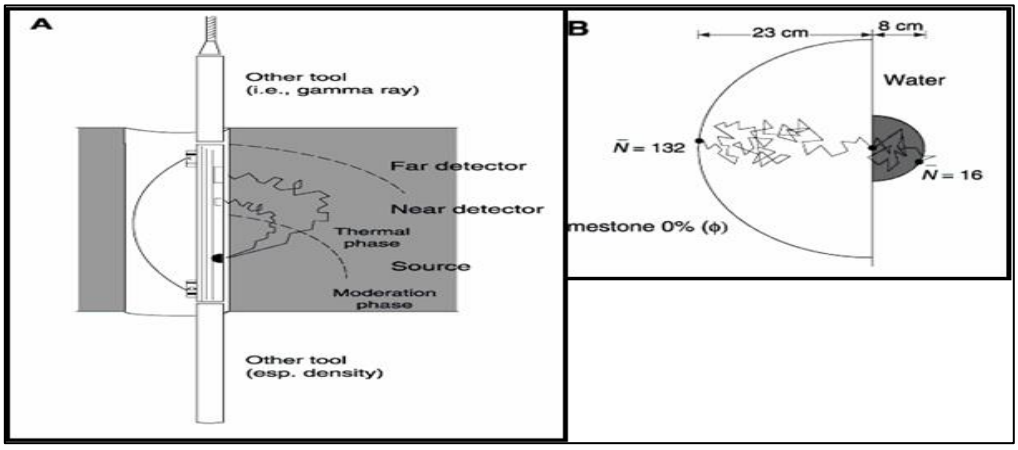

Figure 2. 14: (A) Schematic of Compensate neutron tool (B) Schematic trajectories of neutron in limestone with no porosity and pure water (Rider, 1996).

2.5.4.4 Density Log

The density log measures the bulk density of formations, which includes the overall density of the rocks such as solid matrix and the fluids confined in the pores. Bulk density is the function of matrix and porosity. The density log is quantitatively used to estimate porosity, indirectly hydrocarbon density (fluid types) and acoustic impedance of the formation. The density log is qualitatively used as a lithology indicator, which helps to infer certain minerals in the rock as well as to identify overpressure and fracture porosity. The logging techniques involve exposing the formation to gamma rays, which are backscattered and absorbed by the materials in the formation. However, the rate of absorption and the intensity of the backscattered rays depend on the number of electrons (electron density) that the formation holds, which are closely related to the common density of the material. Dense materials contain more electrons per unit volume (electrons/cm^3), with which the gamma particles can collide and loose energy. Therefore, absorbance of higher energy occurred and backscattering is lower in dense materials. In less dense formations that comprise of lower electron density, enhanced more substantial gamma particles get to the detector and more counts are recorded per unit time.

The detector counts later translated to bulk density as obtainable in the density log. An illustration of a density tool is provided in Figure (2.15). The tool consists of a gamma ray source and two detectors (near or short spacing and far or long spacing). The counting rate recorded by the detector enables the correction for the effects density and thickness of the mud cake. The geometry of the logging tool is designed to minimize the effects of the drilling mud. The source and the detectors are fitted in a plough-shaped skid and pressed against the wall of the borehole by a centring arm. However, the force applied by the arm, and the shape created by the skid, enable the tool to pass across the mud cake in order for the tool and the formation to have contact, also minimizing the contribution of the drilling mud in the recorded signal. The investigation depth is about 10cm (Rider, 1996).

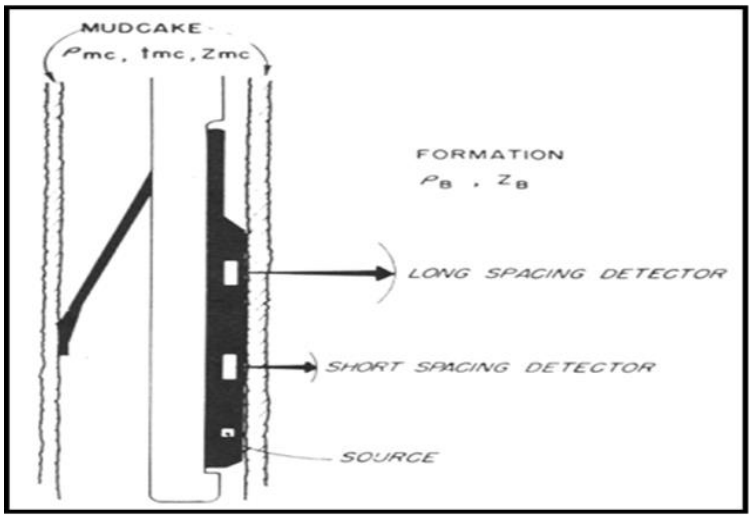

Figure 2. 15: Schematic of dual-spacing density logging device (SPWLA Library).

The differences in the bulk density confirmed changes in porosity, since water and hydrocarbon contain lower densities compared to solid (mineral or rock) materials. The accuracy estimation of porosity from the density log depends on the range of density values used for the matrix and the fluid in the equation on Figure (2.15). The consistent source of these values is from the laboratory analysis. However, an assumed value in log analysis can be used, mostly when the lithology formation is unknown or in an absence of cores. As core is available, a standard rock density of 2.65 g/cm^3 as used in Figure (2.15) is no longer valid. A study of the Jurassic Brent group in the North Sea indicates that, for sandstone of 20 % porosity, the error associated with each 1 % increase in the proportion of siderite controlled porosity, a measured porosity of around 0.8% provided is not valid in the matrix density values (Guest, 1990). In addition, using more accurate matrix density parameters with amount of organic matter and dense minerals present, resulted in at least 10 % increase in porosity values compared with assumed value of 2.65 g/cm^3 (Herron & Herron, 2000).

Conversely, the error in the porosity values acquired with incorrect choice of matrix density is roughly 50 times the error in the matrix value (Granberry, *et al.*, 1968). For instance, an error of 0.01 g/cm^3 in grain density will produce an error of 0.5 % in porosity. The consequences of these are that errors in matrix density parameters could have great effects in the evaluation of reservoirs. In an absence of cores to verify the calculated density log porosity, and if the low values of matrix density are used, the calculated porosity will be low, so that the reservoir potential could be extremely under-estimated. In addition, the fluid density values commonly accepted in density log analysis is that of water (1 g/cm^3) although,

the definite fluid density could be lower when the reservoir is saturated with gas or light hydrocarbons. Evaluation from the density log can therefore result in an extremely high porosity estimate.

2.5.4.5 Sonic Log

The sonic log is a device for seismic velocity determination, thereby measuring the velocity of transmitting sound waves in the formation. Quantitatively, it is a porosity detection tool that is used to extract porosity values of a formation. It also enhanced the seismic interpretation by given interval velocity and velocity profile which can be calibrated with the seismic section. When cross-plotted with the density, sonic log is used to deduce the acoustic impedance log which is the first step of creating a synthetic seismic trace. The sonic log can be also used in combination of other logs (e.g. density and neutron logs) for porosity, shaliness and lithology interpretation.

Qualitatively, the sonic log is used to identify lithology, compaction and overpressure to some extent fractures for correlation purposes, as well as an indication of source rock, because the presence of organic matter in the sediments lowered the sonic velocities. The sonic tool comprises of transducers and receivers. The transducers translate electrical signals into ultrasonic vibrations while the receivers change pressure waves into electromagnetic pulses, which can be amplified to create the logging signal, (Figure 2.16). It consists of numbers of both transducer and receiver, separated by defined distances. However, the averaging interval transit time recorded by each receiver decreases the unwanted borehole effects such as; the Sonde tilt effect and borehole size effect.

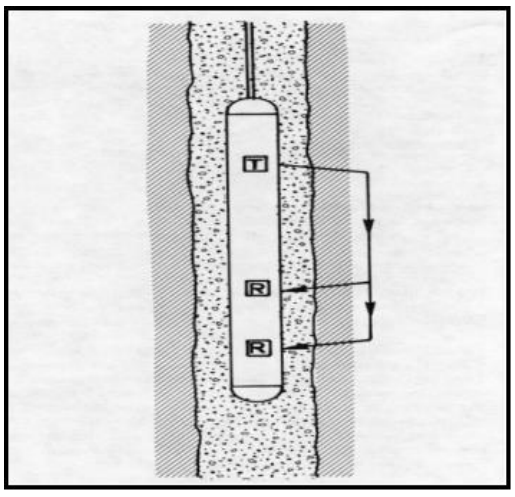

Figure 2. 16: Sonic Logging tool showing Receiver (R) and Transmitter (T) (http://www.spwla.org/library_info/glossary).Availble on 16th June, 2017.)

When a sonic log is running, various acoustic waves are affected by the measurements. The compressional wave is amplified and measured by this tool. The wave pulse travelled from the transducers to the formation is refracted at the borehole wall and travelled within the formation and before it gets back to the receivers as a fluid pressure wave (Schlumberger, 1989). Integrating transit time is also helpful in interpreting seismic records and the most common interval transit time of the arithmetic sensitivity scale ranges between 40μs and 140μs.

2.5.4.6 Spontaneous potential Log

The spontaneous potential (SP) log is a measurement of the natural potential difference (Pd) or self-potential between an electrode in the borehole and a reference electrode at the surface: no artificial currents are applied in the measurements. The currents were actually called "potential spontaneous" or spontaneous potentials by Conrad Schlumberger and H.G. Doll who discovered them. They originate from the electrical disequilibrium that is created by travelling through the vertical formations (in electrical sense) when in nature they are in fact isolated. The SP is primarily used to calculate formation water resistivity and to denote permeability. The SP log curves record the electrical potential (voltage) generated by the interaction of the formation's connate water, conductive drilling fluid and certain ion-selective rocks (shale). It can also be used to estimate shale volume, as well as indicating facies and occasionally for correlation (Figure. 2.17). However, the three factors that are necessary to trigger an SP current are:

(i) A conductive fluid in the borehole.
(ii) A porous and permeable bed surrounded by an impermeable formation.
(iii) A difference in salinity or pressure between the borehole fluid and the formation fluid.

These differences produce spontaneous currents when the fluids made contact through a porous medium or when in contact through shale which acts as semi-permeable membrane (Rider, 1996). Mud filtrate and formation water are however the major fluids considered in an oilfield well when running SP in a wellbore. The SP log was among the first logs launched for determined correlation in sand-shale sequences, primarily because certain intervals developed typical log shapes. Thus, the shapes in sand-shale sequences indicated shale abundance, with the full SP value appearing over clean (sand) intervals, and a diminished SP value occurring over shaly zones. The relationship is considered as linear and the shaliness is

correlated to grain size. The SP curve reading depends on the salinity contents in the fluid, if the formation water salinity is higher than the mud filtrate salinity, the deflection is to the left, for the reverse case, the deflection is to the right.

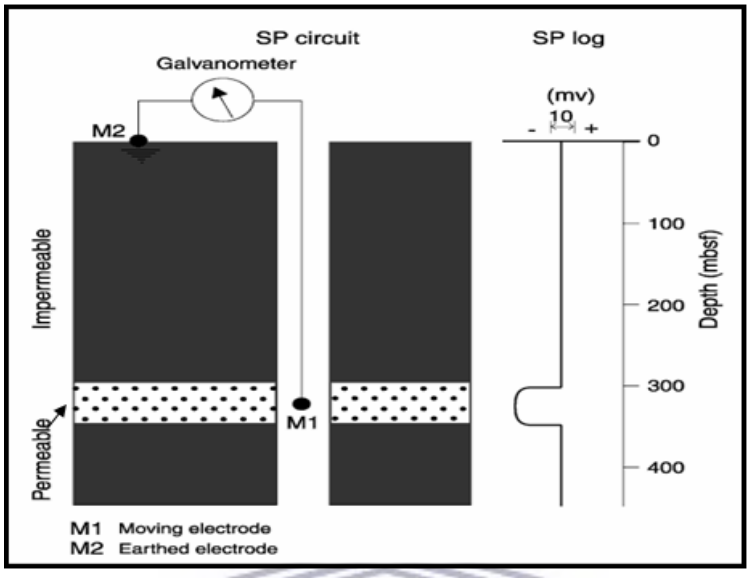

Figure 2. 17: Spontaneous Potential Logging tools (Rider, 1996).

2.5.4.7 Resistivity Log

The resistivity log is a measurement of a formation's resistivity, i.e. its resistance to the passage of an electric current. Conductivity logs measure a formation's conductivity or its capacity to conduct an electric current but this value is usually changed directly to resistivity. However, most of the rock materials are basically insulators, while their surrounded fluids are conductors (Rider, 1996). Hydrocarbons are exceptional contrary in terms of fluid conductivity in that they are extremely resistive. In a porous formation which contains salty water the overall resistivity is usually low, while the same formation, if containing hydrocarbons, usually has a very high resistivity. This is the characteristic that is utilized by resistivity logs in oil wellbores. A high resistivity value may indicate a porous, hydrocarbon bearing formation. In addition, the resistivity of a formation is a key parameter in determining hydrocarbon saturation. Thus, resistivity logs were developed to find hydrocarbons, which serves as the principal quantitative usage. To interpret the geological significance of resistivity logs, it is important to understand that the same porous bed can have a variety of resistivity responses, depending on the fluid content. Subsurface formations have finite, measurable resistivity due to the presence of water in their pores or absorbed in their interstitial clay. Thus, the resistivity of a formation depends on resistivity of the formation water, the amount of water present and the pore structure geometry.

2.6 The Description of Petrophysics and Petrophysical Parameters Characteristic

2.6.1 Introduction

Petrophysics is considered as the study of physical and chemical properties of porous media, particularly of reservoir rocks and their contained fluids. The objective of Petrophysics is to identify and quantify hydrocarbon resources in the subsurface by evaluating rock properties. The Petrophysical measurements of the rock properties are carried out in the borehole and on cores in the laboratory to determine the major reservoir properties such as porosity, permeability, capillarity and fluid saturations. The Petrophysical parameters obtained from the core are used in calibrating the borehole measurements. The borehole measurements are later used to calculate the volume of the hydrocarbon present in the reservoir. This Petrophysical parameter will be evaluated.

2.6.2 Porosity

The Porosity is an important rock property for measuring the potential storage volume for hydrocarbons. It reflects the fraction of the total rock volume that could be filled with oil, gas, water or mixtures of these fluids. Porosity in the carbonate reservoirs ranges from 1 to 35% and in sandstones from 1 to 45% (Schmoker, *et al.*, 1985). For a Petrophysicist, porosity is the first parameter to evaluate because it determines the amount of hydrocarbon that can be present in the reservoir. Porosity is determined from the grain volume and bulk volume of the sample. In Sedimentary rock, porosity developed based on the grain size distribution, grain shape, orientation and sorting. The degree of sorting and the grains' packing are dependent upon textural parameters, roundness and fabric of the grains. When the grains are equal in size, the sorting is regarded as good, while grains of various sizes mixed together are known as a poorly sorted. By definition, porosity is the pore volume per unit volume of a formation; it is the fraction of the total volume of a sample that is occupied by pores or voids spaces i.e. porosity is calculated as the ratio of the pore volume in a rock to the bulk volume of that rock, expressed in percentages, denoted as (Φ) and mathematically expressed as equation 1 in Figure 2.18). Due to the definition of porosity (Φ), porosity (Φ) of a rock sample can be determined by measuring any of these three following quantities: bulk volume, pore volume and grain volume. The sources of the porosity data can be obtained either by direct measurement from core analysis in the laboratory which requires measurement of bulk and pore volume of the core sample, or indirect measurement from well logging analysis and well testing.

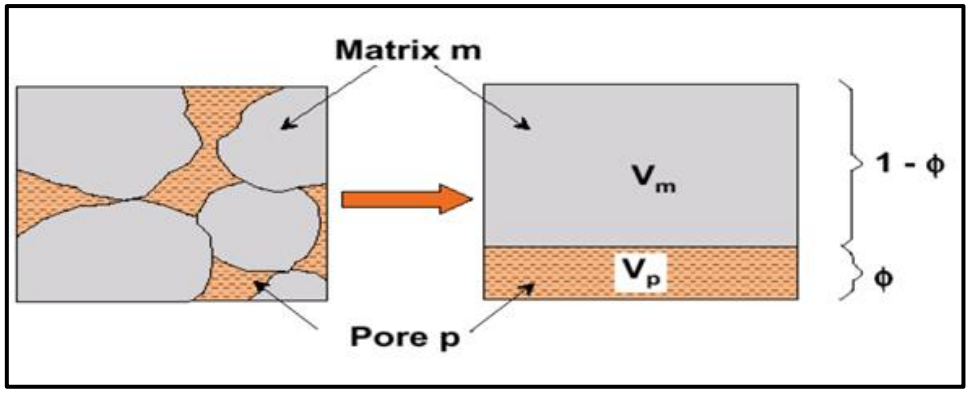

Figure 2. 18: illustrates the mathematical expression of porosity (Torres-Verdin.C., 2001).

$$(\Phi) = \frac{\text{Pores Volume} * 100}{\text{Bulk volume of sample}} = V_p/V_b * 100 \ldots\ldots\ldots\ldots\ldots\ldots \text{equation 1}$$

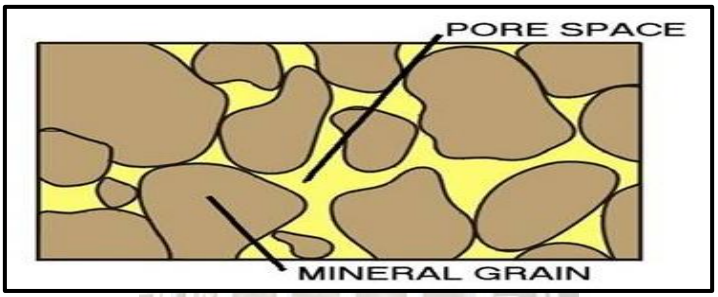

Figure 2. 19: Example of pore space and mineral grain space in sedimentary rock. (Adini, A. 2006).

There are several classifications of porosity which have been defined based either on the degree of connectivity or the period of pores development in sediment, these are called primary porosity and secondary porosity respectively. The primary porosity is the porosity that formed during the deposition of the sediment; i.e. intergranular or intercrystalline (Figure 2.19). Secondary porosity is developed by diagenetic process that occurred subsequently to the deposition of the sediment; i:e fracture and vugs. But the terms commonly used in engineering are Total porosity (Φ_T) and Effective porosity (Φe) (Figure 2.20). Total porosity (Φ_T) is the ratio of the total pore space of the media (rock) to the total bulk volume. The effective porosity (Φe) is the ratio of the interconnected pore space to the bulk volume of the rock. The effective porosity (Φe) or connected pore spaces are usually used to indicate the porosity (Φ) that mostly used to establish fluid flow.

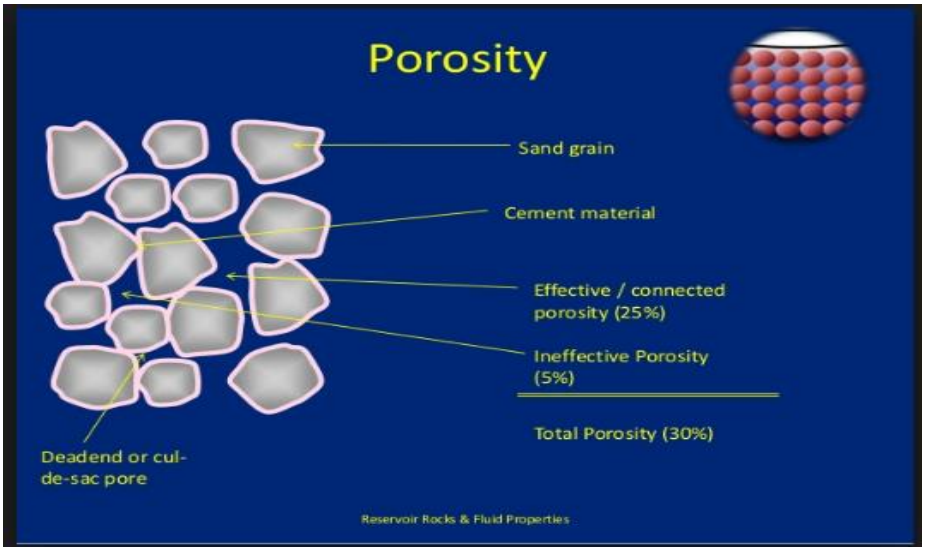

Figure 2. 20: An example of effective, non-effective or isolated, and total porosity of a rock. (http://www.slideshare.net/MTaherHamdani/porosity-38903458), (Dated; 05/3/17)

In very clean sand where shale or clay is absent, the total porosity (Φ_T) is equal to the effective porosity (Φe), effective porosity (Φe) signifies the pore space that confines hydrocarbon and non-clay water. The non-clay water is the free formation water that is neither bound to clay nor to shale. Thus, effective porosity (Φe) is total porosity (Φ_T) minus volume of clay-bound water. The relationship between total porosity (Φ_T) and effective porosity (Φe) can be represented for a shaly sand model as shown in Figure 2.21.

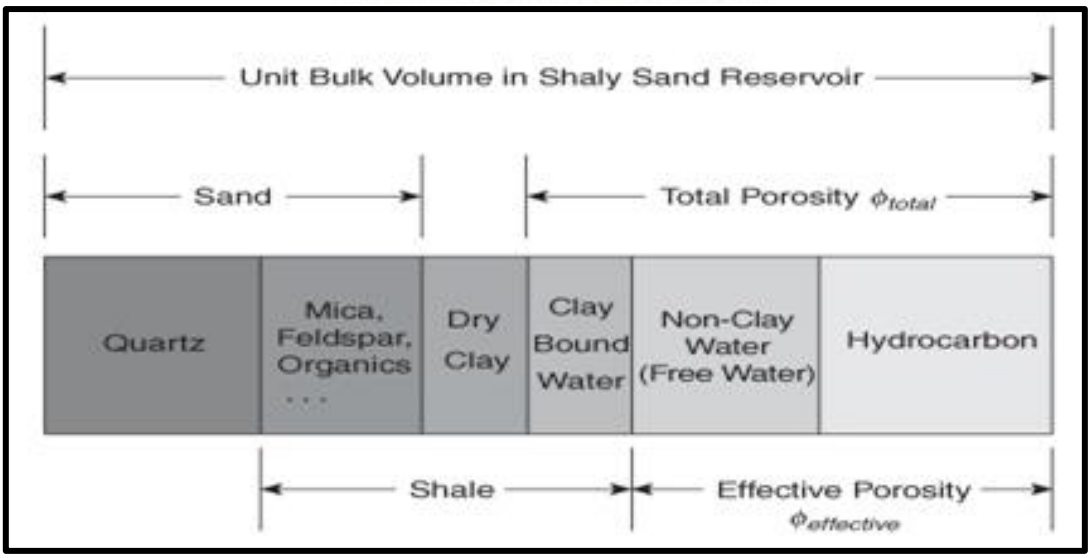

Figure 2. 21: Porosity model for a shaly sand reservoir (AI-Ruwaili & AI-Waheed, 2004).

2.6.2.1 Porosity Alterations

The primary porosity that is formed during the deposition of the sediments has undergone an alteration over some geological period by the following factors: Diagenesis, Cementation, Compaction, Leaching, Bioturbation and Clay coating.

- Diagenesis occurred as a result of lithified sediments which became hard sedimentary rock by mean of physical, chemical and biological processes after the sediments deposited. It's the physio-chemical precipitation of minerals from the pore fluids. The diagenesis effect influences the amount and distribution of porosity and permeability in sandstone thereby determining the reservoir capacity and fluid flow movement in the pore spaces of rock.
- Cementation is the most diagenetic effect due to its influence to bind grains together and consequently reduces the porosity. It's the major process of porosity loss in sandstone where Silica, calcite and clay can be precipitated as cement thereby filling the pore space and decreasing both permeability and porosity.
- Compaction of the sediments is as a result of mechanical loads overlying sediments, i:e the function of the mechanical strengths of the grains. It is a mechanical phenomenon which depends on the pore fluid type, rock type and overburden weight. Compaction of clay is intensely influenced by the clay mineralogy, pore fluid composition and burial history. The more compacted the sediments are, the lower the porosity will be due to dewatering and closer packing of the grains.
- Leaching: This occurs due to the dissolved minerals in the pore fluids. The dissolved minerals created cement which binds the pore spaces thereby reducing the porosity and permeability effect. It's a type of secondary porosity that occurred after the sediments have been deposited.
- Bioturbation alters the confines of the grains in the hosting sediments. They are burrowing bio-organisms in the sediment, which later became fossils. The trace fossils commonly have geochemical characteristics that differ from the surrounding sedimentary rock (Gingras, *et al.*, 2012). Therefore, trace fossils can influence the distribution of porosity and permeability in the sediments by physically changing the pore-throat distribution. They can also behave as lock of the cementation and dissolution processes during the early and late stages of diagenesis.

- Clay coating is the process where crystals grow on the surface of the grains as results of dissolutions over geological periods of time and can completely fill the pores (Schtjens , 1991).

In general any of these transformations can extensively impact porosity and permeability and therefore modify reservoir volume and flow rate.

2.6.3 Permeability

Permeability is the measured capacity of a porous medium to transmit fluids through its interconnected pore spaces. The fluid flow is proportional to the pressure gradient. Permeability is the function of grain-size and size of pore space connectivity, shape of grains and shape of pore space, type of the cement materials between the grains and the degree of interconnected pore space. It is very important because it is a rock property that tells the rate at which hydrocarbon can be recovered. The concept of permeability as proportionality constant controls the rate at which fluid flow is established by Henri Darcy in 1856. The following equation was Darcy's expression for single phase, linear, horizontal flow in a porous material.

$K = Q\mu/A\ (\Delta P/L)$……equation 2.

Where;

K = Permeability (Darcy's).

Q = Flow rate per unit time (cm/s).

μ = Viscosity of fluids flowing (cp).

A = Cross sectional area of rock (cm^2).

L = Length of the rock (cm).

ΔP = Pressure difference (psi).

Permeability is a rock property, while viscosity is a fluid property and ΔP/L is the measure of flow potential. The measurement units for permeability are Darcies, commonly expressed in millidarcies (md). A reservoir's productive capacity is mainly determined by its permeability, where highly productive reservoirs usually have permeability values in the Darcy range. Permeability is measured in the laboratory in horizontal (Kh) and vertical (Kv) position (Figure 2.22). However, measured horizontal (Kh) permeability is accepted in evaluating rock permeability due to it being measured parallel to the bedding which is the essential

mode of fluid flow into a reservoir (Figure 2.22). Horizontal permeability (Kh) varies in different directions and Vertical permeability (Kv) is generally less than Horizontal permeability (Kh) due to the layering effects of sedimentation (Hughes , 2002).

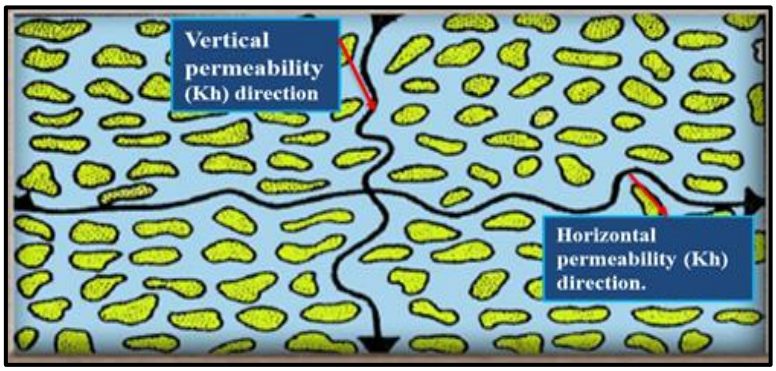

Figure 2. 22: illustrating the direction of measurement permeability (Hughes , 2002).

In Petroleum application, three types of permeability measurement are utilized they are absolute, effective and relative permeability. The permeability is absolute (K_a) if the pore space of the porous medium or the rock is completely saturated (100% saturated) with a single fluid. Absolute permeability is a fundamental property of a porous medium and its magnitude is independent of the types of fluid in the pore space. Effective permeability (K_e) is defined as when the pore spaces of the porous medium are occupied with more than one fluid. For instance, in a rock that contains oil, gas and connate water, the effective permeability of that porous medium to oil is the permeability to oil when other fluids including oil itself, occupy the pore spaces. Relative permeability is the ratio of an effective permeability (K_e) to absolute permeability (K_a) of a porous medium (equation 3).

$K_{re} = K_e/K_a$ .....equation 3

Where:

K_{re} = Relative permeability of the porous medium to the fluid e".

K_e = Effective permeability of the porous medium for fluid e"

K_a = Absolute permeability of the porous medium.

The effective (K_e) or relative (K_a) permeability is commonly utilized to describe the fluid flow in the reservoir rock. The bulk of permeability data is measured from the Core sample analysis in the laboratory, pressure test, drill stem test and Well log. The permeability data derived from the Core analysis in the laboratory are the most reliable in reservoir evaluation.

The horizontal permeability data that are measured on Core plugs taken from whole core sample, are between 1 to 10md (Very good is from 100 to 1000md and good is from 10 to 100md). Figure 2.23 shows the permeability ranges for various rock types.

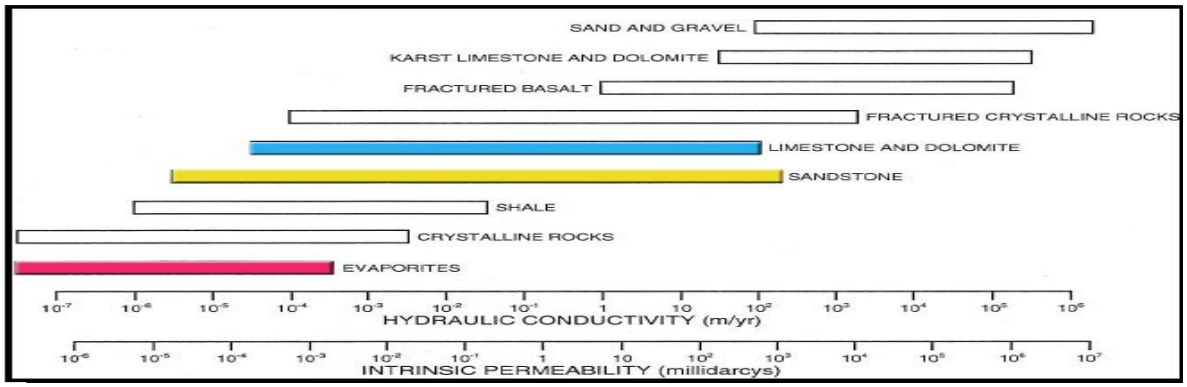

Figure 2. 23: illustrating the rock permeability ranges (Graven, 1986).

2.6.4 Fluid Saturations

The pores space of a reservoir that are occupied by fluid is expressed as the fraction of the volume of fluid in a given core sample to the pore volume of the sample i:e the fraction of the pore volume occupied by a particular fluid.

$$Fluid\ Saturation = \frac{Volume\ of\ occupied\ fluid\ spore\ pace}{Total\ pore\ Volume\ of\ core\ sample} \quad \text{.....equation 4a}$$

$$Sw = {}^{Vw}/_{Vp}\ ,\ So = {}^{Vo}/_{Vp}\ ,\ \text{and Sg} = {}^{Vg}/_{Vp} \quad \text{.....equations 4b}$$

Where:

Sw, So and *Sg* are water, oil and gas saturation fractions respectively.

Vw, Vo and *Vg* are the volume of the given fluids respectively.

Vp is the pore volumes of the rock sample.

In a petroleum reservoir, the fluids are typically water and hydrocarbon such as oil, or gas. Commonly the fluid saturation used to evaluate the petroleum reservoir is water and/or hydrocarbon. The relative volumes of water and hydrocarbons in the pore volume of the reservoir rocks are known as Saturation.

Water saturation (*Sw*) in the reservoir rock is the fraction of pore volume occupied by water; also **Hydrocarbon saturation (*Sh*)** in the reservoir rock is the fraction of pore volume

occupied by hydrocarbons. However, the sum of water and hydrocarbon saturation reservoir in a reservoir rock is equal to one; this relationship can be expressed as:

$Sh + Sw = 1$ ……equation 4c.

Where:

Sh = is hydrocarbon saturation, fraction; and *Sw* is water saturation, fraction. If the hydrocarbon in the reservoir occurs in oil and gas phases, the equation 4c can be re written as:

$So + Sg + Sw = 1$ ……equation 4d

These equations 4c and 4d are very important, as they are applied quantitatively to determine the accurate fluid saturations in the reservoir, mostly at the discovery event, to assess the potential hydrocarbon occupied in the reservoir after it has been penetrated with a well.

2.6.4.1 Determination of Water Saturation by Archie's Experiments

The determination of water saturation for reservoir fluids by Archie in 1942 was based on theory of the electrical resistivity log techniques applied in petroleum engineering called Archie's equation. This empirical equation was derived for clean water-wet sandstone over a moderate range of water saturation and porosities based on relationship between the conductivity of electrical properties and saturation of wet and oil bearing rock. The total saturation of fluids in a reservoir rock is 100%, and reservoir fluids often contain either oil and water, or gas and water or gas, oil and water. Oil and gas are non-conductors while water conducts current mostly when it contains dissolved salt such as NaCl, $MgCl_2$, KCl usually found in formation reservoir water by movement of ions known as electrolytic conduction. Archie noted that resistivity of an electric current in a porous rock is mainly due to the movement of dissolved ions in the brine that occupied the porous rock. He also observed that the resistivity varies with temperature due to the increased ion activity in solution as temperature increases. He thus presented the following main parameters and related them with electrical properties of the reservoir rocks. The most fundamental concepts considering electrical properties of the rock by Archie is the formation factor (F), as expressed below.

$F = {}^{Ro}/_{Rw}$ ……equation 5a

Where: F = is the formation factor, which indicates the relationship between the water saturated rock conductivity and bulk water conductivity. It depends on pore structure of the rock.

Ro = is the resistivity of the rock when saturated 100% with water (formation resistivity) (Ωm).

Rw = is the resistivity water formation (Ωm.)

Archie's experiments showed that the formation resistivity (*Ro*) and water resistivity (*Rw*) can be related by Formation resistivity factor *(F)* as expressed below (equation 5b)

Where: $Ro = F * Rw$ ……equation 5b

However, Archie also derived the second fundamental concept of electrical properties of porous rocks containing both water and hydrocarbon from the resistivity index (I_R).

The resistivity index *(I_R)*, which is defined as the ratio of resistivity of a reservoir rock partially saturated with water (*Rt*) to the resistivity of the rock if fully saturated with water (*Ro*). Therefore, resistivity index *(I_R)* is defined as follow by Archie:

$(I_R) = {}^{Rt}/_{Ro}$ ……..…equation 6a

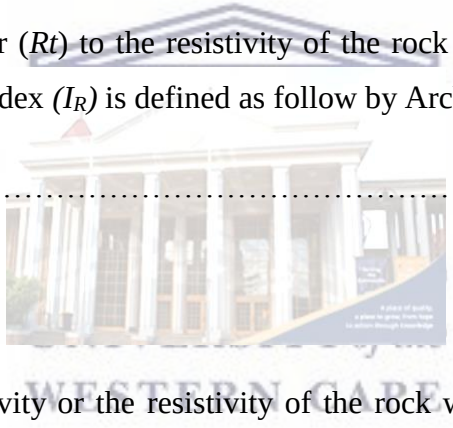

Where:

I_R = is the resistivity index

Rt = is the formation resistivity or the resistivity of the rock when partially saturated with water, (Ωm).

Ro = is the resistivity of the same rock when saturated with 100% water, (Ωm).

Wyllie developed another relationship between the formation factor (F) and other rock properties such as porosity (Φ) and tortuosity (α). Tortuosity is defined as the effective movement path of the fluid through the porous medium. The following relationships were derived by Wyllie.

$(F) = {}^{\alpha}/_{\Phi}$ ……6b.

Where;

F = Formation factor

α = Tortuosity of the rock.

Φ = Porosity.

Archie's experiment also reveals that the formation factor (F) can be related to porosity (Φ) and a slight difference between them can be corrected by introducing cementation exponent (m) as expressed below:

$F = \Phi^{-m}$ ……equation 6c, rewritten in equation 6d

$F = \frac{1}{\Phi^{m}}$ ……equation 6d

Where:

F is the formation factor.

Φ is the porosity.

"m" is the cementation exponent, which ranged from 1.8 to 2.0 for consolidated sandstone and 1.3 for clean unconsolidated sands. This value varies with the grain size, grain size distribution and the complexity of the paths between the pore (tortuosity, α), sorting and packing arrangement of a particular system, compaction as a result of overburden pressure, and type of pore arrangement (Helander, 1984). Fresh water indicates low formation factor and cementation values. The higher the value of "α" the higher the cementation value**"*m*"**. Table 2.2 presents various cementation factors observed for difference rock types (Pirson, 1958).

Archie's finally derived an equation to evaluate reservoir water saturation (S_w) from relationship of resistivity index with water saturation (S_w) of the rock, thereby introducing the saturation exponents (n) which know as Archie's famous equation of water saturation (S_w).

$(I_R) = {Rt}/{Ro}$ ……From equation 6a

Resistivity index can be related to water saturation as:

$I_R = S_w^{-n}$ …….. equation 7a

Where:

S_w = is the water saturation, fraction;

n = is the Saturation exponent.

By combining the equations 6a and 7a:

$S_w^{-n} = {Rt}/{Ro}$ ……equation 7b

The formation factor, which is the formation resistivity factor for clean rock that is fully saturated with water is derived from equation 5a : $F = {Ro}/{Rw}$,

From equation 5b, $Ro = F * Rw$

By combining equations 7b and 5a we get:

$S_w^{-n} = {Rt}/{FRw}$ ..... equation 8

From equation 6d, $F = \Phi^{-m}$, (Winsauer , *et al.*, 1952) (Bassiouni, 1994).

Modified equation 5b later after Archie's by inserting the tortuosity (α) reads;

$F = \alpha\Phi^{-m}$ .....equation 9

Substituting equation 9 into equation 8 gives:

$S_w^{-n} = {Rt}/{\alpha\Phi^{-m} Rw}$ .....equation 10

Equation 10 can be rearranged to give:

$S_w = \left(\frac{\alpha}{\Phi^m}\frac{Rw}{Rt}\right)^{1/n}$.....equation 11

Equation 11 is the Archie's equation for calculating water saturation (S_w) in the reservoir rock.

Where:

S_w = is the water saturation expressed in percent, α = is the tortuosity factors, Φ = is the porosity, *m* = is the cementation exponent, *Rw* = is the resistivity of the water formation.

Rt = is the formation resistivity or the resistivity of the rock when partially saturated with water, and "n = is the Saturation exponent.

Archie's equation relates the porosity (Φ) and resistivity with the quantity of water saturation (S_w) present in the formation. An increase in porosity will reduce the amount of water saturation for the similar formation resistivity (*Rt*). When the water saturation (S_w) is known, hydrocarbon saturation can be calculated as: $S_{HC} = 1 - S_w$.

Where:

S_{HC} = is the Hydrocarbon saturation,

$S_{w.}$ = is the Water saturation.

Archie's equations are generally accepted to calculate the water saturation in clean sand formation and carbonate reservoir only. Due to the complex behaviours of shaly sand formation as result of clay minerals present added more parallel conductive path together with formation salinity. Thus, others model used to evaluated water saturation in shaly sand formation are Waxman-Smits model, Simandoux equation, Poupon-Leveaux equation and Dual-water model.

Table 2. 2: indicating various cementation factors observed for difference rock types by (Pirson, 1958).

Lithology	**Cementation Factor (m)**
Sandstones	
Loose un-cemented sand	1.3
Slightly cemented sands	1.3 – 1.7
Moderately cemented sands	1.7 – 1.9
Well cemented sands	1.9 – 2.2
Limestones	
Moderately porous limestones	2
Oolitic limestone	2.8

2.6.5 Capillary Pressure.

Capillary pressures are generated where interfaces between two immiscible fluids occur in the pores (capillaries) of the reservoir rock; it's a major factor which controls the fluids distributions in a reservoir. The amount of pressure difference between the two fluids is basically coordinated by pore geometry, rock wettability and the interaction of interfacial tensions between rocks and fluids. It is usually considered as having two phases such as a wetting phase and a non-wetting phase. For petroleum reservoir engineering, capillary pressures are important for three main reasons as follows, for the prediction of reservoir initial fluid saturation, to know the cap-rock seal capacity (displacement pressure) and as additional data for assessment of relative permeability data. This characteristic of a rock can be measured from the core samples examined in a laboratory setting and related to the other

measurements taking in the field. This allowed reservoir engineers to find the degree of hydrocarbon accumulation and avoid drilling into water. The capillary pressure concept is also an important parameter in volumetric studies which used to calculate field wide saturation-height correlation from core and log information. It is used to understand the free water level (FWL) from an oil transitional zone of the saturation-height relationship, when correct pressure gradient data for both oil and water legs are not available. The saturation-height function is able to calculate the saturation of the reservoir for a particular height above the free water level and reservoir permeability and porosity or to estimate permeability in an uncored region once the water saturation is known (Harrison & Jing, 2001).

The difference in pressure *Pc* is known as capillary pressure, also the pressure in the non-wetting phase minus the pressure in the wetting phase, (equation 12) as follows:

$P_c = P_{non\text{-}wetting} - P_{wetting}$ .....equation 12.

Thus, the capillary pressure may be either a positive or negative value, for oil – water, gas – water or gas – oil system. Capillary pressure is defined by the following equations:

$P_c = P_{Oil} - P_{Water}$ .....equation 13.

$P_c = P_{Gas} - P_{Water}$.....equation 14.

$P_c = P_{Gas} - P_{Oil}$ .....equation 15.

The wettability is defined as the ability of one fluid to spread on solid surface in the presence of another immiscible fluid. In terms of reservoir fluid, wettability is the ability of one fluid in the presence of another fluid to spread on the surface of the rock, i.e. it is the measure in which fluid adheres to the rock. It is usually figured out by the value of the contact angle that a liquid-liquid interface makes with a solid. Based on the wetting index, if the value is less than 90 degrees indicates a water-wet system, and a value higher than 90 degrees indicates an oil-wet system as illustrated on table 2.3 (Torsater & Hendraningrant, 2013) and (Mirzaee, 2015). (Figure 2.24). The fluid-fluid interaction is held together by intermolecular van der Waal forces which are known as interfacial tension. Gravity plays a major role in both wettability and interfacial tension states.

In reservoir rock, most of the reservoir rocks are water-wet, water is positioned at the pore walls while the oil is in the middle of the pore. Due to the behaviour of respectively water and oil at the pore wall of the reservoir rock, it is very important to note that reservoir rocks

vary hardly in strongly water-wet or strongly oil-wet reservoir rocks and that the wettability varies within a rock. A porous medium can be mixed-wet or fractionally-wet in nature. Mixed-wet can be of mixed-wet large and mixed-wet small wherever respectively the large pores and small pores are oil-wet. A rock with fractionally wet nature has no connection between pore size and wettability, however with small or large pores it can be oil wet.

Table 2.3: Wettability (wetting index WI) by contact angle (Torsater & Hendraningrant, 2013).

Wetting index (cos ɵ)	Contact angle ɵ	Wetting condition
1.0	0^0	Completely water wetted
0	90^0	Neutral system
-1.0	180^0	Completely oil wetted.

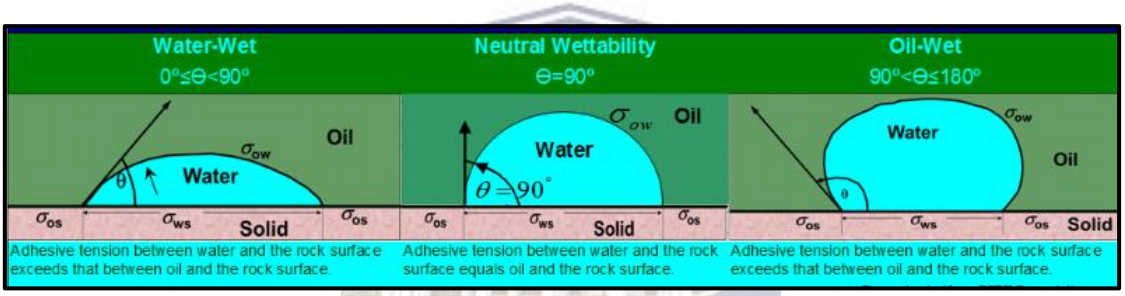

Figure 2. 24: illustrates the relationship between wettability and contact angle (wetting angle) of water and oil. (Mirzaee, N., 2015).

2.6.5.1 Capillary Pressure curves

The capillary pressure curve of a porous medium is a function of pore size, pore size distribution, pore geometry, fluid saturation, fluid saturation history, wettability and the interfacial tension. The wettability of a reservoir rock fluid can be described based on contact angle. A value of the contact angle less than 90 degrees indicates a water-wet system, and a value higher than 90 degrees indicates an oil-wet system (Figure 2.24). In capillary pressure measurement, a non-wetting fluid occupies the pore system that was initially occupied by a wetting fluid and later displaced by the former. The capillary pressure of non-wetting fluid which occupied the pores is described by the Young - Laplace's equation (Dullien, 1979). The Young-Laplace's equation shows how capillary pressure correlates to the rock and the fluids within for an immiscible fluid set in a circular cross-section at lab condition.

$Pc = {}^{2\gamma}/_{r\ \text{pore}} = {}^{2\gamma Cos\theta}/_{r\ pore}$ ……equation 16

Where:

Pc is the Capillary pressure (psi),

γ is the Interfacial tension,

r = is the average radius of the pore

θ = is the contact angle.

The Laplace equation (16), describe the connection between the radius of the pore and the capillary pressure needed by fluid to infiltrate the pores. The laboratory values of the capillary pressure could be converted to equivalent reservoir condition values as follows:

Pc $_{(reservoir)}$ = Pc $_{(Lab)}$ (γCos θ) reservoir / γ Cos θ) lab……equation 17.

The laboratory reservoir conversion method only measures the difference in capillary pressure due to interfacial tension and contact angle. The interfacial tension can be measured at laboratory and reservoir conditions, however, the contact angle is complex to measure mostly in the system that is a devoid strongly wet, i.e. most oil reservoir. The typical values for interfacial tension and contact angle measured from the Core laboratory manual are given in table 2.4 (Harrison & Jing, 2001).

Table 2. 4: Interfacial tension & Contact angle values Core Laboratories, 1982), (Harrison & Jing, 2001).

Wetting Phase	Non-Wetting Phase	Condition: Temperature (T), Pressure (P)	Contact Angle (θ)	Interfacial Tension (dynes/cm)
Brine	Oil	Reservoir, T, P	30	30
Brine	Oil	Laboratory, T,P	30	48
Brine	Gas	Laboratory, T,P	0	72
Brine	Gas	Reservoir, T, P	0	50
Oil	Gas	Reservoir, T, P	0	4
Gas	Mercury	Laboratory, T,P	140	480

2.7 Biostratigraphy

Biostratigraphy by definition is the element of stratigraphy which deals with the distribution of fossils based on stratigraphic record and the organization of strata into units according to the fossils found in them (Ogg, *et al.*, 2014). It relies on the study of in-situ fossil distribution that allows recognition of stratigraphically restricted and geographically widespread taxa or populations which allows subdivision and correlation of lithostratigraphic successions. Such taxa may be selected as index fossils which can be used as a basis for biostratigraphic correlation. However, biostratigraphy is also a branch of sedimentary geology that banks on the physical zonation of biota, both in time and space, in order to recognise the relative stratigraphic position in terms of older, younger and same-age sedimentary rocks between different geographic locations.

Apart from assigning the age based on fossil record this branch of geology helps to understand and interpret the environment of deposition and depending upon the presence of faunal groups helps to demarcate the unconformity surfaces, the duration of hiatus , the depth of deposition (benthic fossils) , identification of maximum flooding surfaces and condensed sections. In oil exploration and particularly in basin analysis application of biostratigraphy spread very rapidly for the last 70 years period throughout the world.

In South African sedimentary basins not much work has been done so far related to biostratigraphic work particularly using important microfossil groups like foraminifera, radiolaria or diatoms for sequence stratigraphic work. Whatever little published references are available are mostly from the sediments of Aptian or younger groups of sediments by a few workers. Very little account is available for biostratigraphic studies from Late Jurassic to earliest Cretaceous marine succession in this area. Notable work on biostratigraphic studies for South African sedimentary basins are by McMillan (1986, 1990, 1992 and 2003), McMillan (2003) first time published a broad integrated account and correlation of different basins across the South African coast. However, all of the sections studied in this work belongs to rocks Barremian and younger group of sediments. The generic identification of most of the foraminifera microfossils were carried out using standard text books (Leoblich and Tappan, 1988) and the species level identification using several publications from DSDP/ODP reports. Detail account of all these references including identification, interpretation is given in chapter six of this thesis.

CHAPTER THREE

3. The Geological setting of Gamtoos Basin

3.1 Introduction.

The recent exploration for hydrocarbons in South Africa is one of the key factors for economic growth, and is playing a major role in the upstream sector. It plays a significant role in the evolution of the South African oil industry to satisfy the country's thirst for oil. South Africa is one of the larger countries in Africa both in land mass and coastline area. Its land area is more than 1.1 million km^2 while the coastline of South Africa is about 3000 km in length. This includes the western coast which is about 900 km long and stretches from the Orange River to Cape Point. From Cape Point the coast stretches a further 2000km along the southern edge of the continent. There is also exploration activity along the eastern coast through Durban and the Zululand Basin up to the Mozambique border (Petroleum Agency of South Africa, 2004/2005). Besides the coastline of South Africa, is the continental margin that forms the South African offshore environment which is characterized by deep basins filled with thick sedimentary sequences. The continental shelf along the west coast is about 20 – 160 km wide off the coast, while along the south coast it ranges from 50 – 200 km off the southern coast and is about 30 km wide off the eastern coast. The continental slope which connects the continental shelf to the deep marine environment has a similar style in breadth and is extensive along the west and south coasts but tends to be narrower along the eastern coast (Figure 3.1). The Agulhas current and Benguela current are two major ocean currents that flow along the coastline of South Africa. The Agulhas current is a warm current flowing south-westerly along the east and south coasts up to Cape Point. It is at its maximum strength along the shelf break and covers the continental slope. The Benguela current on the other hand is cold, flows northwards from the Antarctic along the west coast of Africa to Angola (Figure 3.2).

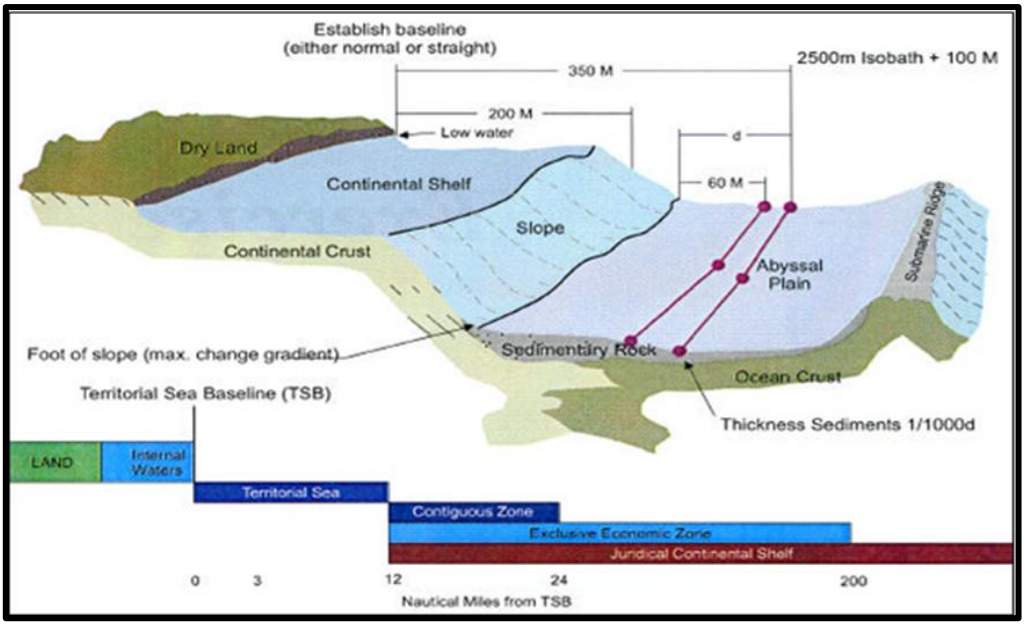

Figure 3. 1: South Africa continental margin and oceanic crust (Broad , 2004)

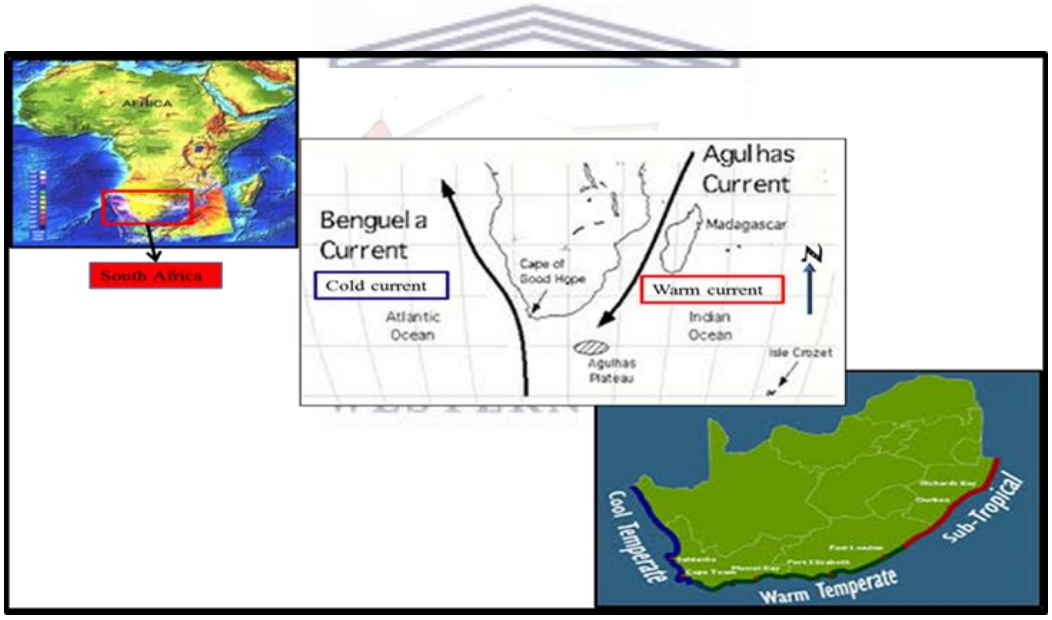

Figure 3. 2: The two major Ocean currents controlled South Africa Coastline. (Modified from http://www.oceanwanderers.com/SouthAfrica.html). Available 6th May 2015.

The Gamtoos Basin which is the focus area of this study, has numerous economic to marginal economic discoveries of gas-to-oil prone source rocks that are found in the synrift, the early drift, the canyon fill and the good oil show source rocks found in the Port Elizabeth troughs, in late Jurassic to early Cretaceous deposits. The borehole intersected an average of 60 m of marginally matured Portlandian, anoxic marine shales which have been recorded to occupy about 8.1 kg/metric ton of rock (Malan, 1993) as well as good sand reservoirs of Valanginian

(Early Cretaceous) age. South Africa's prospects for natural gas production improved recently with the discovery of offshore reserves. The continuous exploration in the Gamtoos Basin is to assess the extent of the available reserves and their economic potentials. However, South Africa's offshore region has not yet been subjected to deep-water exploration. A recent discovery of oil in 1990s shows that giant oil discoveries are more frequently found in the deep-water area of the oceans in the world than the shallower-water regions. It also indicated that turbidite sandstones account for 87% of the deep-water discoveries of oil-prone source rocks.

In addition, based on structural elements, the South African offshore basins were divided into three separate tectonostratigraphic zones, such as the Western offshore, the Eastern offshore and the Southern offshore region respectively (Petroleum Agency of South Africa, 2004/2005). **The Western offshore region**, where the Orange Basin is located consists of a broad passive margin basin that developed after the opening of the South Atlantic during the Early Cretaceous. Conversely, **the Eastern offshore region** that comprises the sedimentary section of Zululand and Durban Basins is a narrow passive margin known as "Africa rift" which formed due to the breaking up of Africa, Madagascar and Antarctica during the Jurassic, consequently limiting the sedimentary deposition of the region. T**he Southern offshore region** known as the Outeniqua Basin comprises of five en-echelon sub-basins namely the Bredasdorp Basin, Pletmos Basin, Gamtoos Basin, Algoa Basin and the Southern Outeniqua Basin. This last basin demonstrated a strong strike slip movement during the breakup and separation of Gondwana in the late Jurassic to Early Cretaceous period (Petroleum Agency of South Africa, 2004/2005). The en-echelon sub-basins of the Outeniqua Basin comprise a complex of rift half-grabens that are overlain by drift sediments of different thicknesses. Rift half grabens formed when normal fault acting on the sedimentary basin dips in a similar direction, thus creating adjacent blocks slipping relatively down and tilting, forming a set of tilted blocks separated by normal faults. Often the sedimentary layers bend along the fault plane (Figure 3.3). However, the deepwater extensions of these en-echelon basins except Algoa Basin are fused in the southern part of the Outeniqua Basin (Figure: 3.4).

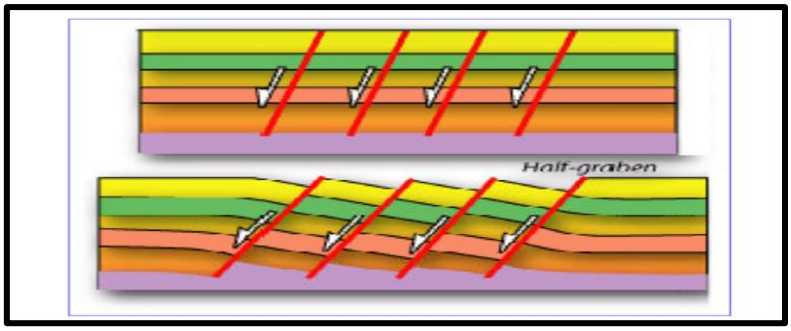

Figure 3. 3: Formation of Half graben from a sequence of normal faults dipping in the similar direction (Hudson, 1998).

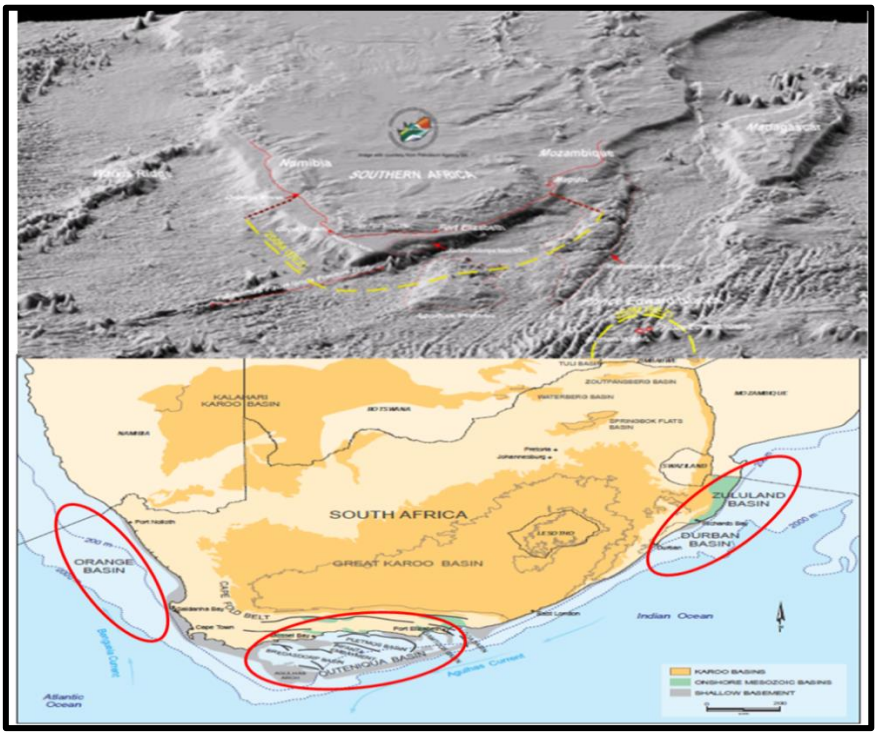

Figure 3. 4: Topography of satellite image of the sea floor and continental margin surrounding South Africa and Structure elements and sedimentary Basin of South Africa (modified from (Petroleum Agency of South Africa, 2004/2005).

3.2 Tectonic settings of Outeniqua Basin

Gondwanaland formed between 800 and 530 Ma years during a sequence of collision events of earlier supercontinent fragments (Meert & Van der Voo, 1996) such as East Africa, Brasiliano and Kuga Orogeny (Figure 3.5). The tectonic settings of the Outeniqua Basin can be traced back to the stretching and break-up of the Gondwanaland lithosphere in the Late Jurassic to Early Cretaceous between ~180 and 130 Ma, when South America rifted away from Africa along the Agulhas-Falkland Fracture Zone (AFFZ), (Ben-Avraham, et al., 1993; McMillan, et al., 1997); (Thomson, 1999; Broad, et al., 2006), and formed the continents of

Africa, South America, Antarctica, Australia and the smaller fragments like the Falklands (Figure 3.6). However, for Southern Africa, three plate-tectonic episodes are of great significance, the Cape Fold Belt formation of the supercontinent orogeny, the intracontinental extension which resulted in the formation of present day offshore basins and the continental break-up responsible for the formation of present-day continentals margins. The post Gondwana period marked the appearance of intra-continental stretching and breaking-up at about ~ 167 Ma with rifting in the Mozambique and Somali Basins (Koning & Jokat, 2006), Most of the common development is plume related break-up (Dalziel, *et al.*, 2000). The intracontinental extension which results in the formation of present day offshore basins started with the rifting process at the early break up of Gondwana and formed the Outeniqua Basin offshore in Southern Africa (McMillan, *et al.*, 1997) (Figure 3.4). The Outeniqua Basin is found between the southern African coast and the Agulhas-Falkland Fracture Zone (AFFZ) (Figure 3.7). It consists of six shallow and deep en-echelon basins, including Bredasdorp, Infanta, Pletmos, Gamtoos, Algoa Basin and the deep Southern Outeniqua Basin, which is more than two km deep and has strong ocean currents thereby creating difficult conditions for hydrocarbon exploration.

The Southern Outeniqua Basin, covers an area of about 22000 km^2, formed the larger part of the Outeniqua Basin along the coast of South Africa as a result of rift tectonics during the break up of Gondwana. These conditions dictated the seafloor depths as well as land elevation of Southern Africa, and defined the limits of the continental margin within which the Outeniqua Basin falls. However, no well has been drilled until recent 2D seismic data acquired by Canadian Natural Resources (formerly Ranger Oil) in 2001 and 2005 confirmed the presence of major structures in the deep water front which are associated with synrift structure within the oil window believing to contain gas (Petroleum Agency SA Brochure, 2008). Also, confirmed from the latest seismic data was the gigantic basin floor fan complex called “Paddavissie” which potentially contains billons of barrels of oil. This basin has been highly regarded for oil in the central and southern extent of the basin as well as more gas-prone along the northern margin with thick overburden. A regional study also recommends drilling the occurrence of source rocks in shallow marine and turbidite sandstones with large structural and stratigraphic traps.

As discussed above, these sub-basins are formed as a result of dextral shearing of the South African margin in the Early to Mid-Cretaceous. The rift stage of the South coast terminated in

the Late Valanginian connecting with a drift-onset unconformity (1At1) (Petroleum Agency of South Africa, 2004/2005). The drift-onset unconformity is of the same age as the initial oceanic crust in the South Atlantic. A complex sequence of micro-plates such as the Falkland Plateau steadily moved west south-westwards past the southern coast of Africa (Figure 3.8a, b). These movements formed some oblique rift half graben sub-basins, including the Bredasdorp and Pletmos basins, which were interpreted as failed rifts, and which are the youngest in the west and the oldest in the east respectively (Figure. 3.9).

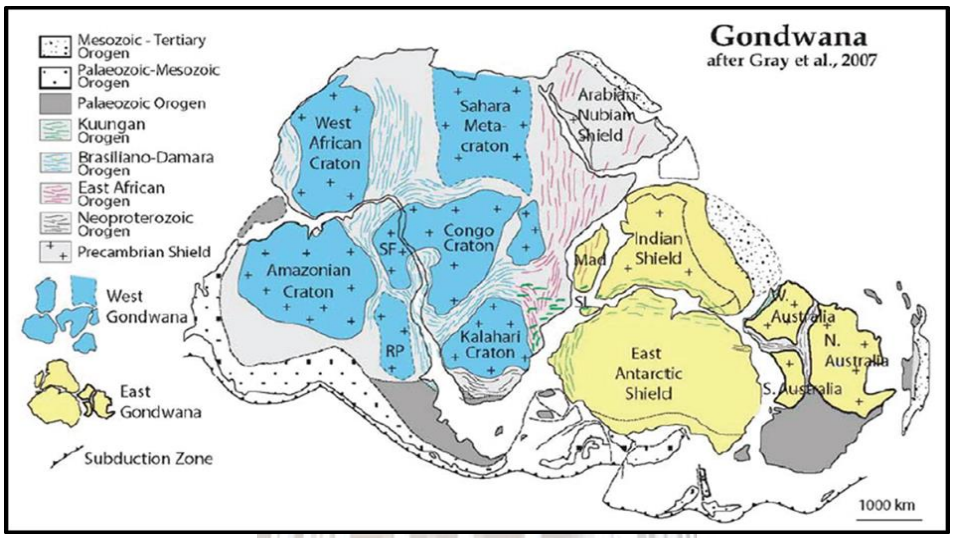

Figure 3. 5: Map of Gondwana after its amalgamation (~530 Ma) indicating its cratonic cores and the orogeny during which super continental fragments were combined (Gray, et al., 2008). The Kalahari craton consists of the Kaapvaal craton, the Zimbabwe craton, and the Limpopo belt.

Figure 3. 6: The rift stage in the Late Jurassic-Lower Valanginian indicating the break-up of Africa, Madagascar and Antarctica (Broad , 2004).

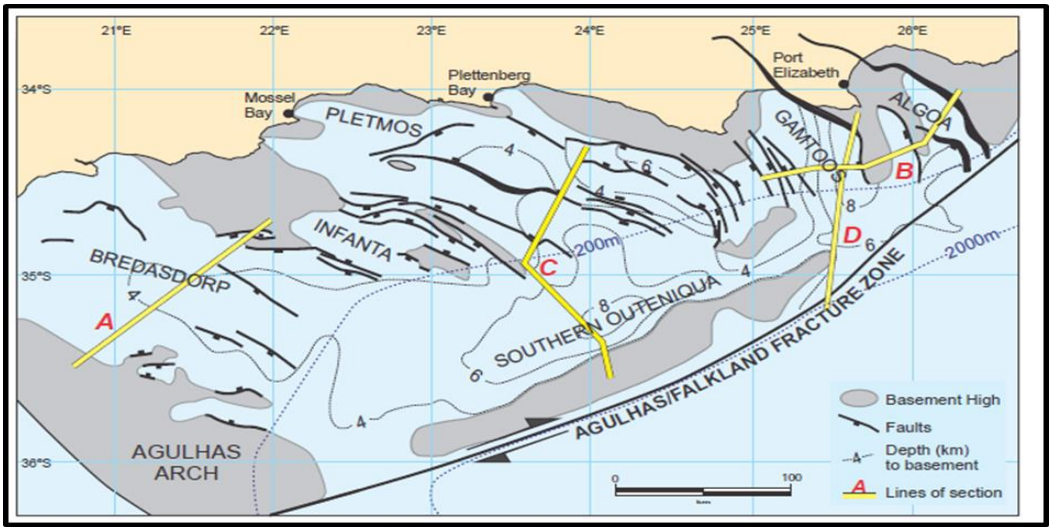

Figure 3. 7: Map of the southern African offshore basins (Broad, et al., 2006). The Bredasdorp, Infanta, Pletmos, Gamtoos, Algoa and Southern Outeniqua Basins collectively are called the Outeniqua Basin.

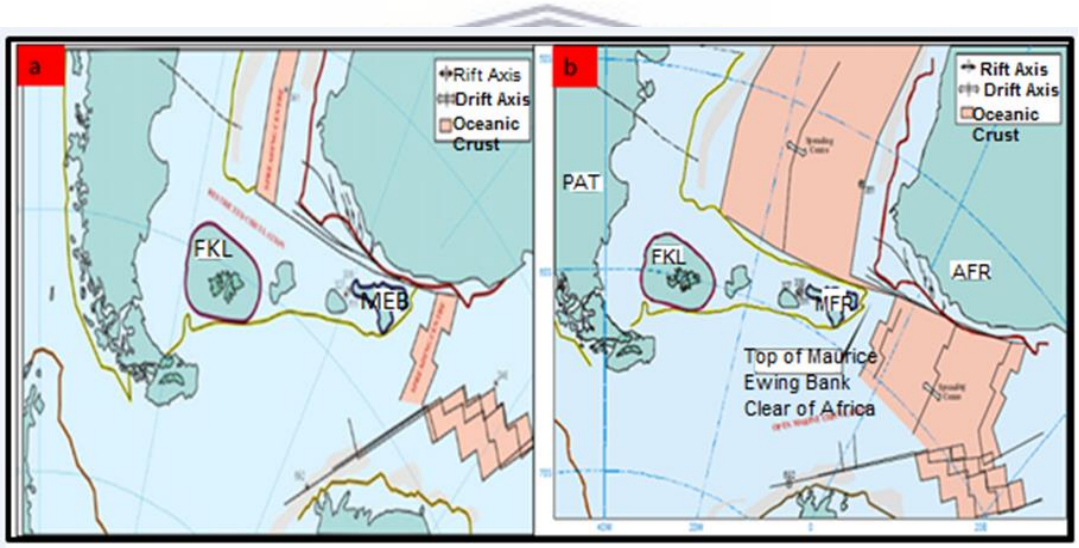

Figure 3. 8: (a) Early drift stage in the Valanginian (1At1) till Hauterivian (6At1) showing the movement of micro plates: Falkland Plateau (FLK) Patagonia (PAT) and Maurice-Ewing Bank plates (MEB) past south coast of Africa (Broad, 2004). (b) Late drift stage in the Hauterivian (6At1) onwards (Broad, 2004).

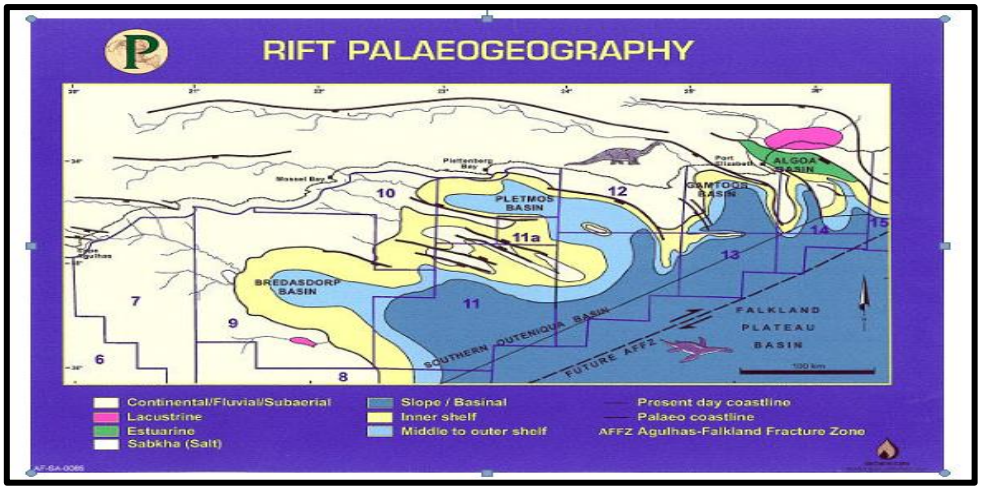

Figure 3. 9: Oblique rift half-graben sub-basins of Outeniqua Basin: Bredasdorp, Pletmos, Gamtoos and Algoa basins (Broad , 2004).

3.3 The Evolution of the Gamtoos Basin

The development of the Gamtoos Basin occurred during the late Jurassic and earliest Cretaceous, but has been initiated in the middle Jurassic (Malan , *et al.*, 1990). The oldest sediments encountered during the drilling, dated to be Kimmeridgian, but significant thickness close the depocentres remains unexplored in the basin where the depocentres contain approximately 7000 m of undrilled Mesozoic section, in which the sediment horizon D exceeds 5.5s two-way-time (TWT) implying approximately 12 km thickness of the undrilled rift sediments may be middle to late Jurassic age (Figure 3.10),(Malan , *et al.*, 1990).

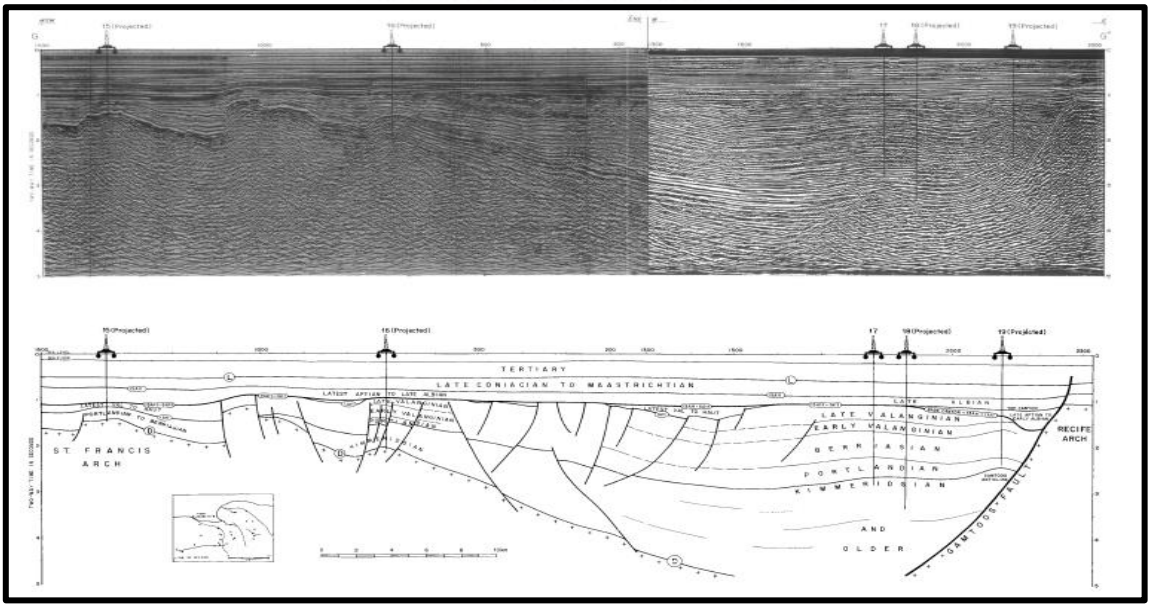

Figure 3. 10: Seismic profile and Geological interpretation across the southern Gamtoos Basin, illustrating the basin characteristics. Profile G-G' (Modified from (Malan , et al., 1990).

3.4 Geology and Tectonic history of Gamtoos Basin

The Gamtoos Basin, within the en-echelon sub-basins in the Outeniqua Basin Offshore South Africa, is a late Mesozoic basin which lies at the southernmost tip of the African plate (Malan, 1993). The Outeniqua Basin, which extends from the Agulhas arch in the southwest to the Port Alfred arch in the northeast, comprises a complex of en-echelon half-grabens. These half-grabens were developed during the early stages of rifting before the separation of east and west Gondwana. In addition, the Gamtoos Basin is comprised of the mostly easterly half graben in the Outeniqua Basin which is defined by the St. Francis, Recife, and the Port Alfred arches and is composed of Paleozoic Cape Super Group rocks. The Gamtoos Basin is basically a simple half-graben feature (Figure 3.11), controlled by the Gamtoos fault extending deep into the crust as well displaying a complex history. The onshore parts of the Gamtoos fault have a throw of about 3,000 m, while offshore the throw increases to about 12,000 m. Further major movement in the offshore Gamtoos Basin occurred on the eastern flank of the St. Francis arch. In the offshore Port Elizabeth and Uitenhage troughs, top of basement (Horizon D) is reached at depths of 6,500 m and 8,000 m, respectively.

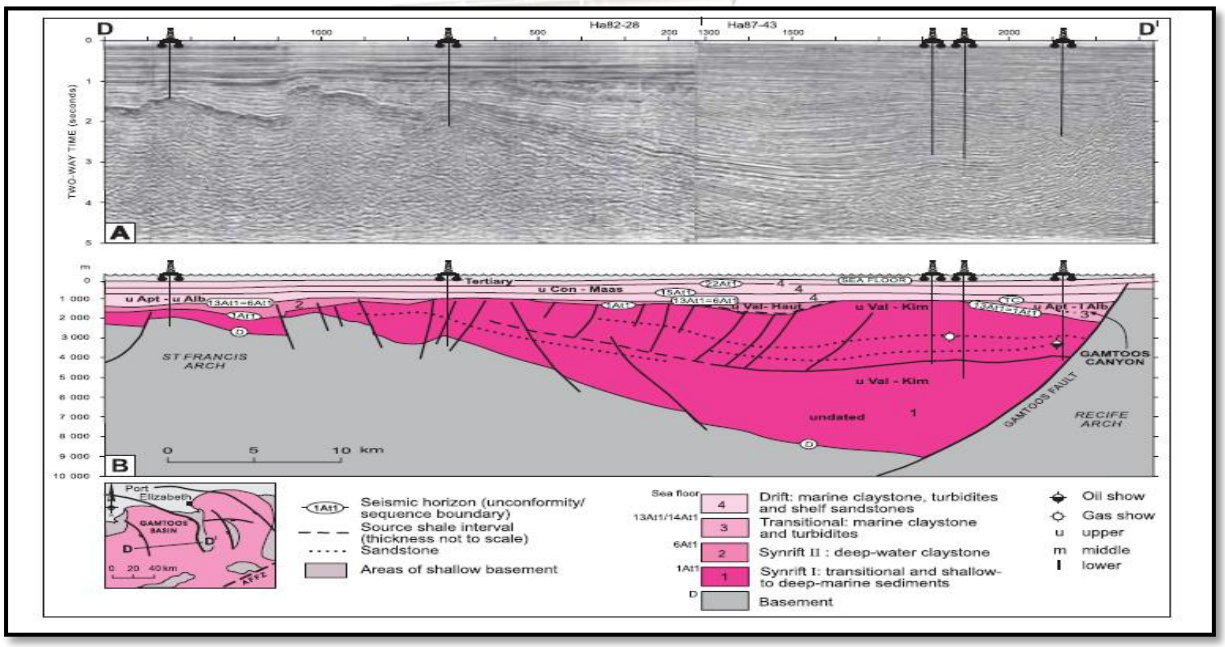

Figure 3. 11: A seismic and geological profile D-D' across the Gamtoos Basin to show the half-graben structural style, stratigraphic subdivision, distribution of organic-rich petroleum source rocks, oil and gas shows. Petroleum exploration wells are shown (McMillan, et al., 1997) A: Two-way reflection time seismic profile, uninterpreted. B: Geological profile based on seismic interpretation and well data.

The sediments of the Gamtoos Basin are divided into four major units as follows:

- Synrift (horizon D to 1At1)
- Early drift (1At1 to 6At1)
- Canyon fill (13At1 to 14At1)
- Transitional-early drift tectonic and sedimentation (6At1 to 13At1)
- Thermal subsidence (post -14At1)

3.4.1 The Synrift (horizon D to 1At1)

The angular unconformity (1At1) at the top of the synrift succession is considered to be the drift onset unconformity. The deep offshore drilling intersected basement rock only on the flanks of basement arches and on the basement highs. The onshore drilling in this basement was terminated once viable economic basements of Ordovician to Silurian Table Mountain Group quartzites or Devonian Bokkeveld Group slates were reached. The rift-, transitional-early drift- and late drift-phases of sedimentation are known as the unconformities D, 1At1 and 13At1 which describe the basin-wide onset of these periods in the Gamtoos Basin (Figure 3.12). The horizon D, which stretches from the top of the basement to horizon 1At1 of Kimmeridgian to Late Valanginian age, records the occurrence of an extensional stress regime that led to horst and graben fill successions (McMillan,, 2003), that resulted in the accumulation of thick sediment deposits.

The horizons D to 1At1 are comprised of the sediments that are composed of inner to outer shelf sandstones and clay stones, such as grey clay stones and glauconitic sandstones, with localised non-marine red and green beds present, and in the proximal setting, occasional conglomerates. These facies depositions occurred during the period of normalized oxygen level in the basin which caused the rare organic enrichment in the rocks. The sediments in the interval 1At1 to 6At1 (Late Valanginian to Hauterivian) are deposits that accumulated in a considerably deep marine environment under deeply lowered oxygen conditions with local organic enrichment that occurred on 1At1 surface.

3.4.2 The Early Drift (1At1 to 6At1)

When Gondwana split up and some of the undocking parts moved along the dextral Agulhas Falkland transform fault, the textural features which are attributed to tectonic strain, developed. These features were preserved in the form of several inverted faults and anticlinal features in the Gamtoos region and developed during the Barremian to Early Aptian. As a

result major basin-wide erosion formed the 6At1 unconformity as well as the incision of numerous canyons into the synrift and early drifts sediments. Thus, 6At1 and 1At1 form the major unconformities in the Gamtoos Basin (Figure 3.12).

3.4.3 The Canyon fill (13At1 to 14At1)

The Early Aptian (post-13At1) marks the beginning of the canyon infilling and terminated during the middle Albian at 14At1. The canyon fill is overlain by Late Albian to Cenomanian sediments terminating at 15At1. However, a further phase of erosion occurred in the late Cretaceous with a number of channels eroding into the drift platform of the southern Gamtoos and Algoa basins around the region of the paleo-shelf break. At some localities the Santonian (Late Cretaceous) erosion was quite intensely cutting into the synrift region (Figure 3.12).

3.4.4 Transitional-early Drift Tectonic and Sedimentation (6At1 to 13At1)

This was considered as the period of erosion, (McMillan,, 2003). During the period 6At1 to 13At1 (earliest Barremian to Early Aptian), two canyons were scoured out (Figure 3.12). The small canyons is found in the Gamtoos Basin close to the Gamtoos fault and partly eroded the Gamtoos anticline, while the much larger Algoa canyon of 60km long, on average 30km wide and 1km deep, was developed in the Uitenhage Trough, in the Algoa Basin. This Algoa canyon cuts across the Uitenhage Fault, revealing basement on the up-thrown side. A likely arm of the canyon, probably formed by late reactivation of the Port-Elizabeth Fault, lies in the northern Port-Elizabeth Trough. The erosion that formed 6At1, locally cut down as deep as well below 1At1. The evidence from the two-way time contour map of the canyon floor's hinterland illustrates the extent of this feature. The above implies that tectonic uplift was accountable for the formation of these unconformities.

3.4.5 Thermal Subsidence (post-14At1)

The southern offshore has experienced a series of phases of thermal subsidence since the beginning of the mid-Aptian, during which the margins of the Gamtoos Basin were uplifted relative to the subsiding basin center (Malan , *et al.*, 1990).This resulted in the erosion of the thermal subsidence region that is marked by truncations at 15At1 and 22At1 (Figure 3.12). The unconformities at 15At1 and 22At1 became the regional unconformities that marked the end of the Cretaceous sediments. The offshore Cenozoic sediments are thin and can be

related to Pliocene to Holocene deposits which are preserved over parts of the onshore Algoa Basin.

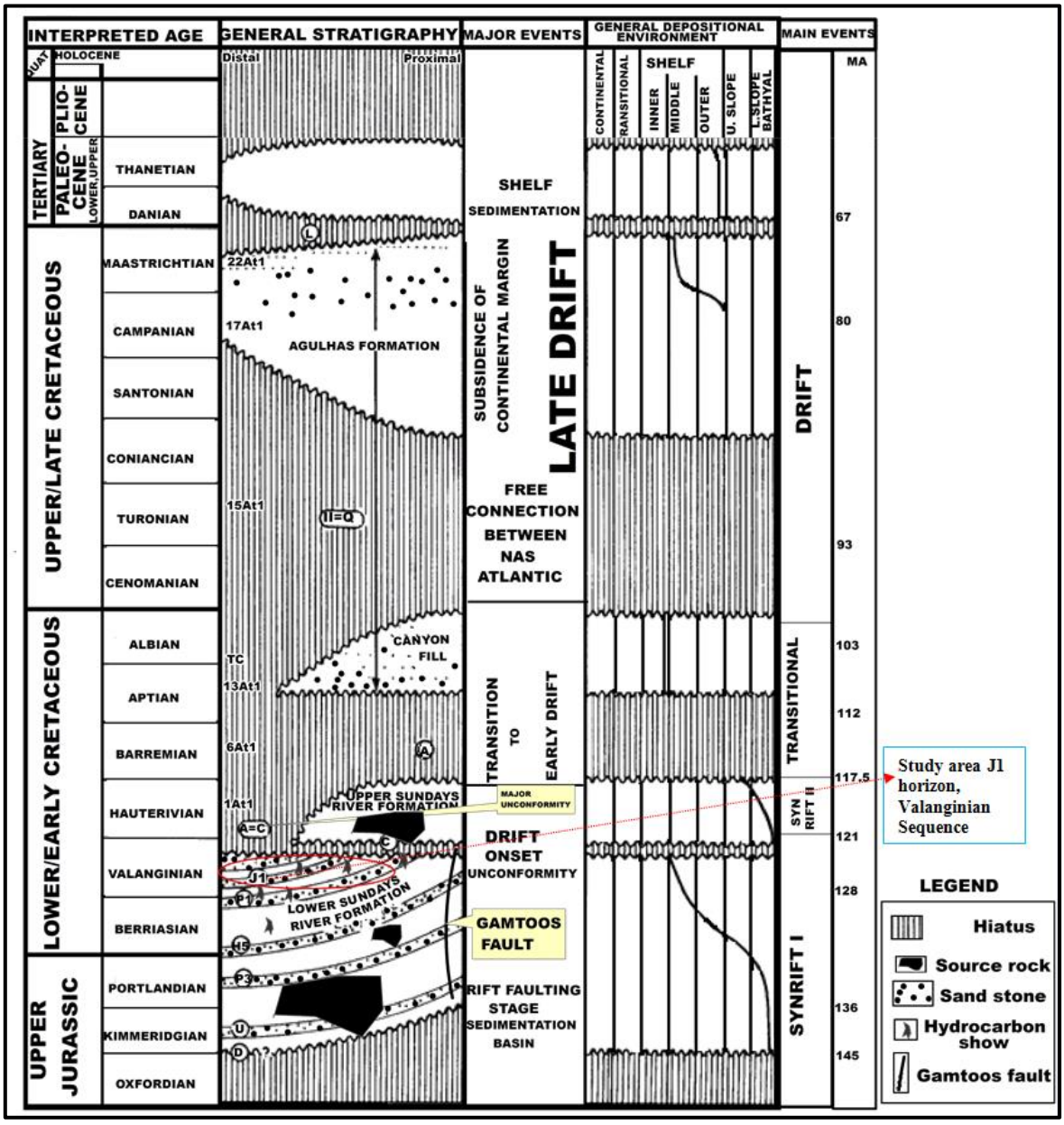

Figure 3. 12: Simplified chronostratigraphic table for Gamtoos Basin showing major unconformities, depositional sequences distribution of sandstone, source rocks and hydrocarbon shows, together with time of the events that influence the developments of the basins. Based on Soekor (1994b) and adapted & modified after McMillan, et al., (1997).

3.5 Petroleum Geology of the Gamtoos Basin

The potential reservoir sandstones in the Gamtoos Basin are sparingly distributed but occur as shallow marine sandstones which are present in the Kimmeridgian in the western part of the basin and in the Late Valanginian sequence in the remainder of the basin. The Valanginian sandstone sequence shows potential for hydrocarbon exploration (Malan, 1993). Also, numerous stacked gas-charged submarine sandstone fans defining a reservoir of Kimmeridgian to Berriasian age were also interconnected in the southern parts of the Gamtoos Basin. As the geothermal gradient of the Gamtoos Basin is strictly speaking low at $3°C/100$ m on average, suitable maturity is reached. The commencement of the main stage of oil migration in the Gamtoos Basin was well timed for migration into pre-existing traps from the Late Cretaceous forwards. However, most of the synrift reservoirs are overlain by clay stone seals that developed regionally. The unconformities, subcrops, anticline, tilted fault block, and the canyon erosion are characteristic features of the Gamtoos Basin which attest to its complex tectonic history as well as the stratigraphic traps that enhanced the exploration opportunities of this basin.

Dry gas- to oil-prone source rocks are presents in the synrift, the early drift, and the canyon fill. From about 215 km measured from the South African shoreline, dry gas is present in the Kimmeridgian to Portlandian sequences; also, wet gas- to oil-prone source rocks were encountered in the borehole at the central and southern parts of the Gamtoos Basin. These source rocks were revealed to ultimately peak at 3kg/metric ton production, but due to the large depths of its burial, its originally potential could have been up to 4 kg/metric ton or more (Malan, 1993) if the temperature controlled by the geothermal gradient would not have "cooked off" or expelled some of the gas. Good oil shows, which associated with the best source rocks, were revealed to have occurred in the Port Elizabeth trough. The borehole on this half-graben intersected an average of 60 m of marginally mature Portlandian, anoxic marine shale which produced 8.1 kg/ton of rock. Thus, if the source sequence continuous to the deeper parts of the trough as indicated from seismic data (Figure 3.11), a high maturity value of the poorly explored half-graben of the basin is expected. Also, mature oil prone source rocks are similarly expected to occur in the unexplored southern parts of the Uitenhage trough.

In addition, the offshore Uitenhage trough contains about 130 m of a dry-to wet gas-prone source rock sequence of latest Valanginian to Hauterivian age, present in the hanging wall of

the Uitenhage fault. Also, immature, dry gas- to oil-prone source rocks are present in the central part of the Gamtoos Basin: about 130 m of immature gas-prone source rock also occurs in the fill of the Algoa canyon. Conversely, about a maximum of 20% porosity reservoir-quality sandstones with 400 md of permeability, is revealed to have developed in the Algoa Basin (Malan, 1993) where the sandstone is comprised of 40% of the horizon D to the 1At1 (Synrift) succession in the Uitenhage trough, which extends to the Gamtoos Basin. Nevertheless, slightly poorer reservoir quality sandstones of Albian age have been intersected in the canyon-fill sequences for both Gamtoos and Algoa Basins respectively.

CHAPTER FOUR

4. *General Methodology Background for the Study*

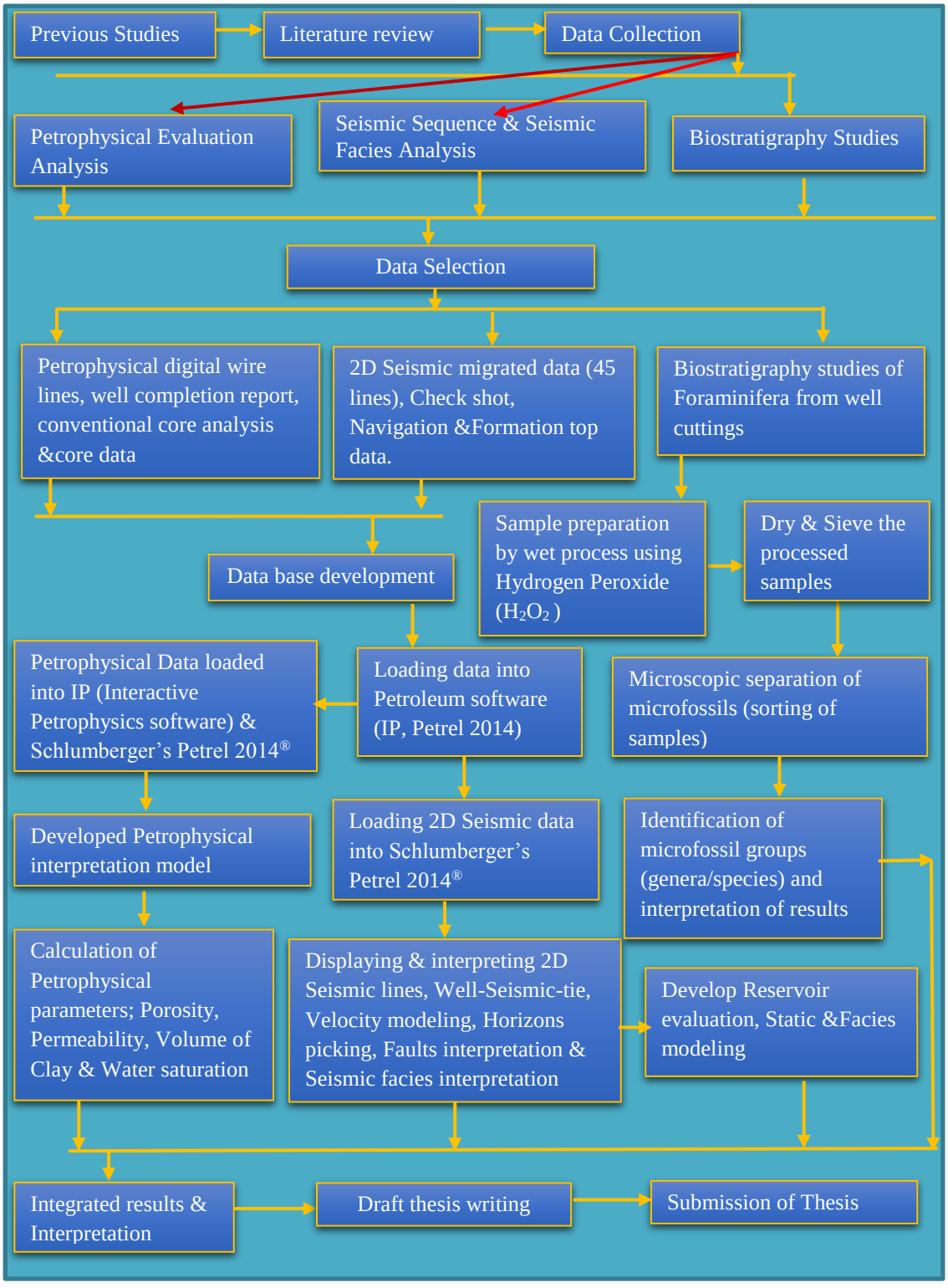

Figure 4. 1: General methodology framework of the study.

4.1. Introduction to the Methodology and Background

This studies utilise Geophysical wirelines logs (LAS Format), Well Core, 45 lines-2D Seismic data profiles in (SEG-Y) acquired by Schlumbeger Services Company, collected from the Petroleum Agency South Africa (PASA), as outlined in the above flow chart.

In order to achieve the objective of the study i.e. to evaluate the petrophysical characteristics of the potential sandstone reservoirs within the pay zones of the selected wells by means of petrophysical well logs and the stochastic modeling method to delineate the petrophysical and facies model of the Valanginian sequence in the Basin. Also, application of seismic facies analysis and seismic sequence analysis was used to delineate the depositional environment of the selected wells in the study area. Drilling cuttings samples were also collected for biostratigraphic studies. The drilling cutting samples were processed and examined through the microscope and the fossil present identified to denote the age of the sediment as well as its depositional environment. These procedures were all put in consideration to achieve the aims and objectives of this study.

4.2 The methodology for the Petrophysical evaluation and reservoir modeling

The quality control (QC) such as log-editing, log splicing, and an environmental correction were performed on the data when loaded into the Interactive Petrophysics software (IP) and Petrel 2014®. Thus, the data quality control (QC) interpretation, modelling and analysis of the provided digitized wireline logs in LAS format data were corrected by means of the software packages before and after loading. The following data types such as digital geophysical wireline logs, Conventional core analysis data reports, Geological well completion reports and 2D Seismic (SGY) format, were used. However, in order to display the log curves and carry out the calculation of the petrophysical parameters, the following basic steps were followed to achieve these objectives:

- Log interpretations were carried out to mark appropriate reservoir zones (pay zones) within the selected wells.
- Computation of reservoir rock characteristic parameters, using various wire line logs.
- Interpretation of the measured calculation parameters for the evaluation of the hydrocarbon potential within the selected wells.
- Merging or splicing logs runs and depth shift curves between logs for the selected wells.
- Applying the environmental corrections for the logs

- Computation of the clay volume from the gamma ray
- Computation of the total and effective porosity from the density, neutron and sonic logs where necessary, depending on the availability of logs for the individual wells used for this study.
- Computation of water saturation using the Simandoux or Indonesian model varieties for the wells.
- Calculating of net pay using the petrophysical industrial standard cut-off value for porosity and permeability for the study wells.
- Facies- and the Petrophysical modeling of the reservoir characteristics of the selected wells.

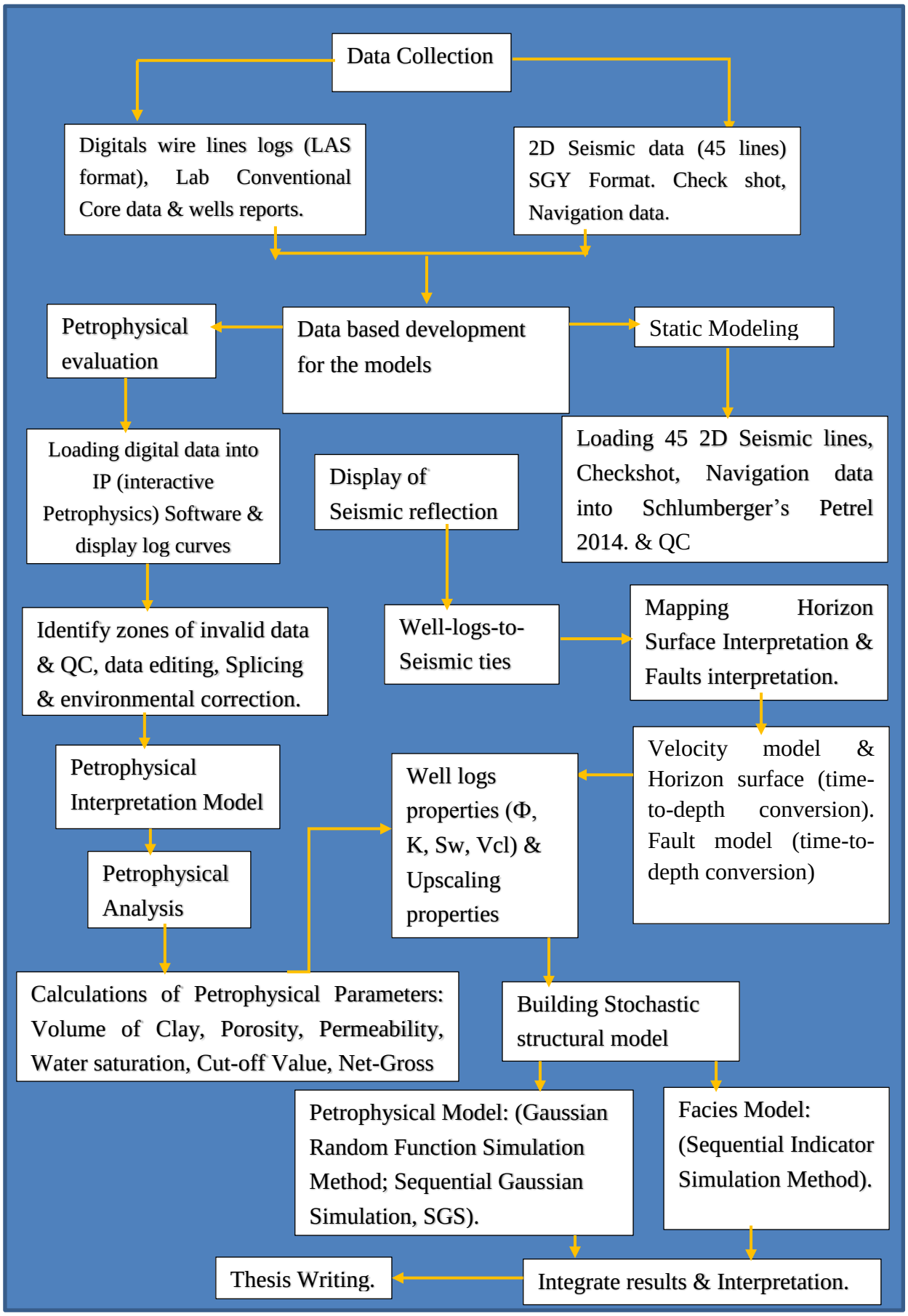

Figure 4. 2: Flow chart depicting the methodology of the Petrophysical evaluation and Static reservoir modelling parameters.

The geophysical data were carefully loaded into the software (IP Interactive Petrophysics®) and the log interpretation was started, to evaluate the possible depths of potential reservoir sandstones within the selected wells. Calculation of petrophysical parameters such as porosity, permeability, water saturation, clay volume, was also performed. By calculating these petrophysical evaluation parameters, the hydrocarbon generation potential of this Basin could now be predicted.

4.2.1 Log Editing

Well logs are the result of physical measurement of subsurface properties obtained within the limited spaces of a borehole (Jarvis , 2006). The probing instruments measure from very close range to the rock under in situ condition. However, these measurements are affected by borehole irregularities such as mud filtrate invasion and casing points, but also depend on the lapse of time between drilling and logging of the hole among other factors. The way this error is handled can affect the quality of the final reservoir characterization model. Therefore, well log data are some time required to be cleaned of the data of measurements associated with errors by means of editing, normalization, corrections and interpretation for consistent and accurate logs well-to-well before it can be used for the reservoir characterization study. Thus, for this study, log editing such as environment corrections and splicing were performed on the selected wells' log data.

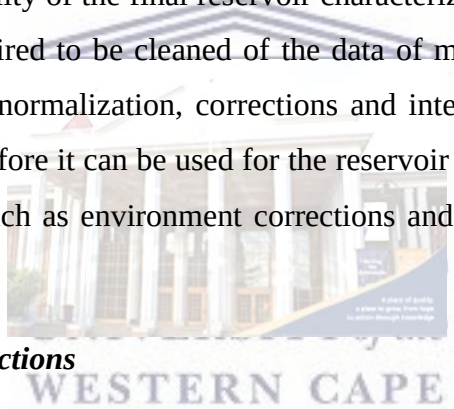

4.2.2 Environmental corrections

The environmental corrections are usually applied to wireline logs by means of using computer programs because logging tools are sometimes affected by borehole and mud conditions. These effects on logs are due to stress, mud weight, salinity content and temperature etc., affecting the logs' measuring instruments during logging, thereby creating unwanted anomalies readings. The environmental corrections are applied to the following wells: Ha-A1, Ha-I1, Ha-N1, Ha-B2, Ha-G1 and Ha-K1. Corrections included are: borehole size and mud weight correction to gamma-ray logs, matrix corrections to the neutron porosity and invasion corrections to the deep resistivity logs, mud salinity of the borehole and hole diameter. These properties for the corrections are obtained from the log headers and make that these logs provide a good set of data with the appropriate mud system required, so as to evaluate the reservoir and characterize the petrophysical parameters encountered on selected wells.

4.2.3 Log splicing

Splicing of logs is the process of generating together dis-jointed runs-logs, logged in a well to produce a single runs-log of a continuous LAS file. The log runs at different depths in a well Ha-K1, were spliced into a continuous log as illustrated in Figures 4.3 and 4.4.This procedure was repeated for the rest of the wells used in this study.

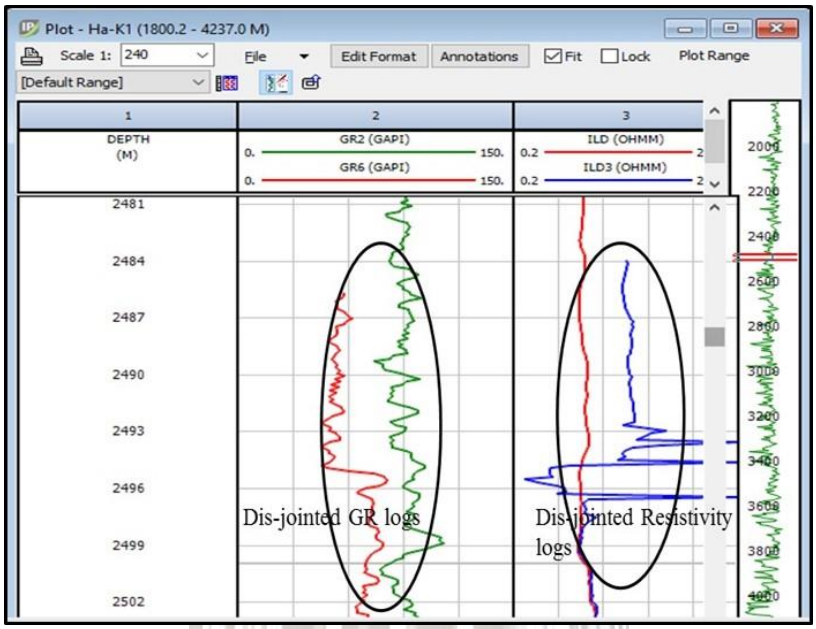

Figure 4. 3: illustrating the dis-jointed runs-logs of Gamma ray (GR) and Resistivity (ILD) on well Ha-K1, before splicing.

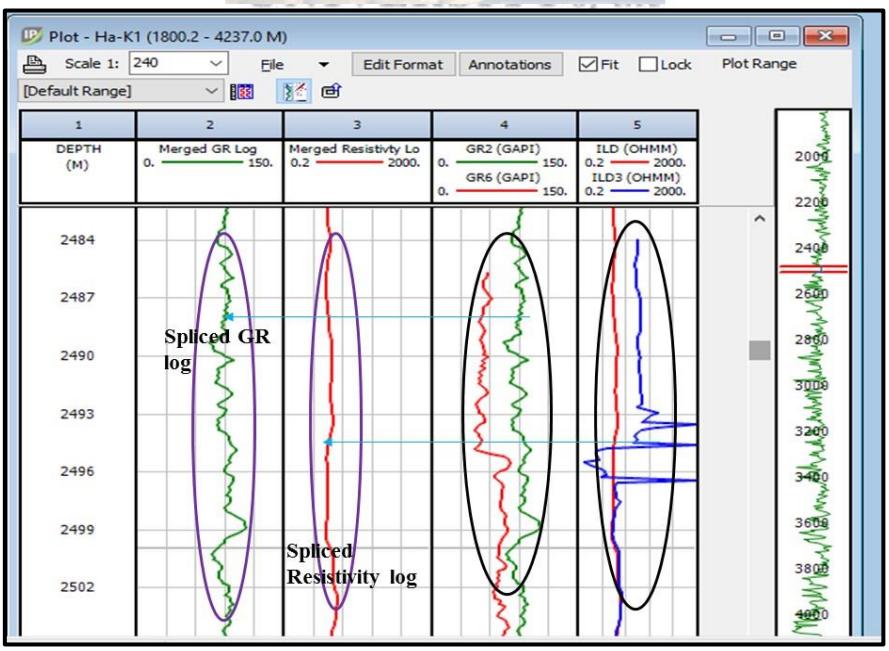

Figure 4. 4: illustrating the spliced runs-logs of Gamma ray (GR) and Resistivity (ILD) of well Ha-K1, from dis-jointed logs runs into a single continuous LAS file.

4.2.4 Identification of a possible Sandstone Reservoir

Identification of a potential sandstone reservoir or zone of interest which is referred to as the clean zone with hydrocarbons is the initial measure taken to interpreting logs during petrophysical evaluation of a reservoir. This can be achieved by clearly defining the baseline cut-off from the gamma ray log. The baseline cut-off of ~ 85.5 (API) defined for this well Ha-K1 was calculated from the mean histogram obtained from the spliced gamma-ray runs logs, during the logging of well Ha-K1, as indicated in (Figure 4.5). The maximum deflection of gamma ray logs to the right indicates a shale formation while the maximum deflection of gamma ray logs to the left suggests clean sandstone (Jensen , et al., 2013). The same procedures were followed for the other wells used in this study. Figure 4.6 illustrates an example of a potential sandstone reservoir from well Ha-K1.

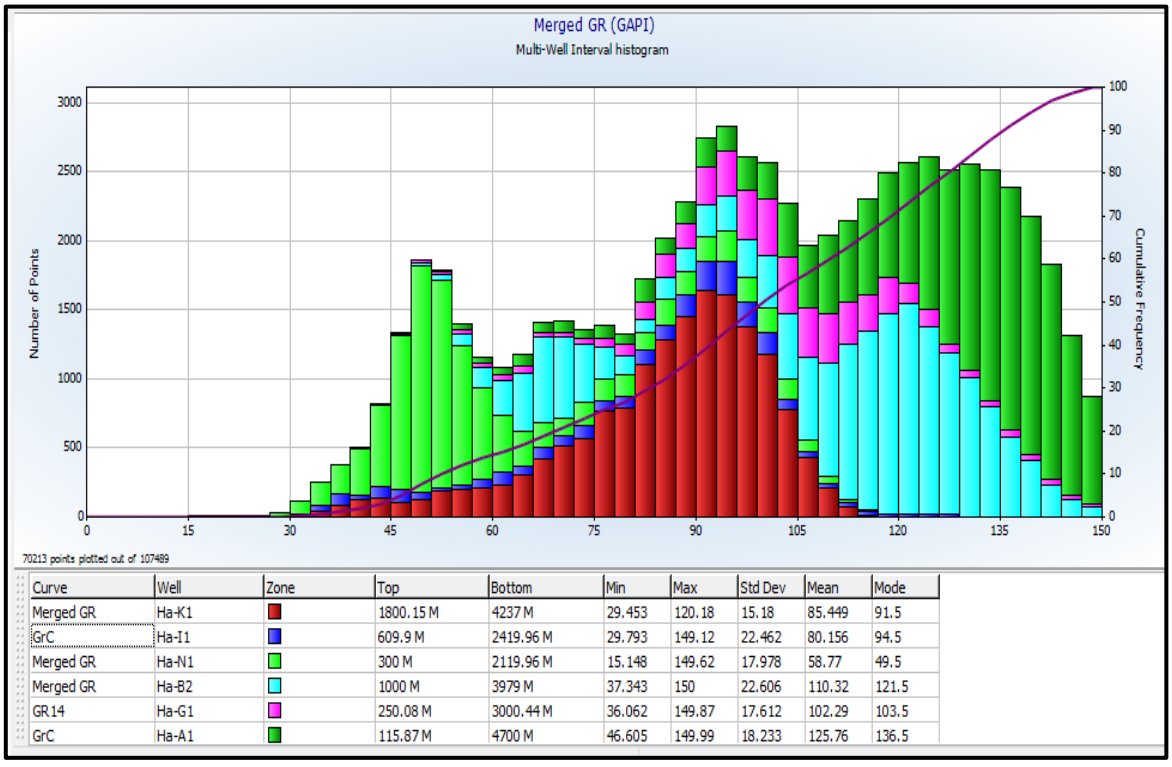

Curve	Well	Zone	Top	Bottom	Min	Max	Std Dev	Mean	Mode
Merged GR	Ha-K1		1800.15 M	4237 M	29.453	120.18	15.18	85.449	91.5
GrC	Ha-I1		609.9 M	2419.96 M	29.793	149.12	22.462	80.156	94.5
Merged GR	Ha-N1		300 M	2119.96 M	15.148	149.62	17.978	58.77	49.5
Merged GR	Ha-B2		1000 M	3979 M	37.343	150	22.606	110.32	121.5
GR14	Ha-G1		250.08 M	3000.44 M	36.062	149.87	17.612	102.29	103.5
GrC	Ha-A1		115.87 M	4700 M	46.605	149.99	18.233	125.76	136.5

Figure 4. 5: indicating the baseline cut-off at 85.5 (API) to define the shale and sandstone formations of well Ha-K1.

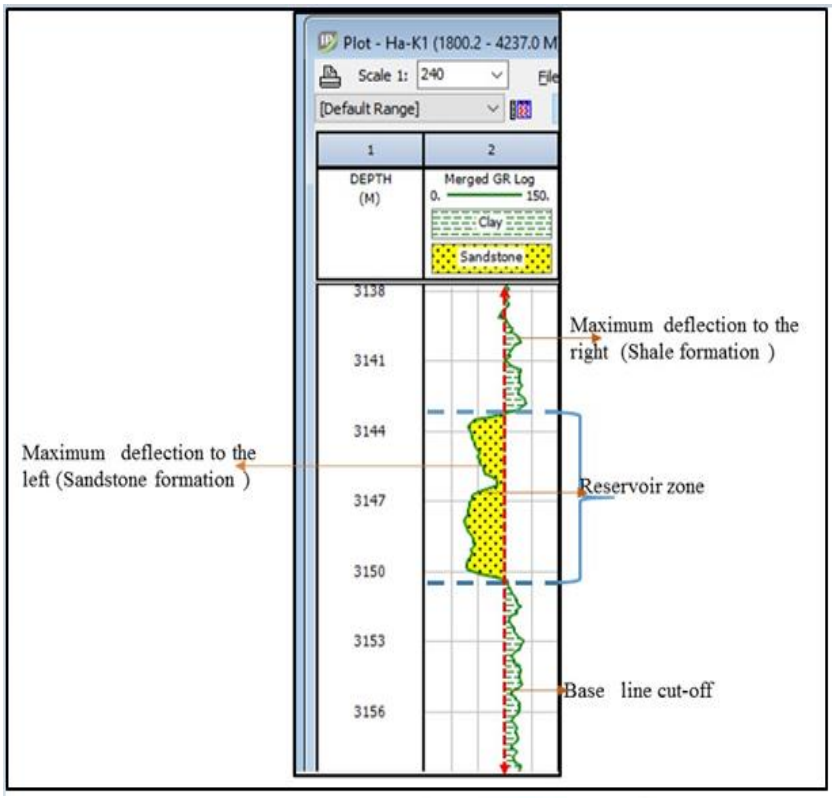

Figure 4. 6: Example of a potential sandstone reservoir from well Ha-K1.

4.2.5 Determination of m, a, n and Rw parameters from Standalone Pickett's plots

For accurate estimation of water saturation of any reservoir evaluation, the determination of the petrophysical exponents' parameters namely: "a" (tortuosity factor) "m" (cementation factor) "n" (water saturation exponent factor) and "Rw" (water resistivity factor) are very important to obtain an accurate estimation of the fluids' saturation present in the reservoirs of wells. For this study the Picketts plot method was utilized to calculate these petrophysical parameters for sandstone reservoirs of the Valanginian sequence of the Gamtoos Basin using five wells (Ha-K1, Ha-B2, Ha-G1, Ha-I1 and Ha-A1). Resistivity and Porosity are plotted against each other in water bearing intervals using Standalone Pickett plots. The results were further discriminated by the volume of clay calculated from the wells' gamma rays logs, to predict the matrix values within the reservoirs of the selected wells so that porosity can be more accurately calculated. These parameters were obtained from the porosity and resistivity taken from the data logs, in each of the runs in each well. Figure 4.7 illustrates the multi-wells Standalone Picketts plots for the six wells with the determined values of each parameter respectively. The straight lines in the cross plot indicate the amount of the water saturation present in the reservoirs; thus, the red line suggest 100% water saturation, 0.5 line represent

50% water saturation, 0.3 line indicates 30% water saturation and 0.2 line suggests 20% water saturation.

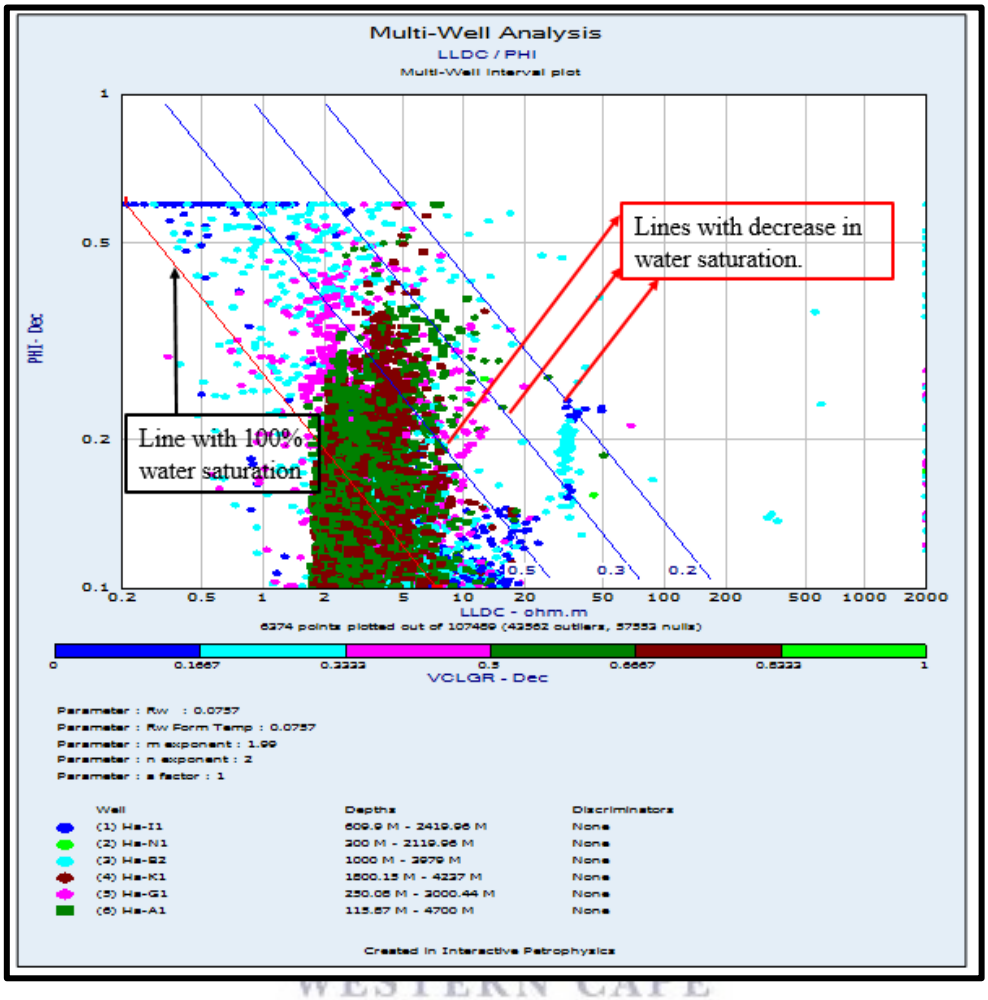

Figure 4. 7: The Standalone Pickett plot from multi-wells adopted to determine the Petrophysical exponent's parameters (a, m, n and Rw).

4.2.6 Determination of Clay Volume

The Shale or Clay volume can be defined as the volume of wetted shale or clay per unit volume of reservoir rocks, expressed in decimal fractions or percentages. Before the calculation of shale or clay volume, the gamma ray index (I_{GR}) was the initial step to calculate by means of using Schlumberger's (1979) formula below (equation 1). The shale volume is determined by using gamma ray logs runs for each of the wells studied in a porous reservoir because shales are usually more radioactive than sand and carbonate.

$$\mathbf{I_{GR} = (GR_{Log} - GR_{min}) / (GR_{max} - GR_{min})}$$ (Schlumberger , 1979)……equation 1.

Where:

I_{GR} = Gamma ray index,

GR_{Log} = Gamma ray log reading of formation.

GR_{min} = Minimum gamma ray (clay free zone i.e.; for clean sand).

GR_{max} = Maximum gamma ray log (100% clay zone or shale zone).

Since the studied reservoir wells are tertiary unconsolidated sandstone rocks, the shale volume are calculated from the gamma ray index (I_{GR}) using the Larionov Tertiary Rock model equation as follows. These procedures are repeated for the wells studied and a detailed interpretation will be explained later in the studies.

$VSH_{LarionovTertiaryRock} = 0.083(2^{(3.7\text{-}IGR)} - 1)$, (Dresser Atlas, 1979) ……equation 2

The various non-linear equations and model used for the volume of shale calculation and the comparison of the models are presented below (Figure 4.8) (Saputra, 2008)

Larionov (1969) for tertiary rock; $Vsh = 0.083(2^{3.7IGR} - 1)$ ……equation 3.

Stieber (1970); Vsh = IGR/ 3-2*IGR ……..……equation 4.

Clavier (1971); $Vsh = 1.7 - [(3.38-(IGR +0.7)^2]^{1/2}$……..……equation 5.

Larinov for older rocks $Vsh = 0.33*(2^{2IGR} - 1)$……...equation 6

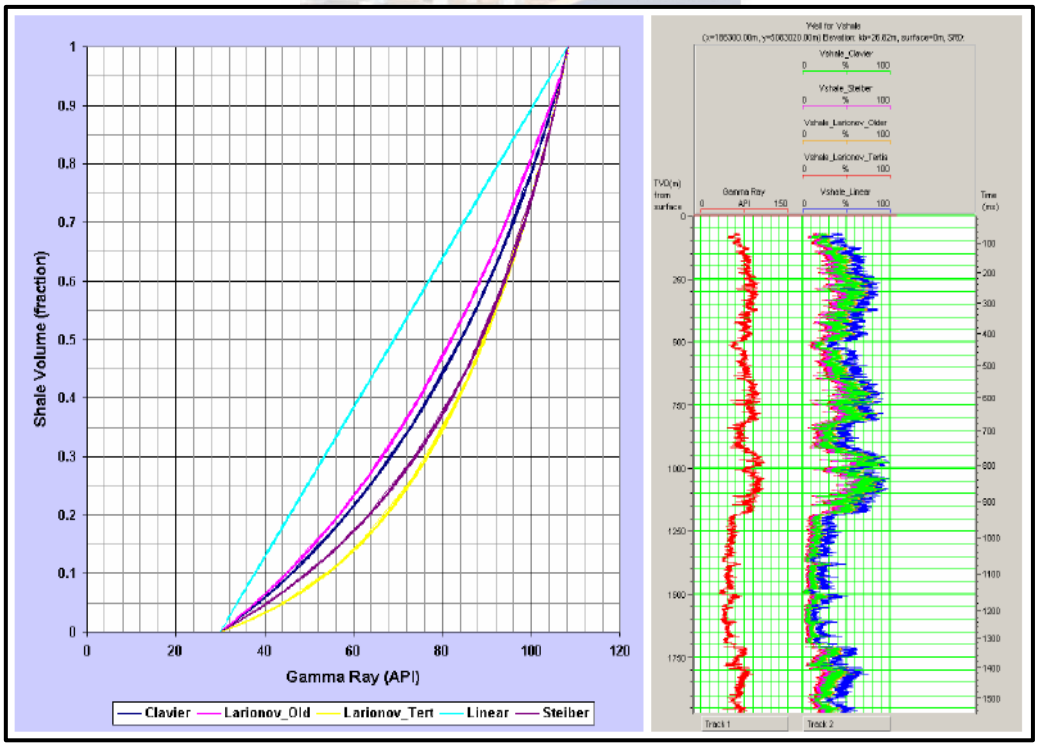

Figure 4. 8: Comparison of various methods used for Shale volume calculation (Saputra, 2008).

4.2.7 Determination of Porosity

The porosity curves were derived from the density, neutron and sonic logs. The combination of neutron-density logs was utilized to calculate the porosity of wells Ha-B2. Ha-K1, Ha-I1, Ha-G1, Ha-A1 to obtain a good indication of lithology and a more accurate estimation of porosity, as presented in the following equation below:

$\Phi = (\rho ma - \rho b) / (\rho ma - \rho fl)$……..….equation 6.

Where:

Φ = is the porosity derived from the density log

ρma = The matrix or grain density (g/cc)

ρb = The bulk density which include the porosity and grain density (g/cc)

ρfl = is the fluid density (g/cc), salt mud =1.0 and fresh water =1.

However, neutron and density logs were not available for well Ha-N2. Therefore the porosity was derived using sonic logs by means of the Wyllie time average formula following the equation below:

$\Phi = (\Delta t_{log} - \Delta t_{matrix} / \Delta t_f - \Delta t_{matrix})$ …….. …….equation 7

Since the reservoirs in the study wells Ha-N2 are the unconsolidated formations, a correction factor for porosity derived from sonic, is necessary. They are expressed below.

$\Phi = (\Delta t_{log} - \Delta t_{matrix} / \Delta t_f - \Delta t_{matrix}) * 1/Cp$ …….equation 8

And, **$Cp = \Delta t_{sh} * C/ 100$**……..…..equation 9

Where:

Φ derived porosity in transit time (µsec/m).

Δt_{log} is the acoustic transit time sonic logs (µsec/m).

Δt_{matrix} the acoustic transit time of the rock matrix (µsec/m).

Δt_f Acoustic transit time taken through the of interstitial fluids (µsec/m).

Δt_{sh} the specific acoustic transit time in shales (µsec/m).

Cp the compaction correction factor,

C is constant = 1

100 Acoustic transit time in compacted shale. Generally the shale compaction coefficient ranges from 1.0 to 1.3, based on regional geology, but for Ha-N2 it was 1.02.

4.2.8 Determination of Water saturation

Porosity logs neutron-density combined with resistivity logs were used to obtain porosity and water saturation curves parameters (n, m, a, Rw) for water saturation from the Standalone Pickett's cross plots (Figure 4.7). Simandoux model (1963) and Indonesia model by Poupon and Leveaux (1971) equations 10 &11, as shown below were used to calculate the water saturation for this study, due to the shaly-sand formation of the study's wells (Ha-B2. Ha-K1, Ha-I1, Ha-G1, Ha-A1 and Ha-N1). It was further used to obtain the best fit curves when calibrated with conventional core data analysis for water saturation. The model has an effective porosity as the input porosity in the water saturation model.

$Sw = aRw / 2\Phi m – Vsh / Rsh + \sqrt{(Vsh / Rsh) 2 + 4/F * Rw * Rt)}$ …….....equation 10

(Simandoux, 1963).

Where:

Sw Water saturation. Rw Formation water resistivity.

Rt true resistivity from deep resistivity log. Φ Effective Porosity fraction.

Vsh Volume of shale calculated. Rsh Resistivity of the shale formation.

a Saturation equation exponent, which is the gradient of the line defined on the plots.

m Cementation factor.

$1/\sqrt{R_t} = \{V^d_{clay}/\sqrt{R_{clay}} + \Phi^{m/2}/aR_w\} S_w^{n/2}$ .....equation 11

Poupon and Leveaux (1971). Thus**, $d = 1 - V_{sh} / 2$**

R_t true resistivity from the deep resistivity log S_w Water saturation fraction.

V_{clay} Volume of shale. R_w Formation water resistivity.

R_{clay} Resistivity of wet clay. n Saturation exponent.

Φ Porosity. a Tortuosity factor. m cementation exponent.

4.2.9 Determination of Permeability

The method used in this study to estimate log-calculated permeability (K) is based on multiple variable regressions. The old wireline logs which were runs in the wells are not directly measuring the permeability from the wells. However, the estimated log calculated permeability (K) was calculated from the regression equations obtained from the porosity versus permeability cross plot known as (PoroPerm) relationship plots. This is done by plotting the Klinkenberg core permeability of the liquid horizontal in the logarithm scale against gas expansion core porosity data in linear scale, obtained from the conventional core analyses of the wells (Ha-B2. Ha-K1, Ha-G1, Ha-A1, Ha-I1). Figure 4.9 illustrates the regression equation from multi-wells (PoroPerm) plots from core permeability versus core porosity. The regression equations were used to predict the permeability (K) for wells respectively, where Core porosity depends on the porosity logs used for each wells.

$K_{multi\text{-}wells}$ = 10^ (-2.11306 + 9.27334 * Core porosity) .....equation 12

Details of these regression equations obtained for each wells (Ha-B2. Ha-K1, Ha-I1, Ha-G1, Ha-A1 and Ha-N1) and diagram would be interpreted in chapter 5 of this study.

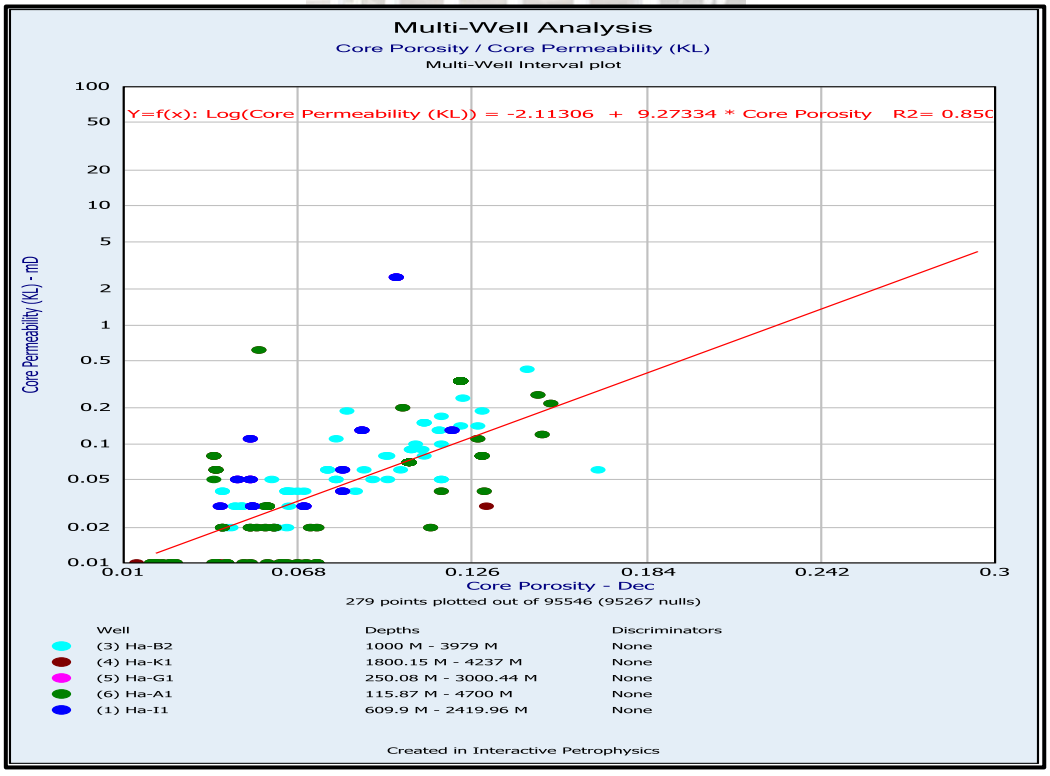

Figure 4. 9: The regression equation from multi-wells (PoroPerm) plots from core permeability versus core porosity.

4.2.10 Core

Only three wells (Ha-B2, Ha-K1 and Ha-G1) were cored in this basin, however no core was recovered within the J1 Valanginian interval of the study formation. The core photograph in Figure 4.10 represents core logs from well Ha-G1 encountered below the Valanginian section in this basin.

Figure 4. 10: Core photograph from well Ha-G1 depths 2399.82 m to 24.88 m used for this study, showing the lithology below the Valanginian section.

4.2.11 Cross- plots Determination

In this study, different types of well log cross- plots between two variables were plotted and the results of the chains of points were used to define the relationships between the variables. The cross-plots include:

- Cross-plots of compatible logs measuring the same parameters such as porosity logs. Neutron-density cross plot and discriminated by the gamma ray log to denote lithology.
- The cross-plots of core sample value Klinkenberg core permeability parameter against the core porosity logs.
- The cross-plots of petrophysical porosity logs versus water saturation and volume of clay plots, to denote the cut-off value used in this study.

These cross-plots can be seen later in their respective chapters in this study.

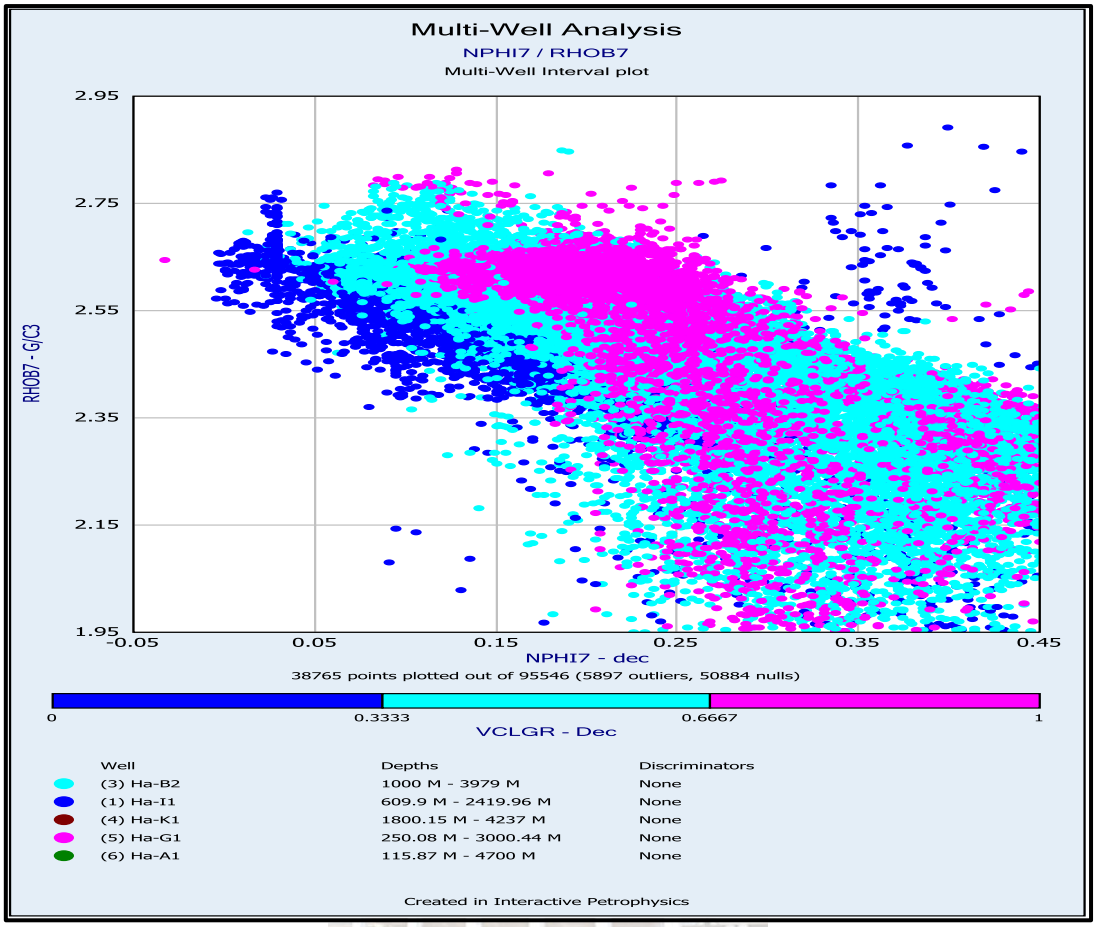

Figure 4.11: The multiple wells (Ha-B2. Ha-K1, Ha-I1, Ha-G1, Ha-A1 and Ha-N1) cross-plots of Density logs versus Neutron logs and Gamma ray logs as discrimination logs for volume of clay determination.

4.3 Petrophysical Static Reservoir Modeling Method

Due to the visual requirements of the dynamic simulation process and to arrive at a final well production and performance, it was essential to build a static model that represents the subsurface reality of the reservoir sands of the Valanginian succession encountered in most of the wells in the entire study area of the Gamtoos Basin as closely as possible. The static geological model was built by integrating relevant sub-surface data and interpretation from after the petrophysical evaluation process. The 2D seismic structural interpretation and properties model such as porosity, permeability, net-to-gross and water saturation; lithological description and facies interpretation, from the log analyses are used to build the static geological model of the Valanginian section for this study.

In addition, Petrophysical reservoir modeling is an important method for reservoir description. This technique has a distinctive advantage in parameter estimation, reservoir

heterogeneity, reservoir characteristic, and comprehensive uses of numerous data. This technique of the reservoir modeling is divided into two categories such: the deterministic and stochastic modeling approaches respectively.

However, in this study only the stochastic modeling approach was utilized, as the vast potential of using stochastic modeling in this study is the possibility of quantitatively integrating a whole range of different types of information and data generated during this study. It is also considered as an improvement on traditional geological modelling techniques (Haldorsen & Damsleth, 1990). Also, petrophysical interpretation of the reservoir rock, defined in well logs quantitative interpretation phase, can be extended to the whole reservoir through stochastic modeling, by means of direct simulating of petrophysical properties, or indirectly by simulating facies, and then associating mean petrophysical values or frequency distribution with these.

Thus, this method was further integrated into the reservoir characterization of the study wells to provide general geological knowledge of the reservoir and a more scientific basis for its interpretation. Also for the geological understanding of the complexity of subsurface sand distributions, improvement of the characterization of heterogeneity and evaluation of the reservoir uncertainty, thus generating a more realistic geological model. The following procedures were taken to achieve this objective for this study. The data analysis, interpretation, and modeling performed in this model study were done using Schlumberger's Petrel 2014® software platform. This software has been developed to provide a "seismic to simulation" workflow, where data may be visualized, interpreted, and integrated for building simulation models.

4.3.1 Loading of Seismic data

45-lines of 2D-Seismic data (SEG-Y) format, check-shot, formation tops, navigation data and geophysical logs (Las file) data of wells Ha-B2. Ha-K1, Ha-I1, Ha-G1, Ha-A1 and Ha-N1 were loaded and imported into the Schlumberger Petrel 2014® and a display of the seismic reflection data was put on the computer screen.

4.3.2 Well-to-Seismic ties

Well-to-Seismic ties were performed in this study to calibrate and compare the units of the wells measured in depths domain, to the Seismic data measured in time domain (Figure 4.12). The well-to-seismic ties also enable one to identify and map the horizon tops of the

formations from the study wells by a specific reflection on the seismic section. This is done by calibrating the sonic logs well data from the wells (Figure 4.13) with the checkshots seismic data, thereby generating the synthetic seismic trace which directly correlates the well log data to the seismic data (Figure 4.14), since compressional sonic log data and check shot data are accurate measures of vertical interval velocity (Luton & Prieto, 2000). As the sonic log measures a travel time Δt, it provides a means to time-convert well data. Therefore, this provides a sonic time-depth relationship used in this study for the synthetic seismic trace generated for the wells.

Checkshots are considered to measure times that are closer to the surface seismic data (Robein , 2003) at the correct seismic scale (Simm & Bacon, 2014). Calibrating of sonic log data by Checkshot survey or a Vertical Seismic Profile (VSP) provides a sequence control of depths corresponding to vertical time (Robein , 2003; White & Simm, 2003). The Checkshot results for wells Ha-K1, Ha-G1, and Ha-N1 generated by the Vertical Seismic Profile (VSP) contractor Schlumberger, are used for the initial inputs of time-depth relationship for this calibration.

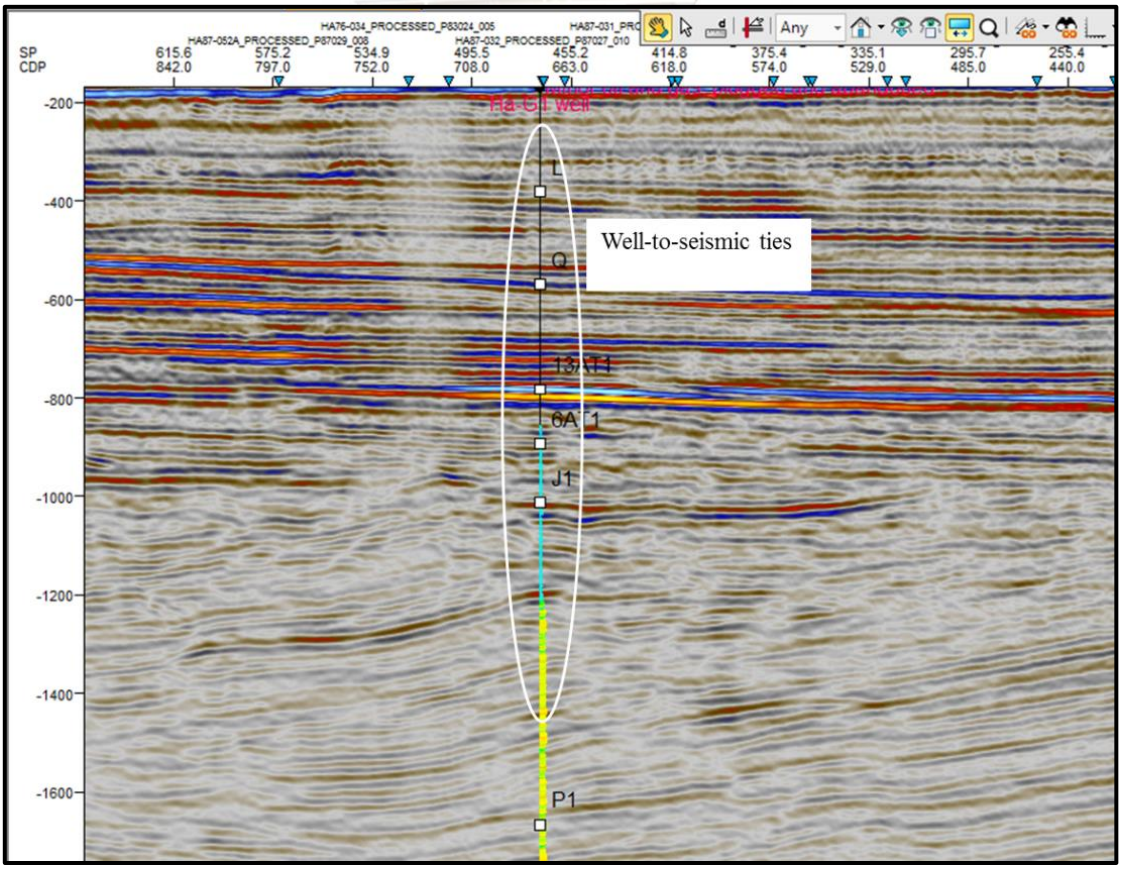

Figure 4. 12: Well-to-seismic ties of well Ha-G1, on 2D processed seismic line Ha87-047.

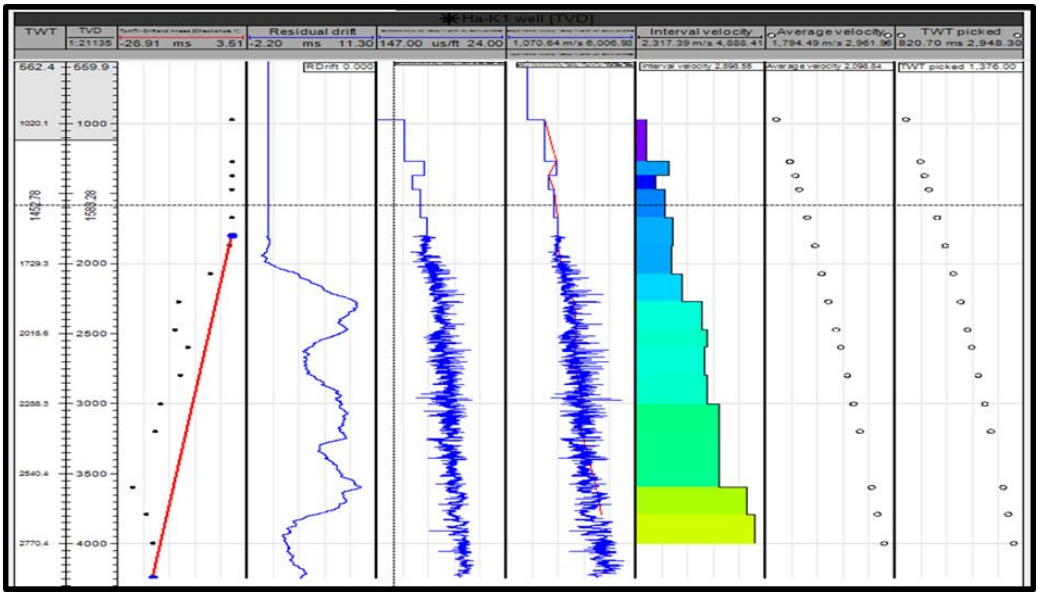

Figure 4. 13: Illustration of calibrated sonic log and Checkshots survey data of well Ha-K1. Track 1, is the curve corresponding to the time of the checkshots minus time of sonic log. Knees (blues- black dots) which applied at each Checkshot point. Track 2, is the residual drift curve. Track 3, the original sonic log curve (blue). Track 4, the calibrated sonic log (red) and the original sonic log curve. Track 5, the interval velocity. Track 6, average velocity curves dots. Track 7, is the two-time curves dots.

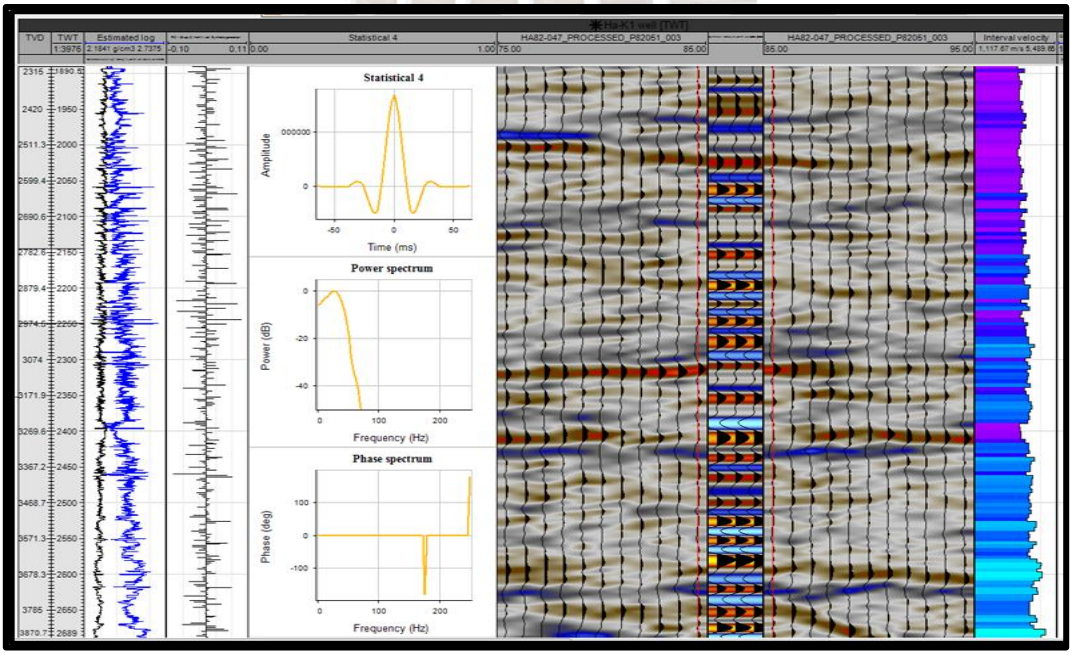

Figure 4. 14: The synthetic seismic trace generated from well Ha-K1, 2D line Ha82-047, processed by means of seismic-to-well ties. Track 1, is the bulk density log (blue) and the calibrated sonic log (black), they are multiplied to produce an acoustic impedance log (AI). Track 2, the reflection coefficient log (RC). Track 3, displays zero phase, at 25 Hz Ricker wave convolved with the reflectivity log (Analytical method and Ricker Algorithm). Its power and phase spectrums are displayed below it. Track4 – 6, illustrate the synthetic seismogram centred between seismic data adjacent to the well Ha-K1. Track7, is the interval velocity.

4.3.3 Time to Depth conversion

Time to depth velocity conversion was performed in this study and Figure 4.15, from well Ha-G1 is a representative example of this conversion. This method allows integration of all data sets, such as well logs, well tops, checkshots data, seismic reflection data and horizon interpretation. A seismic well tie was used to create time-depth relationship (TDR) between depth-domain well log data and time-domain seismic data. Formation well top horizons were interpreted from the well tie, which is used to build the structural basis for the velocity model in this study.

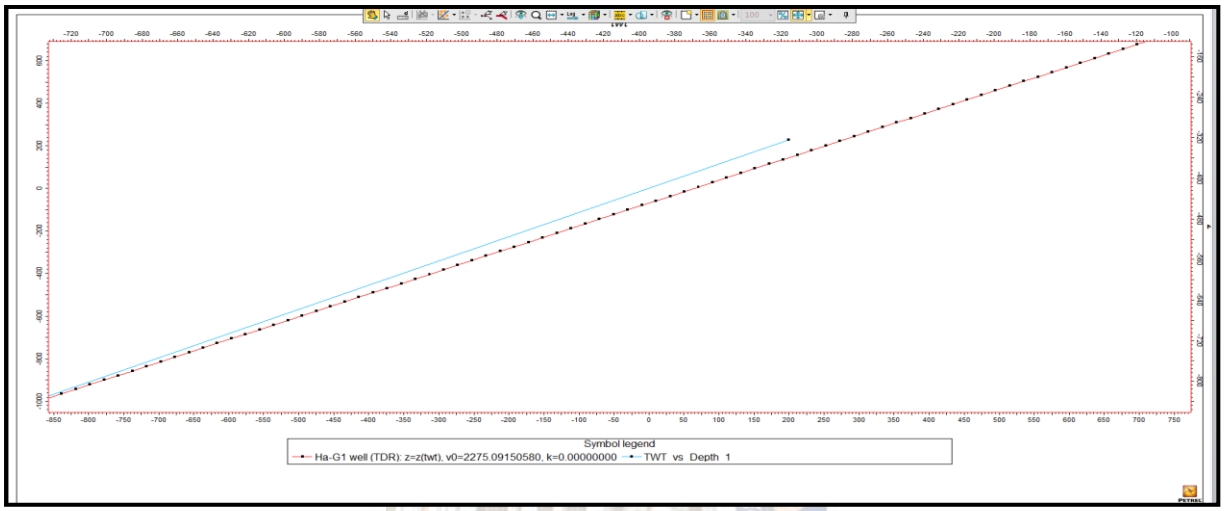

Figure 4. 15: Shows an example from well Ha-G1 of time-depth function plot for the wells.

4.3.4 Horizon interpretation mapping and creation of surfaces

After the depth-domain well data were integrated into the time-domain by means of time-depth conversion relation (TDR). The wells and it well tops formation pick are overlaid on to time-domain seismic intersection, which is also based on the synthetic process. The points corresponding to the well's formation tops indicate the starting point for the horizon mapping across the seismic volume. The horizons were mapped manually for single seismic amplitude reflection along peaks. Then, the seismic horizon mapping interpretations were performed on all the 2D seismic processed lines. For instance in Figure 4.16, line Ha78-003 indicates one of the seismic lines mapped for this study by means of mapping the seismic reflections of the well's formation tops and amplitude reflection peaks or troughs. Positive amplitude reflection which corresponds to the main reservoir sands on seismic data reflection was identified for

mapping. Three major focus seismic reflection horizons were mapped; such sequence formations are P1, J1 and 1At1 representing from the bottom the Berriasian, Valanginian and Hauterivian sequences respectively. These were mapped to generate surfaces in time and depths, to obtain geological formation and essential zones of the Valanginian sequence. Figures 4.16 and 4.17 show the major seismic reflection horizons of P1, J1 and 1At1 Berriasian, Valanginian and Hauterivian sequences mapped, as well as the surfaces in-time created for the study from the respective horizons. The surfaces in-time created from the horizons P1, J1 and 1At1 Berriasian, Valanginian and Hauterivian sequence were later converted to surface depths in metres by means of velocity modeling to build the horizon models (Figure 4.18).

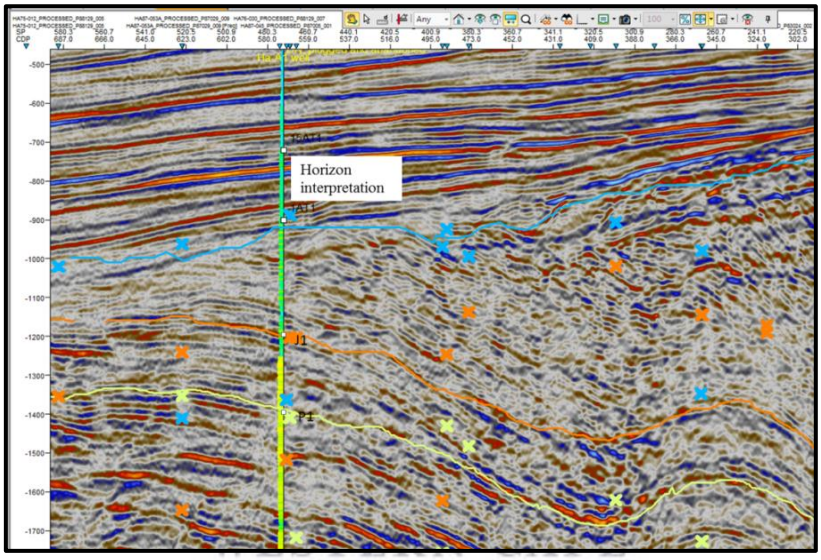

Figure 4. 16: Shows the major seismic reflection horizons P1, J1 and 1At1 mapped from well Ha-A1, 2D seismic processed line Ha78-003 respectively.

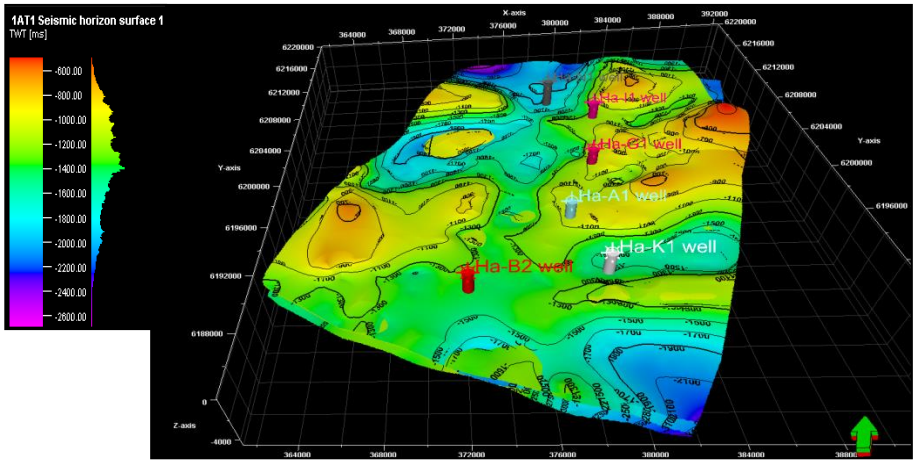

Figure 4. 17: Shows the horizon surfaces in-time created from the horizons P1, J1 and 1At1 sequences, from bottom to the top respectively.

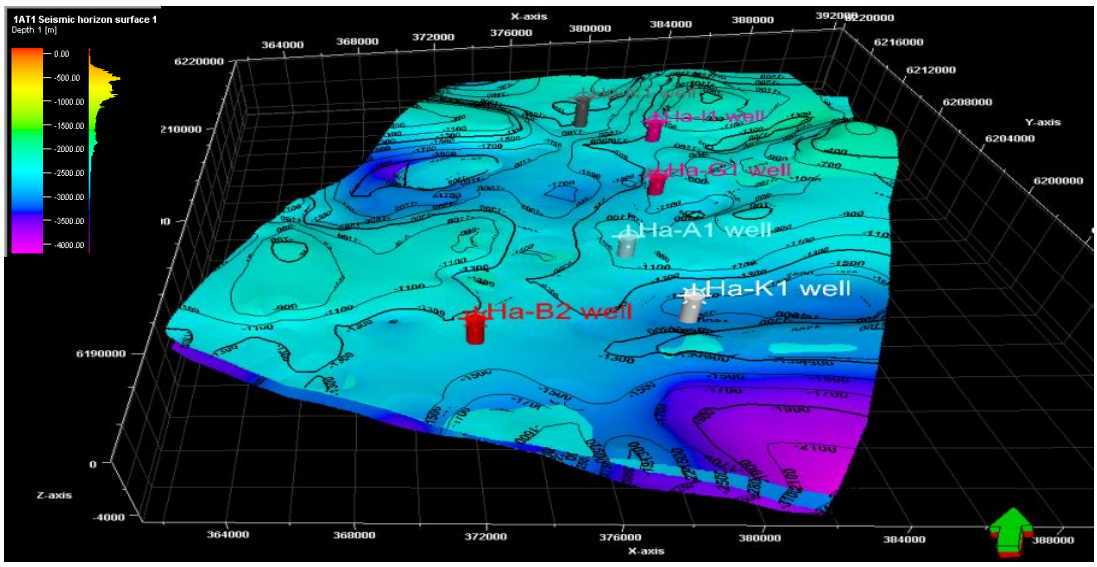

Figure 4. 18 : Shows the horizon surfaces in-depth created from the horizons P1, J1 and 1At1 sequence, from bottom to the top respectively.

4.3.5 Faults interpretation mapping

The two major listric faults identified from the seismic lines are faults F1 and F2, on 2D seismic line Ha82-012A and Ha87-053A (Figure 4.19). These were traced and mapped on time-slices ranging from -497.50ms to -2071.01ms and -433.69ms to -1257.53ms respectively for F1 and F2 at representative levels on the seismic section. Most of the seismic lines do not show significant faults; most faults observed from the seismic lines are minor listric faults which have no significance in mapping. The faults F1 and F2 were delineated, mapped, assigned names and coloured-coded. By geologic definition, these faults formed by an extensional regime during tectonic events in the basin like rifting and drifting as a result of extensional stresses in the Basin.

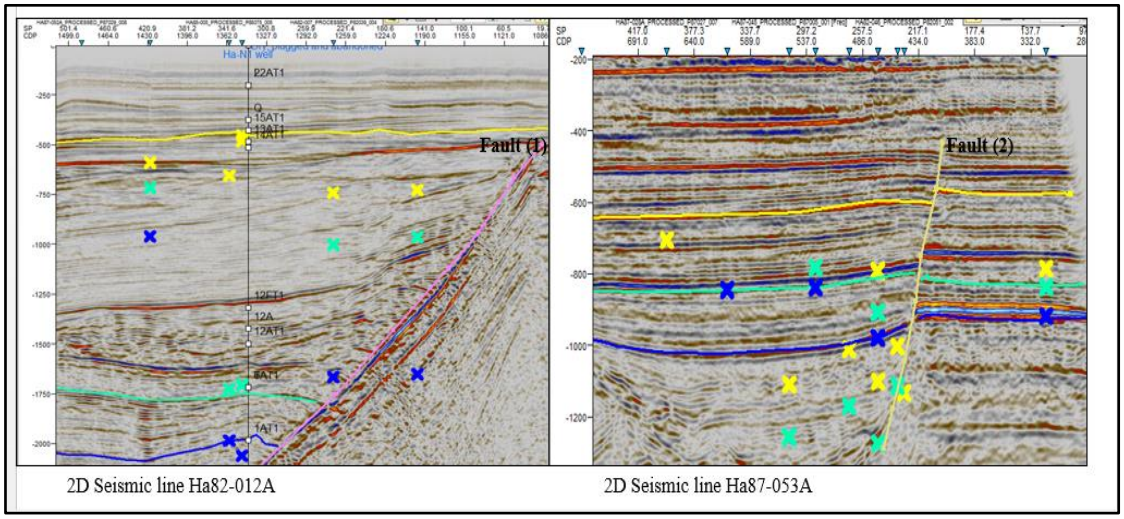

Figure 4. 19: Illustrating the horizons and faults F1and F2 interpretation on 2D seismic lines.

4.3.6 Velocity modeling

Velocity modeling is essential for the domain-conversion of the seismic data. The seismic profiles are measured in two-way time, or the length of time it takes for a seismic wave generated at surface to reflect from a specific subsurface horizon and travel back to a receiver at the surface. In addition, for the purpose of characterization, Velocity modeling is very useful to convert the vertical axis from the two-way-time in milliseconds (ms) to total depth in feet (ft) or meter (m) depending on measuring value taken. This Time–Depth Relationship (TDR) enables the interpreter to correlate the seismic data to other data sets in the depth-domain such as wireline log and core data, facilitating the measurement of the formation thickness. Velocity modeling was performed for the wells Ha-B2. Ha-K1, Ha-I1, Ha-G1, Ha-A1 and Ha-N1 in this study to enabling time-depth-relationship (TDR) i.e. depth-domain functions operation from the seismic time-domain. The Figure 4.20 shows the results of the velocity modeling correction for the wells and the surfaces created in depth (m) from Figure 4.18 above after the velocity model.

	A	B	C	D	E	F	G	H	I
1	**Velocity model**	Velocity model (NEW MODEL)							
2	**User name**	user							
3	**Project**	VALAGINIAN STUDY.pet							
4	**Date**	Monday, September 11 2017 19:37:59							
5	**From:**	TWT [ms]							
6	**To:**	Z [m]							
7	**XY:**	[m]							
8									
9	**1AT1 Seismic**	**Well**	**X-value**	**Y-value**	**Z-value**	**Horizon after**	**Diff after**	**Corrected?**	**Information**
10		Ha-K1 well	379334.0	6193176.1	-1532.00	-1532.00	0.00	Yes	
11		Ha-B2 well	372165.5	6191962.5	-1131.60	-1131.60	-0.00	Yes	
12		Ha-A1 well	377992.3	6197498.7	-901.00	-901.00	0.00	Yes	
13		Ha-G1 well	380092.1	6202877.0	-1071.60	-1071.60	-0.00	Yes	
14		Ha-I1 well	381116.3	6208695.3	-693.00	-693.00	-0.00	Yes	
15									
16	**J Seismic horiz**	**Well**	**X-value**	**Y-value**	**Z-value**	**Horizon after**	**Diff after**	**Corrected?**	**Information**
17		Ha-N1 well	378486.7	6211841.1	-2949.00	-2949.00	0.00	Yes	
18		Ha-B2 well	372165.5	6191962.5	-1504.60	-1504.60	0.00	Yes	
19		Ha-A1 well	377992.3	6197498.7	-1137.00	-1137.00	-0.00	Yes	
20		Ha-I1 well	381116.3	6208695.3	-1202.00	-1202.00	-0.00	Yes	
21									
22	**P1 Seismic hor**	**Well**	**X-value**	**Y-value**	**Z-value**	**Horizon after**	**Diff after**	**Corrected?**	**Information**
23		Ha-K1 well	379334.0	6193176.1	-1773.00	-1773.00	-0.00	Yes	
24		Ha-B2 well	372165.5	6191962.5	-2397.60	-2397.60	0.00	Yes	
25		Ha-G1 well	380092.1	6202877.0	-1514.60	-1514.60	0.00	Yes	

Figure 4. 20: Showing the results of the velocity modeling correction for the wells.

4.3.7 Creation of Polygon

The polygons (Figure 4.21) were created to cover an appropriate area of the different seismic horizons mapped from the 2D-seismic processed data lines based on the well formation tops from the seismic data lines. This was later used to model the surface generated for this study. Figure 4.21 below shows the polygon created around the seismic horizons.

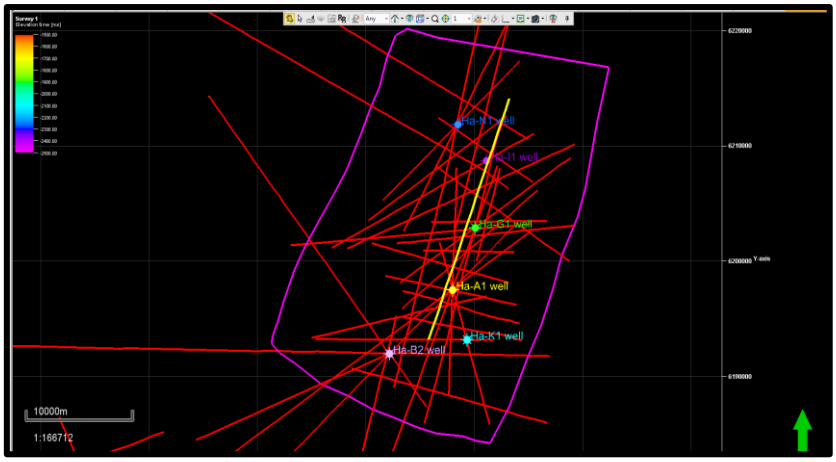

Figure 4. 21: Polygon created covering the maximum area of the horizons mapped from the wells shown.

4.3.8 Simple 3D Grid and Structural Framework

A simple 3D grid process was performed in this study in order to create cell grids that will contain the geometry of the reservoir to denote the geological and petrophysical information of the reservoir properties. This is due to the nature of available data of 2D seismic process data which do not allow enabling of a 3D model directly. The grid cells have an optimized increment of 50 m by 50 m along X and Y direction respectively and limits of 561 * 718 nodes dimension (Figure 4.22). The created 2D horizon surfaces recorded in-time were converted to surface depth and moved into the structural framework and converted to simple 3D grids through structural gridding to enable the discrete populating of the facies and petrophysical property values into the grid cells for the characterization of the geometry. The grid cells were oriented in the north-south direction along the well's position and the 3D grid model.

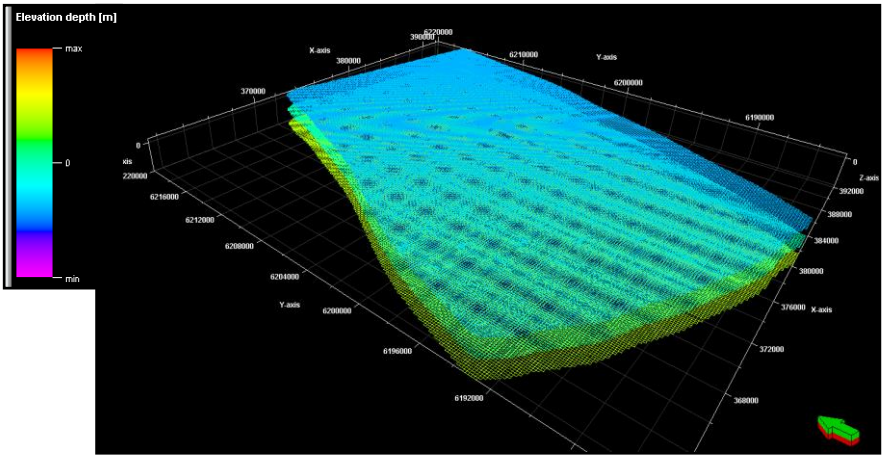

Figure 4. 22: The simple 3D cellular gridding cells (207 x 238 x 21) area built through structural gridding for this study.

4.3.9 Horizon modeling

Horizon Modeling formed part of the structural model of this study to create zones, to honour the stratigraphic relationship established with the seismic technique. Such relationship includes conformable, baselap or truncation as types of contact. Seismic techniques are also used to validate the geologic interpretation as well as to denote the sediment deposition pattern. These are constructed based on the depth-seismic horizon surfaces converted from time-seismic horizons surfaces of the P1, J1 and 1At1 top sequences (Berriasian-to-Valanginian-to-Hauterivian) displayed in Figure 4.23a, from bottom to the top. The volume based modeling method with comformable horizon relationship types was used to model these horizon surfaces. Figure 4.23b, shows the focus zones of the horizon modelling of this study with the conformable sequence surfaces' top sequences of Valanginian (J1) and Berriasian (P1).

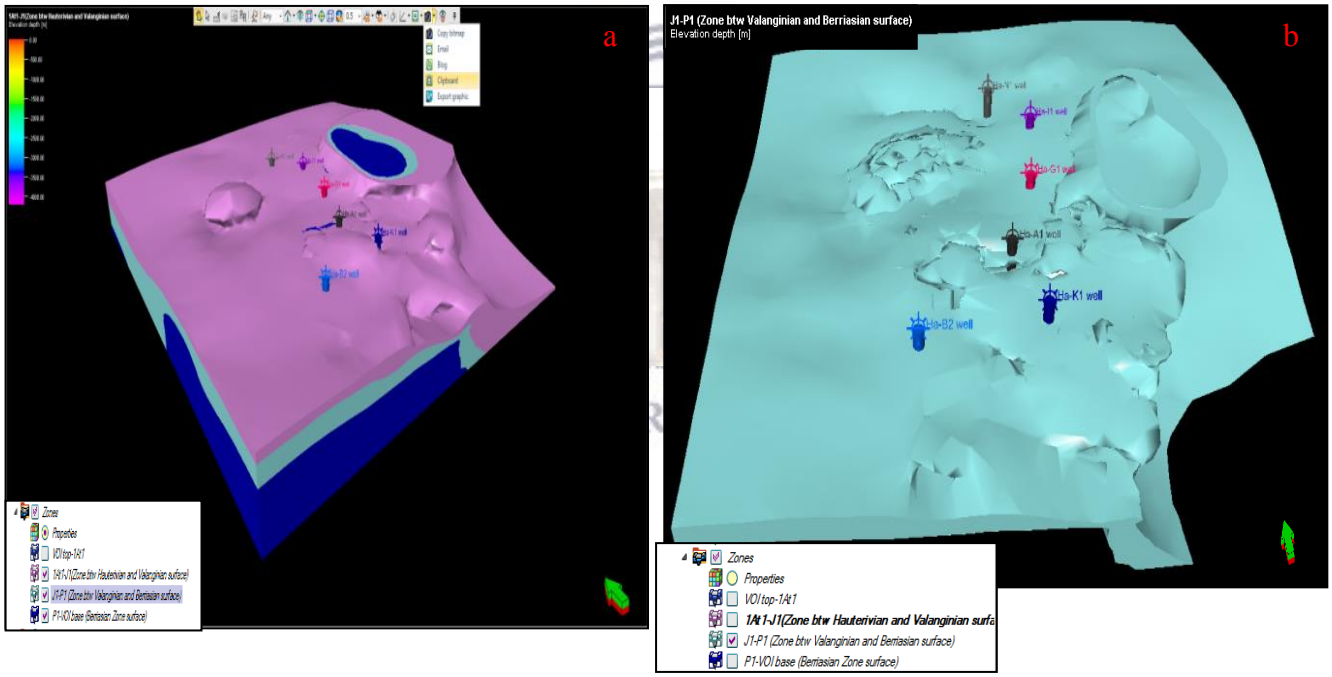

Figure 4. 23: (a): Zones of the horizon modeling with the conformable sequence surfaces P1, J1 and 1At1 top sequences from bottom to the top sequence (Berriasian, Valanginian –to- Hauterivian). (b): Zones of the horizon modeling with the conformable sequence surfaces top sequences of Valanginian (J1) and Berriasian (P1).

4.3.10 Upscaling of parameters method

Upscaling (U), (Figure 4.24), was performed in this study because the volume of data logs is very tiny, and to observe the properties in a cell, the mean of these points has to be displaced in the cell. Another reason for upscaling is to assign the well log value to the cells where it is intersected by the well path. The created geologic facies derived from the gamma ray log and petrophysical properties such as porosity, water saturation and permeability calculated from the reservoir zones in the wells, were exported as LAS format from the IP (Interactive Petrophysics®) software, imported and loaded onto a Petrel 2014® workstation after which Upscaling was performed. The treat-log line and neighbour-cell method which enabled all penetrated cell layers relatively to their variogram distance to populate facies, were adopted for the upscaling of the facies. The averaging method by arithmetic mean was used to upscale the additive petrophysical properties such as porosity and water saturation. The geometric mean method was adopted in upscaling the calculated permeability (K), because of its spatial correlation in the reservoir and because it is log normally distributed, as well as its sensitivity to lower values. The "Most of" algorithm upscale method value, being the most represented in the penetrated cells, was used for the facies upscale. Figure 4.24 illustrates the Upscaling parameter along the well path.

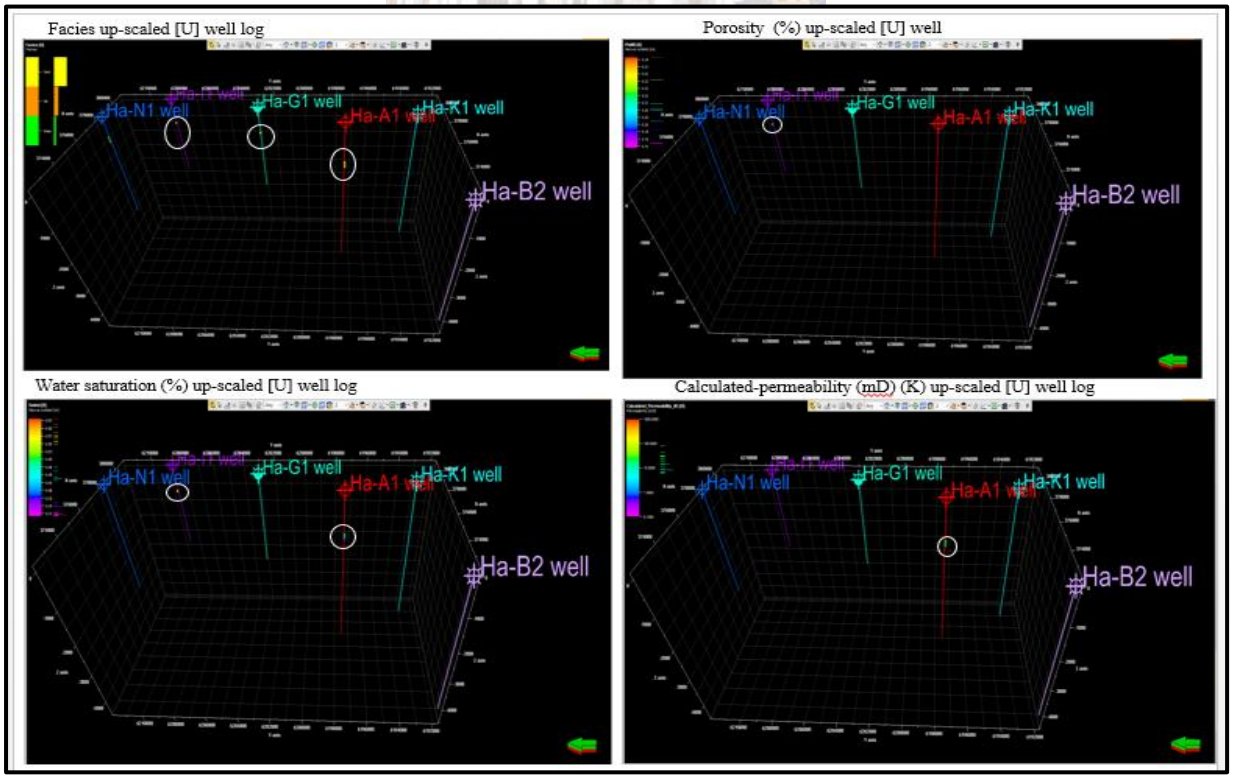

Figure 4. 24: Dots in circles indicate the Up-scaled well logs parameters along the well path.

4.3.11 The Variogram

A Variogram is basically a description of the spatial variation of a reservoir's properties. The variogram was applied in this study because histogram graphs alone cannot disclose the location and directional change of the distribution of reservoir properties, however it can provide a broad information about the details. To understand the varaiability structure of distributed reservoir properties, a spherical variogram model with sills, known as a transition model which describes the data and serves as input into the property modeling, was adopted in this study. However, a variogram model without a sill is also known as a non-transition model. Variogram data for each property upscaled were generated to identify anisotropy and direction of maximum data continuity of the Variogram model properties. The Variogram parameters values such as Sill of 1.0, Nugget of 0.0001, and anisotropy range of 14416, of both major and minor directions in vertical direction for well information and area variation, an azimuth of 63° with dip 0^{o}, in clockwise direction and spherical variogram type was selected and applied to generate an accurate result of the Variogram model. Thus, the resultant model was used in populating the facies and petrophysical properties in the 3D grid cells, using the stochastic simulation algorithm method by means of the Gaussian Random Function Simulation (GRFS) algorithm modeling in this study.

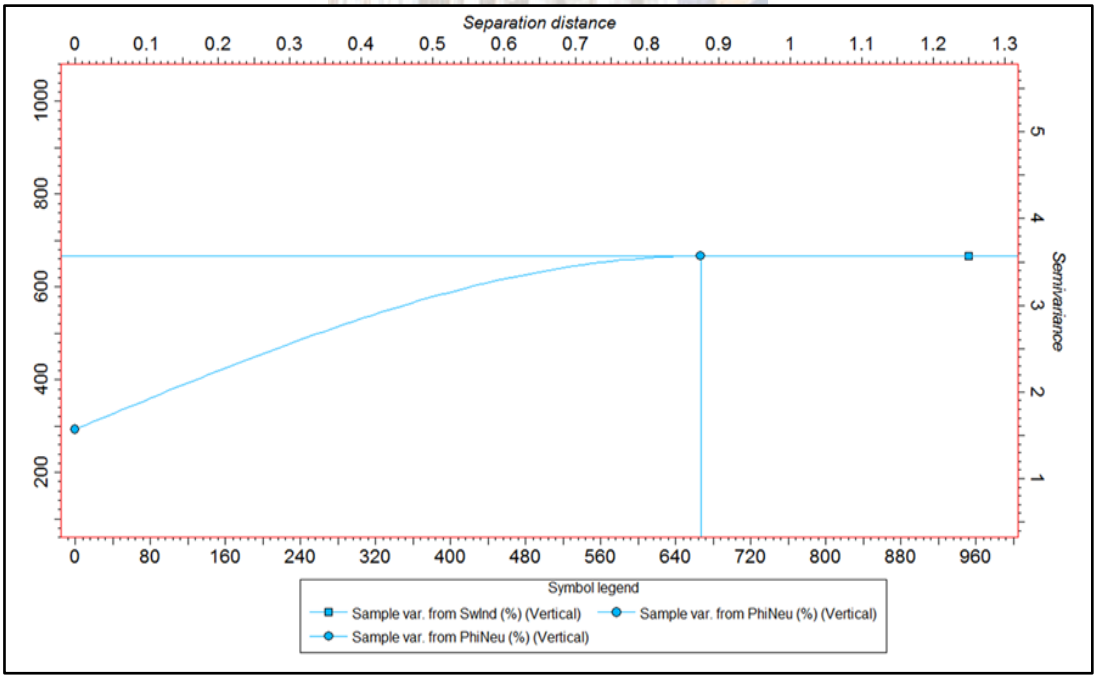

Figure 4. 25: Sample variogram (semi variance) combining neutron-porosity and water saturation generated data analysis.

4.3.12 Facies modeling

After the upscaling of the properties, the next level was to generate the facies model. The facies model was generated for the depositional sequence focus on this study, the J1 top horizon of Valanginian age. The Stochastic Simulation method by means of the Sequential Indicator Simulation (SIS) algorithm using a Kriging indicator was adopted for this model; after the upscaling of the Facies log, (Figure 4.26 a & b indicating the Interface model from the software used). The lithofacies were discriminately coded at the wells based on log data, primarily the gamma ray logs (GR) available for the wells by using Python script; (Gamma Ray (GR 1) < 80, 0, If (GR 1)>80 GR 1< 102, 1, 2)). Where 0 represents sandstone, 1 represents siltstone and 2 represents shale. The GR values less than 80 API are classified 0, (Sandstone), GR values between 80 – 102 API classified as Siltstone, while GR value greater 102 API are classified as Shale.

Finally, the Stochastic method by sequential indicator simulator method was applied to simulate a discrete property (facies) using the Kriging indicator, which is controlled by taking an average frequency and variation of the discrete spatial continuity. This method was considered reasonable for this modeling due to its ability to enabling easy modeling of facies environments where the facies volume shares vary vertical, laterally or both. Also ensure to transform a continuous distribution to a discrete distribution and its drive to simulate complex facies heterogeneity (Yu & Li, 2012).

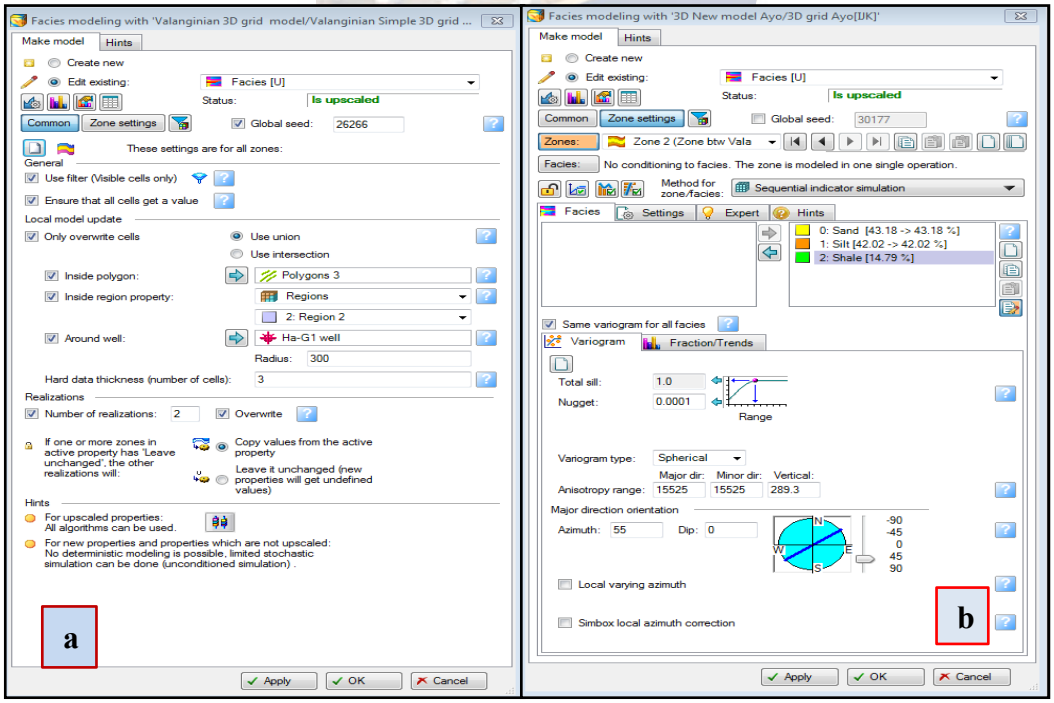

Figure 4.26: a & b shows the interface for facies modeling procedure of the J1 Valanginian sequence study area.

4.3.13 Petrophysical modeling

The petrophysical model was performed in this study for the Valanginian sequence (J1 horizon), after the up-scaling of the petrophysical properties (porosity, permeability and water saturation) logs in order to populate the grid cells. The Stochastic simulation algorithm method by means of Sequential Gaussian Simulation (SGS) method was geostatistically applied in assigning the properties that were adopted for this study. Figures 4.27, 4.28 and 4.29 a-f respectively indicate the Interface model procedures for the various properties as derived from the Petrel2014®software. This method was adopted due to

- its ability to enabling modeling of properties by lithofacies,
- its honouring of the well log data,
- its input parameter distributions,
- its ability to produce histograms, and
- because it provides a clear variogram and trends.

The variogram and distribution are also used to illustrate local variation. Similarly, the simulation is most suitable for use in situations where the shape of a particular facies body is uncertain. Furthermore, the program runs fast and produces an accurate result with variability in distributions.

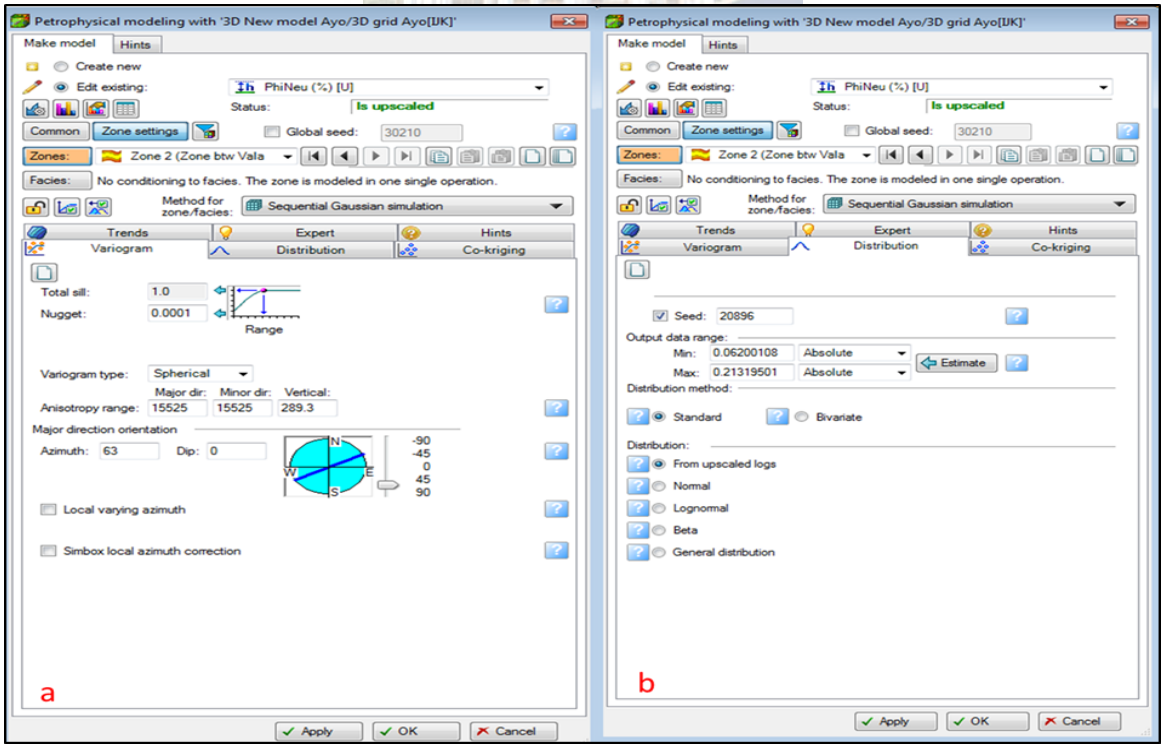

Figure 4. 27 a & b: showing the interface procedures for the distributions of petrophysical properties (porosity) top of Valanginian sequence of the study area.

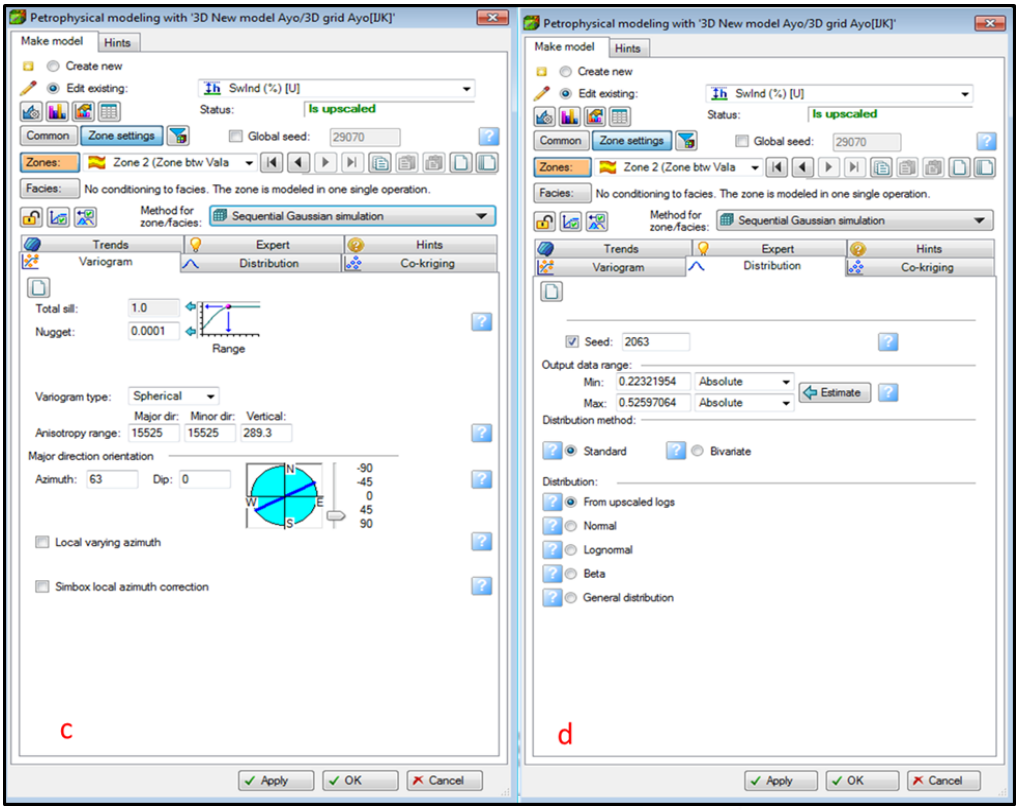

Figure 4. 28 c & d: showing the interface procedures for the distributions of petrophysical properties (water saturation) top of Valanginian sequence of the study area.

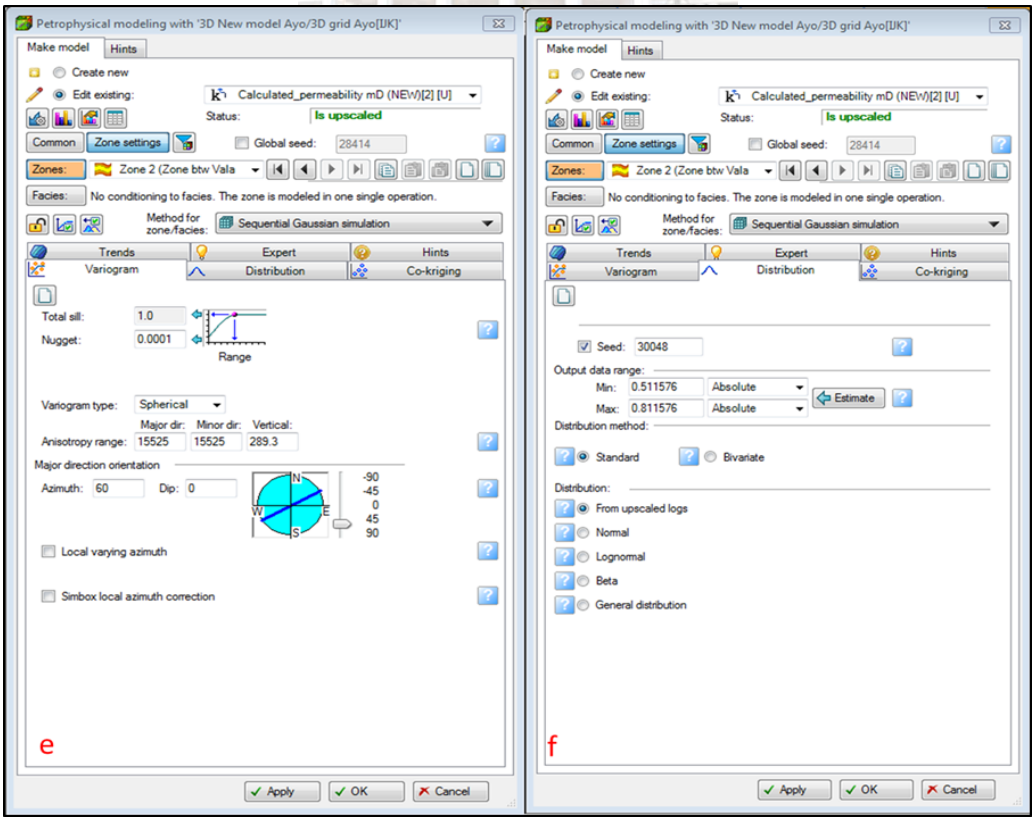

Figure 4. 29 e & f : Showing the interface procedures for the distributions of petrophysical properties (Permeability) top of Valanginian sequence of the study area.

4.3.14. Stratigraphic well correlation

Stratigraphy well correlation was performed for this study. This correlation were carried out using the Gamma ray (GR) log data from the wells through formation well tops loaded into Petrel software workstation. The facies were to deduce the lithology well discriminated based on the gamma ray logs curves cut-off value obtained from the wells. This were performed to enabling well-to-well correlation, with the objective of defining the stratigraphic horizons bounding the main geological sequence trend and depth correlating across the wells along the study sequence. The (Figure 4.30) shows the well correlation across the wells for the main focus J1 horizon Valanginian sequence.

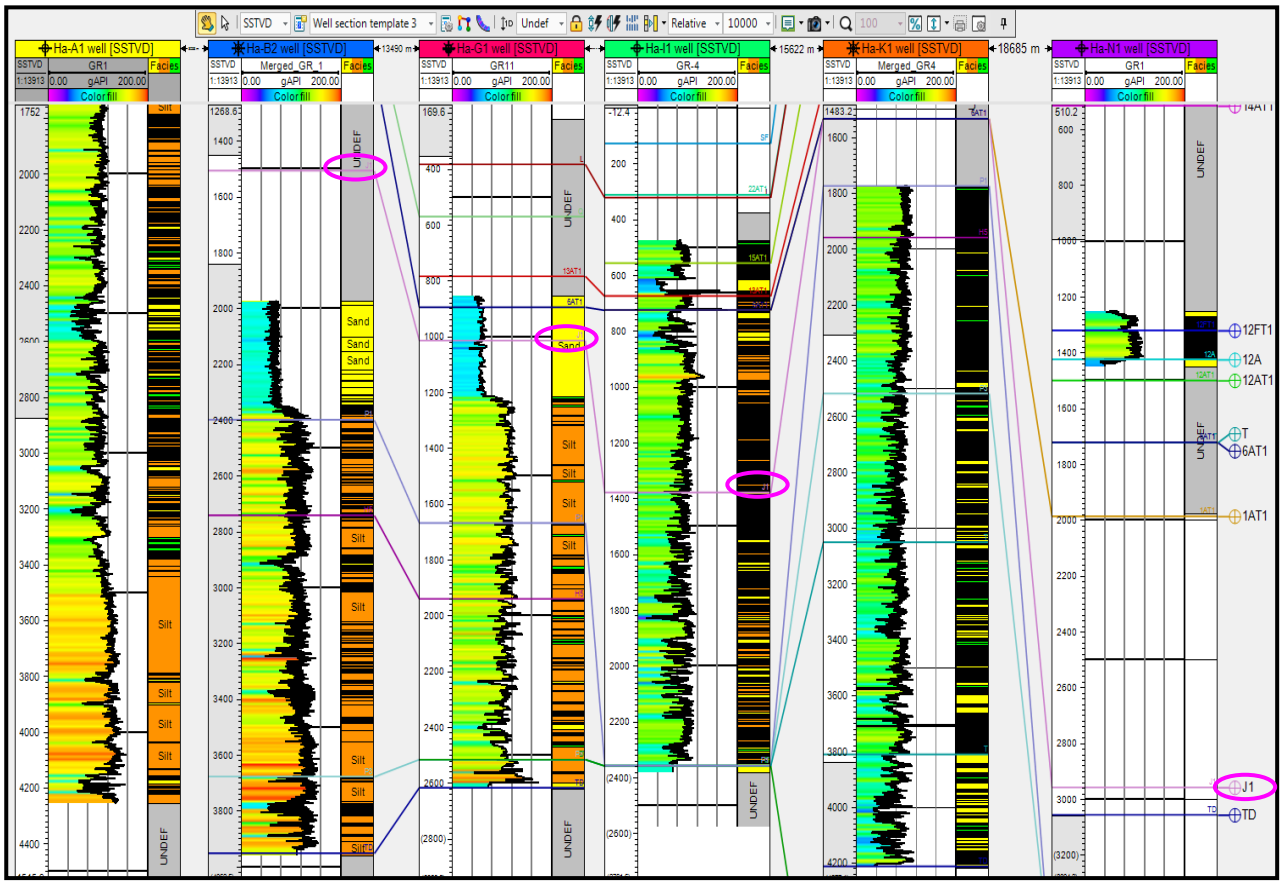

Figure 4.30: Well correlation across the wells for the main focus J1 horizon, Valanginian sequence.

4.4 Seismic Sequence and Seismic Facies Analysis Methods

The seismic analysis that was carried out for the study of the Valanginian sequence involves two procedures, namely, Seismic Sequence Analysis and Seismic Facies Analysis; both are described in detail under Chapter FIVE of this thesis. The lines used are a processed regional seismic line Ha87-047 which was shot from Northeast (NE)-to-Southwest (SW), and a processed local seismic line Ha85-005 shot from North (N) to East (E) at the centre part of the study. Finally, the local processed seismic line Ha82-0214 which was also shot from South (S) to East (E) in the southern party of the study area was used to interpret the seismic sequence and seismic facies analysis of the Valanginian sequence respectively.

The first procedure was the seismic sequence analysis. This involved the identification and mapping of the major seismic sequence boundaries, based on seismic reflections. This was done by subdividing the sedimentary sequence into genetically related units i.e. a depositional sequence by identifying the seismic reflection termination patterns such as toplap, onlap, downlap, and erosional truncation.

The second process is followed by seismic facies analysis that was interpreted by means of identifying the seismic facies units, such as amplitude reflection strength, the frequency reflection, internal reflection configuration, and the external geometry form of the three dimensions that are associated with the facies units. These were recognised and interpreted using simple techniques explained by Mitchum, (1977) i.e. the seismic attributes reflection such as geometric reflection, amplitude reflection, reflection continuity and wave frequency attributes. This was also calibrated with gamma ray (GR) well log for the available wells. These procedures were all combined to predict the depositional environment that controls the sediments deposited in the Valanginian sequence of Gamtoos Basin. Figure 4.31 illustrates the general methodology framework for seismic sequence and seismic facies analysis for this study.

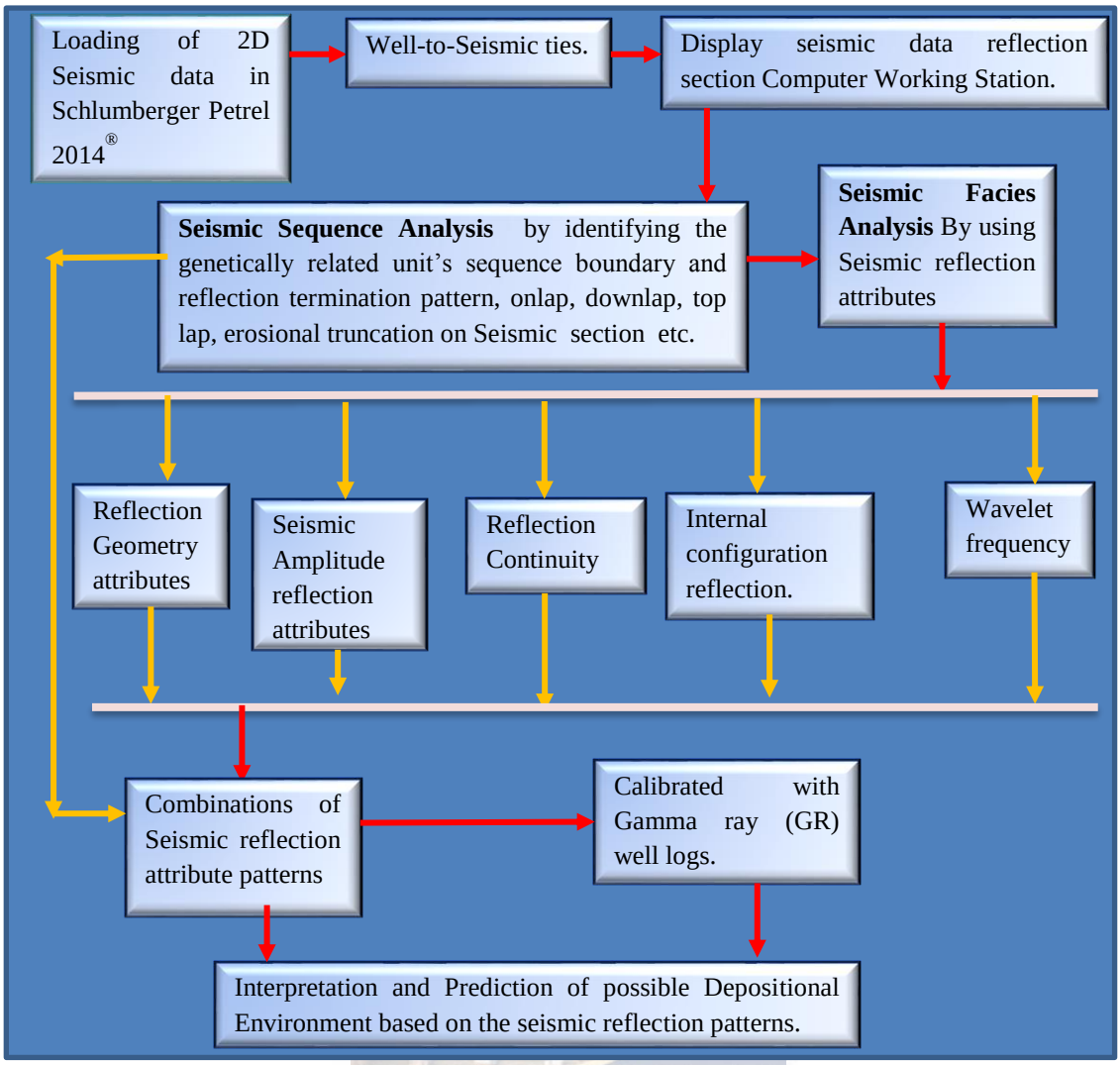

Figure 4.31: The general methodology framework for seismic sequence and seismic facies analysis for this study.

4.5 Biostratigraphic Analysis Methods

For the current biostratigraphic analysis no conventional core samples were available from the Valanginian section of the wells. Only unwashed well cuttings were available for analysis from two wells Ha-G1 and Ha-I1. The samples were selected after careful examination of the well logs and by megascopic examination. The procedure of sample selection and methodology of processing before biostratigraphic analysis is discussed in detail under the Chapter SIX of this thesis.

The biostratigraphic analysis carried out during the course of the present work was initiated with the study the temporal distribution of marine microfossil group 'Foraminifera'. Application of foraminifera is well known in dating the sample deposited under marine environment and it helps to specify the various sub environments within a basin. As already mentioned, only unwashed samples were available for analysis from the Petroleum Agency South Africa (PASA). Samples for two exploratory wells Ha-I1 and Ha-G1 were considered in this work for detail analysis.

An amount of 20g of each sample unwashed samples were considered for processing for biostratigraphic analysis. Lithological detail of each samples were carefully noted before actual processing begins. The sample were mechanically disintegrated initially to free loose debris and thoroughly washed with water to remove any drilling fluid (drilling mud) present. The washed samples free of drilling fluid were then soaked in water and a little amount of H_2O_2 (30% Hydrogen peroxide solution) was added to it for disintegration of the rock chips. A small amount of caustic soda was added to the wet sample to enhance the breaking down process of the sediment particles. The wet sample was kept under this condition for 48 hours. The samples were further boiled for 30 minutes and then washed under running water with a 200 µm sizes mesh to remove excessive clay particles. The washed residue was transferred to the bowl and kept under electric oven to dry the water. Each of these samples were transferred in plastic containers with proper sample depth recorded labels for microscopic separation.

Before visualization of the sample under the Microscope, four sets of micropaleontological sieves such as 30, 60, 85 and 100 µm sizes (mesh) were arranged from bottom to top to subdivide the processed residue into different size fractions. The microfossils were isolated under a Stereozoom binocular microscope with incident light arrangement. The microfossils were picked with a picking brush (0, 00,000 size) and preserved in microfauna slides (single

punch or multiple chambers) for identification and further interpretation. Figure 4.32 below shows the general methodology framework of biostratigraphic analysis for this study.

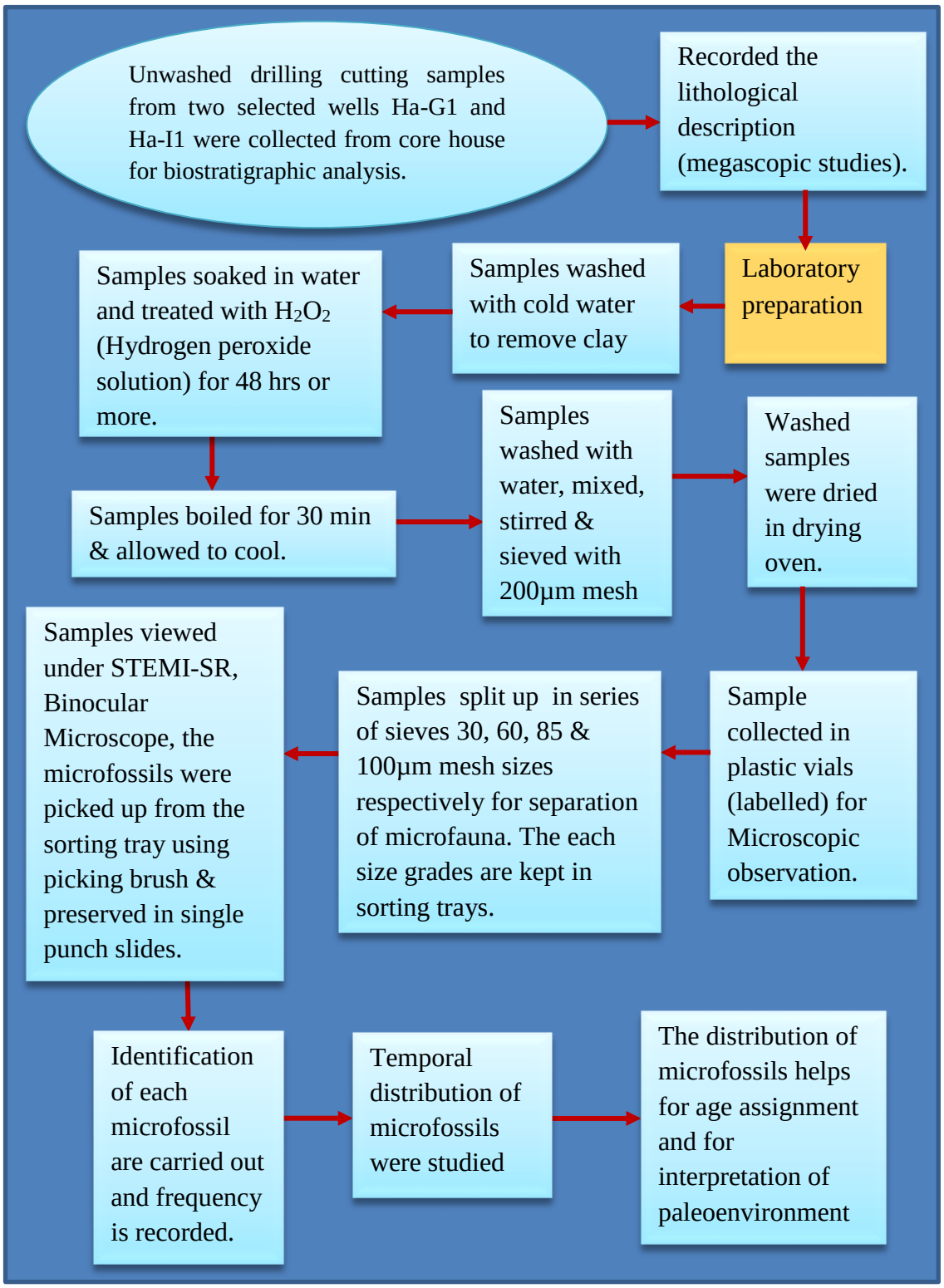

Figure 4.32: General methodology framework of biostragraphic analysis for this study.

CHAPTER FIVE

5 Seismic Sequence and Seismic Facies Analysis and Interpretation of Valanginian Depositional Sequence in the Gamtoos Basin, Offshore South Africa

ABSTRACT

The prediction of depositional environments and reconstruction of the reservoir geometry is of great significance in hydrocarbon exploration. Sedimentary facies distribution within a sequence is controlled by the environment of deposition. The analysis of facies within a basins based on seismic studies has become increasingly important in hydrocarbon exploration and is being used by most of the oil companies. The present study aims to determine and contribute to a better understanding of the depositional sequences by analysing information from the six drilled wells Ha-N1, Ha-I1, Ha-G1, Ha-A1, Ha-K1 and Ha-B2 from the north to the south for the Early Cretaceous Valanginian age group of sediments.

A comprehensive interpretation of the model by Vail, *et al.*, (1977) entails configuration and classification characteristics of seismic data reflection termination patterns, description of the seismic sequence, and seismic facies analysis of the sedimentary sequences. This was tied with well-logs (GR-ray) signatures from the wells and application of 3D-stochastic lithofacies model, were applied in this study.

The depositional sequence was mapped and interpreted on seismic-reflection data for the J1-horizon trending from north to south across the drilled wells in the basin. The interpretation configuration features are associated with seismic data reflection terminations patterns, according to the model by Vail, (1977) & Mitchum et al., (1977) for seismic sequence and seismic facies analysis. These are calibrated with well-logs signatures across the drilled wells from the north to the south of the study area indicating a mass flooding depositional sequence belonging to Valanginian age, deposited as channel-fill, submarine canyon, shallow marine- to deep marine off continental shelf, submarine fan lobe and basin floor depositional environments. The sediments around the study area were deposited in a shelf to deep marine environment.

The 3D stochastic lithofacies model derived from the surfaces attribute-depth-thickness map of the Valanginian depositional sequence revealed the facies and channels of a distributary depositional sequence pattern across the wells in the study area. The lithofacies model

exposed the effect of the erosional events that created hiatuses from the north to the south during this period. The Valanginian marine flooding of high energy density turbidites affected the basin from northeast to southeast of the study area, leading to massive sandstone deposits and intermittent siltstones with minor intercalated shale deposits. In the area between the northwest and the southern part massive silt- and shale deposits with an intermittent sandstone lithofacies of low energy turbidite channels was encountered. The northern part is generally dominated by shale with intercalated sandstones and minor silt.

Keywords; Depositional environments, Lithofacies, Sandstone, Silt, Shale, Turbidite, Well-logs signatures, Shallow marine, Deep marine, Seismic sequence and Seismic facies.

5.1 Seismic Interpretation

5.2 Introduction to Seismic Interpretation

This chapter presents the seismic interpretation based on seismic sequence and seismic facies analyses for the depositional sequence top of P1-to-J1-horizons (Valanginian section) of the Gamtoos Basin and to describe the depositional environment of the sequence. The framework of the seismic analysis and interpretation begins with the seismic sequence analysis which is again based on the depositional sequence identified on a seismic section (Mitchum Jr, *et al.*, 1977), by recognition and descriptions of the surface discontinuities, which are identified and interpreted in orderly patterns of reflection terminations along the discontinuity surfaces.

This is followed by seismic facies associations, which are analysed and interpreted on the basis of configurations of the seismic reflections such as, amplitude, continuity, frequency and the external geometry reflection. This was followed by tying the interpretations among all lines to obtain traces on similar surfaces of different lines, either parallel to or across each other. This was connected further into the study area to trace the surface in a larger possible area. Some of the surface lines are of regional significance passing through wells, while others are local lines passing through a particular well in some section of the study area.

The 2D regional extent seismic line (Ha75-12) shot from North-northeast (NNE) to South south-west (SSW), line (Ha87-047) shot from Northeast (NE)-to-Southwest (SW), cut across the wells Ha-G1 and Ha-A1 in the northern and southern part of the study area respectively. While the 2D-seismic lines Ha85-005 (NNE-NNW), line Ha82-12 (N-to-E), line Ha82-14(S-to-E), and line Ha76-031(E-to-W) were shot locally in the Northern and Southern part of the study area and cut across wells Ha-B2, Ha-I1,Ha-K1, Ha-N1 respectively. All these lines were used for the interpretation of the seismic sequence and seismic facies analysis and to examine the lateral changes patterns of the sedimentary succession across the study area.

For a detail interpretation understanding of the depositional environment of the sedimentary succession, the information collected from the seismic facies analyses were calibrated with electrical well logs available from the wells that are drilled through the Valanginian succession (JI horizon). However, for the wells where such logs are not available the interpretations were carried out on their seismic reflection attributes, centred on the internal reflection configuration, the three-dimensional external geometry form, that is associated

with the facies units, using simple techniques as explained by Mitchum Jr, *et al.* (1977a). Figure 5.1 shows the map window of the 2D-seismic lines across the wells for the interpretation of the seismic sequence and seismic facies analysis.

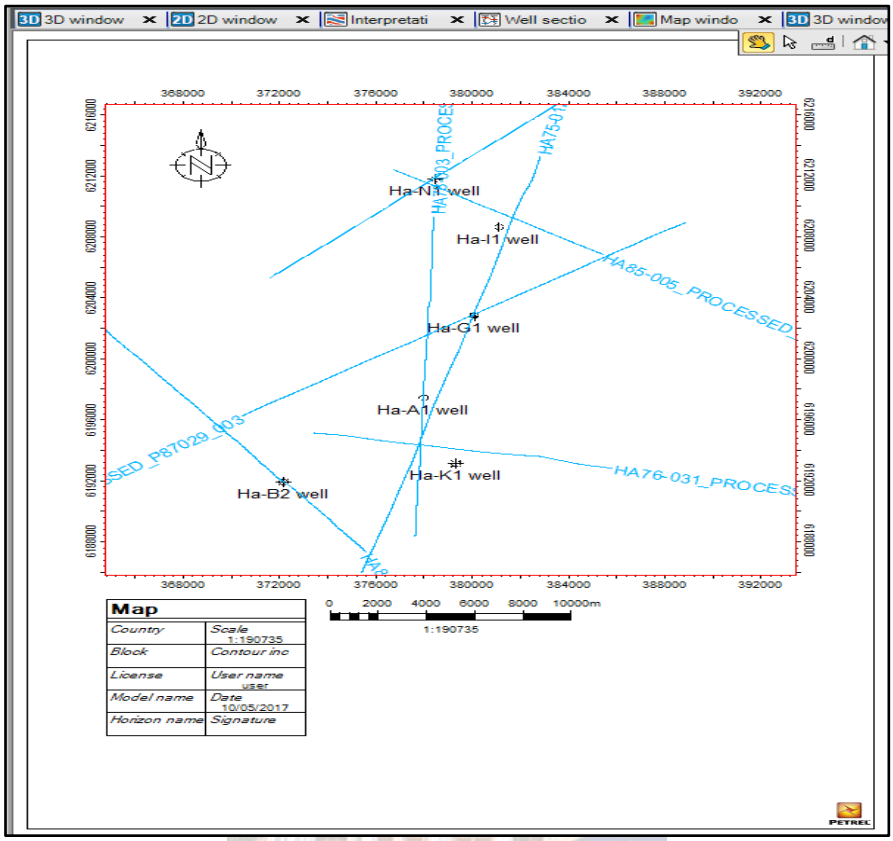

Figure 5. 1: Map window of the 2D-seismic lines across the wells utilized for the interpretation of the Seismic sequence and Seismic facies analysis (Seismic stratigraphy analysis).

5.2.1 Seismic Sequence Analysis and Interpretation of Results

5.2.1.1 Introduction to Results of Seismic Sequence Analysis and Interpretation from Seismic Lines

The objective of the seismic sequence analysis is to interpret the depositional sequence on seismic section by demarcation of discontinuities based on reflection terminations. The techniques and concepts for seismic sequence analysis are worked out by the Exxon group in the late 1970's (Vail, *et al.*, 1977) where the seismic sections were subdivided into packages of concordant reflections separated by sequence boundaries. The identification of a sequence boundary is focused on the reflection termination deposition patterns, such as toplap, erosional truncation, onlap and downlap (Figure 2.2).The regional extension 2D-seismic

interpretation was done for the seismic sequence analysis of line Ha87-047 shot from the Northeast (NE)-to Southwest (SW) , which is intersected by well Ha-G1, and is perpendicular to the 2D-seismic line Ha75-012 that intersected wells Ha-I1 and Ha-A1, shot from North-northeast to South south-west. As stated above, this was done to delineate the depositional pattern of the Valanginian section (P1 - JI horizons) from the northern part of the study area to the south.

The 2D-seismic line Ha87-047 was interpreted corresponding with its sequence boundaries and the intersected wells. The J1 horizon corresponding to the Valanginian section of Early Cretaceous of the Gamtoos Basin has been subdivided into three seismic depositional sequences, on the basis of their geometry and nature of the sequence boundaries surfaces (SB I, SB II, SB III, and SB I) within the area. These are named as sequence I, II and III respectively (Figure 5.3). The seismic sequence under these studies was defined based on unconformities and their correlative conformities. However, within each of the seismic sequences, seismic facies were interpreted based on criteria of the classification summarized by Mitchum Jr, *et al*., (1977a) and Sangree & Widmier, (1977); Sangree & Widmier, (1979).

The sequence boundaries were mapped within a time window of -1617.29ms, -1434.25ms, -1193.55ms and -1019.83ms two-way travel time (TWT) respectively throughout the study area. The sequences were mapped from discordant relationships of lithological units at the sequence boundaries. These intervals were defined based on seismic reflection patterns, configurations and lithofacies, the sequence boundaries are laterally extensive and conformable in stratigraphic order from the oldest sequence (Sequence I) to the youngest sequence (Sequence III); these sequences are affected by erosion, thus developing erosional surfaces.

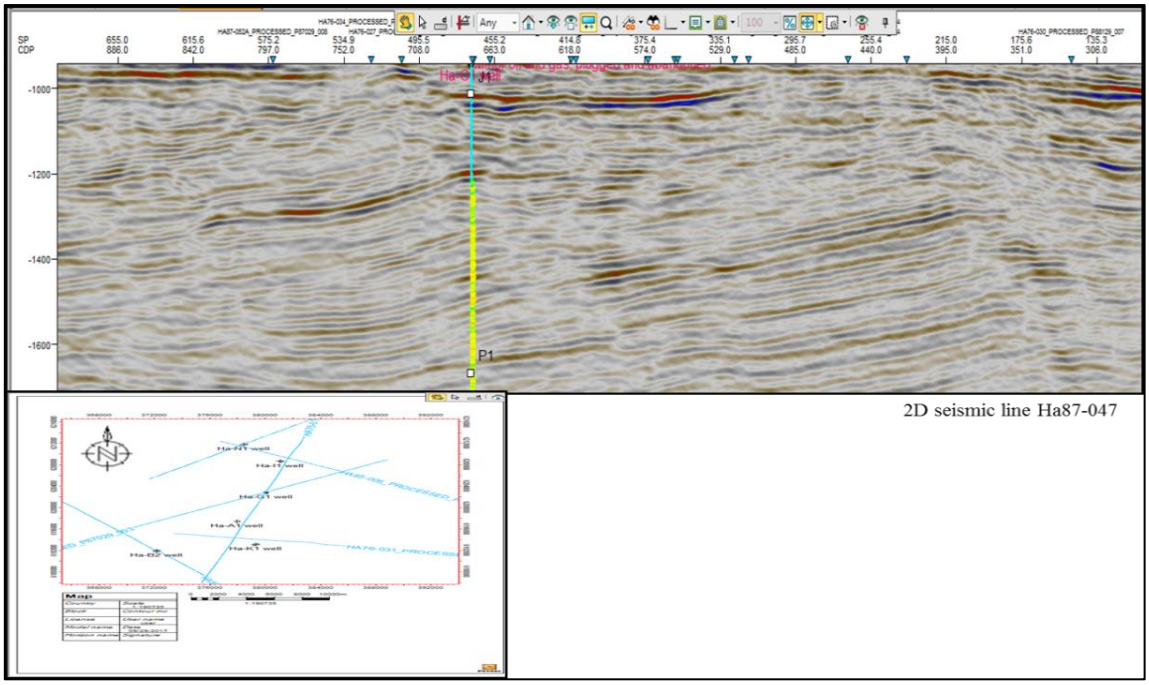

Figure 5. 2: Un-interpreted 2D-seismic line Ha87-047 seismic cross section reflection shot from NE-to-SW direction intersected by well Ha-G1, Northern part of the study area.

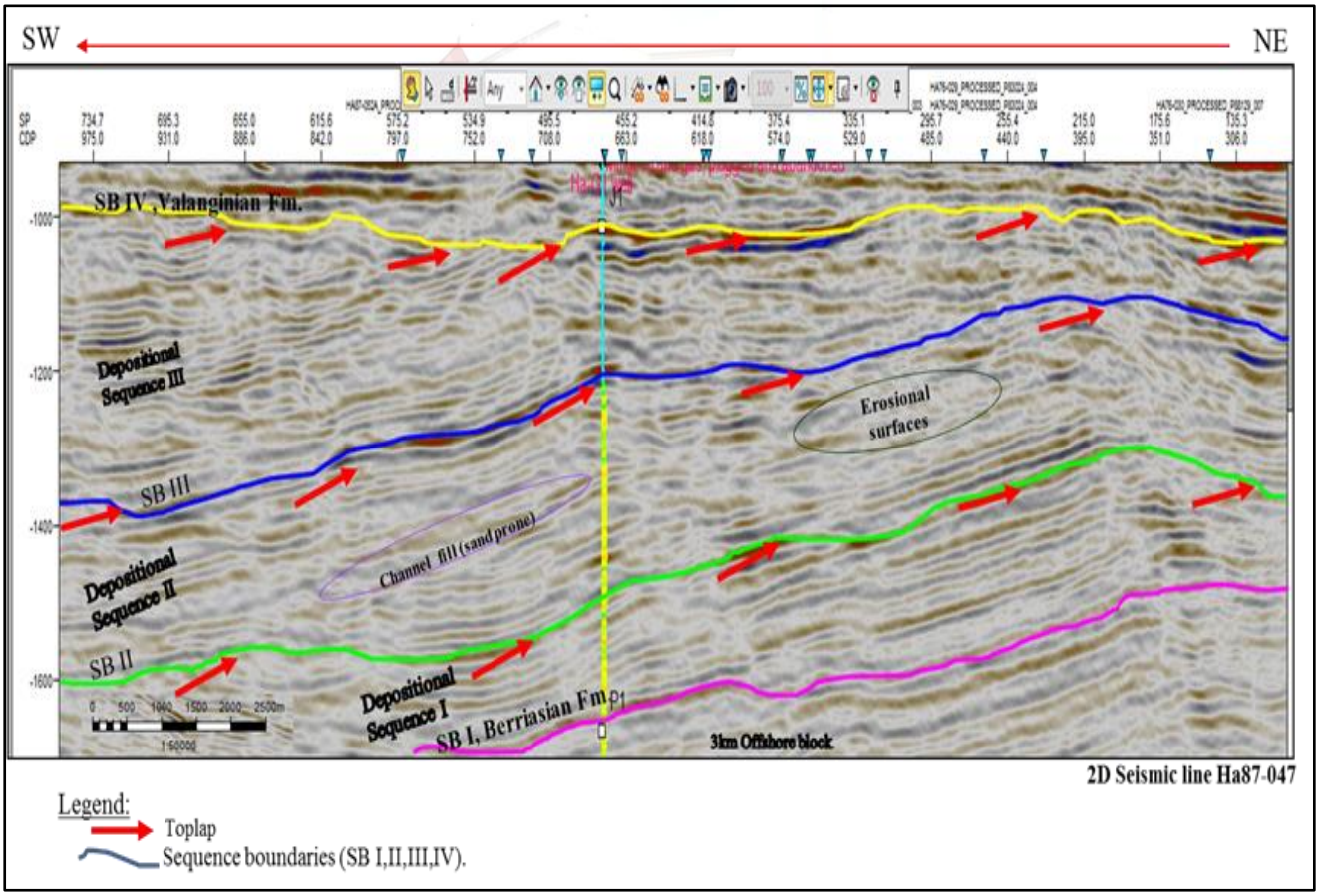

Figure 5. 3: Interpreted 2D-seismic line Ha87-047 and well Ha-G1 seismic sequence analysis cross section reflection shot from NE-to-SW in the Northern part of the study area with sequence boundaries SB1, SBII, SBIII and SB IV separating different geological units.

5.2.1.2 The Analysis and Interpretation of Seismic sequence of Valanginian Section (top of P1-J1 horizons) around the well Ha-G1 Northern part (North east-to-Southwest) of the study area

The seismic sequence analysis of the Valanginian succession around well Ha-G1 was interpreted based on the seismic reflection of 2D-seismic line Ha87-047 shot from Northeast to Southwest and intersected well Ha-G1 which was located and drilled at the northern part of the study area. Within this Valanginian succession, three depositional sequences were identified and defined on the basis of their sequence boundary surfaces. The sequence boundary (SB 1) represents the top of P1 formation of Berriasian sequence, (base of J1 horizon belonging to Valanginian age, Early Cretaceous) on seismic reflection in this basin. While the sequence boundary SB IV represents the top of J1 horizon (Valanginian), the sequence boundaries SB II and SB III are the successive sequence boundaries within the entire succession below J1 horizon (Valanginian) to the P1 horizon of the Berriasian age.

These sequence boundaries were characterized by a series of depositional sequences namely sequence I, II, and III (Figure 5.3). Conversely, based on the observation from the cross section of the seismic reflection termination pattern of the depositional sequences I, II, and III of the 2D-seismic line Ha87-047 in the northern part of the study area, the reflection termination discordance patterns were marked by characteristic strong toplap terminations of the sediments associated within the horizon. A toplap is a discordant relationship, and marks the termination of strata at the top against the younger units above i.e. the older horizons sequence boundaries are terminating against younger horizons sequence boundaries such as SB1, SBII, SBIII and SB IV respectively (Figure 5.3).

This represents a period of non-deposition and development of minor erosion surfaces above the wave base in still-stand sea level, while the deposition is moving gradually towards the proximal part of the basin. This type of discordant termination is commonly found in deep marine environment. Therefore, it is concluded that in the northern part of the study area around well Ha-G1, the depositional environment on the top of P1-to-J1 horizons (Valanginian succession) is deep marine and possibly was a submarine fan under abyssal depth. It also indicates the period of non-deposition of sediments and the development of an erosional surface in later stage.

5.2.1.3 The Analysis and Interpretation of Seismic sequence of Valanginian Section (top of P1 - J1 horizons) around well Ha-I1 (North-to-East) in the northern part of the study area

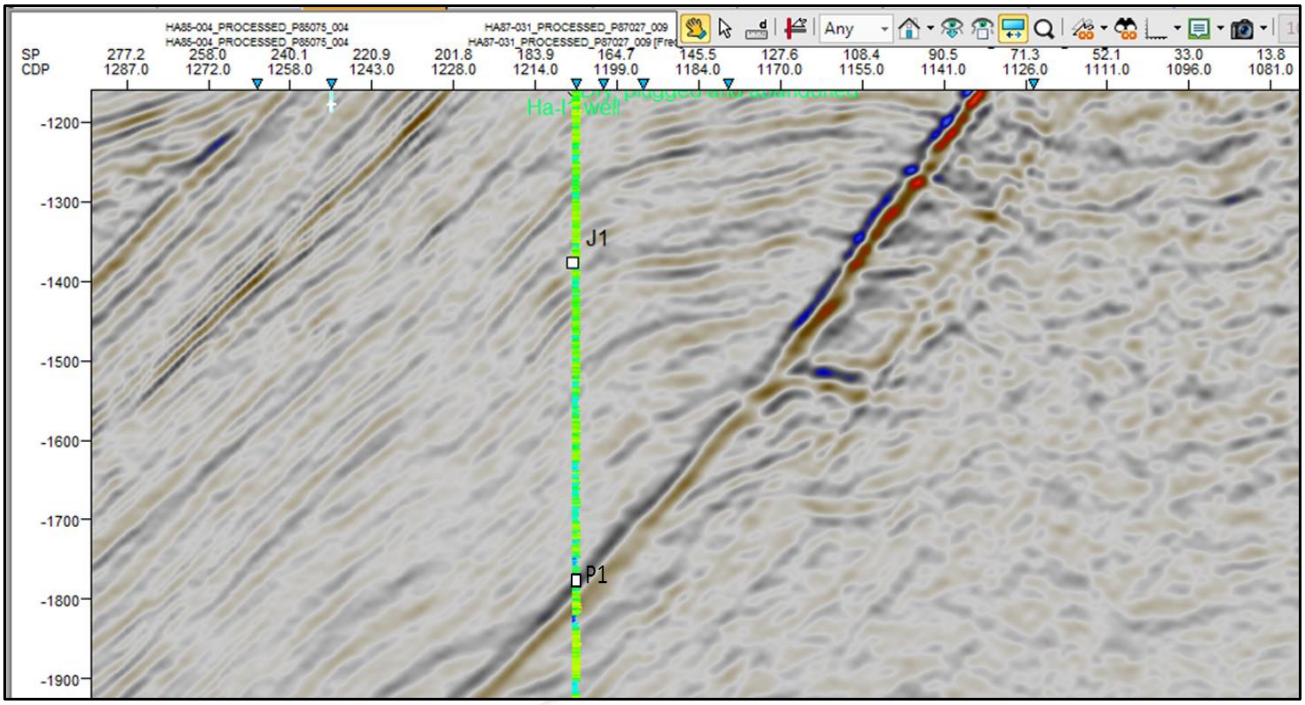

Figure 5. 4: Un-interpreted 2D-seismic line Ha85-005 seismic cross section reflection shot from North to East intersected by well Ha-I1, Northern part of the study area.

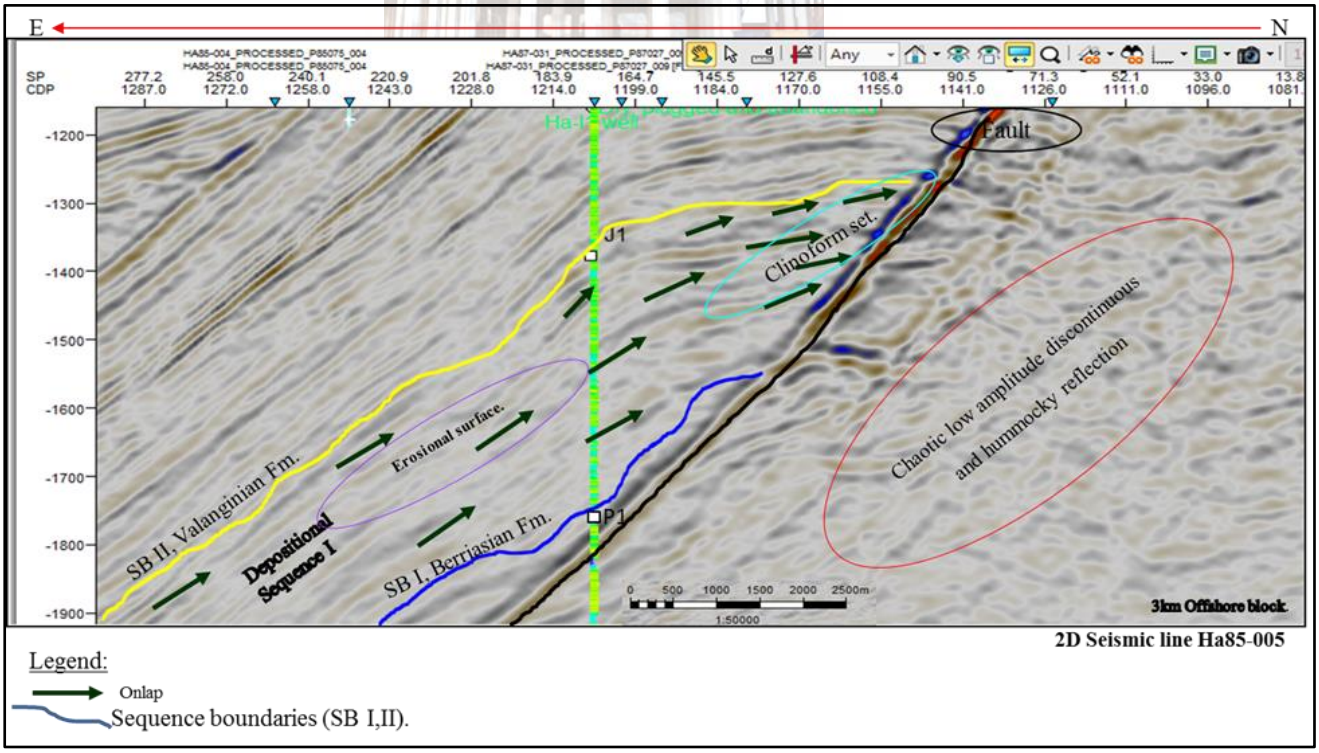

Figure 5. 5: Interpreted 2D-seismic line Ha85-005 (well Ha-I1) seismic sequence analysis cross section reflection shot from N-to-E direction in the Northern part of the study area with (SB1 and SBII) sequence boundaries separating different geological units.

In the Northern part of the study area, 2D processed seismic line Ha85-005 which was shot in the direction from the North to East, was used to interpret the seismic sequence analysis of this region, to understand the depositional environment settings. In this region, the 2D-seismic line Ha85-005 was intersected by well Ha-I1 at -1317.33 ms and -1753 97 ms two-way-time through the well formation tops of J1 horizon of the Valanginian sequence and the P1 horizon of the Berriasian sequence respectively (Figure 5.5). There is evidence of deformation which resulted in an inclined normal fault that trends NE to SW, encountered at -973.6 ms to 1905.16 ms TWT on the seismic cross section reflection on this sequence (Figure 5.5).

The two sequence boundaries SB I and SB II identified on the seismic reflection cross-section represents the top of P1 horizon (Berriasian) and the J1 horizon (Valanginian) respectively. In-between the sequence boundaries, depositional sequence I was recognised. This was based on related characterization of termination depositional sediments showed as an onlap discordant pattern (Figure 5.5).

The definition of an onlap is a base-discordant reflection termination relationship, in which horizontal strata progressively terminate against an inclined surface, indicating a proximal deposition of sediment i.e. sediments deposited close to the sediments' source. This reflection termination pattern is commonly observed in marine depositional environments as aggrading marine sediments on basin slopes in a deep marine environment. The depositional sequence I sediments between the sequence boundaries SB I and SB II of P1 horizon of the Berriasian and J1 horizon of the Valanginian respectively, show on cross section reflection of 2D-seismic line Ha85-005, a classical reflection of an angular unconformity, (Figure 5.5) in which the depositional sediments patterns are onlapped associated with these horizons. Hence, it is suggested that the depositional environment setting of formation J1 at the top of the Valanginian section in the northern part of the study area deposited in a deep marine environment probably as basin floor environments and deposited close to their source.

In addition, the seismic surface of marine onlap has been proposed to represent the marine hiatus (time gap) i.e. the period of non-deposition or condensed interval (Mitchum Jr, *et al.*, 1977a). This hiatus surface can be observed on the cross section 2D-seismic reflection line Ha85-005 (Figure 5.5) as the remnant erosional feature (channel sand) of Valanginian section.

5.2.1.4 The Analysis and Interpretation of Seismic sequence of Valanginian Section (top of P1 - J1 horizons) around well Ha-B2 Southern part (South-to-East) of the study area

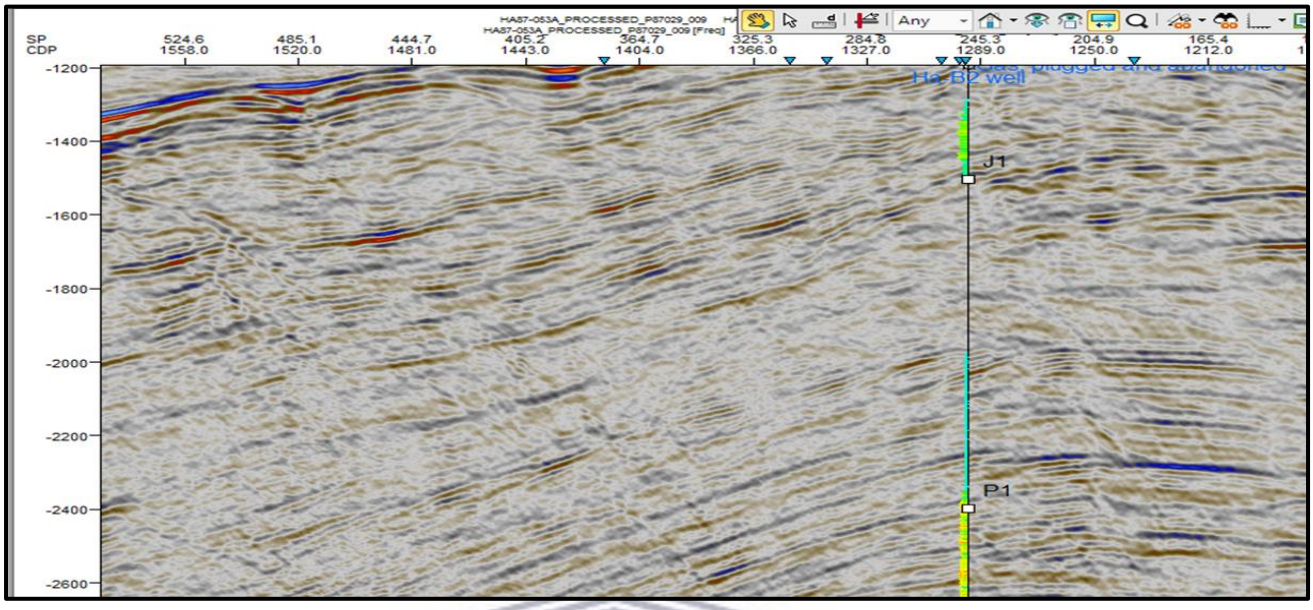

Figure 5. 6: Un-interpreted 2D-seismic line Ha82-014 (well Ha-B2) seismic cross section reflection shot from South- to- East intersected by well Ha-B2, in Southern part of the study area.

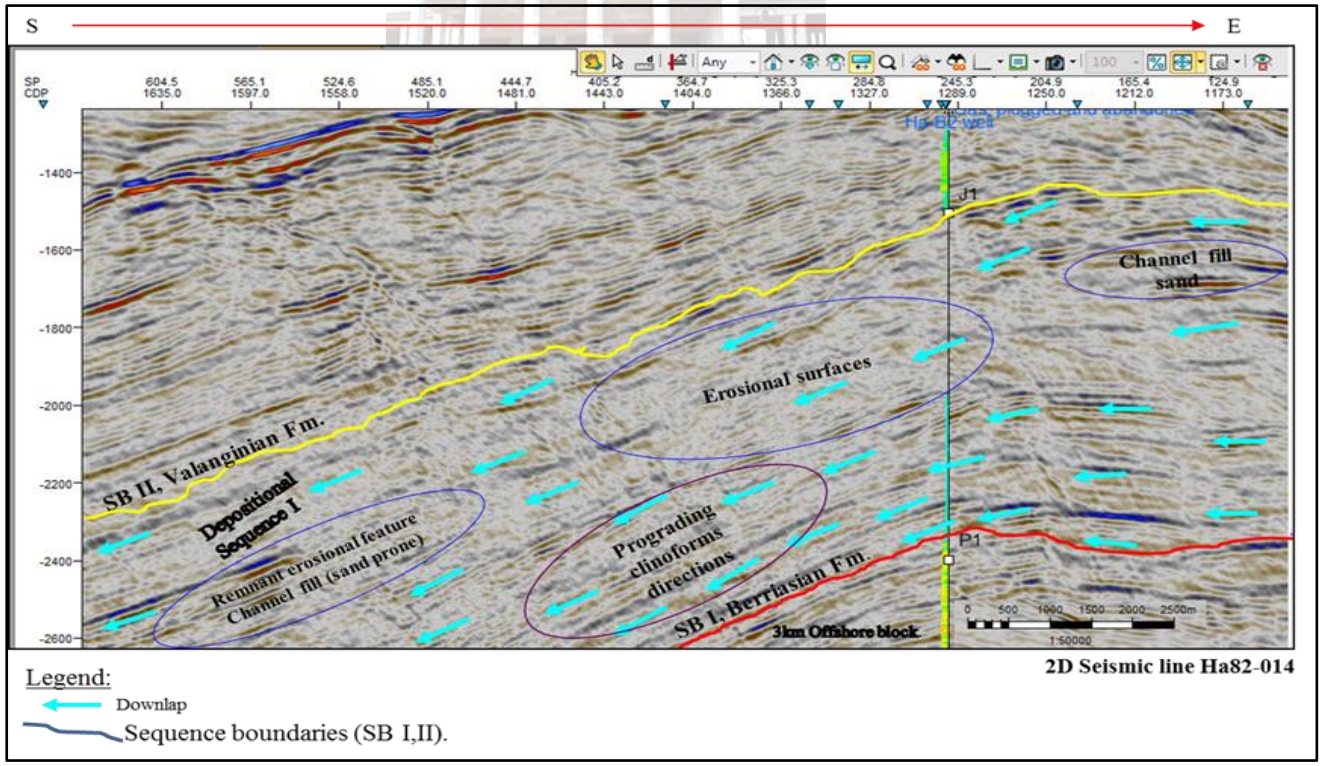

Figure 5. 7: Interpreted 2D-seismic line Ha82-014 (well Ha-B2) seismic sequence analysis cross section reflection shot from South-to-East in the Southern part of study area with (SB1 and SBII) sequence boundaries separating different geological units of sequence I.

In the southern part of the study area, three wells Ha-B2, Ha-K1 and Ha-A1 were drilled. The interpretation of the depositional environment of these three wells was based on 2D-seismic line Ha82-014, which was shot locally in South-to East direction in the southern part of the study area. This 2D-seismic line intersected by well Ha-B2 at -2382.84 ms and -1528.55 ms TWT on P1 horizon of the Berriasian sequence and J1 horizon of the Valanginian sequences respectively (Figure 5.7). These horizons make up the two sequence boundaries SB I and SB II for P1 and J1 horizons respectively, which are identified on the seismic cross section reflection terminations by discordant surfaces.

These sequence boundaries are regionally extensively conformable with each other in stratigraphic order on the seismic cross section. Between these sequence boundaries is the sequence I, denoted as Valanginian sequences that are characterized with strong base discordant relationships of downlap termination reflectors associated with the horizons (Figure 5.7), in which the seismic reflections of inclined strata terminate down dip against an inclined or horizontal surface. Downlap termination related reflectors also show the lateral extent of strata or sediment deposited basin ward, indicating distal deposition condition far from the sediment source. This is usually observed at the base of a prograding clinoform and commonly represents the progradation of a basin-margin slope system into deep water can be seen on the seismic cross section reflection (Figure 5.7).

The down dip and gradient of the sedimentary strata reveals the transport direction also the rate of sediment supply. Large and fast sediment dumps are liable to show steep gradients. Thus, downlap signifies a change from marine (or lacustrine) slope deposition, to marine (lacustrine) condensation or non-deposition. These surfaces of downlap also represent a marine condensed unit. This type of base-discordant relationship is commonly found in the top of basin floor fans, top basin slope fans and maximum flooding surface depositional environment i.e. deep marine environment.

Thus, it is suggested that the depositional setting of the top formation of Valanginian section in the southern part of the study area was under a deep marine environment which may be either a basin floor fan or a basin slope fan depositional environment, outboard of the continental shelf where the sediments were deposited far from their source. The sequence I is also affected by erosion and characterized by remnant erosional sand deposit on channel surfaces which can be regarded as surfaces of downlap that represent the marine condensed unit in the section as observed on the seismic reflection cross section (Figure 5.7).

5.2.1.5 The Analysis and Interpretation of Seismic sequence of Valanginian Section (top of P1-J1 horizons) around well Ha-A1 Southern part (South-to-East) of the study area

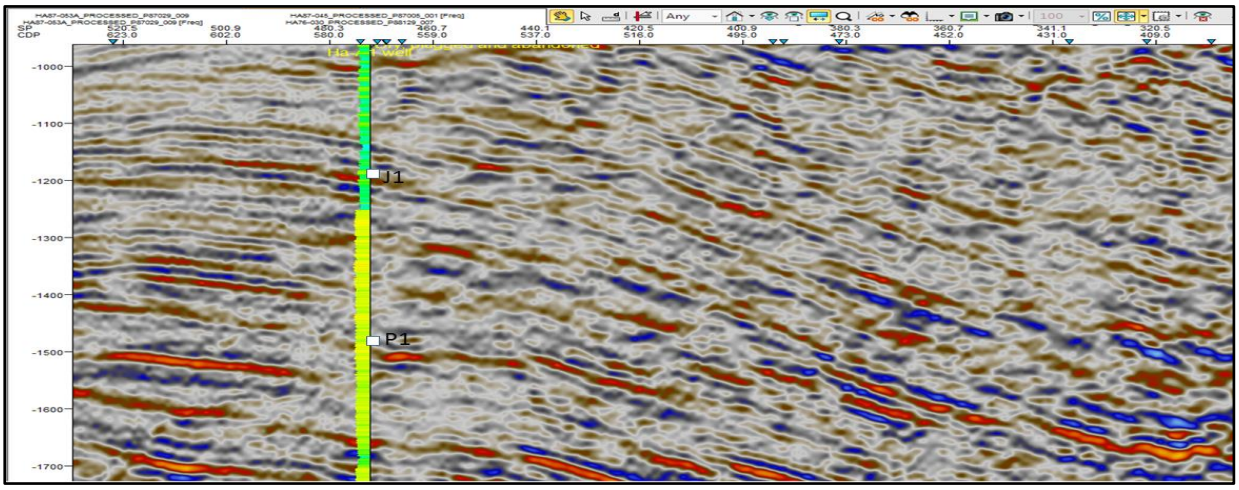

Figure 5. 8: Un-interpreted 2D-seismic cross section on seismic line Ha782-003. Reflection shot from South- to- East in the Southern part of the study area intersected by well Ha-A1.

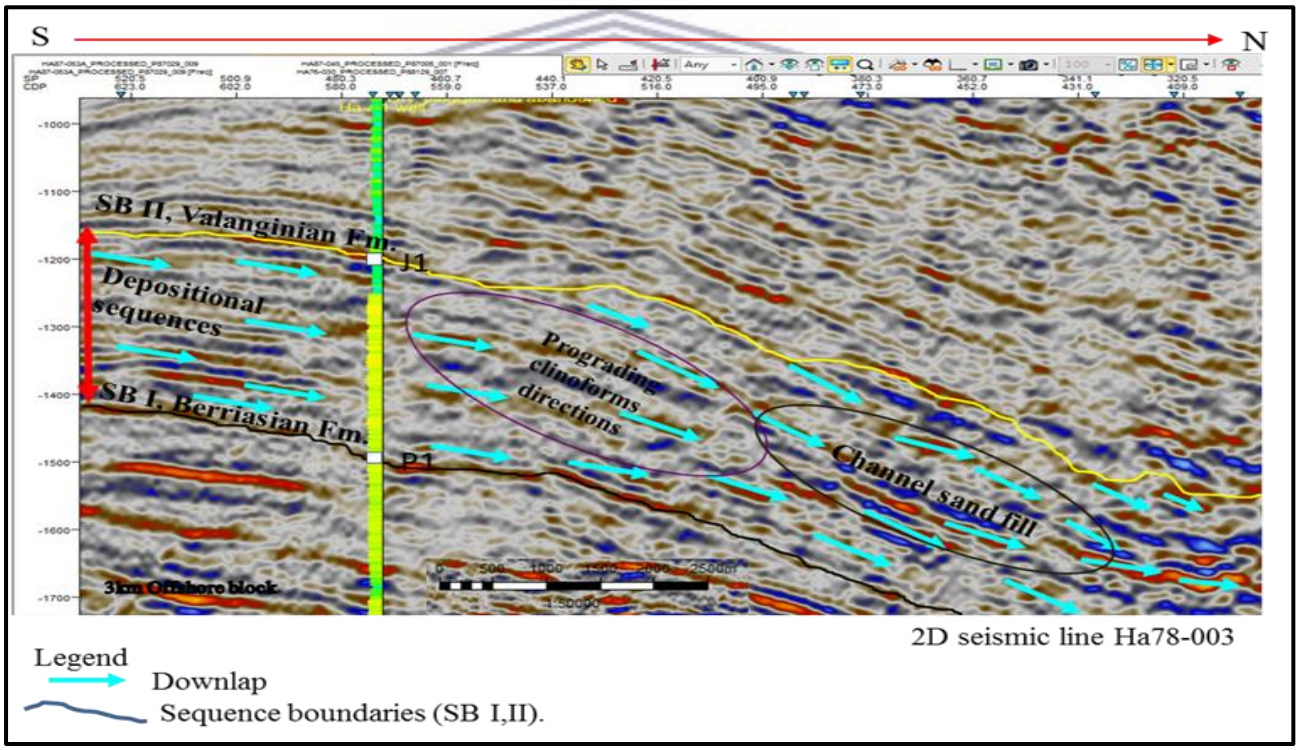

Figure 5. 9: Interpreted 2D-seismic sequence analysis cross section line Ha78-003 (intersecting well Ha-A1) reflection shot from South-to-North in the Southern part of the study area with (SB1 and SBII) sequence boundaries separating different geological units of sequence I.

The depositional environment of well Ha-A1 drilled in the southern part of the study area, was established on regional extended 2D-seismic line Ha78-003, that was shot in south-to-north direction of the basin. The well cuts across the 2D-seismic line Ha78-003 at -1198.17 ms and -1405.07 ms TWT on sequence boundaries SB I and SB II, which are P1 and J1 horizons respectively denoted as top formations of the Berriasian and Valanginian sequences respectively (Figure 5.9). The sequence boundaries are regionally extensively conformable with each other in stratigraphic order. In between the sequence boundaries (SB I and SB II), are the depositional sequences (Valanginian) characterised by a base-discordant termination reflector relation of downlap features as observed on the seismic reflection cross section.

Based on the characteristics of a downlap truncation relation pattern in which inclined strata terminate down dip against an initially horizontal or inclined surface, the down dip and gradient of the strata show the transport direction and the sediment supply. The large and fast sediment dumps resulted in steep gradients. It also indicates lateral extent of the sediment deposition basinward and distal deposition of the sediments (i.e. deposition of sediment far from the sediment source). Downlap is usually observed at the base of prograding clinoforms and represents the progradation of a basin-margin slope system toward deep water. This is interpreted as representing a change of the depositional environment of the sediment from marine slope deposition to marine condensation or non-deposition. The surface downlap signifies a marine condensed unit.

The above interpretation suggests that in the southern part of the study area of the Valanginian section in south-to-north direction of the basin, the depositional environment of the sediments is a deep marine environment, which can be either a basin floor fan or a basin slope fan, outboard of the continental shelf in which sediments are deposited towards the basin, inward of the deep sea and far from the sediments' source. The surface downlap as observed on 2D-seismic line Ha78-003 signifies a condensed marine unit, which suggests the presence of remnant channel sediments (Figure 5.9).

5.3. Results of Seismic Facies (SF) Analysis and Interpretation

5.3.1 Introduction to Seismic Facies (SF) Analysis and Interpretation from the Seismic Lines

The seismic facies analysis is the next step to seismic stratigraphy interpretation and is defined as descriptions and geologic interpretations of seismic reflection parameters, by means of determining the depositional environment from seismic reflection characteristics (Roksandic, 1978). The objective of this seismic facies analysis is to enable the correlation of seismic reflection attributes to the stratigraphic characteristics of identified sequences and provide a correlating framework between the seismic and well data. In addition, these reflection characteristics are believed to correspond to the unique geological and depositional history of a sequence (Mitchum Jr, *et al.*, 1977a). Seismic facies associations are analysed and interpreted on the basis of configurations of the seismic reflections such as, amplitude, continuity, frequency and the external geometry reflection of the strata within the depositional sequence to determine the depositional environment's setting and to estimate the lithology (Roksandic, 1978).

Consequently, in this study five seismic reflection attributes are employed to discriminate between the seismic facies associations. These include reflection amplitude and frequency strength, reflection continuity, internal configuration and external geometry reflection, to further ascertain the depositional environment of the Valanginian sequence of the study area in-between J1 and P1 horizons respectively. The seismic facies units are interpreted and calibrated with well logs for detailed geologic information, based on the environment of deposition and lithofacies distribution. In wells where no electrical logs are available the interpretations were made on the basis of the seismic facies reflection attributes. Thus, in this study the seismic facies attributes are utilized as outlined in the following sections of this chapter.

5.3.1.1 The Analysis and Interpretation of Seismic Facies (SF1) of the Valanginian Section around well Ha-G1 in the Northern part of the study area along the North north-East-to South south-West line

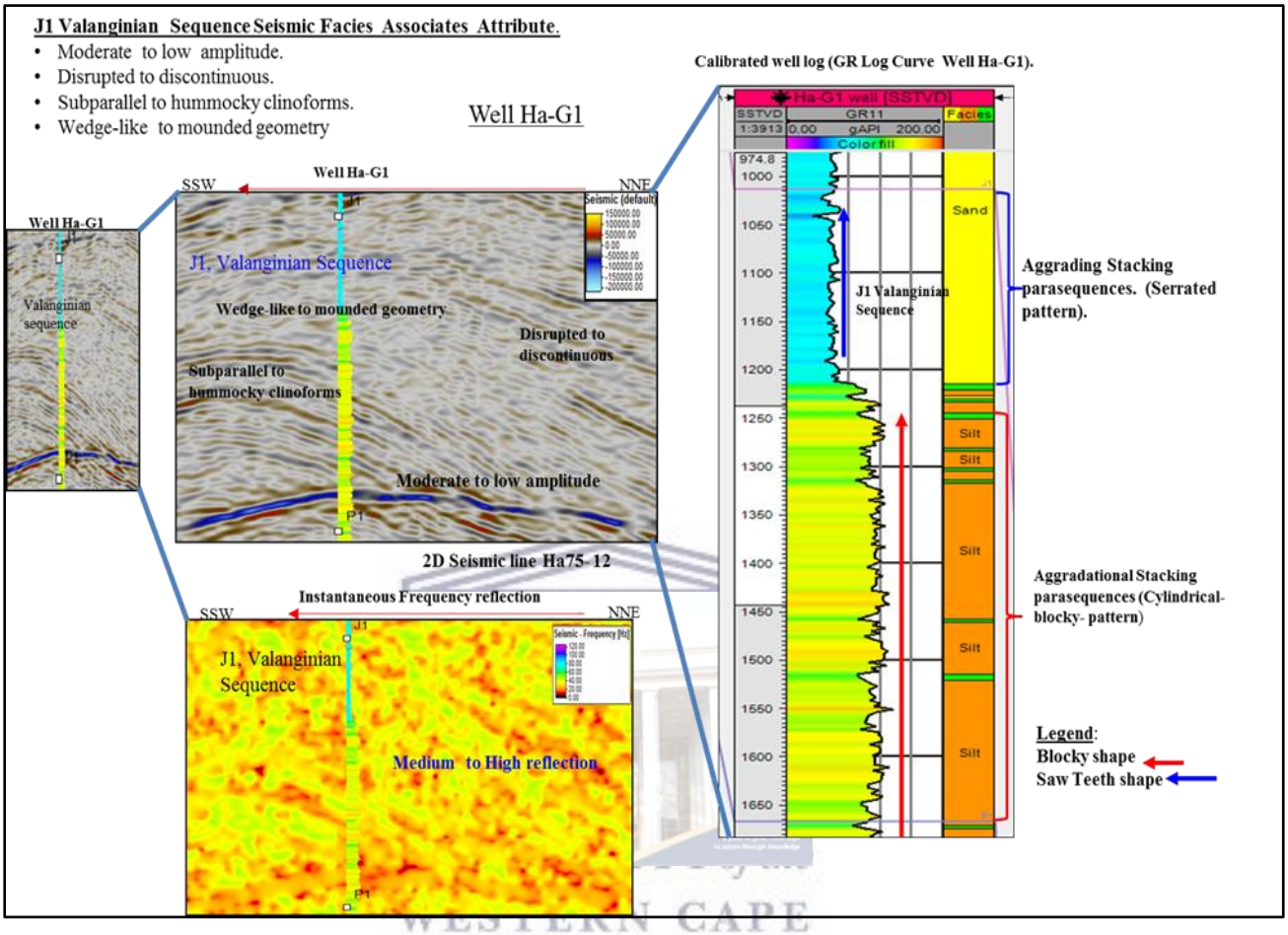

Figure 5. 10: Interpreted Seismic Facies Associations Analysis in the Northern part of the study area on 2D-seismic line Ha75-12 around well Ha-G1,shot from NNE-to-SSW direction, based on seismic reflection attributes: reflection amplitude and frequency strength, reflection continuity, internal-configuration and external geometry related seismic features with calibrated well GR-log curves.

In the Northern part of the study area, the seismic facies association was analysed for J1 horizon on 2D-seismic line Ha75-12, shot from the North-northeast to South-southwest, which also intersected well Ha-G1 (Figure 5.10). On this line, five seismic facies reflection attributes such as amplitude, continuity, frequency, internal configuration and the external geometry reflections were used and interpreted to delineate the stratigraphic information about the lithology and the depositional environment on Valanginian section (top of P1 – J1horizons) and integrated with well log interpretation.

The amplitude of the associated seismic facies indicates low to moderate reflection on seismic cross section (i.e. weak reflection) which varies laterally and changes from a disrupted to a discontinuous facies (Figure 5.10). Based on stratigraphic information about this facies, it is suggested that the depositional environment of the Valanginian section varies from continental shelf to deep marine and probably even a submarine fan.

The internal configuration seismic facies association describes the energy levels involved during the depositional process and thus identifying the type of depositional environment: low energy levels are related to the deposition of fine clastics such as clay while high energy levels are linked to coarser clastics such as sand. Based on internal configurations of Valanginian section (top of P1-to-J1 horizons) observed from the 2D-seismic line Ha75-12 in the Northern part of the study area, the seismic facies were interpreted to represent sub-parallel to hummocky internal-configuration facies associations (Figure 5.10). Hummocky facies is linked with low energy environment like inter-deltaic and pro-deltaic environments of deposition; the clay or shale encountered here are also linked to low energy environment like a continental shelf environment. Sub-parallel facies characteristics describe the stability and the uniform sedimentation conditions of a depositional sequence reflecting consistent subsidence or an area close to the basin shelf. It is thus suggested that the depositional-environment settings of the section, based on internal-configuration of the seismic facies associations, are either deltaic, continental or marine environments, where the marine environment is either a shallow or a deep marine environment.

The external geometry of the seismic facies attributes of the top of the Valanginian section (in-between J1-P1 horizons) on the 2D-seismic line Ha75-12, displays the wedge-to-mound seismic facies reflection (Figure 5.10). The wedge-like feature describes a sudden break and lateral change in the sedimentation pattern during the deposition of the sediments with gradual change of depositional environments from continental to sub marine fan. The mound facies reflection on the other hand reveals the possibility of a depositional build-up of sediments deposited in a higher energy condition within the basin, which are usually associated with submarine fan complexes. It is thus concluded that the succession in the northern part of the study area has been deposited within shallow or deep marine environments.

The frequency reflection strength of the seismic facies indicates the thickness (e.g. bed spacing) of the stratigraphic units. In frequency-dependent seismic facies, the thinner bed has

a relatively higher instantaneous frequency reading than that of the thicker bed which normally indicates a low instantaneous frequency (Zeng, 2010). The instantaneous frequency seismic facies attribute reflection was also examined on 2D-seismic line Ha75-12, for the Valanginian succession (top of P1-to-J1 horizons) to determine the thickness of these sequences and infer the depositional environment in the Northern part of the study area. Medium to high reflections between 30-50Hz were observed (Figure 5.10). This suggests that the Valanginian succession deposited as thin bedded sediments with shallow depth of penetration and high resolution power (Figure 5.10). This seismic facies association is usually observed in shelf platform margin environments, indicating a massive-bedded build-up of an aggradational stacking sequence. The variable high frequency is usually observed in a submarine canyon and on the lower slopes of proximal turbidites' slumped clastic sediments (Badley, 1985). The depositional environment setting of the Valanginian succession is thus most likely that of a shallow marine environment (Figure 5.10).

In addition, the calibrated GR logs of well Ha-G1 that is intersected by the 2D-seismic line Ha75-12 were used to obtain a detailed lithological interpretation of the Valanginian succession. Sediment build-up known as an aggradation stacking parasequence was observed in this succession made up predominantly of sandstone and silt as indicated from the gamma ray signatures by their cylindrical-blocky and serrated log signatures (Figure 5.10). This is interpreted as a sequence of thick, uniformly graded, coarse-grained sandstone, and medium-fine grained silt units, probably deposited in a braided channel, or tidal channel or as a result of subaqueous slump within the sequence. This type of stacking pattern can be used to denote the absence of significant movement of a shoreline over a period of time and the rapidly increasing accommodation space in the formation to be taken up by sediment deposits. This could be recognised in either of the following depositional environments:

- channel-fill,
- submarine canyon–fill,
- braided fluvial and deltaic environments,
- fluvial flooding plain,
- storm dominated shelf and
- distal deep marine slope environment.

The Valanginian section depositional environment can therefore vary between deltas and shallow marine to deep marine depositional environments.

In conclusion, based on the observation from all the seismic facies reflection attribute studies of Valanginian section in the Northern part of the study area to discriminate the depositional environment of well Ha-G1 as intersected on the 2D-seismic line Ha75-12, the depositional environment was found to be shallow marine to deep marine.

5.3.1.2 The Analysis and Interpretation of Seismic Facies (SF2) of the Valanginian Section (top of P1-to-J1 horizons) around well Ha-I1 in the Northern part of the study area along a North-northeast to North-northwest line

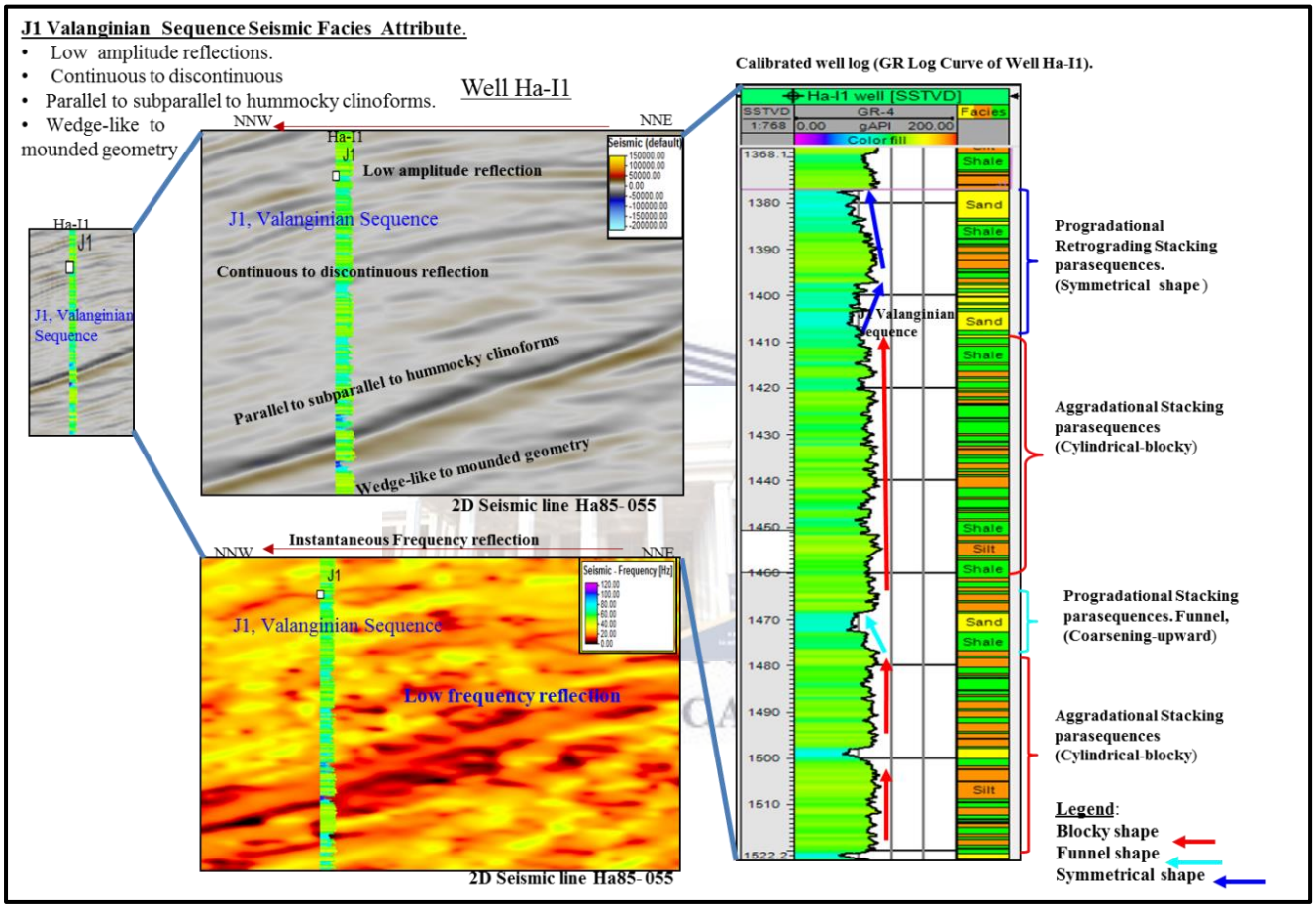

Figure 5. 11: Interpreted Seismic Facies Associations Analysis in the Northern part of the study area on 2D-seismic line Ha85-055 around well Ha-I1,shot from NNE-to-NNW direction, based on seismic reflection attributes; reflection amplitude and frequency strength, reflection continuity, internal-configuration and external geometry related seismic features with calibrated well GR-log curves of well Ha-I1.

In the Northern part of the study area, another 2D-seismic line Ha85-005, that was shot along a line from North-northeast to North-northwest and intersected by well Ha-I1, was used to delineate the seismic facies and the depositional environment for the Valanginian succession in that region. The seismic facies associations observed based on this 2D-seismic line Ha85-

005, were characterised with low amplitude seismic facies and other facies associations as follows: poor amplitude reflections with variation in continuity indicates monotonous lithology, mostly inferred as marine shale, though it could be the massive continental sands deposited in a specific type of geological basin (Niranja, 2016). The low amplitudes (weak reflection) as illustrated in Figure 5.11, and the continuous to discontinuous continuity-reflection seismic facies, geologically signifies that there are lateral changes in facies of the section during the depositional period and that there are rapid changes in energy levels available to the depositional processes in the environment. This is usually associated with continental depositional environments of higher energy facies, which are interpreted to be channel fill sediments from an environment such as a braided, meandering stream, or a flood-plain as well as the proximal deposits by a fluvial channel in offshore. Thus, the depositional environment of the succession based on the seismic facies associations indicates a shallow marine to deep marine depositional environment. A low amplitude reflection suggests similar lithologies on both sides of the interface e.g. sand/silty shale (Figure 5.11), while the high amplitude reflection characteristic commonly points to a vertical change of different lithologies across the interface e.g. sand/shale.

The internal configurations observed from the 2D-seismic line Ha85-005, for the Valanginian succession (top of P1-to-J1 horizons) in this part of the study area were characteristic for parallel-to-subparallel-to-hummocky seismic facies reflection associations (Figure 5.11). Generally, the internal configuration of seismic facies is geologically interpreted to denote the energy level of the depositional environment and some description of sedimentary structures. The parallel-to-subparallel-to hummocky seismic facies attributes associated with the succession indicates that there was a uniform energy environment causing stable conditions, producing low energy facies as in inter-deltaic and pro-deltaic environments depositing clay or shale on a continental shelf.

The above interpretation however, also means that section could be associated with some sedimentary structure formed at deeper depth. Therefore, it suggests that succession formed with balanced uniform rate of sedimentation along the uniformly subsiding, nearly stable basin shelf. At shallow depth sedimentary structures such as ripple marks, cross bedding, prograding bar dunes, separating delta complexes, and prograding shelf or slope systems of the deposited sediment in the sequence would be formed. This seismic facies reflection is commonly associated with coastal plain or shallow marine shelf, or basin-margin depositional environments. Thus it is concluded that the deposition within the Valanginian section (based

on this internal-configuration of seismic facies association) took place within the shallow marine (i.e. continental shelf) to deep marine environment.

The external geometry of the seismic facies association of the Valanginian section observed on the 2D-seismic line Ha85-005 shot along NNE-to-NNW line indicates a strong seismic facies association of wedge-like to mounded geometry. Geologically, this indicates a gradual variation in the environment of deposition and lateral change in sedimentation rate within this depositional sequence, with the possibility of depositional build-up of the sediments deposited in a higher energy environment. Wedges are usually associated with fluvial to shallow marine shelf facies, while mounded facies are usually linked with the submarine fan complexes. Therefore, the depositional environment of the of the Valanginian section based on this 2D-seismic line Ha85-005 in the northern part of the area is that of a shallow marine to deep marine environment.

The instantaneous frequency seismic facies attributes which are geologically used to infer the bed spacing (thickness) of the depositional sequence (Zeng, *et al.*, 2010), were also interpreted for the Valanginian section to delineate the bed thickness. The seismic facies association indicates low-reflection between 0-20Hz which can be observed along the continuous strata (Figure 5.11). Accordingly, this implies that this section was deposited as thick-bedded unit with greater depth of seismic penetration but less seismic resolution power. These seismic facies associations are related with the slope fan, basin-floor fan, on-shelf delta, on-shelf incised valley, as well as a coastal delta and inner-shelf marine deposits. Consequently, the results suggest that Valanginian section was deposited under a shallow marine to deep marine environment in the northern part of the study area.

In addition, the GR log motifs of well Ha-I1 were also calibrated with the 2D-seismic line Ha85-005 cross section facies reflection, to facilitate the detailed lithological interpretation of the J1 horizon based on gamma ray log curves (Figure 5.11). The Valanginian section was characterised by both low and high gamma ray values indicating the presence of shale, silt and sand deposits respectively (Figure 5.11). The series of depositional cycle patterns on gamma ray log signature such as aggradation stacking parasequence (cylindrical or blocky shape), progradational stacking parasequence (funnel shape, coarsening-upward), and progradation retrograding stacking parasequences (symmetrical shape), suggests an offshore shoal of transgressive sand bodies deposited in shelf environments. The aggradational stacking parasequence (cylindrical or blocky shape) indicates sediment build-up of thick

uniformly-graded coarse-to-medium-to-fine-grained sandstone-silt-shale units as observed in this stacking (Figure 5.11).

This style of stacking pattern can be used to indicate the presence of a stable shoreline over a period of time and more rapidly increasing accommodation space in the formation to be taken up by sediment deposits. This could be recognised in the following depositional environments:

- channel-fill,
- submarine canyon –fill,
- braided fluvial,
- delta,
- fluvial flooding plain,
- storm dominated shelf ,
- distal deep marine slope environment.

Valanginian section was furthermore characterized with a progradational stacking parasequence (funnel shape, coarsening-upward), signifying a decreasing clay content up-section or coarsening upward trend i.e. changes from shale-rich into sand-rich lithology with an upward increase in depositional energy; in deep marine setting this indicates an increase in sand content of turbidite bodies, which can occur in deltaic and turbiditic progradation environments.

The last depositional cycle of Valanginian succession is a progradational-retrograding stacking parasequences pattern characterized by symmetrical or barrel shape (Figure 5.11), suggesting the gradual increase and decrease in gamma ray response; this occurs usually by progradation and retrogradation of clastic sediments. These lithology types were observed in the Valanginian section and are usually found to be the result of the reworking of an offshore bar or transgressive shore face delta. The depositional environment of top formation's Valanginian section around well Ha-I1 on the 2D-seismic line Ha85-005, calibrated with gamma ray log curves, in the northern part of the study area, varies from a shallow marine (delta, continental shelf) to a deep marine depositional environment.

5.3.1.3 The Analysis and Interpretation of Seismic Facies (SF3) of the Valanginian Succession (top of P1-to-J1 horizons) around well Ha-B2 in the Southern part of the study area, along a South-to-East line

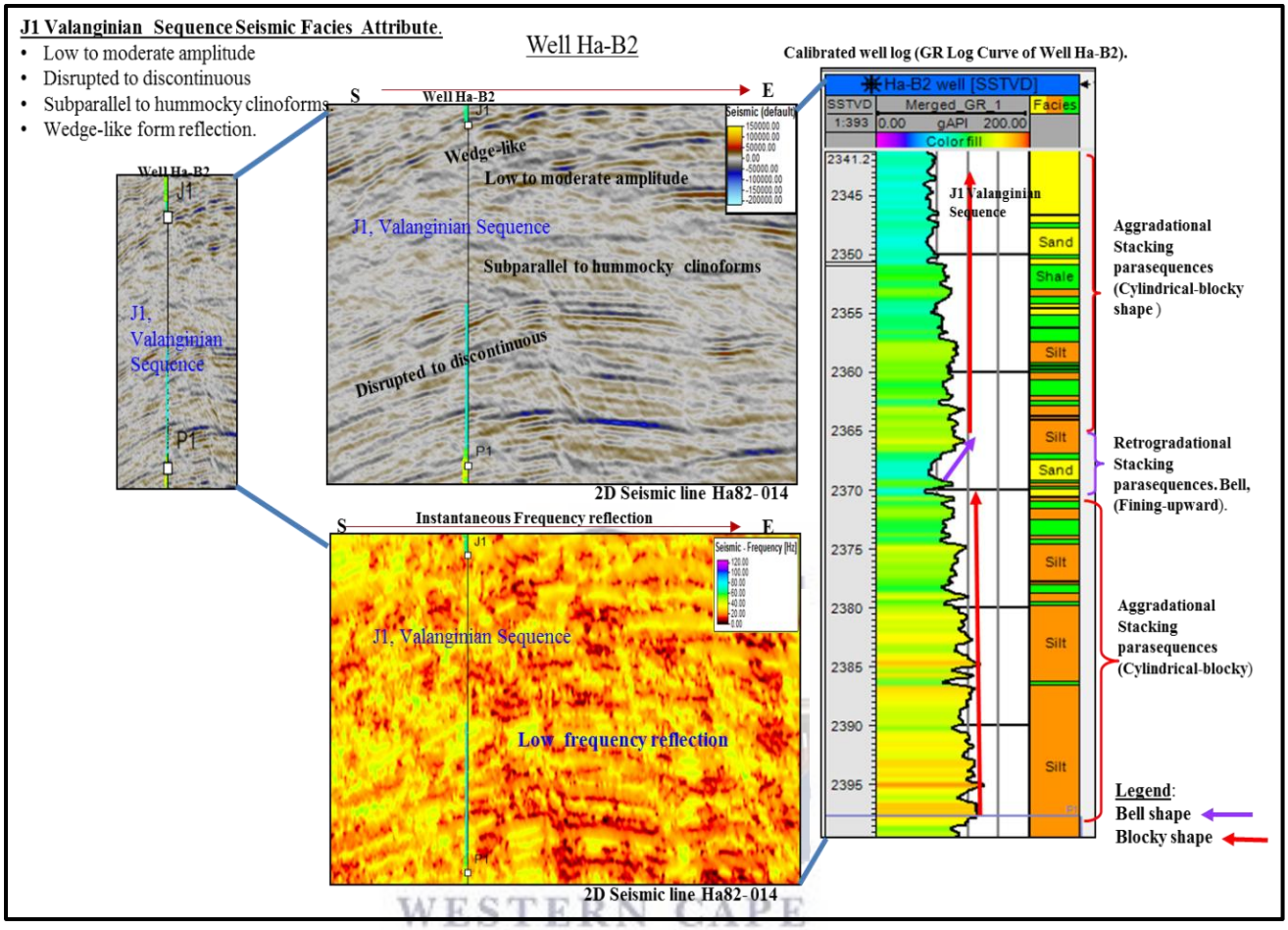

Figure 5. 12: Interpreted Seismic Facies Association Analysis in the Southern part of the study area on 2D-Seismic line Ha82-014 around well Ha-B2,shot along a line from South-to-East, based on seismic reflection attributes; reflection amplitude and frequency strength, reflection continuity, internal-configuration and external geometry related seismic features with calibrated well GR-log curves.

In the southern part of the study area the seismic facies attributes such as reflection amplitude and frequency strength, reflection continuity, internal-configuration and external geometry related seismic features with calibrated GR-log curves of well Ha-B2, were used to decipher the depositional environment of the Valanginian section (top of P1-to- J1 horizons). The 2D-seismic lines that were used for the study in the southern region, Ha82-014 and Ha76-031, are shot from South to East and East to West respectively, and are intersected by drilled wells Ha-B2 and Ha-K1 respectively (Figure 5.12).

The 2D-seismic line Ha82-014 is intersected in well Ha-B2 at 1199ms two-way-time on the contact between J1 horizon and P1 top formation of Berriasian sequence boundary. However, based on 2D-seismic line Ha82-014, the seismic facies attribute associated with top formation J1 horizon (Valanginian section) was characterized with weak amplitude (low to medium amplitude) reflection with disrupted to discontinuous seismic facies association (Figure 5.12). Poor amplitude reflections with variation in continuity indicates monotonous lithology, mostly inferred as marine shale, though it could sometimes be the massive continental sands which deposited in a specific type of geological basin (Niranjan, 2016). Geologically, this implies that there were lateral changes in facies during the depositional process associated with continental to marine depositional environments of higher energy facies. The depositional environment commonly found with this seismic facies varies from the continental with channel fill sediments to marine, probably a submarine canyon with a canyon fill deposit and sub marine fan lobe environment. Based on seismic facies of weak amplitude to disrupt to discontinuous facies, Valanginian section is suggested to have been deposited in a deep marine environment.

The internal reflection-configuration seismic facies attributes indicate the depositional energy of environments. The low-energy is related to deposition of finer clastics such as clay while the high energy is linked to coarser clastics such as sands. The seismic sequence facies association indicated by the 2D-seismic line Ha85-014 is characterized with subparallel to hummocky clinoforms reflections (Figure 5.12) Valanginian section. A subparallel sequence seismic facies association geologically implies stability with uniform sedimentation conditions of deposition that is either subsiding or close to the basin shelf. The hummocky pattern on the other hand is frequently linked with low energy facies such as interdeltaic and prodeltaic clays or shales deposited close to the continental shelf. Based on these seismic facies attributes, Valanginian section can be regarded as a sequence with low energy facies such as silts and shales as observed in the calibrated gamma ray log curves of well Ha-B2 (Figure 5.12), with a uniform sedimentation of the sequence deposited within a shallow marine environment (e.g. prodelta, continental shelf or basin shelf).

The external geometry seismic facies association observed from the 2D-seismic line Ha85-014 of the Valanginian section is characterized by a wedge-like seismic facies association (Figure 5.12). This facies association helped in validating geologically the inferred depositional features and provide reliable information on depositional energies and association of facies of the geologic bodies (Niranjan, 2016). Geologically, wedge-like

seismic facies association represents the sudden break of sedimentation patterns and is commonly associated with fluvial to shallow marine shelf facies. It is thus suggested that the Valanginian section has undergone a break in sedimentation and was deposited along the continental shelf or shallow marine environment in the southern part of the study area.

The instantaneous frequency seismic facies reflection attributes are geologically interpreted to infer the thickness (bed spacing) of a depositional sequence. Based on 2D-seismic line Ha82-014, for the J1 horizon (Valanginian section), low instantaneous frequency attribute seismic facies reflection between 0-20Hz (Figure 5.12) was observed which can be seen along the disrupted to discontinuous strata. This indicates that the sequence within Valanginian section developed thick deposits with great depth of penetration (Figure 5.12) but with low resolution power. This seismic facies is related with a slope fan, basin-floor fan, on-shelf delta, on-shelf incised valley, and also a coastal delta or inner-shelf marine deposits. Therefore, it is suggested that in the southern part of the study area, the Valanginian section was deposited between shallow marine and deep marine environments according to the characteristics of this seismic facies attribute.

The 2D-seismic line Ha82-014 cross section facies reflection results were also calibrated with the GR log curves of well Ha-B2 to delineate the detailed lithological interpretation of Valanginian section based on gamma ray log signatures (Figure 5.12) in the southern part of the study area. The Valanginian section (top of P1-to-J1 horizons) was characterised as a series of depositional cycles of low and high gamma ray values, with a dominance of sand, silt and shale deposits respectively (Figure 5.12). The series of depositional cycle patterns comprises of gamma ray log signatures such as an aggradation stacking parasequence (cylindrical or blocky shape) or a retrogradational stacking parasequence.

The aggradational stacking parasequence indicates sediments that are built-up out of thick uniformly graded medium-to-fine-coarse grained silt-shale-sandstone units observed in the stacking pattern (Figure 5.12). This stacking pattern usually indicates a stable shoreline over a period of time, as well as more rapidly increasing accommodation space for sediment to be deposited. This is commonly found in the following depositional environments: channel-fill, submarine canyon–fill, and delta deposits, fluvial flooding plain, storm dominated shelf deposits and a distal deep marine slope environment. In addition, in the southern part of the study area, Valanginian section is also characterized with a retrogradational stacking parasequence (fining-upward, bell shape). This indicates increasing clay contents up-section

in gamma ray value and is commonly found in a fluvial point bar, tidal point bar, deep tidal channel-fill, tidal flat or in transgressive shelf environments, thus suggesting that there is a presence of clay or shale deposits in this section. It is thus concluded that based on the characteristics observed from the gamma ray log signature from silt-to shale-to sandstone in well Ha-B2 in the southern part of the study area, the lithofacies and depositional environment of Valanginian section (top of P1-to-J1 horizons) were deposited during the period of more accommodation space which resulted in sediment built up stacking parasequence patterns and further interpreted as deposited in a continental to shallow marine depositional environment.

5.3.1.4 The Analysis and Interpretation of Seismic Facies (SF4) of Valanginian Succession (top of P1-to- J1 horizons) around well Ha-K1, Southern part of the study area along an East-to-West line

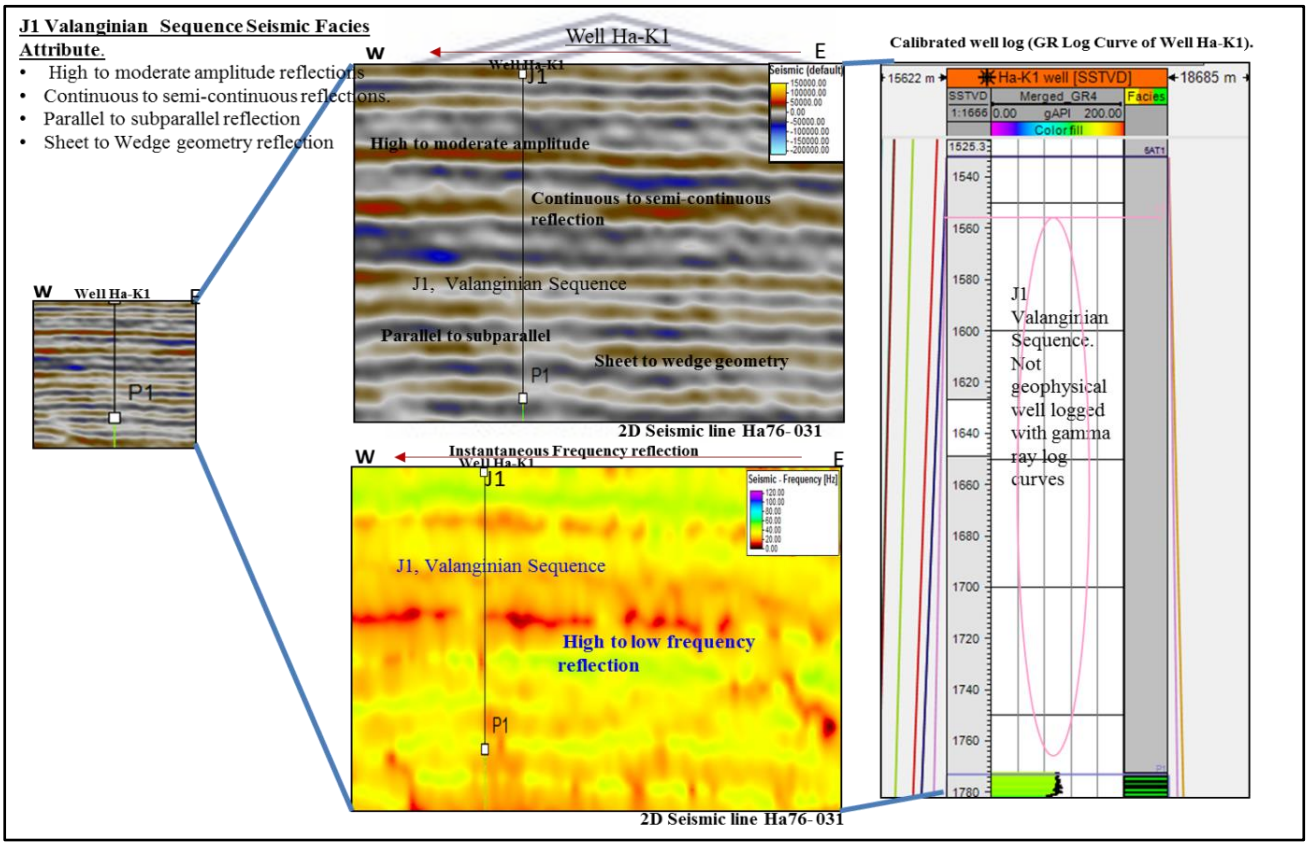

Figure 5. 13: Interpreted Seismic Facies Associations Analysis in the Southern part of the study area on 2D-Seismic line Ha76-031 around well Ha-K1,shot from East-to-West, based on seismic reflection attributes; reflection amplitude and frequency strength, reflection continuity, internal-configuration and external geometry related seismic features with calibrated well GR-log curves.

Seismic facies attributes were also interpreted on 2D-seismic line Ha76-031 around well Ha-K1 drilled in the southern part of the study area, to delineate the depositional environment of the Valanginian succession in the region. There was however no geophysical log data (GR log curves) available to be calibrated with the formation to help in detailed interpretation of the lithofacies and the trend of the depositional environments (Figure 5.13), as they were not logged geophysically through the Valanginian section (J1 horizon). Hence, the interpretations were only on the basis of seismic facies reflection attributes.

According to the seismic facies association on the 2D-seismic line Ha76-031 around well Ha-K1, Valanginian section (tops of P1-to-J1 horizons) was characterized with high to moderate amplitude seismic facies attributes with continuous to semi-continuous reflection (Figure 5.13). High amplitude seismic facies with continuous reflections are usually suggestive of sandstone or limestone, the consistency of these facies is indicative of wide spread and uniform depositional sequences that imply marine facies as the environment of deposition (Niranjan, 2016). Geologically this implies that Valanginian section was occupied with channel fill sand sediments deposited in a marine depositional environment; the moderate amplitude to semi continuous amplitude of the facies may indicate a partially monotonous lithology such as silt or shale that was present in the sediments during the depositional sequence of the formation.

The internal configuration of the seismic facies association of the Valanginian section in the southern part of the area, based on 2D-seismic line Ha76-031 around well Ha-K1 is described with parallel to sub-parallel facies association reflection. This seismic facies suggests a balanced uniform rate of sediment deposition under uniform subsidence near the stable basin shelf (Niranjan, 2016). Geologically, it also implies the description of the sedimetary structure with relative formation depths, as well as the depositional process of the sediments. In a shallow depositional environment sedimentary structures such as ripple marks, crossbedding, prograding bar dunes, separated deltal complexes and prograding shelf or slope systems of the deposited sediment in the sequence are usually associated with this facies. This seismic facies reflection is commonly linked with a coastal plain on continental or shallow marine shelf, or basin margin as depositional environments. It is thus suggested that Valanginian section was deposited uniformly with well-defined sedimentary structures in a shallow to deep marine depositional environment.

The external geometry form of the seismic facies attributes observed for the J1 horizon from the 2D-seismic line Ha76-031 around drilled well Ha-K1 indicated a sheet to wedge geometry reflection. This seismic facies helps in validating the geological bodies and inferred depositional features (Niranjan, 2016). The seismic facies attributes geologically illustrate a uniform, sudden break followed by a gradual variation in sedimentation rates including lateral change in sedimentation pattern during the depositional process. This type of seismic facies is usually associated with fluvial to shallow marine facies and can also be found in the continental rise, mainly as slope-front fill sediments (Badley, 1985). Slope-front fill sediments are composed of mass flow (thick) sediments laid down in submarine fans which form the locus of deep marine sand deposits, also on the continental slope and abyssal plain depositional environments. This observation indicates that the Valanginian section (J1 horizon) has undergone a break in deposition under continental to shallow marine environment in the southern part of the study area.

The instantaneous frequency seismic facies which was used to denote the bed spacing (thickness) of the Valanginian section, indicates medium to high frequency of 20-40Hz reflections (Figure 5.13), based on this interpretation on 2D-seismic line Ha76-031 around drilled well Ha-K1 in the southern part of the study area. This implies that the thickness of bedding of the Valanginian section as thin bedded sediments with shallow depth penetration and high resolution power. These seismic facies reflectors are commonly found in prodelta and slopes, associated with prograding shelf delta or fan delta or shelf-margin delta, (Badley, 1985). It is therefore concluded that the depositional environment of the Valanginian section can be regarded as a shallow marine to deep marine environment with thick, massive sediment deposits.

5.3.1.5 The Lithofacies Surface Attributes Depth Thickness (Between J1-to-P1horizons) Map Analysis and Interpretation of the J1 horizon of the Valanginian Sequence (Seismic Facies Map)

A lithofacies depth thickness model map (Seismic facies map) was created for the Valanginian section. The objective of the modeling was to delineate the flooding of the depositional sequence pattern via 3D view. The identification and interpretation of the lithofacies gives better detailed understanding of the pattern of the depositional environment viewed in a 3D model (Figure 5.14). However, based on interpretation from the seismic sequence and seismic facies analysis of the horizons (Valanginian section) as described above around the study's wells Ha-N1, Ha-I1, Ha-G1, Ha-A1, Ha-B2 and Ha-K1, the common

features associated with the seismic sequence and seismic facies are found in the depositional environment varying between shallow marine to deep marine of the continental shelf, submarine fan lobes and basin floor depositional environments.

The 3D perspective view of the depth surface map attribute of the facies model of J1 horizon (Valanginian section) of the study area, indicates a mass flooding thick bedded siltstone lobe (siltstone facies) with intercalated fine mud-rock (shale facies) and minor sandstone in low energy turbidite channel depositional environment area in the south-western part of the study area. The Northern part of the section indicates a diachronous deposition dominated by sandstone intercalated with minor siltstone and shale. This is probably deposited in a high energy turbidite channel, followed by low energy settling of the siltstones and shale before the next pulse of high energy sandstone was deposited.

The depositional sequence from the north-east to the south-east around the well Ha-K1, of the study area suggests that many high energy turbidites might be encoutered, whereby many marine depositions dominated by sandstone intercalated with siltstone and minor shale are observed. Similarly, the formations are also characterized by erosional surfaces, this might be due to tectonic processes resulting in erosional events due to uplift. This created a sediment hiatus in the formation.

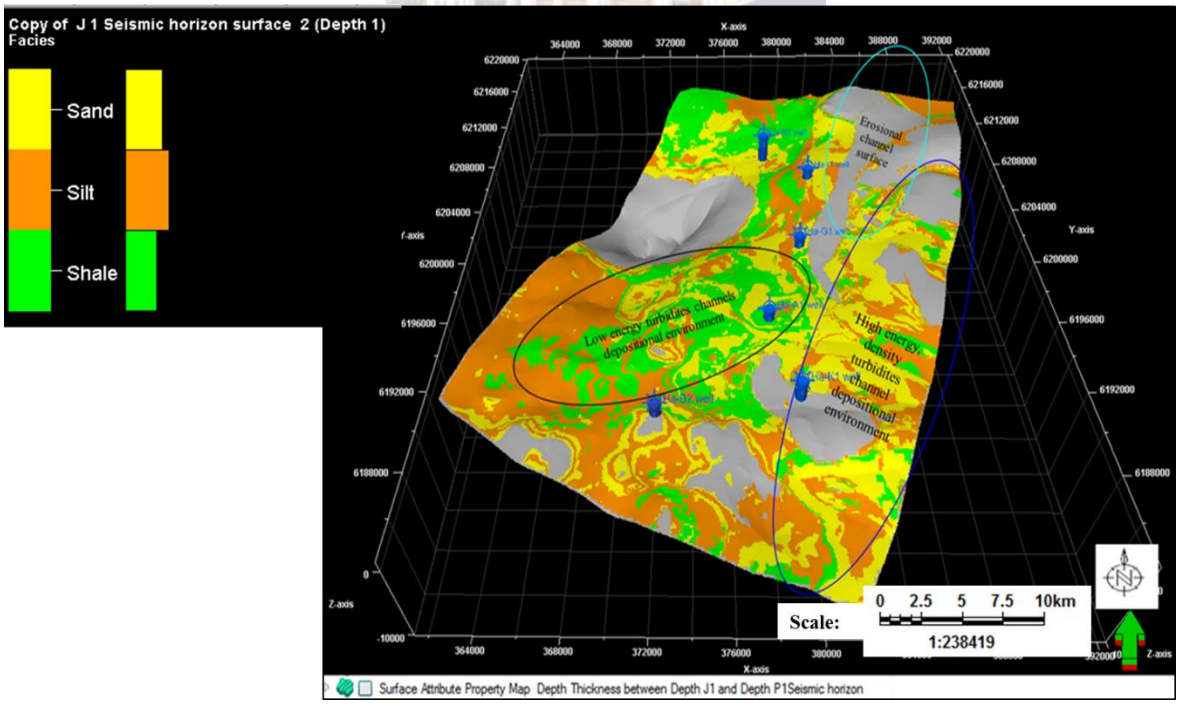

Figure 5. 14 :Seismic facies map of the 3D perspective view of Lithofacies surface attributes depth thickness map model of J1 horizon across the study area.

5. 3.1.6 The Time (ms) Structure Maps Analysis and Interpretation of J1 Valanginian Sequence (J1 horizon)

Figure 5.15 represents the 3D perspective view of time structure map of J1 horizon (Valanginian section). The two-way-time of the map across the formation ranges from 250ms to 2500ms. The time variations in the study area were due to both structural deformation such as the formation of minor listric faults, and erosional events observed on seismic reflection in the study area which formed as a result of tectonic uplift that has occurred in the area.

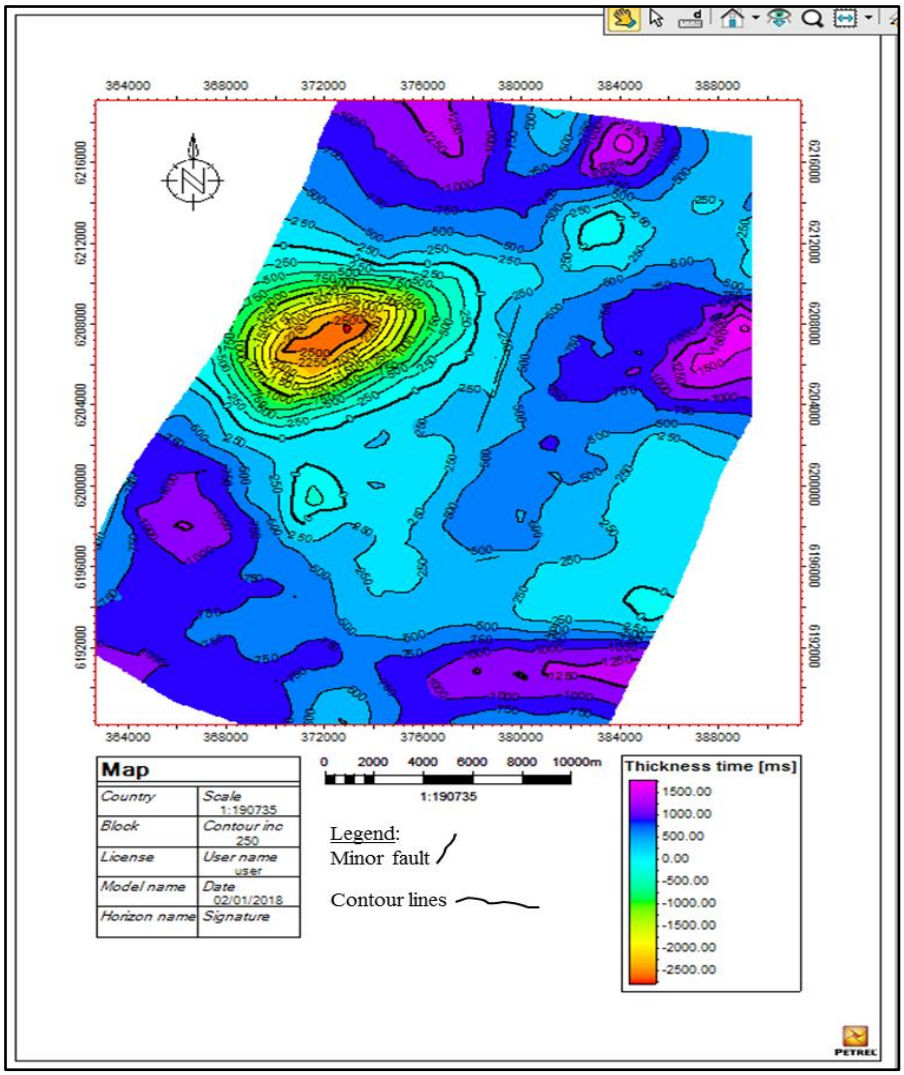

Figure 5. 15: 3D view of time structured thickness map model of J1 Valanginian section across the study area.

5.3.7.1 The Depth (m) Structure Maps Analysis and Interpretation of J1 Valanginian Sequence (J1 horizon)

The depth structure map was also described for the J1horizon based on a 3D assessment view of the map (Figure 5.16). The depth ranges from 0 to 4500 m, where the variation in depth suggests deformation in the study area that occurred as a result of a tectonic event. The minor listric fault in the central part of the formation is trending North-South, as a result it can be observed that the sediments are thinned-out and range about 0 m to -1500 m thickness from the North-east toward the Southern part of the study area . This might be due to the uplift and erosional event that occurred during the period (McMillan, *et al.*, 1997). Further, non-deposition of sediment occurred, caused by a low-stand situation during the period. In addition, considering the pattern of sedimentation in the North-West to the South-Western part of the area (Figure 5.16), this part of the basin appeared to have developed thick sediments ranging from about 2250 m to 3000 m in thickness. The latter is as a result of progradational deposition of sediment towards the region, as preserved in the area. Through uplift and its accompanying intense erosional event that occurred and the progradation of fluvial sediments from the Sunday River troughs depositing sediment at the northern part of the basin (McMillan, *et al.*, 1997), this region retains more sediment accumulations due to its accommodation space. The interval contours on the map in Figure 5.16 below, have been drawn at 250m thickness intervals; the 0m line in the eastern part trending from north to south represents the point at which the section within the depositional sequence is no longer present due to the post-depositional erosion.

Conversely, in terms of hydrocarbon trapping potential, the section lacks potential reservoir traps around the wells located in the study area as illustrated in Figure 5.16. There are no prospects for potential reservoir traps that can be recognised in the depth thickness map of the J1 horizon (Valanginian section) around the location of the wells. The wells location on the map shows absence of stratigraphic or structural traps such as anticlines or synclines, neither do they show four or three ways closures. There was also no significant fault observed that could explain the hydrocarbon fill mechanism of the formation in the wells.

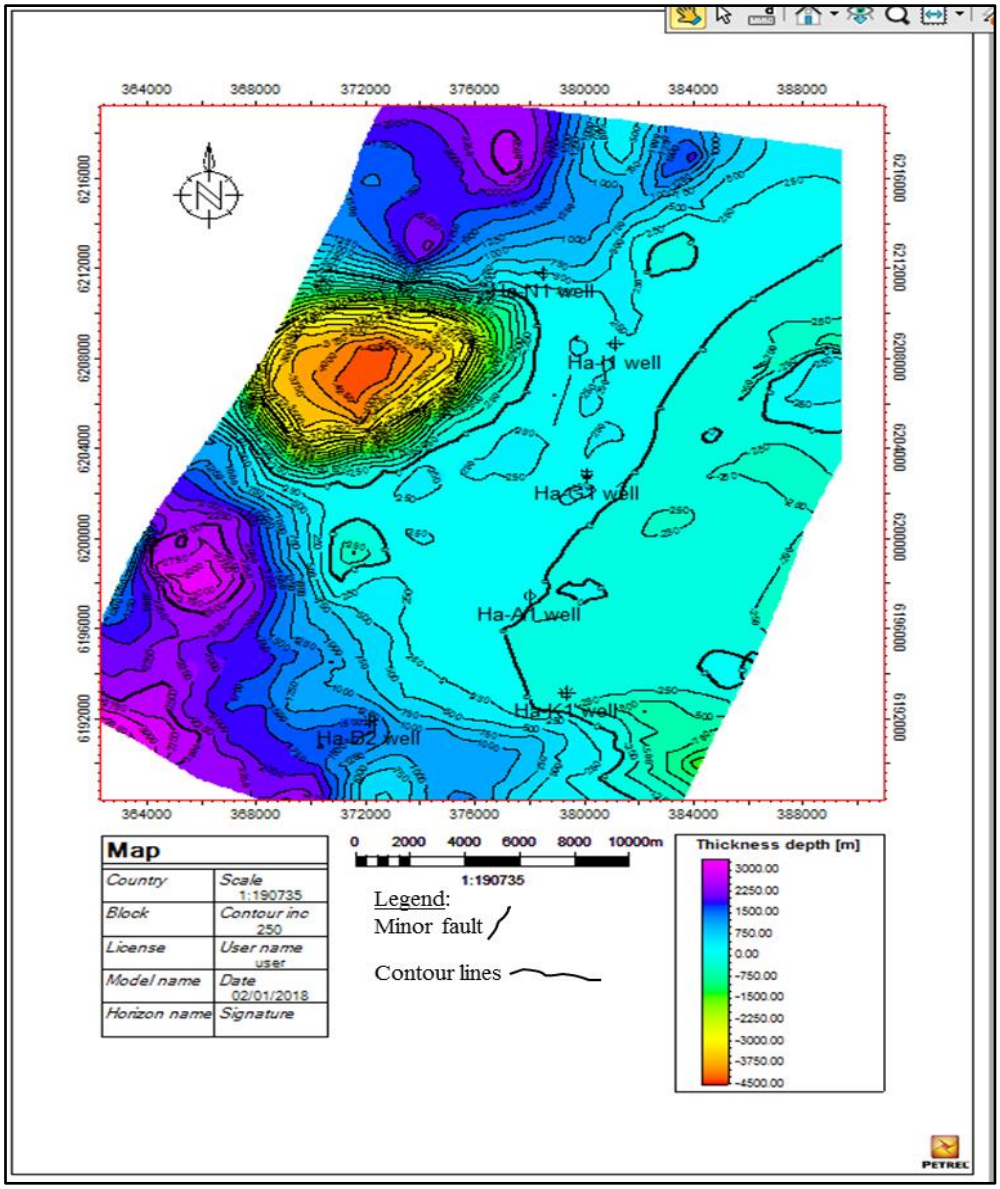

Figure 5. 16: 3D perspective view of depth (m) structured thickness map model of J1 horizon across the study area.

Table 5. 1: Overview of Seismic Facies that have been defined in this study.

Well Names	Well Location	Seismic Facies:	Amplitude	Continuity	Internal Configuration	External Geometry	Frequency	Seismic sequence: Boundaries (Upper, Lower)	Depositional System	Depositional Environment	Lithofacies Association
Ha-G1	North (Central)	SF1	Moderate-to-Low	Disrupted –to-discontinuous	Subparallel – Hummock clinoform	Wedge-like to Mounded geometry	Medium to High Reflection	Top lap; Erosional	Aggradational stacking pattern.	Delta, Submarine fan, Shallow-to-Deep Marine	Sand-to-Silt-dominated & Shale.
Ha-I1	North	SF2	Low	Continuous - Discontinuous	Parallel-to-Subparallel-to-hummock clinoform	Wedge-to-mounded geometry	Low Frequency	Onlap; Erosional	Aggradational & Progradational -retrograding stacking pattern.	Basin floor close to the source, Shallow marine shelf & Deep marine.	Shale dominated Silt, & Sand.
Ha-B2	South	SF3	Low-to - Moderate	Disrupted to discontinuous	Subparallel-to-hummock clinoform	Wedge-like form	Low Frequency	Down lap	Aggradational, (Condense), Retrogradational stacking pattern	Basin floor fan, Basin floor shelf edge, Shelf-delta, Slope fan, & Maximum flooding surface (MSF)	Silt dominated, Shale & Sand
Ha-K1	South	SF4	High-to-Moderate	Continuous-to-Semi continuous	Parallel-to-Subparallel	Sheet-to-Wedge geometry	High to Low Frequency	Down lap	Aggradational, (Condense), Retrogradational stacking pattern	Basin floor fan, Basin floor shelf edge, Shelf-delta, Slope fan &Maximum flooding surface (MSF).	Sand dominated, Erosional channel sand, silt.

5.4 Conclusions

The seismic stratigraphy and depositional environments of the sediments of Valanginian (Early Cretaceous) age, in the Gamtoos Basin, Offshore South Africa, have been studied using characteristics of the seismic reflection termination pattern analysis approach as outlined by Vail, *et al.*, (1977) and Mitchum Jr, *et al.*, (1977). The seismic sequence and seismic facies results were calibrated with well logs from drilled wells. This approach was done by classifying the layers between major unconformities of the Valanginian age of sediments based on seismic reflection patterns.

The seismic reflections terminations patterns characteristics such as toplap, erosional truncation, onlap and downlap, for the seismic sequence analysis interpretation for the studied wells from the north to the south in the study area respectively, indicated a deep marine depositional environment, that comprises a submarine fan, basin floor fan, and abyssal depositional environments, with an indication of periods of erosional surfaces and non-deposition of sediments. The sequences studied were deposited during the same geologic time i.e. Valanginian stage of Early Cretaceous. The studies reveal that the sediments in the northern part were deposited under deep marine condition.

The seismic facies analysis was interpreted based on the seismic reflections attributes such as amplitude, continuity, frequency and the external geometry reflection from these drilled wells in the study area from the north to the south. The depositional succession belonging to the Valanginian age indicate a low energy facies , inter-deltaic / pro-deltaic to continental shelf, shallow marine to deep marine environments in the north. This suggests shallow to deep marine sediments were deposited in the northern part of the study area.

The southern part of the study area also indicated almost identical depositional environment similar to the northern part where the mass flooding of the Valanginian age group of sediments were deposited within a shallow marine-shelf (pro-delta, continental shelf and basin shelf) to deep marine environment with channel fill sediments. Some of the deposition took place as a submarine canyon fill deposit and as sub marine fan lobe. It is thus concluded that the mass flooding depositional sequence of sediments deposited in this part of the study revealed a shelf to deep marine environment.

The electrical log signatures from the studied well sections indicates a lithology mainly dominated by sand and silt as indicated from the gamma ray curves of cylindrical-blocky and serrated log signatures of graded coarse grained sand-stone to medium-fine grained silt units. This further shows an aggradation stacking pattern. These log signatures along with the identified parasequence sets after calibration with the seismic facies indicates that the environment of deposition varies from submarine channel-fill, submarine canyon–fill to shallow continental shelf. It is thus concluded to have been a shallow marine to deep marine depositional environment in the northern part of the study area.

The electrical log pattern from the southern part of the studied area also indicates a similar aggradation stacking parasequence (cylindrical or blocky shape) of sediments built-up of thick uniformly graded medium-to-fine-to-coarse grained-silt-shale-sandstone units. This indicates deep tidal channel-fill, shallow marine, submarine channel to deep marine depositional environments, similar to the northern part, thus suggesting a transgressive system tract set of sediments.

The 3D-lithofacies surface depth attribute facies map indicates a mass flooding characterised by thick bedded siltstone lobe (siltstone facies) with intercalated fine mud-rock (Shale facies) and minor sandstone in low energy turbidite channel depositional environment in the south-western part of the study area. The northern part indicates a diachronous deposition dominated by sandstone, intercalated with minor siltstone and shale, probably deposited in a high energy turbidite channel, followed by low energy settling of the siltstones and shale before the next pulse of high energy sandstones were deposited. The north-east to the south-east of the Valanginian sequence suggests that high energy turbidites might be encoutered, the marine deposits dominated by sandstone intercalated with siltstone and minor shale that are characterized by erosional surfaces due to tectonic processes as a result of uplift that created a sediment hiatus in the section .

Based on the results, these approaches are proven technique to understand the environments of the sediments belonging to the Valanginian stage within the basin.

CHAPTER SIX

6. Foraminiferal Biostratigraphy of the Early Cretaceous Succession in Gamtoos Basin, Offshore South Africa

ABSTRACT

Importance of biostratigraphy as a tool for basin analysis is very well known for last several decades. Apart from the fixing the stratigraphic position (geological age), biostratigraphic analysis helps to understand the depositional environment and bathymetric fluctuation during the course of sedimentation. Various biostratigraphic tools are commonly used for this interpretation. Foraminifera are considered the best microfossils for marine succession particularly for late Mesozoic sediments. In the present chapter an attempt has been made to confirm the geological age of the studied succession often referred as Valanginian section in various chapters in this thesis.

In the South African sedimentary basins the lithological succession between the seismic markers P and J1 is represented by thick piles of clastic sediments commonly referred to as Valanginian section. In a few drilled exploratory wells in the Gamtoos Basin this section was encountered out of which the wells Ha-G1 and Ha-I1 are studied for biostratigraphy. In absence of planktonic foraminifera only two major benthic groups viz. calcareous and agglutinated were studied and compared with known Valanginian succession from different areas. The benthic foraminiferal assemblage in this work confirms early Cretaceous Valanginian age for the studied intervals.

Temporal distribution of foraminifera from both the sections reveal that throughout the Valanginian time deposition took place in marine slope under bathyal environment with an average bathymetry of ~500m with minor fluctuations. The sections in both the wells are dominated by fine clastic (shale with minor siltstone). At some interval development of reservoir facies (sandstone) are noticed in the deeper slope as marine fan complexes. This observation supports the conclusion drawn from the seismic facies analysis.

Keywords; Biostratigraphy, Foraminifera, Depositional environments, Bathyal, Deep marine, Paleobathymetry

6.1 Introduction to Foraminiferal Biostratigraphy

In the continental margin around the South Africa's coastline there is about 165 000km^2 continental shelf (up to 200 m isobath) and approximately 400 000km^2 out to the 2000m isobath. Most part of this area is middle to late Mesozoic time and the basins were originated before middle Jurassic (Board *et.al.* 2006).

Located on the southern part of the Africa continent the Outeniqua Basin comprises a series of rift sub-basins from west to east, the Bredasdorp, Pletmos, Gamtoos and Algoa sub-basins. From the study of calcareous nannofossils under the Deep-Sea Drilling project (DSDP) leg 71, it was postulated that the oldest datable sediments belong to late Jurassic (Kimmeridgian /Portlandian) age (Wise, 1983).

The synrift stratigraphy of the present research area of Gamtoos sub-basin is not clearly understood as the synrift sediments were not penetrated in the offshore wells. In the onshore part the synrift sediments comprises mainly continental clastics (shale, siltstones and sandstones) belonging to the Kirkwood Formation (Winter, 1973; McLachlan and McMillan, 1979). This was followed by marine shales and sandstones of the Sunday River Formation which was dated as Late Valanginian to Hauterivian (Valicenti and Stephens, 1984). These two units (continental and marine) are later brought together as Uitenhage Group and broadly dated as Portlandian (Tithonian) to Early Valanginian.

As reported by McMillan *et.al*, (1997), the development of the Gamtoos and Algoa basins were initiated in the middle Jurassic (?) and continued during the late Jurassic and earliest Cretaceous time. The oldest datable sediments encountered during exploratory well drilling is of late Jurassic (Kimmeridgian) age. The depocenter area is around 7000m thick with undrilled Mesozoic succession. All the above age assignments are based on stratigraphic positions of the unconformity surfaces as observed in seismic sections. Sediments within the drilled sections are characterised by basal non-marine conglomerate and red beds (McMillan et.al, 1997) followed by interbedded sandstones and siltstones. In the area close to the Gamtoos Fault and near the Gamtoos Basin depocenter black claystones (anoxic) are reported with presence of sparse microfauna (mainly agglutinated foraminifera with Radiolaria flooding). Details of these microfauna were not reported in these reports.

6.1.1 Foraminifera Microfossil Biostratigraphy in Gamtoos Basin

History of oil exploration in South African sedimentary basins started about six decades ago however, barring for a very few publications (McLachlan and McMillan 1976, 1979; McMillan 1990a &1990b, 2003; McMillan et.al., 1997) detail work on the microfossil biostratigraphy for the drilled succession is relatively unknown for these basins. Most of these publications are related to the reference of foraminifera of Aptian-Albian stages of the early Cretaceous and from younger sections. Although reference of further deeper succession (Berriasian–Valanginian-Hauterivian–Barremian) within the earliest Cretaceous has been mentioned in some publications, no significant record of foraminiferal biostratigraphy has been reported. An integrated work based on foraminiferal biostratigraphy and sedimentation pattern from the post drift succession (Early Barremian to Late Maastrichtian) of the seven South African basins are referred by McMillan (2003), this covers mainly post Valanginian sediments and no information on the older sections are available.

An attempt has been made in the present research to confirm the stratigraphic position of the sedimentary succession penetrated in the subsurface (referred as called Valanginian sediments) and to confirm the age from the studies of temporal distribution of the marine microfossil group 'foraminifera'. The present work also helps to understand the environment of deposition and paleo depth aspects using benthic foraminifera as referred by several researchers from time to time. For the present work well cuttings available from the two exploratory drilled wells were considered and the preparation technique has already been discussed in Chapter FOUR of this thesis. All the samples available in this work are unwashed drill cuttings received from the core house facility of the Petroleum Agency of South Africa, Cape Town. For some intervals in both the wells samples were not available for examination. All the well cuttings were processed in the departmental laboratory for microscopic examination.

6.1.2 Sample Preparation for Biostratigraphic Work

A total of 54 selected well cuttings from the two exploratory wells (26 well cutting samples from the Well Ha-G1 and 28 samples from the well Ha-I1) of Gamtoos Basin were made available for biostratigraphic interpretation. The samples were selected after careful examination of the well logs and avoiding the sandstone intervals. Most of the samples were collected from fine argillaceous shale/claystone/siltstone intervals for a better faunal recovery. However, samples from a few intervals were either not available or not selected (due to high arenaceous nature) from both the wells (1650-1700m, 1780-1850m, 1970-2190m of well Ha-I1 and 1410-1480m, 1550-1600m of well Ha-G1). In biostratigraphic studies argillaceous samples (preferably shale or siltstone) are always preferred for processing for better faunal recovery.

Standard amounts of unwashed sample (20grams) were processed for each interval. The processed residues were manually sorted and then were classified under different morphogroups and their generic status was determined using standard taxonomic reference books (Loeblich Jr., A., Alfred R., Tappan, H., 1988). The identification for different species were carried out using several journals and catalogues of foraminifera.

The temporal distribution of foraminifera with the frequency against each 20 grams of samples from the selected intervals of the two wells Ha-G1 and Ha-I1 are presented in Tables 6 .1 and 6.2 respectively. The foraminifera biostratigraphy from the two wells are discussed in the following paragraphs.

6.1.2.1 Foraminiferal biostratigraphy of Well Ha-G1, Gamtoos Basin

The exploratory well Ha-G1 located in the offshore Gamtoos Basin (figure.5.1) was drilled up to a depth of 2645m to explore hydrocarbon below Berriasian and older sediments. For foraminiferal biostratigraphic studies only unwashed cutting samples were available from the Petroleum Agency of South Africa, Cape Town core house. A total of 26 unwashed drill cutting samples between the intervals 1265m -1670m were selected available for this study. Samples for a few intervals were not available in the core house, moreover samples from sandstone dominated intervals are not preferred due to poor faunal yield. These intervals are between 1410-1480m, and 1550-1600m. All the samples examined in the present work were selected after careful examination of well logs followed by megascopic examination of the lithology. The frequency of foraminifera along with other microfauna groups like ostracod, pteropods etc. are also presented in Table 6.1, the interpretation of the biostratigraphy along with paleoenvironmental detail is presented in Figure 6.1.

Table 6. 1: DISTRIBUTION OF DIFFERENT MICROFOSSIL GROUPS WITHIN THE INTERVAL 1265M TO 1670m IN THE WELL Ha-G1, GAMTOOS BASIN

Sample Interval (mts.)	Calcareous benthic foraminifera													Agglutinated benthic foraminifera																	
	Epistomina caracolla	*Epistomina oronata*	*Epistomina hechti*	*Lenticulina guttata*	*Lenticulina muensteri*	*Lenticulina* sp.	*Gavelinella sigmoicosta*	*Dentalina* sp.	*Lagena hauteriviana*	*Lagena* sp.	*Nodosaria* sp.	*Robulus vortex*	*Marginulopsis* cf. *robusta*	*Bathysiphon* sp.	*Haplophragmoides cushmani*	*Haplophragmoides* sp.	*Dorothia kummi*	*Dorothia subtrochus*	*Hyperammina gaultina*	*Trochammina* sp.	*Ammobaculites agglutinans*	*Ammobaculites* sp.	*Textularia bettenstaedti.*	Ostracoda sp.	Bryozoa	Pteropods	Micro bivalves	Algal fragments
1265-70														1																
1275-80					1			1																						
1280-85		1						1																						
1285-90														1																
1300-05		1	1		1									1																
1305-10		1												2																
1315-20						1																1								
1325-30														1																
1355-60																2														
1360-65																						1								
1375-80	1	1		1																		1			3		2			
1395-1400	2	3		4				1							1		1		3			1		1	2					
SAMPLE GAP																														
1485-90				1	1									1																
1495-1500	2	2		4										1	3					4						1				
1510-20				1																										
1520-25	10	3		2					1	1					2		2	1	1			3								
1525-30																														
1530-35	3	2		2	2					1				6			1							2		4			
1535-40	4	3	3								1			8	1								1							
SAMPLE GAP																														
1610-15	1				1									1									1							
1615-20					1																		1							
1620-25	5				8								1		1								17			1				
1625-30					1																1									2
1635-40													1		1	1														
1655-60					2							1							3				2							
1665-70																										1				

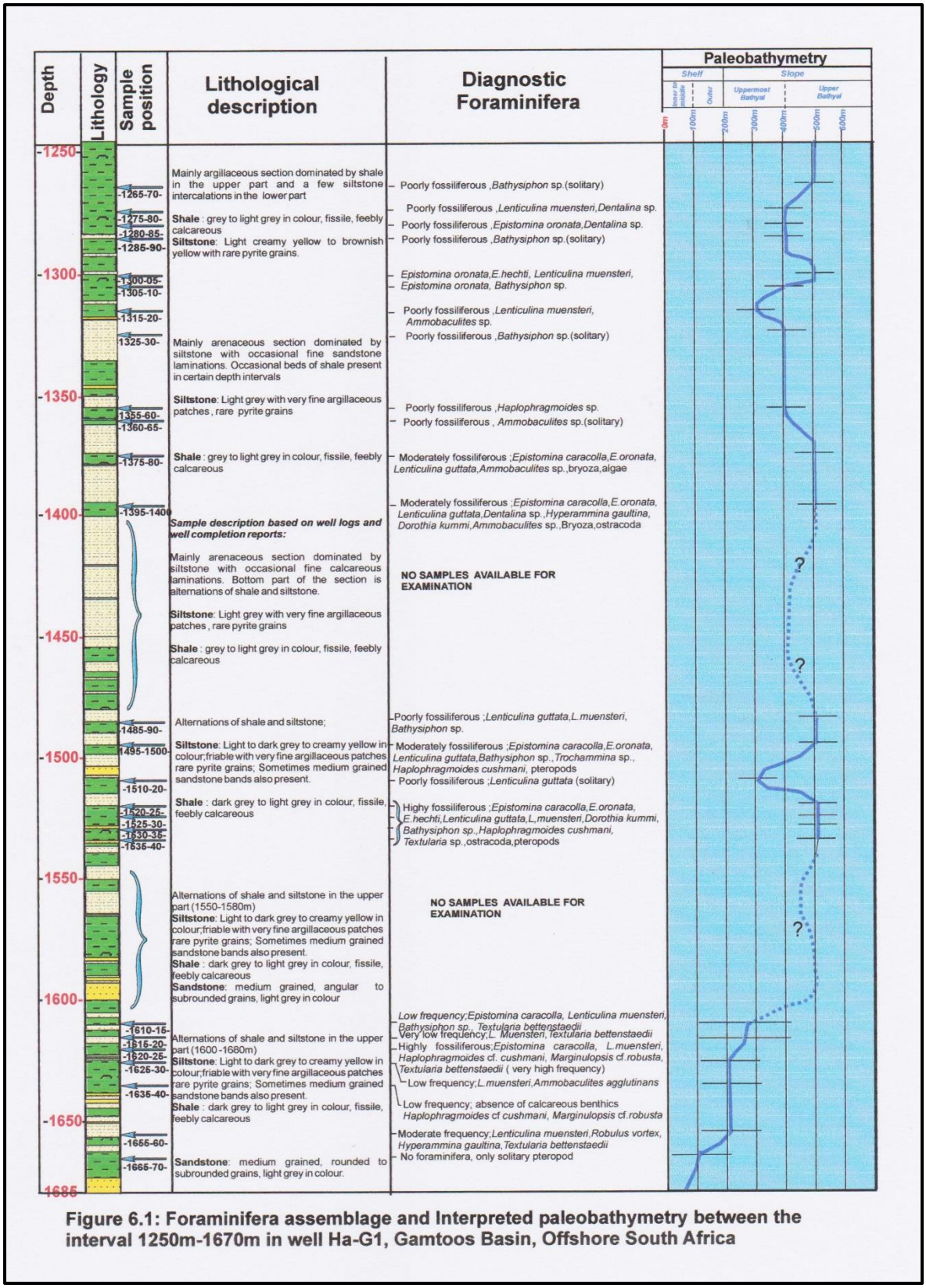

Figure 6.1: Foraminifera assemblage and Interpreted paleobathymetry between the interval 1250m-1670m in well Ha-G1, Gamtoos Basin, Offshore South Africa

Figure 6. 1: Foraminifera assemblage and interpreted Paleobathymetry between the interval 1250m – 1670m in well Ha-G1, Gamtoos Basin, Offshore South Africa.

The temporal distributions of the microfauna reveal that foraminifera are the most dominant microfossil group present in well Ha-G1. However, presences of any planktonic foraminifera were not recorded in within the studied intervals. Only benthic foraminifera represented by both calcareous and agglutinated varieties are present and are almost equally dominant in most of the samples. This indicates a well oxygenated bottom condition during the time of deposition. Apart from foraminifera, rare / occasional presence of ostracods, bryozoan, pteropods and micro bivalves (rare) are present in a few samples between the intervals 1375m to 1670m.

The lower most few samples the foraminiferal frequency was poor but increased gradually around the interval 1610m-1640m. The lithology in the bottom is dominated by sandstone and followed by alteration of finer clastic shale-siltstone laminations indicating a gradual increase in bathymetry. The benthic foraminiferal assemblages are dominated by calcareous benthics (*Lenticulina muensteri* and *Epistomina caracolla*) along with agglutinated benthics represented by *Textularia bettenstaedri, Haplophragmoides* sp.etc. The gradual increase in faunal frequency along with presence of both calcareous and agglutinated foraminifera in general indicates good oxygenated condition and the deposition within outer - middle shelf to upper bathyal (>300m). Above this interval samples between 1540m till 1600m was not available for examination. The lithology interpreted from well logs and from the Well Completion Report suggests presence of thick sandstone and shale/silt cyclic deposition.

The frequency and diversity of both calcareous benthics and agglutinated foraminifera gradually increased within the interval 1485-1540m. This interval is represented by a lithology of mainly alternation of shale and siltstone with a few fine sandstone beds. Frequency and diversity of calcareous benthics represented by several species of the genus *Epistomina* like *E. caracolla, E. oronata, E. hechti* along with *Lenticulina guttata, L. muensteri, Lagena* spp. is the characteristics for this interval. Among the agglutinated foraminifera constant presence of *Bathysiphon* sp., in many samples along with *Dorothia kummi* and *D. subtrochus* indicates undisturbed uppermost to middle bathyal condition (> 400m depth) with minor fluctuation in between some interval. Presence of bathyal species like *Trochammina, Ammobaculites* sp., *Hyperammina* sp. in some samples also suggests paleodepth of 400m to 500m under the marine slope. For the overlying succession between 1400m to 1485m no samples were available for examination. The well

logs and information available from the Well Completion Report (Well Ha-G1) suggests that except the lower part (1460m-1485m) the interval is dominated by shale with progressive increase in siltstone with a few calcareous bands in the upperpart indicating a slight decrease in water depth.

The uppermost section between 1265m to 1400m is again a siltstone dominant section with a few arenaceous intervals in the lower part. The uppermost part above 1325m is entirely a shale dominant section. The lower argillaceous part (1375m to 1400m) is moderately fossiliferous where calcareous benthics *Epistomina caracolla, E. coronata* and *Lenticulina guttata* continues from the underlying intervals. Agglutinated foraminifera frequency within this interval decreases. Presence of *Bathysiphon* sp., *Haplophragmoides* sp. and *Ammobaculites* sp. indicates a fluctuating bathymetry between 300-500m (uppermost bathyal to upper bathyal) during the time of deposition.

6.1.2.2 Biostratigraphy of Well Ha-I1

The exploratory Wildcat well Ha-I1 located around 5.9 km North East of the Well Ha-G1 (Fig 5.1) was drilled upto a depth of 2420 m. Available unwashed cutting samples (total 28 numbers), selected mainly from the highly argillaceous (shale/siltstone dominant) interval 1410m to 2780m from this well were considered for analysis. Samples between 1770-1850m and 1960m-2000m were not available or were sandstone dominated intervals, therefore not considered for the present work. The laboratory processed samples were sorted for microfossils and their frequency recorded. Detail of the vertical distribution of the micro fauna (foraminifera and other microfossil groups) recorded for this well is presented in Table 6.2 and the detail integrated biostratigraphy and paleoenvironment is presented in figures 6.2 and 6.3 respectively.

The overall microfaunal assemblage in well Ha-I1 shows a strong similarity in faunal composition with the well Ha-G1. The lower most interval from below 2320m and 2400m is a highly arenaceous section dominated by sandstone and silt and is poorly fossiliferous, only presence of solitary ostracoda is recorded .The overlying argillaceous interval between 2310m to 2380m comprising mainly shale with a few siltstone beds is also moderately to poorly fossiliferous, a few benthic foraminifera like *Epistommina caracolla* and *Reophax* sp. along with Radiolaria dominated interval indicates gradual increase in

bathymetry. The shale dominated interval from 2320m to 2210m is moderately fossiliferous with diverse assemblage of calcareous and agglutinated benthics. The calcareous benthic assemblage comprises of *Epistomina caracolla*, *E. oronata* and some indeterminate *Epistomina* species. Presence of *Lenticulina guttata, L. subgaultina, L.*cf. *muensteri* along with rare occurrence of *Gavelinella sigmoicosta, Robulus nitidus* and *Marginulina* sp. and rare *Polymorphina* sp. The agglutinated foraminiferal assemblage mainly comprises of *Bathysiphon* sp., *Haplophragmoides* sp. and *Trochammina* sp. with rare occurrence of *Reophax* sp., *Rhyzammina* sp. and *Hyperammina elongata*. Throughout this interval presence of ostracods was recorded. The microfauna gradually decrease towards the top. This interval is followed by a thick arenaceous unit (sandstone) between 1920m-2210m devoid of fauna.

The next higher unit comprises of the claystone/shale association between 1870m to 1920m. Only three samples were available for study within this interval. The two samples in the bottom part (between 1890m to 1920m) yielded a rich assemblage of benthic foraminifera and both calcareous and agglutinated benthics are present. This sudden increase in frequency of both the benthic groups suggests an increase in bathymetry (~500m) and more oxygenated open marine environment prevailed during the period. The calcareous benthic foraminiferal assemblage comprises of *Epistomina caracolla, E. oronata* and *Lenticulina* cf. *muensteri* along with solitary *Polymorphina* sp. Agglutinated foraminifera with relatively low frequency and diversity continues from the bottom section. The increase in the frequency of *Bathysiphon* sp. and presence of *Haplophragmoides cushmani* indicates an upper bathyal (possibly marine slope) environment. There is a decrease in bathymetry above this interval as revealed by low of the foraminifera and increase in arenaceous content (mainly sandstone with few intermittent shale bands) in the immediate younger succession. Above this between 1760m- 1860m and 1670m- 1720m no samples were not available for examination. However almost all the samples available for analysis above 1750m yielded deep water foraminifera *Bathysiphon* sp. with Textularia sp., *Ammobaculites acquale*, *Reophax* sp., and *Textularia* sp. in a few intervals. Most of these forms are common in the marine slope environment

Table 6. 2: DISTRIBUTION OF DIFFERENT MICROFOSSIL GROUPS WITHIN THE INTERVAL 1410M TO 2380m IN THE WELL Ha-I1, GAMTOOS BASIN

Sample Interval (mts.)	Calcareous benthic foraminifera										Agglutinated benthic foraminifera																				
	Epistomina caracolla	*Epistomina oronata*	*Epistomina* spp.	*Lenticulina guttata*	*L. subgaultina*	*L.cf. muensteri*	*Gavelinella sigmoicosta*	*Robulus nitidus*	*Marginulina* sp.	*Polymorphina* sp.	*Bathysiphon* sp.	*Rhizammina algaeformis*	*Gyroidinoides* sp.	*Reophax* sp.	*Haplophragmoides* sp.	*H.globus*	*H.cushmani*	*Hyperammina elongata*	*Hypermmina* sp.	*abrupta*	*T. depressa*	*.Haplophragmium* sp.	*Ammobaculites acquale*	*Textularia* sp.	*Glomospira* sp.	*Saccammina lathrami*	Ostracoda sp.	Radiolaria	Pteropods	Algal fragments
1410-20											2																		6	
1430-40				1															1										2	
1450-60	1										1												1				1			
1470-80											3												2		1					
1510-20											1												2						4	
1530-40											4												1			1				
1560-70	1										3			2										2					3	
1600-10											1			2															1	1
1620-30			2																											
1640-50											5																			
1720-30											4																			
1730-40			2																											
1740-50			1								1																	1		
1750-60											2																			
							S	A	M	P	L	E				G	A	P												
1870-80	1					1					4						1													
1890-1900	7	3				4					3		1				5										1		2	
1910-20	18	6				2					6						2					2					4		1	
							S	A	M	P	L	E				G	A	P												
2210-20								1			1				1												2			
2230-40											2					1				2							1		3	
2250-60	2								1			1			1												6			
2260-70				1							1			2	3					1							1			
2270-80															4					1							1			
2280-90	4	3	2			1	1											2									3			
2310-20	2			1	3						1																1			
2330-40																												10		
2350-60	2													1																
2370-80																											2			

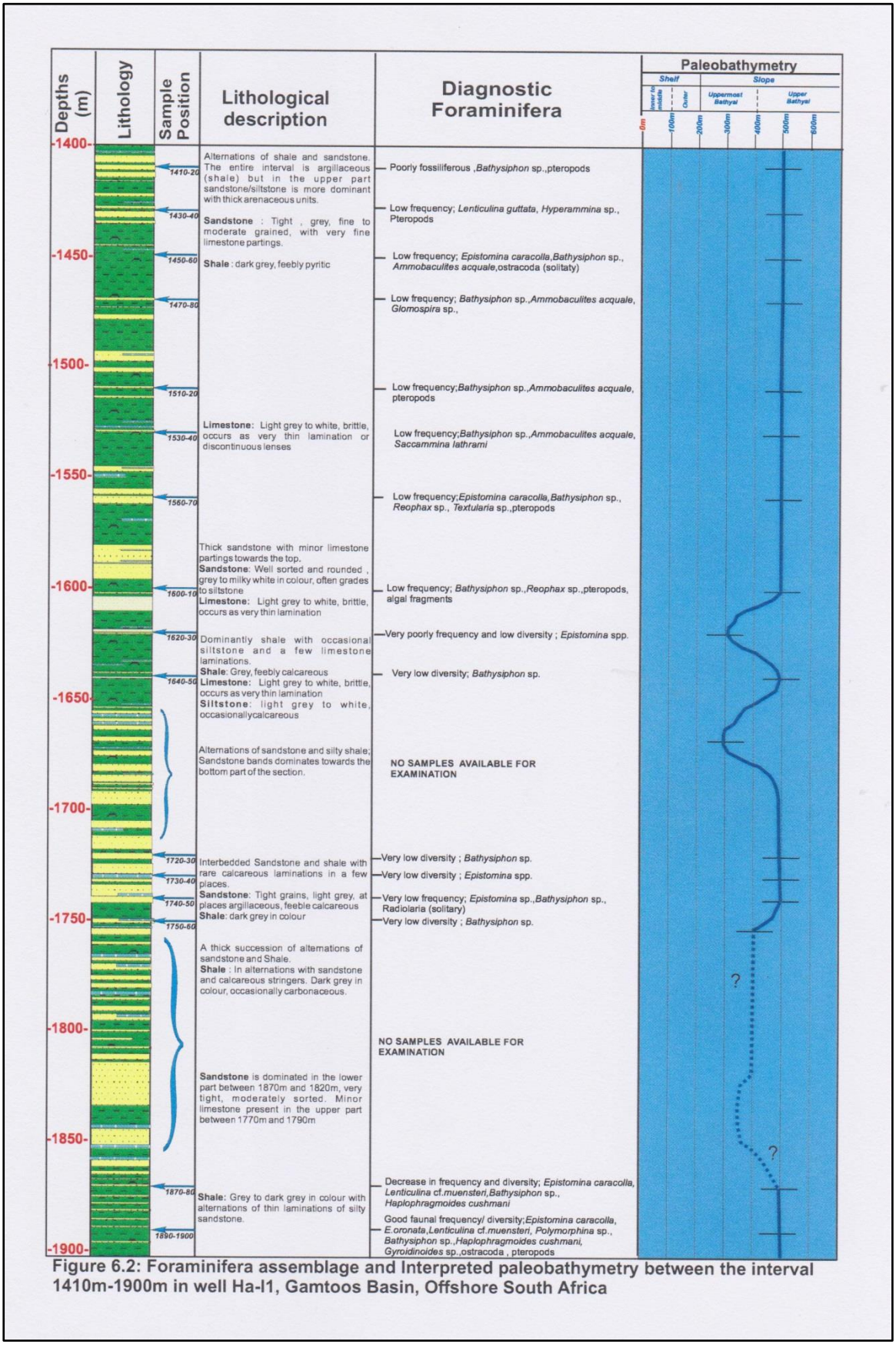

Figure 6.2: Foraminifera assemblage and Interpreted paleobathymetry between the interval 1410m-1900m in well Ha-I1, Gamtoos Basin, Offshore South Africa

Figure 6. 2: Foraminifera assemblage and interpreted paleobathymetry between the interval 1410m – 1900m in well Ha-I, Gamtoos Basin, Offshore South Africa.

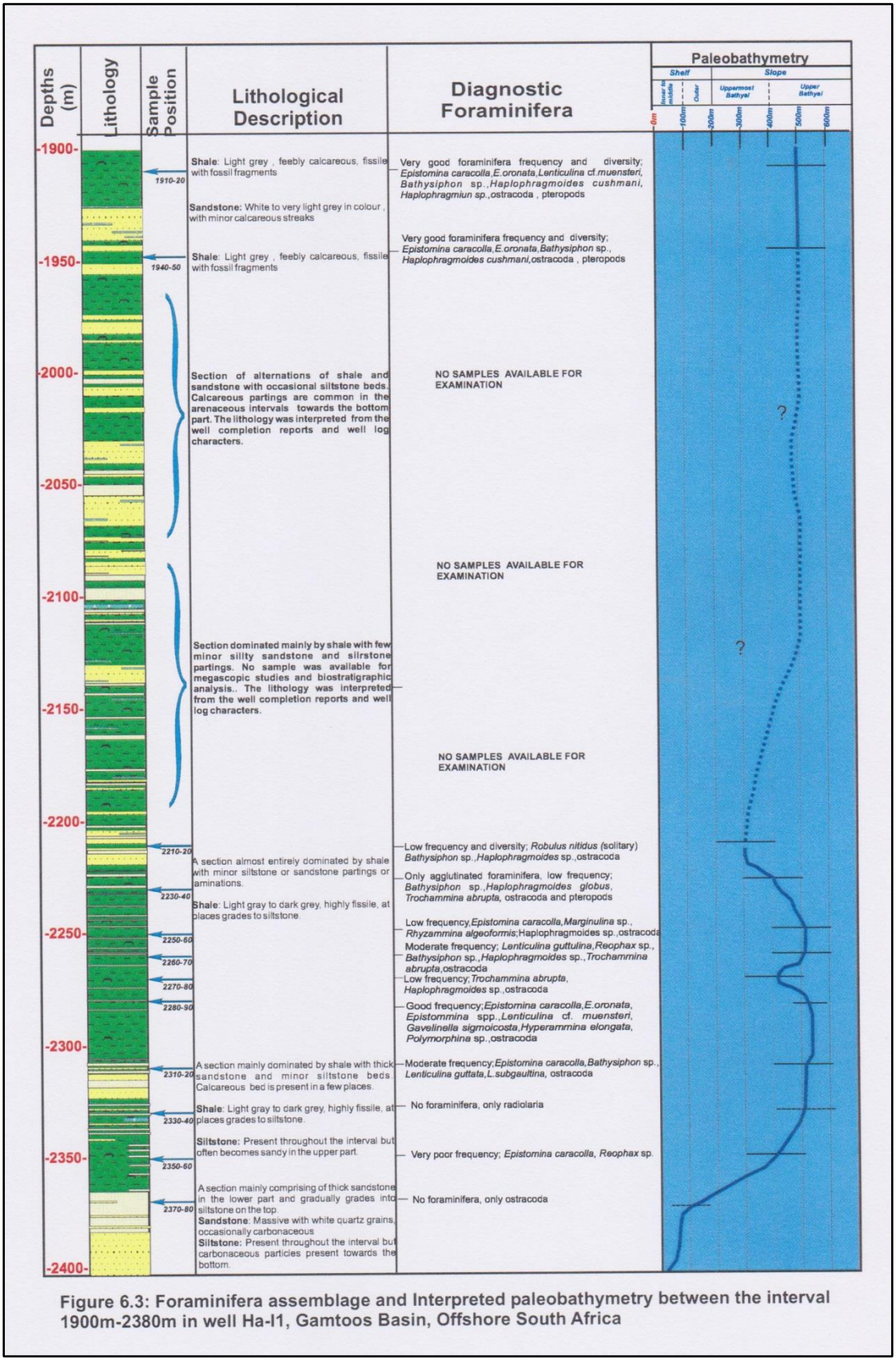

Figure 6.3: Foraminifera assemblage and Interpreted paleobathymetry between the interval 1900m-2380m in well Ha-I1, Gamtoos Basin, Offshore South Africa

Figure 6. 3: Foraminiferal assemblage and Interpreted paleobathymetry between the interval 1900m -2380m in well Ha-I1, Gamtoos Basin, and Offshore South Africa.

6.2 Discussion about the geological age OF THE SUCCESSION

Foraminiferal biostratigraphic study carried out in the two exploratory wells Ha-G1 and Ha-I1 indicates some similarities in the assemblages of calcareous and agglutinated benthics. In both the wells no planktonic foraminiferal assemblages were recorded. Similar observation was also found from the nearby surface sections especially in the coastal areas by McLachlan et.al (1979). The benthic foraminifera assemblage in the two studied sections indicates presence of calcareous foraminifera with very good frequency in the lower part and gradually the frequency decreased in the upper part. Several species of the genus *Epistomina* represented by *E.caracolla, E.oronata* and the genus *Lenticulina* (*Lenticulina* cf. *muensteri* and *L.guttata*) are common in almost equal proportion in both the wells. The agglutinated foraminifera from the two wells also show a similarity in distribution with frequent presence of *Bathysiphon* sp. in most of the studied samples. Several species of other agglutinated foraminifera like *Haplophragmoides cushmani*, *Dorothia kummi*, *D.subtrochus*, *Hyperammina gaultina*, *Ammobaculites* spp. and *Textularia* spp. are also present in several samples. Similarity in both the assemblages indicates that both the studied sections are almost from the identical age. However, no record of detail information about the earliest Cretaceous foraminiferal assemblage from any wells of Gamtoos Basin or from any nearby basins like Algoa or Pletmos Basin are available.

There is a strong similarity in benthic assemblages in several DSDP/ODP studies carried out from the Indian Ocean sites and in some other areas. Some of the notable works includes the study of early Cretaceous foraminifera from Barrow Group sites 762 and 763, Northwest shelf Australia (Jones and Wonders, 1992), DSDP site 263 (Hobbourn *et. al.*, 1995), Sites 259 and 261 (Bartenstein, 1974) and from Polish Lowlands (Sztejn, J.,1969).

The Barrow Group sites 762 and 763 have yielded a similar assemblage of benthic foraminifera. A rich assemblage of agglutinated foraminifera species viz. *Haplophragmoides cushmani*, *Dorothia kummi*, *Textularia bettenstaedti* and calcareous benthics *Epistomina caracolla* and *Lenticulina muensteri* are like the assemblages from the present work on Gamtoos Basin. In Barrow Group sites this interval is placed under Valanginian stage (Early Cretaceous). In the Polish Lowlands known surface exposures from the Valanginian stage were studied by Sztejn (1969) to understand the foraminiferal assemblage. The Valanginian age of this section was confirmed earlier due to rich index species of invertebrate ammonoid fauna. Microfossils recovered from this section have also yielded *Epistomina caracolla, E. oronata, Lenticulina muensteri, L. guttata, Haplophragmoides cushmani.* Studies of Late Jurassic /

Cretaceous Epistominidae of Canada and Europe (Williamson and Stam, 1988) have yielded the same *Epistomina* assemblage from the Valanginian section.

In absence of any age diagnostic planktonic foraminifera and on the basis the calcareous benthic association of *Epistomina* spp. along with *Lenticulina* spp. and the agglutinated foraminifera assemblage the studied section can be placed under Valanginian age of early Cretaceous epoch.

6.2.1 Paleobathymetry and Depositional Environment

Temporal distribution of the microfossil group foraminifera from the Valanginian section of the two wells Ha-G1 and Ha-I1 shows a strong similarity in faunal composition. As already mentioned, both the sections are mainly comprising of lithology dominated by shale and fine siltstone with few sandstone intervals. However, no planktonic foraminifera were recorded in both the sections. Both the studied sections recorded presence of agglutinated and calcareous benthics in various frequencies.

Studies on the benthic foraminifera morphology and its relationship with depositional environment in marine realm is a well-known subject of biostratigraphic research (Nagy, 1992; Szydlo, 2005; Reolid *et.al.*, 2008; Nagy et.al., 2009; Lob *et.al.*, 2012 and others). In most of these research major benthic morphogroups (foraminifera microfossil) analysis was carried out to identify changes in depositional environment through time. This often helps in identification of transgressive – regressive sequences in the subsurface sections. In the present work all the samples studied were essentially well cuttings (as no conventional core samples were available for biostratigraphic studies) and a fixed amount 20gms were only available for examination. For some intervals samples were not available also samples from sandstone intervals were not collected.

Comparison between the data obtained from the two well sections reveal some similarity in microfaunal composition. The calcareous benthics present in the lower part of both sections comprises of *Epistomina* spp. in the lower part of both the two well. Their frequency gradually decreases towards the upper part. The other common calcareous benthic is *Lenticulina* spp. and their presence is noticed in both the sections although the frequency is relatively low. Rare occurrence of *Dentalina* sp., *Lagena* sp., *Robulus* sp., *Marginulopsis* sp. etc. are present in a few intervals. In general, the genus *Lenticulina* are epifauna with a living habit in outer shelf to bathyal environment.

The other important benthic foraminifera group present in the two Valanginian sections are the agglutinated foraminifera which are well known from bathyal to abyssal marine environment. They are represented by erect epifaunal groups like *Bathysiphon* spp. common throughout the studied intervals and *Rhyzammina* sp. (rare). Both these two agglutinated foraminifera are well known depth indictors and are common in bathyal to abyssal depths. The other epifauna groups represented in both the sections are *Trochammina* spp., and *Glomospira* sp. (only in well Ha-I1) known to occur in a wide range of oceanic depths from outer shelf to abyssal. The common infauna groups such as *Haplophragmoides* spp., *Ammobaculites* spp., *Textularia* spp. are present in several intervals throughout the well sections are known to occur from outer shelf to bathyal environment. The temporal distribution of the depth indicator benthic foraminiferal group suggest that the Valanginian sediments comprises of the finer clastics were deposited within uppermost bathyal to upper bathyal (300m to 500m+) throughout within the marine slope .

CHAPTER SEVEN

7. Petrophysical Formation Evaluation of the Valanginian Depositional Sequence Gamtoos Basin, Offshore South Africa

ABSTRACT

In order to understand the heterogeneity of the reservoir and hydrocarbon accumulation and production capacities within the Valanginian section of Gamtoos Basin, offshore South Africa, petrophysical formation evaluation from the sandstone reservoirs has been performed. The Gamtoos Basin is an en-echelon sub-basin comprises of onshore and offshore components. Structurally it is a complex rift type basin and comprises of onshore and offshore components made up of relatively simple half grabens bounded by a major fault to the northeast, and contains comparable thickness of sediments of organic-rich shale rock for petroleum generation (Malan, 1993; McMillan, *et al.*, 1997). The early and late rift subsidence of these half grabens is reflected by the development of thick sediments containing Kimmeridgian-to-Hauterivian wet gas to oil prone shale with sandstone reservoir potential in the Valanginian.

The objective of the work presented under this chapter is to quantify the heterogeneity of the hydrocarbon bearing Valanginian sandstone reservoir from the five drilled wells (Ha-B2, Ha-G1, Ha-K1, Ha-A1, and Ha-I1) located from the north to the south of the study area. Formation evaluation from well logs using the petrophysical approach was applied by extensive utilization of Interactive Petrophysics (IP) ® software throughout the evaluation process. The data set used for this study contained wireline logs (Las format), core data and geological well completion reports.

Detailed petrophysical analyses were carried out on the selected sandstone dominated intervals of the studied wells. The log analysis from the drilled wells indicates presence of gas in the sandstone intervals. The cut-off parameters were applied on the eleven sandstone reservoir intervals studied from these wells to differentiate between the pay and non-pay interval sands, seven of the sand intervals were proven to be hydrocarbon bearing . Parameters like Porosity, permeability, water saturation and volume of clay were calculated within the pay sand intervals. The estimated average effective porosity for the pay sand intervals of the wells ranged from 12.5% to 16.2%, the average water saturation from 35.9% to 55.2% and the average volume of clay from 10.0% to 20.6% for the wells HA-K1, Ha-B2, Ha-I1 and Ha-A1

respectively. The predicted permeability obtained for the intervals lower than 1mD which indicates an interval with poor permeability that has no ability to transmit fluids.

The three pay sandstone intervals in well Ha-G1 indicated no hydrocarbon show with any effective porosity, water saturation and volume of clay respectively by cut-off value, the predicted permeability ranged from 0.08mD to 0.1mD. This suggests that the well Ha-G1is a dry hole as indicated in the Geological well completion reports.

This data available from the four wells indicates a hydrocarbon bearing reservoir (gas) with fair-to-good effective porosity and poor permeability with lower water saturation. The Interactive Petrophysics (IP) ©software gives a good account of the petrophysical evaluation of this formation.

Key words: Hydrocarbon, Reservoir, Effective Porosity, Permeability, Water saturation, Volume of clay, Formation Evaluation, Petrophysical properties.

7.1 Introduction to Analysis and Interpretation of Petrophysics

Petrophysical parameter studies are very important during the development and production stages of a well and for estimation of hydrocarbon reservoir potential in any oil and gas field. Furthermore, it facilitates the building of the geological model of a hydrocarbon reservoir based on reservoir properties such as lithology, porosity, permeability, water saturation and fluid type. Petrophysical analyses of the argillaceous sandstone reservoir of the Valanginian sequence of Gamtoos Basin, offshore South Africa were carried out using well logs and seismic data for static modeling of the reservoir. This study was motivated by the fact that the gas-bearing reservoir of the Gamtoos Basin drew instant attention as a result of its high economic potential. This basin was characterized as having both oil and gas generating source rocks with unknown hydrocarbon bearing capacity of the reservoir potential, in terms of the petrophysical properties based on the porosity, permeability and water saturation (Broad, 1990).

The aim of this study is to integrate petrophysical evaluation and seismic data analysis and interpretation the results to characterize the reservoir quality of the Valanginian sequence. The objective was to make use of details of the available well logs and 2D-seismic data to delineate the quality of the reservoir zones of the selected wells in the field. The delineation of the reservoir zones were performed based on porosity, permeability, water saturation and volume of clay, subsequently integrated with 2D-seismic data to determine the spatial distribution of the discrete and continuous reservoir rock geometric properties (porosity, permeability and water saturation), using stochastic modelling techniques (Chapter eight of this study). The detailed analysis of the Petrophysical data of the Valanginian section helps in better understanding of the hydrocarbon bearing reservoir units, variation in thickness and in the petrophysical parameters across the studied areas and possible hydrocarbon entrapment.

Five wells viz: Ha-B2, Ha-K1, Ha-A1, Ha-G1, and Ha-I1 from the North to the South of the study area, were selected for this analysis. However, due to insufficient data available for this analysis, the present work used the data of three wells Ha-B2, Ha-K1 and Ha-G1 only for Petrophysical evaluation of the reservoir. For the remaining two wells Ha-A1 and Ha-I1 data of conventional core analysis were not available and therefore to characterize the reservoir the data from the other three wells were extrapolated since they are relatively adjacent wells within the Valanginian section.

7.1.1 Introduction to Conventional Core Analysis

Conventional Core obtained from the subsurface during drilling operation represents a continuous section by providing a record of subsurface geology and data that might not be accessible in surface exposures particularly where weathering process damages the preserved organic matter.

The objective of coring is to offer information that will advances to more efficient oil or gas production, through geological information which includes the lithology types, nature of pore space, mineralogy or geochemistry, depositional environment as well as petrophysical and engineering information. The later includes permeability and porosity correlation, relative permeability, capillary pressure, grain density, electrical properties, thus enhancing the oil recovery studies and estimate the reserve that involves porosity and fluid saturation. Finally core analysis provides drilling and completions information that deal with fluid formation compatibility studies, rock mechanics data and grain size information for gravel pack design.

There are different ways of obtaining core during drilling that include conventional coring systems, special coring systems, wireline sidewall coring systems and coring bits systems. Proper care must be taken while placing the coring fluid, transporting and storage of cores in order to retain the desired fluid saturations. Sometimes, the initial reservoir condition and the coring fluids utilized may affect the saturation of water, oil or gas in the core arriving at the laboratory, as noticeably higher or lower than expected in its original state of the formation (Bateman, 1985).

The conventional core analyses are performed in the Petrophysics laboratory on the reservoir rock to obtain detailed measurements of reservoir parameter evaluations which include porosity, permeability and saturation (oil, water and gas), which are fundamental reservoir properties needed for the assessing of hydrocarbon in-place, productivity and overall economics. These types of analysis are mainly focused on the interval of selected areas to be analysed, and it is usually performed on homogeneous formations such as sandstones, carbonates and shaly sands, at about three or four inches of each foot of the core (Opuwari, 2010).

This analysis was performed on the wells Ha-G1, Ha-B2 and Ha-K1 used in this study and the core analysis was carried out from depths below the Valanginian sequence. The conventional core analysis measurements include grain density, gas expansion (core porosity), air permeability (Ka), liquid permeability (KL), saturation of fluids (gas, water and oil) and

calcimetry (calcite and dolomite). These were performed for the wells Ha-G1, Ha-B2 and Ha-K1.

The average core porosity ranges from 4% to 10% with an average of 5%, which indicates poor porosity. In the three wells permeability values of 0.08 mD, 0.05mD, and 0.09mD respectively were recorded from the cores indicating poor permeability. There was no oil show, but high water saturation (%) with recorded values of 65, 72 and 80% respectively and lower gas saturation (%) with recorded values of 35, 28 and 20% respectively, from the cored wells Ha-G1, Ha-B2 and Ha-K1. The conventional core analysis results of the wells utilized for calibration in this study were obtained from the core conventional description reports provided by the Petroleum agency of South Africa (PASA).

7.2 Analysis and Interpretation of the Geophysical Wireline Logs for the Selected Wells

The interpretation of the well logs utilized in this study to characterise the formation evaluation of the Valanginian section. This was based on the mode of its application in the geological and Petrophysical methods. These logs can be used as single for lithology identification e.g. GR log (gamma ray log) or in combination e.g. neutron and density logs, to obtain information both about the lithology and fluid types present in the reservoir. In terms of lithology identification penetrated by a well involves either a single or a combination of different logging curves: the Gamma ray, Neutron and Density logs, as well as Sonic log. A lithology of sandstone with variable thickness up to 5m with above and below that sandstone non-reservoir shales, can be referred to as sandstone reservoir and the fluids (gas and oil) within the spore spaces of that reservoir are known as hydrocarbons. In the present work a suite of logs from five wells Ha-G1, Ha-K1, Ha-B2, Ha-A1, and Ha-I1 was presented comprises of gamma ray (GR), resistivity (ILD, LLD and MSFL), Bulk density (RHOB), neutron (NPHI), caliper (CAL); other tracks in the suites included depths (track 1) and formation top (track 2). Figures 7.1 indicate one of the logs suites of the wells studied, with the interval of interest.

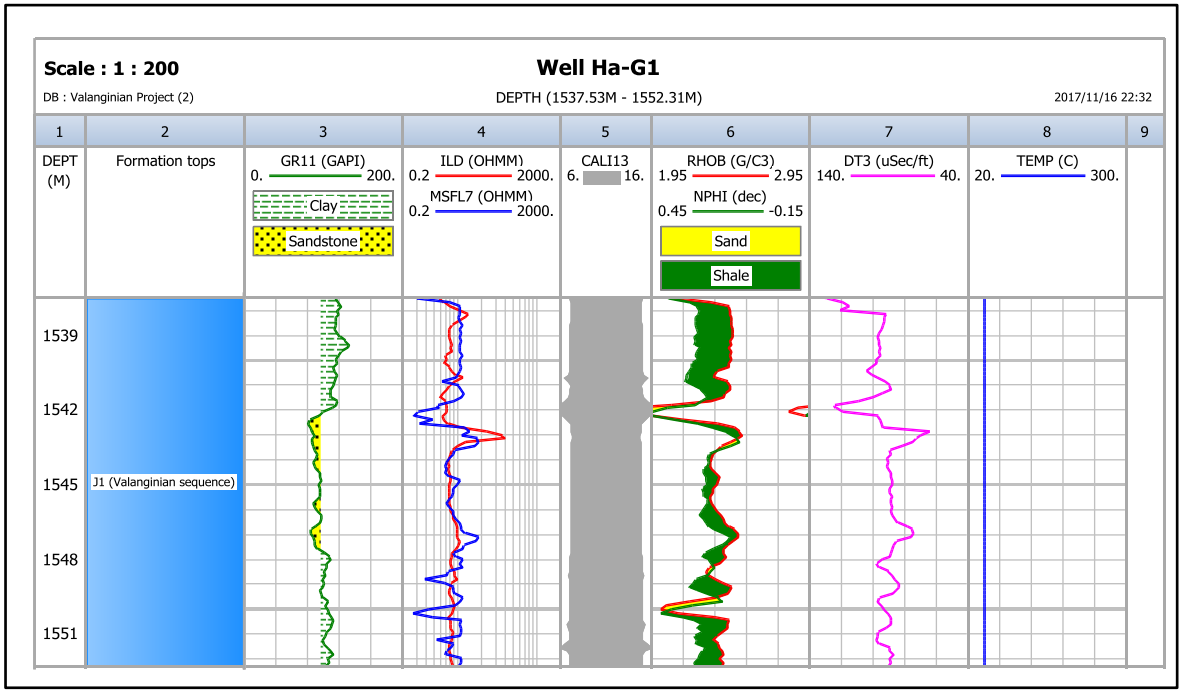

Figure 7. 1: Different log curves of well Ha-G1in different tracks.

The interpretation of the logs in this study begins with identification of intervals of interest or potential sandstone reservoirs i.e. the clean zones with hydrocarbon, followed by defining a clean sandstone and shale baseline or cut-off line on gamma ray log. This is done by using gamma ray log, where maximum deflection to the right indicates a shale lithology (high readings of gamma ray log) while the maximum deflection to the left indicates a clean sandstone (low readings of gamma ray log). The baseline or cut-off line was obtained from the mean value (API unit) of the histogram of the gamma ray plotted for each of the wells. Figure 7.2 indicates a histogram plot for well Ha-G1 with mean value 98 API for the baseline or cut-off line.

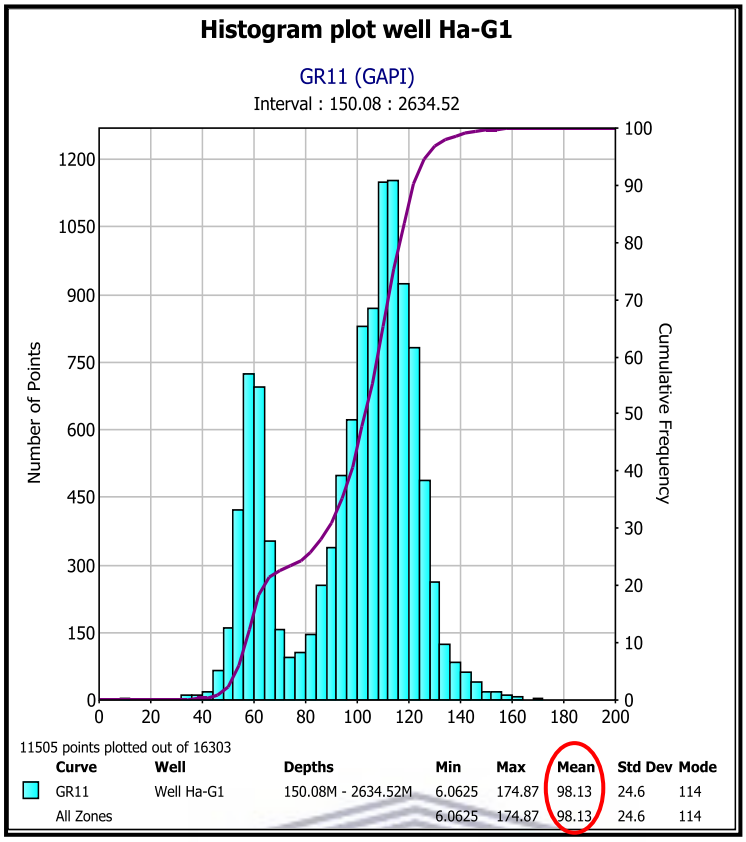

Figure 7. 2: Histogram for well Ha-G1 with mean value for the baseline or cut-off line.

7.2.1 Wireline logs interpretation of well Ha-G1

Well Ha-G1 was drilled in the Northern part of the study area, allowing consideration by means of gamma ray log (Figure 7.3, track 3) of the thickness and lithology of the Valanginian section of the well, which is ranging from depths 1040.1m to 1715.8m. Only three zones that can be recognised as potential reservoir (clean sand zone) were encountered within this sequence varying from depth 1537.53m – 1552.31m, 1669.81m – 1684.14m and 1692.37 – 1706.24m respectively; they are shallow zones. These zones were selected based on gamma ray behaviour and combination of density and neutron logs. Figure 7.3, 7.4 and 7.5 indicates the respective zones of the Valanginian section evaluated for this study.

Both Lateral Deep Log Resistivity and Micro-Spherically Focused Log (LLD & MSFL) (Figure 7.3, 7.4 and 7.5 Track 4) were used to identify the formation fluids (gas/oil/water) and possible fluid contacts in well Ha-G1. True resistivity and flushed zone resistivity within the borehole were also measured. Hydrocarbon bearing zones are indicated by high resistivity readings while decrease in resistivity readings suggests a salty water formation in the wellbore.

In zone 1, interval 1537.53m – 1552.31m depth, the resistivity effects from both logs are generally low within the reservoir interval which is an indication of the presence of salty water within the interval, except within the interval 1541.89m – 1543.34m where both resistivity logs are slightly higher; this slightly high reading in the resistivity suggests a possible hydrocarbon presence within this interval which can be confirmed by the slight cross-over of porosity logs of neutron-density which suggests a slight gas effect within the interval (Figure 7.3,7.4 and 7.5 Track 4). The little separation between the resistivity logs curves within the intervals may be owing to small contrast between formation water resistivity and mud filtrate used.

Zone 2, interval 1669.81m – 1684.14m indicates low resistivity readings from the logs which suggests the presence of salty water within the interval.

Zone 3, interval 1692.37m – 1706.24m is characterised by high and low resistivity readings from the logs within the interval of the section, this suggests the presence of conductive and non-conductive fluids of salty water and hydrocarbon respectively. This can be explained as the presence of gas within the interval of 1693.30m – 1695.65m as a slight cross-over of porosity logs of neutron-density was observed, while the interval 1696. 03m – 1706.24m indicates a low resistivity reading from the logs (Figure 7.3, 7.4 and 7.5 Track 4) indicating the presence of salty water. The sonic log (Figure 7.3, 7.4 and 7.5 tracks 7) which is also a porosity log, was used to identify the lithology of well Ha-G1 as the sonic logs are sensitive to negligible textural variations in both sand and shale, and thus help to identify the source rock as being shale. The temperature was recorded for this borehole across the intervals. In general, the uses of Micro-Spherically Focused Logs (MSFL) to determine the resistivity of the wellbore formation suggests that the formation has experienced flushing in which drilling fluids have displaced the formation fluids from the well borehole during the drilling. MSFL are known to provide measurements of flushed zone resistivity (Rxo) of formations with low mud cake correction. This can be confirmed by the calliper log mirror image of the wellbore (Track 5, Figure 7.3) with the presence of mud cake build up along the well bore in some depths which indicate the permeable zones within the intervals of the well Ha-G1. The temperatures (Figure 7.3, 7.4 & 7.5 tracks 8) within the selected zones were low range between 54^0C to 57^0C, which suggests that the temperatures are below the hydrocarbon generation window for most oil generation.

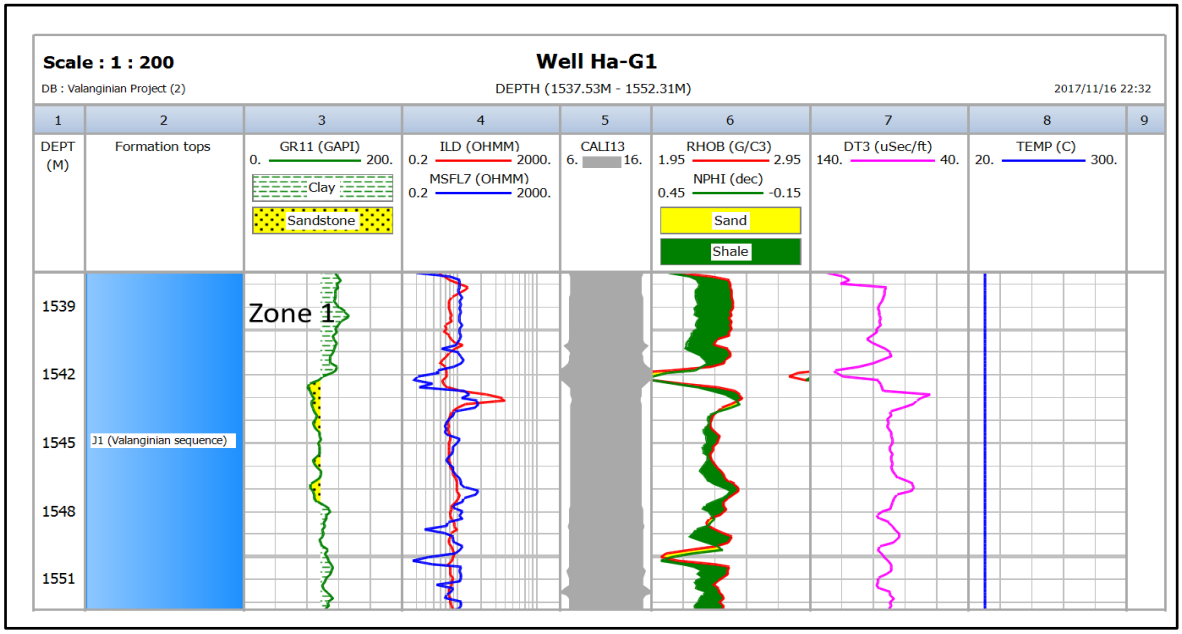

Figure 7.3: Reservoir interval well Ha-G1 (Zone 1, 1537.53m – 1552.31m depths) of the Valanginian sequence.

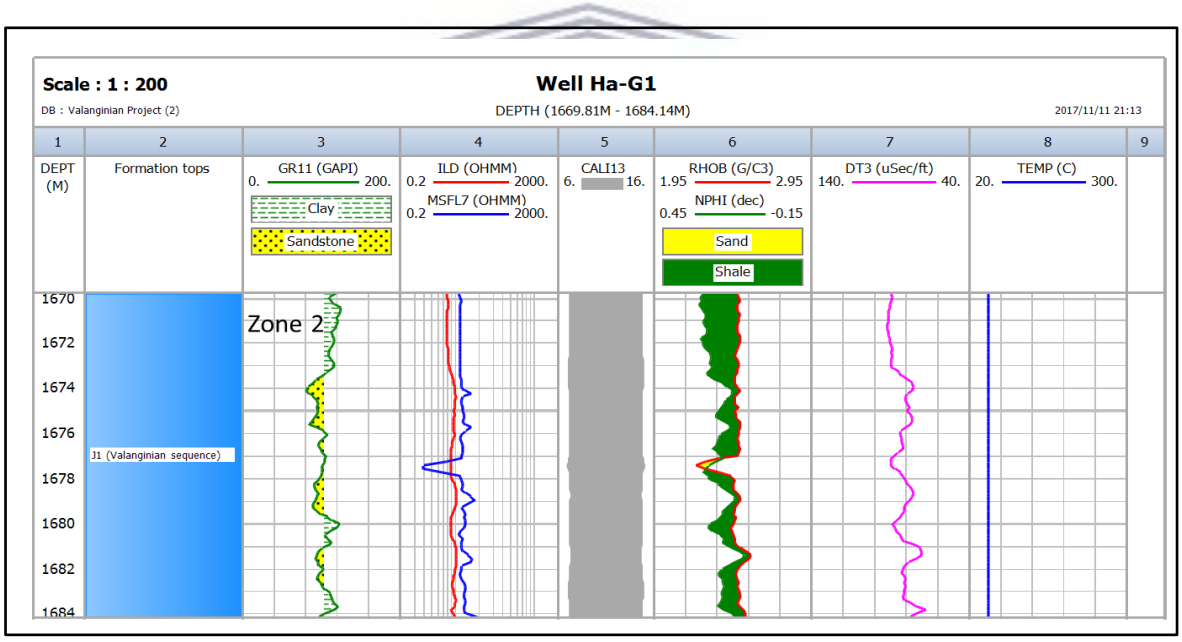

Figure 7.4: Reservoir interval well Ha-G1 (Zone 2, 1669.81m – 1684.14m depths) of the Valanginian sequence.

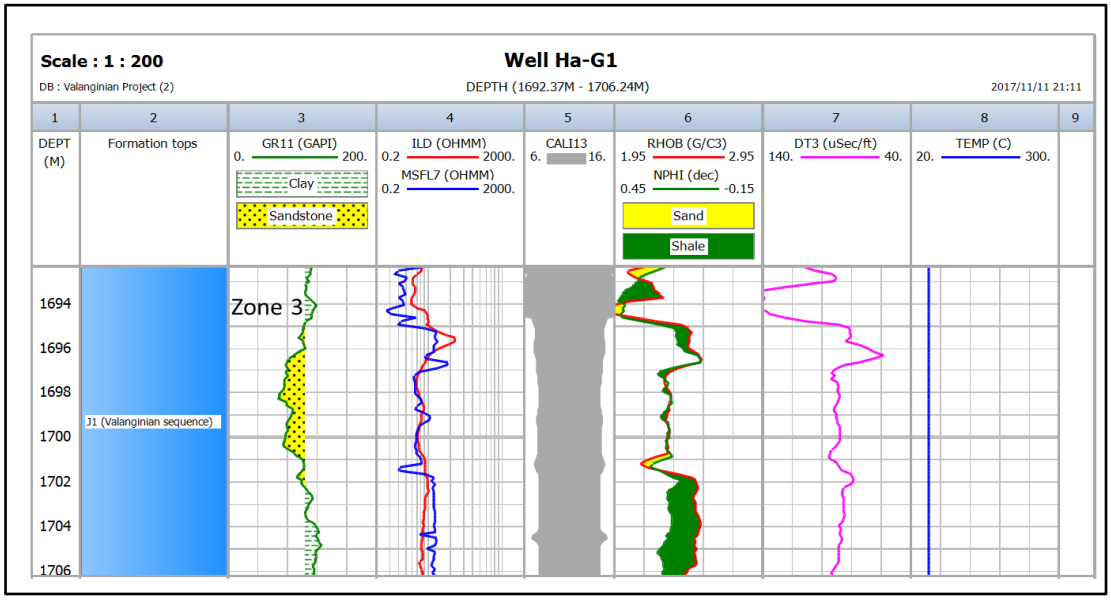

Figure 7. 5: Reservoir interval well Ha-G1 (Zone 3, 1692.37m – 1706.24m depths) of the Valanginian sequence.

7.2.2 Wireline logs interpretation of well Ha-B2

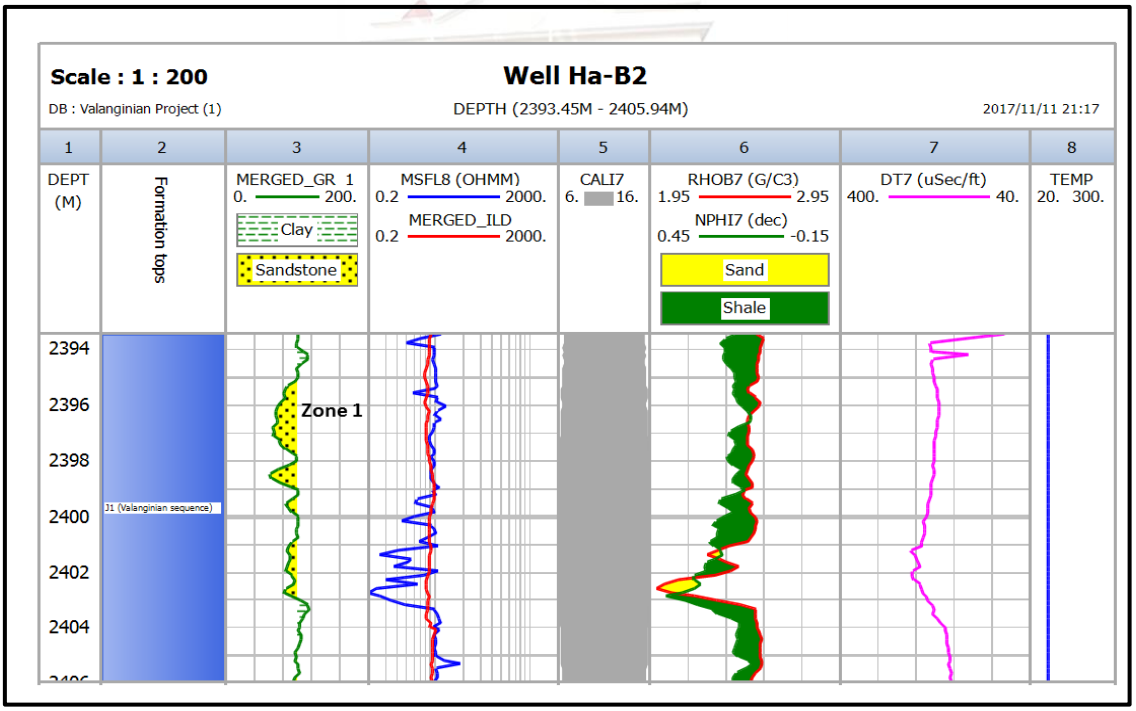

Figure 7. 6: Reservoir interval well Ha-B2 (Zone1, 2393.45m – 2405.94 m depths) of the Valanginian sequence.

Well Ha-B2 was drilled in the southern part of the study area. In the Valanginian section of these wells the interesting interval is in between 2003.90 m - 2676.87 m. Above and below this interval is a thick deposit of shale which serves as a cap rock for the reservoir interval encountered within the Valanginian sequence ranging between 2393.45m – 2405.94m depth. This lithology within this interval could be identified by means of merged gamma ray log (Track 3, Figure 7.6) and combinations of neutron-density logs and others logs (Sonic log) as stated above. Lateral Deep Log Resistivity and Micro-Spherically Focused Logs (LLD & MSFL) were also used to identify the formation fluids (gas/oil/water) and possible other fluid contacts in the borehole, to carry the same functions as explained in the previous well description above. Within intervals 2393.45m – 2405.94m depth low resistivity readings from both logs are indicated which suggests the presence of salty water. The slightly higher reading of deep lateral resistivity at the interval of 2400.87 – 2403.65 m with the cross-over of neutron-density log curves indicates the presence of gas in the reservoir. A lower reading of Micro-Spherically Focused Log indicates the permeable depths of the flushed zone within the intervals. The sonic logs (Figure 7.6, track 7) also help in identifying the cap rock within the selected reservoir intervals. The temperature (Figure 7.6, track 8) was 67^0C which suggests that the interval selected was within the hydrocarbon generation window.

7.2.3 Wireline logs interpretation of well Ha-K1

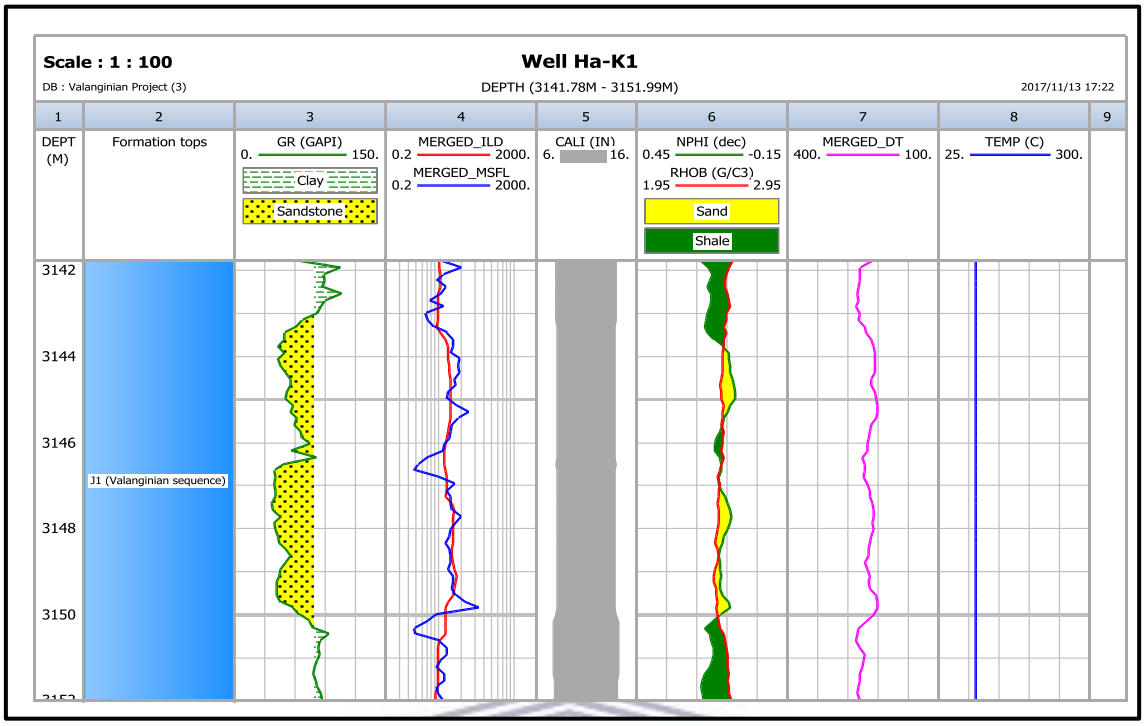

Figure 7. 7: Reservoir interval well Ha-K1 (3141. 78 m – 3151.99 m depths) of the Valanginian sequence.

The well Ha-K1 was also drilled in the southern part of the study area. The thickness of the JI formation of this well ranges from interval 3101.4 m - 3200 m, which can be classified as a deep interval sequence. The potential reservoir was encountered within the interval 3141.8 m – 3152.31m was identified by gamma ray (GR) log (Figure 7.7, track 3), in combination with neutron-density logs and sonic logs. This interval indicates presence of a huge thickness of shale both above and below. Deep Log Resistivity and Micro-Spherically Focused Logs (LLD & MSFL) (Figure 7.7, track 4) were also used to identify the formation fluids (gas/oil/water) and possible fluids contact in the borehole and to measure true resistivity and flushed zone resistivity within the borehole respectively. Within the reservoir interval 3141.8 m – 3152.31m are clear indications of the high resistivity readings indicating presence of hydrocarbons in the reservoir and could be confirmed by cross-over of neutron-density log (Figure 7.7, track 6), displaying a clear presence of gas effect within the reservoir interval.

Lower resistivity readings were also observed within the intervals above and below the reservoir, which also suggests a presence of salty water with a constant fluids salinity signature that gives an excellent log for the lithological distinction within the borehole formation of well Ha-K1. The wellbore formation was well consolidated as the caliper log (Figure 7.7, track 5)

runs through the formation borehole and measures the size and shape of the hole, indicated a gauge as no washed-out or caved sections of the hole were observed on the Caliper log. The temperature (Figure 7.7, track 8) was 68^0C which suggests that the interval selected was within the hydrocarbon generation window.

7.2.4 Wireline logs interpretation of well Ha-A1

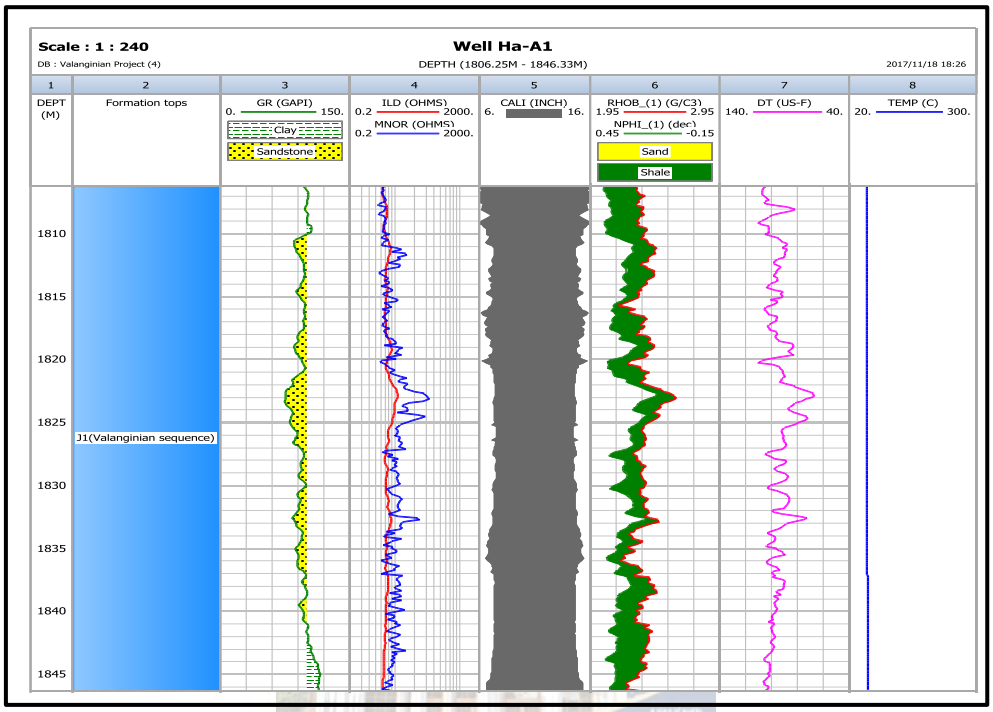

Figure 7. 8: Reservoir interval well Ha-A1 (1806.25 m – 1846.33 m depths) of the of the Valanginian sequence.

Well Ha-A1 is one of the well located in the southern part of the basin that was drilled through the Valanginian sequence. The lithologies encountered in the wellbore were identified by gamma ray logs and a combination of neutron-density logs reveal that the sedimentary succession is predominantly shale and lack the well-developed reservoir character. No potential reservoirs were encountered within these intervals except between 1806.25 m -1846.33m (Figure 7.8, track 3). The intervals are well capped with shale (seal) above and below the sequence. The Induction-Deep Log resistivity (ILD) and Micro-log normal resistivity (MNOR) were used to identify the fluid contacts in the wellbore, as well as to measure true resistivity and flushed zone resistivity within the borehole respectively. The resistivity readings in these selected intervals were high, which suggests the possible presence of hydrocarbons within the intervals, but neutron-density log did not indicate clear presence of any gas. (Figure 7.8, track 6). Not much separation was observed between the resistivity logs. The selected intervals are

observed as permeable zones based on the indication of the presence of mud cake and washed-outs from the caliper log (Figure7.8, track 5) that runs through the formation and was used to measure the borehole size, revealing the shape of the well. A high temperature of 76^0C (Figure 7.8, track 8) was noticed within the selected intervals, which suggests that source rocks in these intervals are within the hydrocarbon generation window particularly oil.

7.2.5 Wireline logs interpretation of well Ha-I1

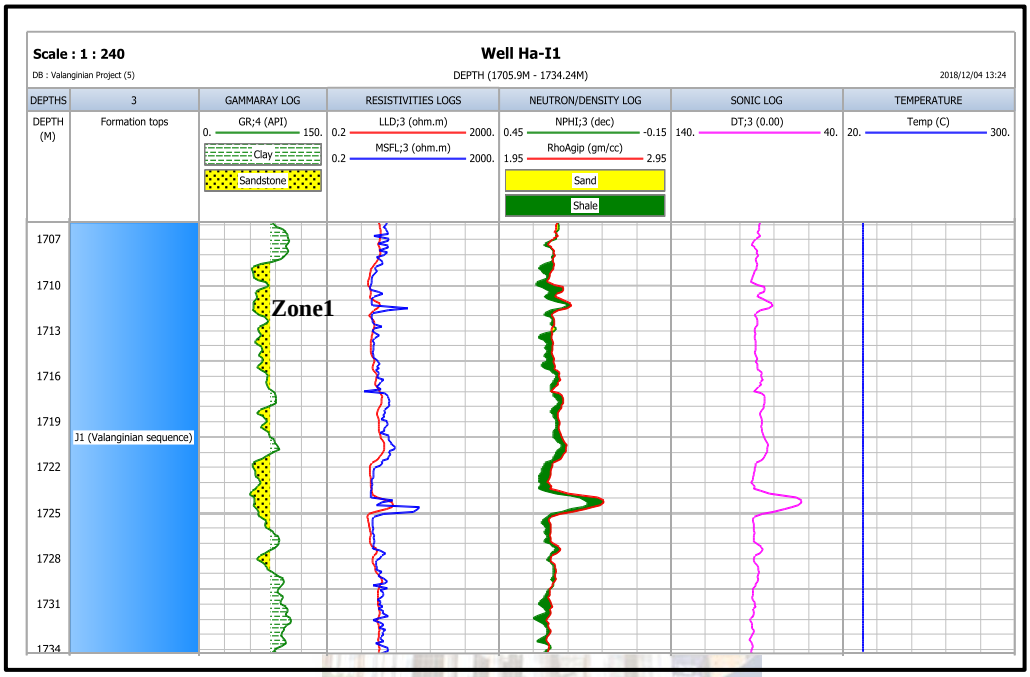

Figure 7. 9: Reservoir interval well of Ha-I1 (Zone 1, 1705.94 m – 1734.23 m depths) of the of the Valanginian sequence.

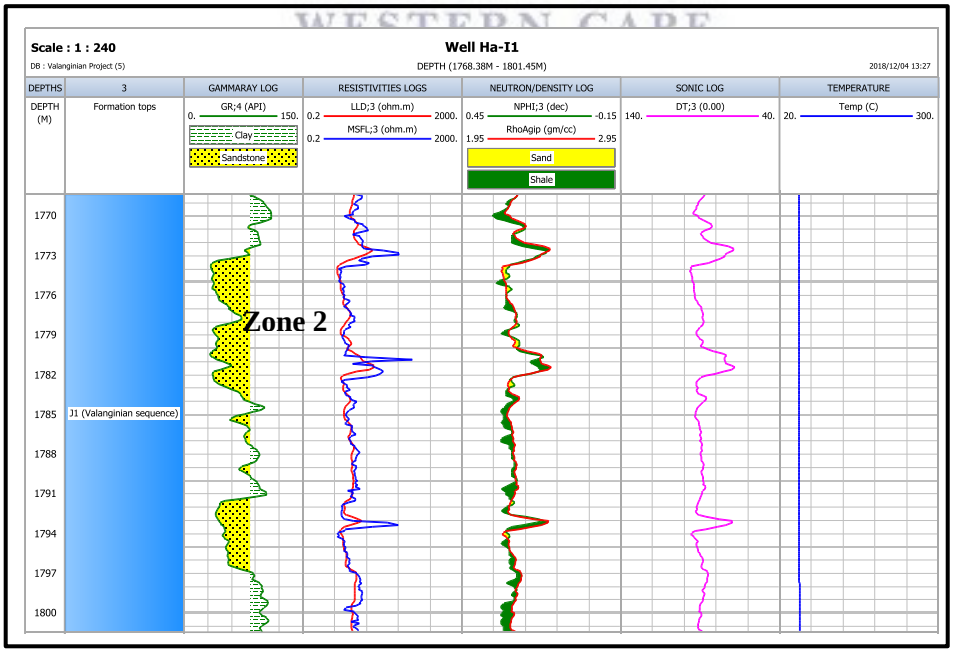

Figure 7. 10: indicate reservoir interval well Ha-I1 (Zone 2, 1768.38 m – 1801.45 m depths) of the Valanginian sequence.

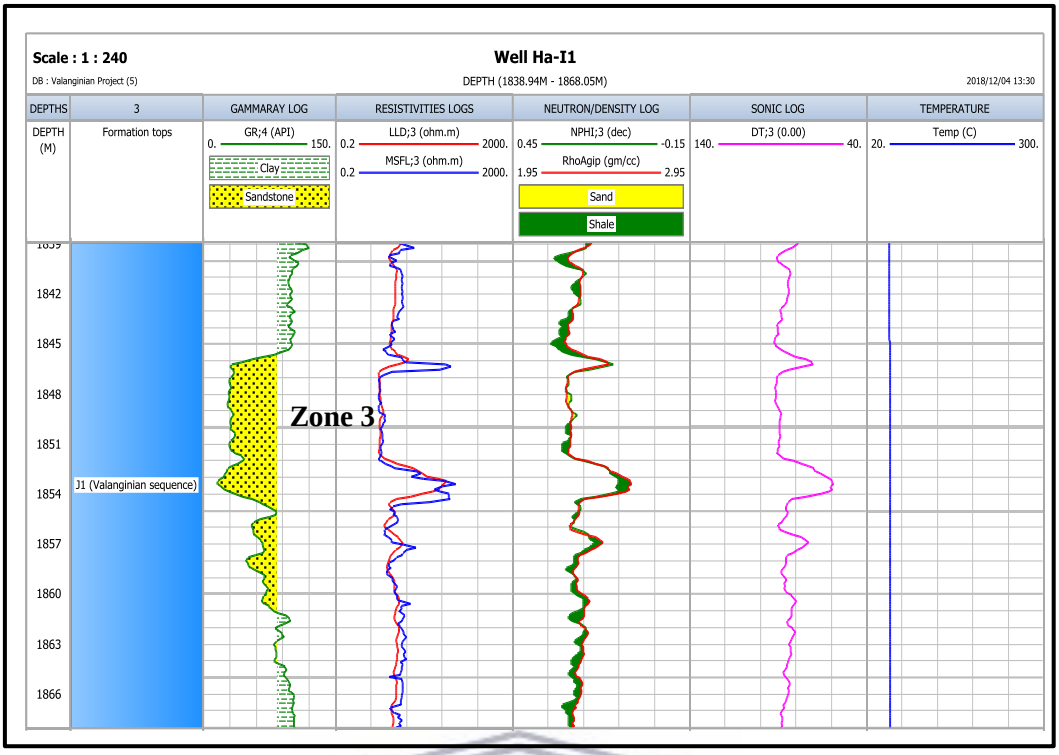

Figure 7. 11: indicate reservoir interval well Ha-I1 (Zone 3, 1838.94 m – 1868.05 m depths) of the Valanginian sequence.

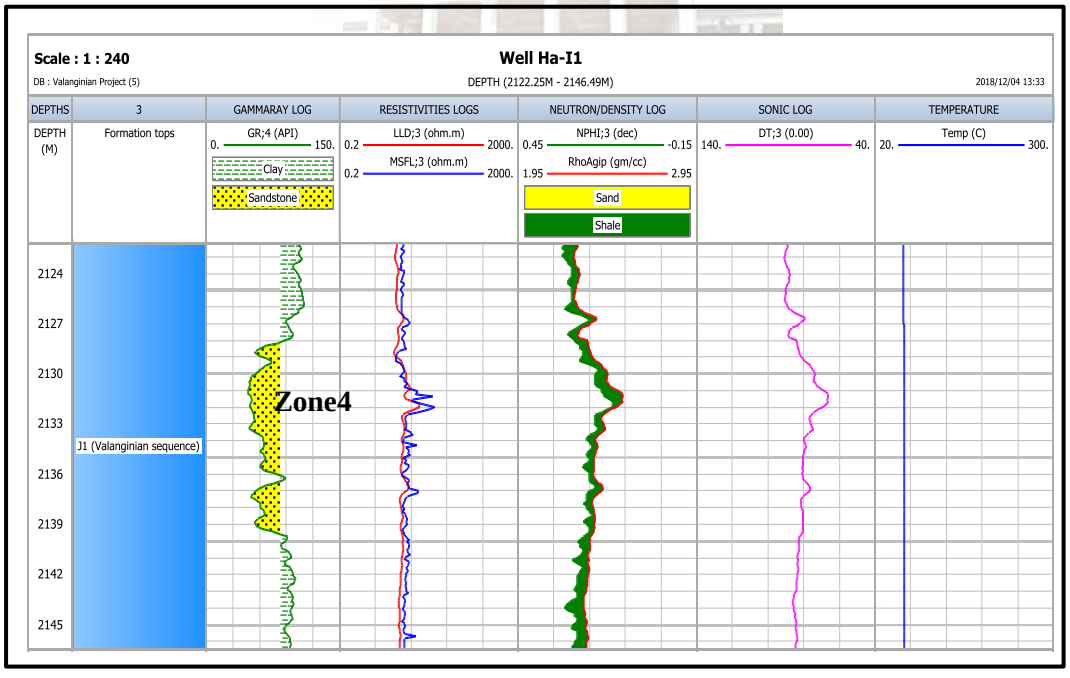

Figure 7. 12: Reservoir interval well Ha-I1 (Zone 4, 2122.25 m – 2146.49 m depths) of the Valanginian sequence.

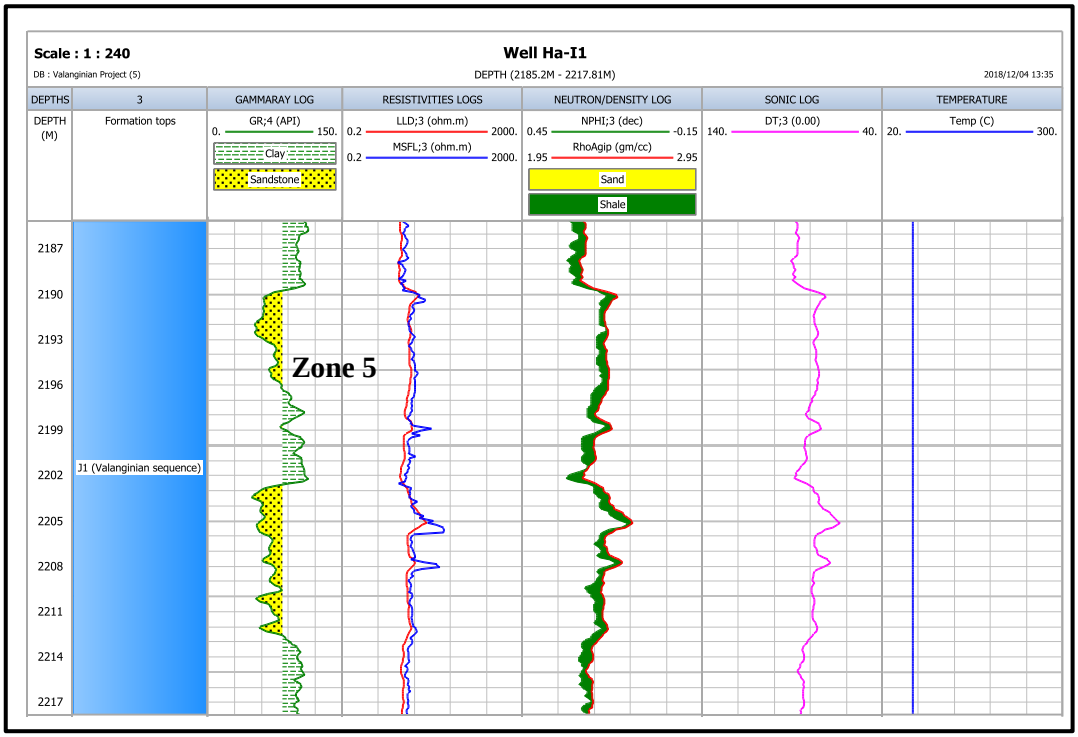

Figure 7. 13: Reservoir interval well Ha-I1 (Zone 5, 2185.25 m – 2217.81 m depths) of the Valanginian sequence.

The well Ha-I1 was drilled in the northern part of the basin (Figure 1.3, chapter one above). The Valanginian section in this well is quite thick and lies within the interval from 1402.40 m – 2380.63 m. Within these interval five potential reservoirs (clean sand zones) were encountered between depths 1705.94 m – 1734.23 m, 1768.3 – 1801.45 m, 1838.94 m – 1868.05 m, 2122.25 m – 2146 m, and 2185 m – 2217.81 m (zones 1 to 5). These potential reservoirs were identified by gamma ray logs (Figure 7.9 -7.13 GR; 4, track 3).

In these reservoir intervals (zone 1 to 5), there was no separation was noticed between the Deep Log Resistivity and Micro-Spherically Focused Logs (Figures 7.9 -7.13, LLD;3 & MSFL;3) which were used to identify the formation fluids (gas/oil/water) as well as to measure the true resistivity and flushed zone resistivity within the borehole. The low resistivity readings within the reservoir intervals suggest the presence of water and high resistivity readings therefore, indicates possible presence of hydrocarbons, this can be observed with slight crossing-over of the neutron-density logs (Figures 7.9,7.10 & 7.11 track 6) in zones 2 and 3 and indicates the presence of gas within the reservoirs. The sonic transit time logs also help in identifying the cap rock within the selected reservoirs intervals as being shale.

The calliper log which measures the hole size and shape, was not used in this well. Consequently it was not possible to ascertain whether there is an indication of washed out or permeable zones in selected reservoir intervals of the well. This suggests that the well was gauged during the drilling process. The temperature (Figures 7.9 – 7.13, track 8) within the reservoirs intervals gradually increases further from 50^{o}C, to 64^{o}C, 68^{o}C, 71^{o}C and 76^{o}C respectively, which suggests that some intervals within the reservoirs are within the window of hydrocarbon generation.

7.3 Determination of Petrophysical Properties

The determination of petrophysical properties parameters is a vital step in formation evaluation to determine the economic viability of a hydrocarbon-bearing reservoir (Fens, 2000). These parameters include lithology and fluid identification, shale volume, porosity, water saturation and permeability estimation. The following section outlines the models related to these parameters used in this study.

7.3.1 Lithology determination

The lithology of the well sections were identified using the neutron versus density cross plot combined with gamma ray log motifs. Lithology determination analysis for all the well depths and the depth of the reservoir units were cross plotted to identify the major sediments within the well (Figure 7.14 a &b). Based on the majority of the cloud points that populated the multi-well cross plot, it is concluded that the lithology within the reservoir interval indicates sandstone to silt/clay as compared with the entire reservoir's intervals depth which is predominantly silt/clay with minor sandstone and shale as shown in Figures 7.14 a & b respectively.

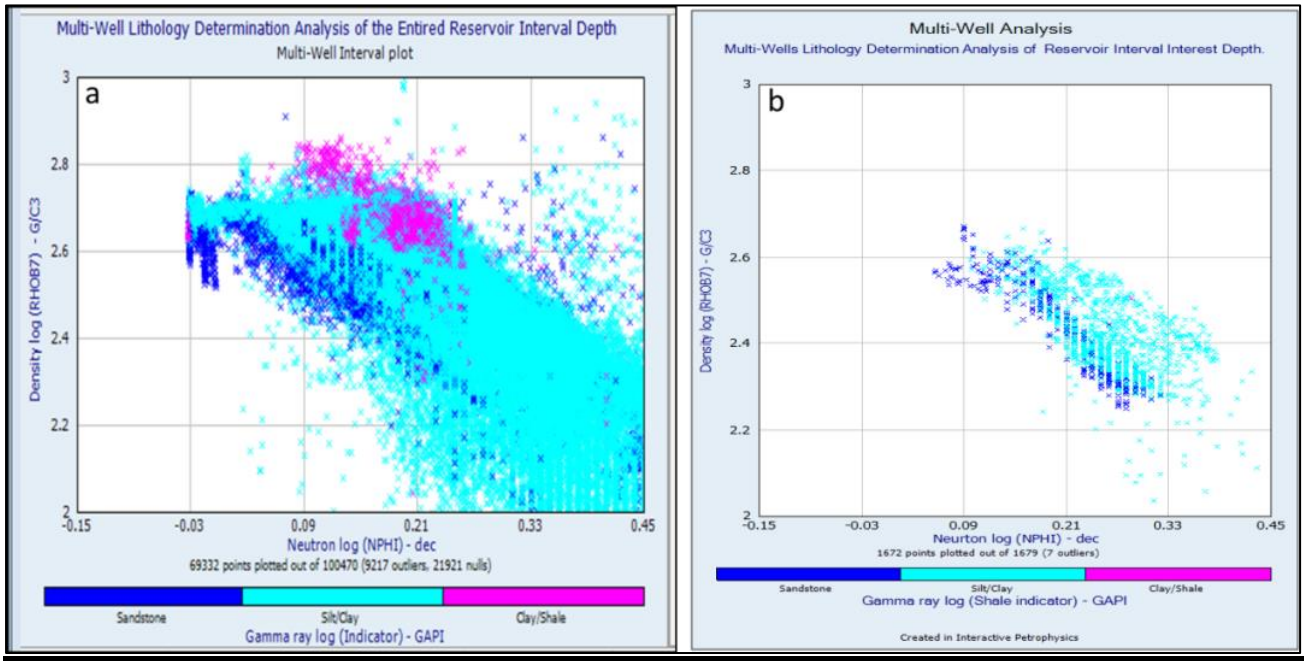

Figure 7. 14 a & b: Multi-well cross plot for the lithology determination of the entire reservoir intervals and the reservoir interval of interest depths of the studies wells respectively.

7.3.2 Volume of shale determination

The presence of conductive clays and shales is a factor considered complicating the interpretation of resistivity data of a partially saturated formation (Hamada, 1996). The shale type, the amount present and the mode of distribution in the formation have different effects on resistivity and porosity. Commonly, the presence of clay or shale in a sand bed lowers the true formation resistivity (R_t) and, if not corrected, will result in overestimating water saturation (Sw), i.e., interpreting as water-bearing zones that are oil-bearing. Shale or clay comprises many proportions of clay minerals such as illite, montmorillonite, and kaolinite, as well as silt; all these minerals affect the porosity and permeability of the formation. All these factors were considered in the study in order to have accurate results in estimating water saturation and porosity for the formation studied.

In the present work the estimation of reservoir quality was made for parameters like porosity types and distribution of reservoir fluids and is mainly based on the evaluation of the shale volume (Vsh). Qualitatively evaluating of shaly sand involves an accurate estimate of the amount of shale (Soto Becerra, 2010). The quantity of shale volume (Vsh) is defined as the volume of wetted shale per unit volume reservoir rock. Shale Volume (Vsh) indicators are generally determined by gamma ray log in a permeable reservoir due to the radioactive elements present in shale, as shale is more radioactive than sand or carbonate (Jensen, *et al.*, 2013). The units of Shale volume (Vsh) are either expressed as decimal fractions or

percentages. To estimate the Shale volume (Vsh), the initial measure is to calculate the gamma ray index (IGR), based on the linear equation below.

$IGR = \frac{GR\log - GRmin}{GRmax - GRmin}$ ..... equation1.

Where;

IGR = Gamma ray Index.

GRLog = gamma ray readings in the zone of interest.

GRmin = minimum value for gamma ray reading in clean sand zone or interval.

GRmax= maximum value for gamma ray readings in shale interval.

Thus, for the study, the minimum and maximum gamma ray values of the lithologies used were obtained from the histogram plots. The clay volume values used for each zone were obtained from the volume of clay curves derived from the gamma ray log (VCLGR). Figures 7.16 below represents the example of the multi-well gamma-ray histogram and Figure 7.14 a & b above show the cross-plot of the lithology identification of the wells with their value as shown in Table 7.1. However, the clay volume/shale volume values obtained must be corrected by effective formula in order to obtain optimum values valid for the interpretation (Jensen, *et al.*, 2013). The use of linear and non-linear equations to estimate the shale volume (Vsh) of a reservoir depends on the minimum and maximum values that are defined in the sand line and shale line (baseline) respectively. The sand line and shale line (baseline) could have one gamma ray (GR) in some areas but differ in some deeper levels of the well. Thus, in the event of inaccurate calculations of the Shale volume (Vsh), the influence of the formation porosity and water saturation affect the original oil reserves or in place. The different non-linear (correction) equations and models available to calculate the shale volume (Vsh) are given below and the comparison of the model is shown in Figure 7.15.

Larinov (1969) for tertiary rocks, $Vsh = 0.083(2^{3.7IGR} - 1)$..... equation 2.

Stieber (1970), $Vsh = \frac{IGR}{3 - 2*IGR}$ ..... equation 3.

Clavier (1971), $Vsh = 1.7 - \{(3.38 - (IGR + 0.7)^2\}^{1/2}$..... equation 4.

Larinov for older rocks, $Vsh = 0.33*(2^{2IGR} - 1)$..... equation 5.

The Stieber (1970) equation model was used in this study for correction effect from the gamma ray Index values obtained.

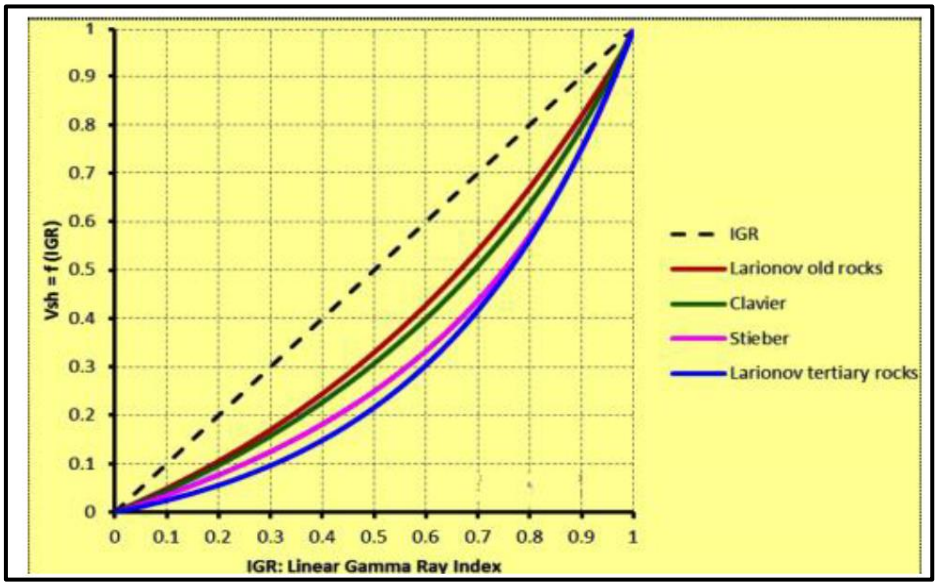

Figure 7. 15: Shale volume (Vsh) as a function of gamma ray Index (IGR), (David, 2015).

Table 7. 1: Parameters used to calculate volume of clay within the reservoir intervals.

Well Name	Reservoir Name	Top Depth (m)	Bottom Depth (m)	GRmin (API)	GRmax (API)	GRlog (API)
Ha-B2	1	2393.45	2405.94	61.875	116.75	93.145
Ha-G1	1	1537.53	1552.31	80.937	133.37	103.99
Ha-G1	2	1669.81	1684.14	80.937	124.87	104.27
Ha-G1	3	1692.37	1706.24	69.125	126.25	99.76
Ha-K1	1	3141.78	3151.99	37.093	106.0	62.198
Ha-A1	1	1806.25	1845.33	75.53	116.53	94.59
Ha-I1	1	1705.9	1734.24	60.79	108.84	81.973
Ha-I1	2	1768.38	1801.45	33.37	110.42	70.314
Ha-I1	3	1838.94	1868.05	16.44	119.47	71.07
Ha-I1	4	2122.25	2146.49	48.0	110.06	80.2
Ha-I1	5	2185.20	2217.81	49.67	112.79	83.873

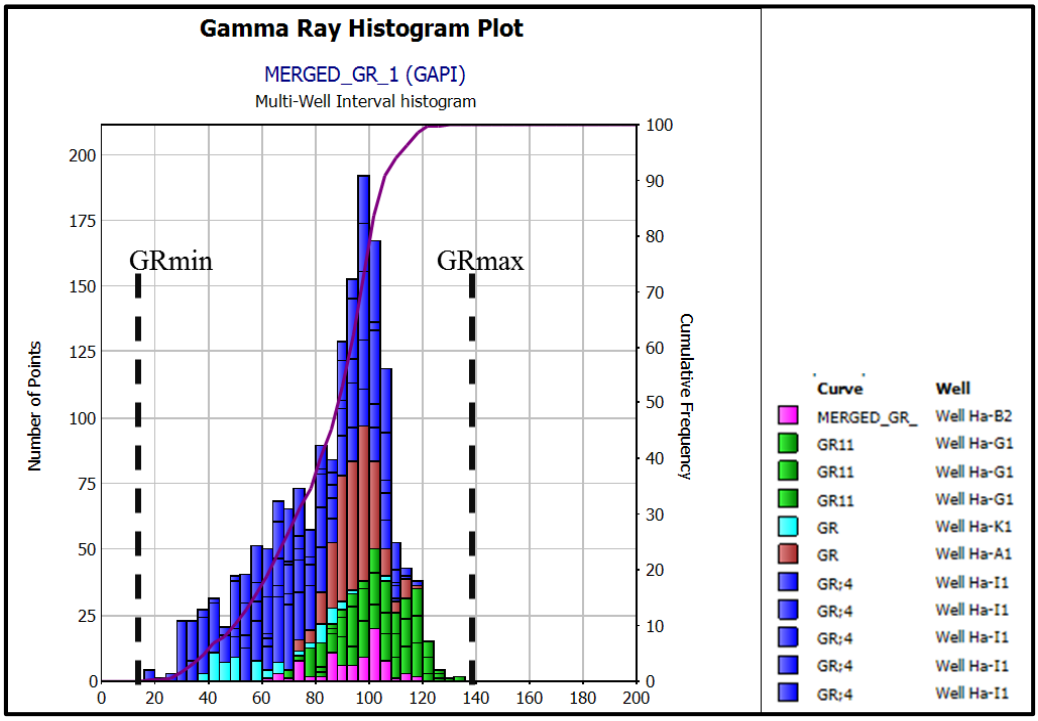

Figure 7. 16: Multi-well gamma-ray histogram.

7.4 Porosity and Water saturation determination.

The porosity curve was derived from the neutron, density and sonic logs. For the wells Ha-B2, Ha-G1, Ha-K1, Ha-A1 and Ha-I1 studied, the porosity and water saturation were calculated from neutron-density combination logs. The equations below were used to derive density porosity log curves evaluated for these studies.

$\Phi = P_{ma} - P_b / P_{ma} - P_f$ ....equation 6.

Where:

Φ = Porosity (dec).

P_{ma} = Density of the matrix material (g/cc)

P_b = Density log reading (g/cc)

P_f = Density of the saturated fluid (g/cc), such as salt mud = 1and fresh water = 1.

The equation used to derived neutron-porosity log curve is:

PHIN =PHIe * Sxo * PHINw.....equation 7.

Where:

PHIN = log reading

PHIe = effective porosity.

SXo = water saturation of the invaded zone.

PHINw = log reading (100%) water.

Porosity calculated from sonic log was also considered, by adopting the Wyllie Time Average equation for sonic porosity. Since the sonic log is a porosity log that measures an interval's transit time (Δt) of a compressional sound wave through the formation, the interval transit time (Δt) depends on both lithology and porosity. The porosity derived from the sonic slowness is different from that derived from the density or neutron tool, which only have an effect on primary porosity and do not react with fracture or vugs (secondary porosity). The Wyllie Time Average basic equation for sonic porosity calculation is given below.

$\Phi = \Delta t_{log} - \Delta t_{ma} / \Delta t_f - \Delta t_{ma}$ ……equation 8.

Where:

Φ = porosity (fraction)

Δt_{log} = sonic log interval transit time reading in the formation (μsec/ft).

Δt_{ma} = interval transit time in the matrix (μsec/ft).

Δt_f = interval transit time in the fluid within the pore space of the formation (μsec/ft).

In order to have good calculated porosity and water saturation curves for the selected interval zone studies, groups of different models of effective porosity and water saturation curves were plotted from the database. The model curves derives from the IP software such as Phie Density (PhiDen), Phie Neutron (PhiNeu), PhieDen/Neu (PhiND), PhieNeu/Son (PhiNS), PhieSonic (PhiSon) and SwSimandoux (SwSim), Sw Mod Simondoux (SwModSim), Sw Indonesian (SwInd) and Sw Mod Indonesian (SwModInd) had to be calibrated with core data and then the best model curves that agreed with the trend position from core data was selected.

However, for this study, core data were only available for wells Ha-B2, Ha-G1 and Ha-K1; the core data obtained within the intervals of selected wells below the Valanginian section were utilized as the reference base for correlation at relative depths, to calibrate the models of effective porosity and water saturation respectively for the sequences studied. Effective porosity Phie Neutron (PhiNeu), PhieDen/Neu (PhiND) and Sw Indonesian (SwInd) were found to be the best fit curves when calibrated with core data of wells Ha-B2, Ha-G1 and Ha-K1 respectively. Figures 7.17 – 7.19 show the example of the calibrated model log curves with core data and the agreed best-fit model log curves.

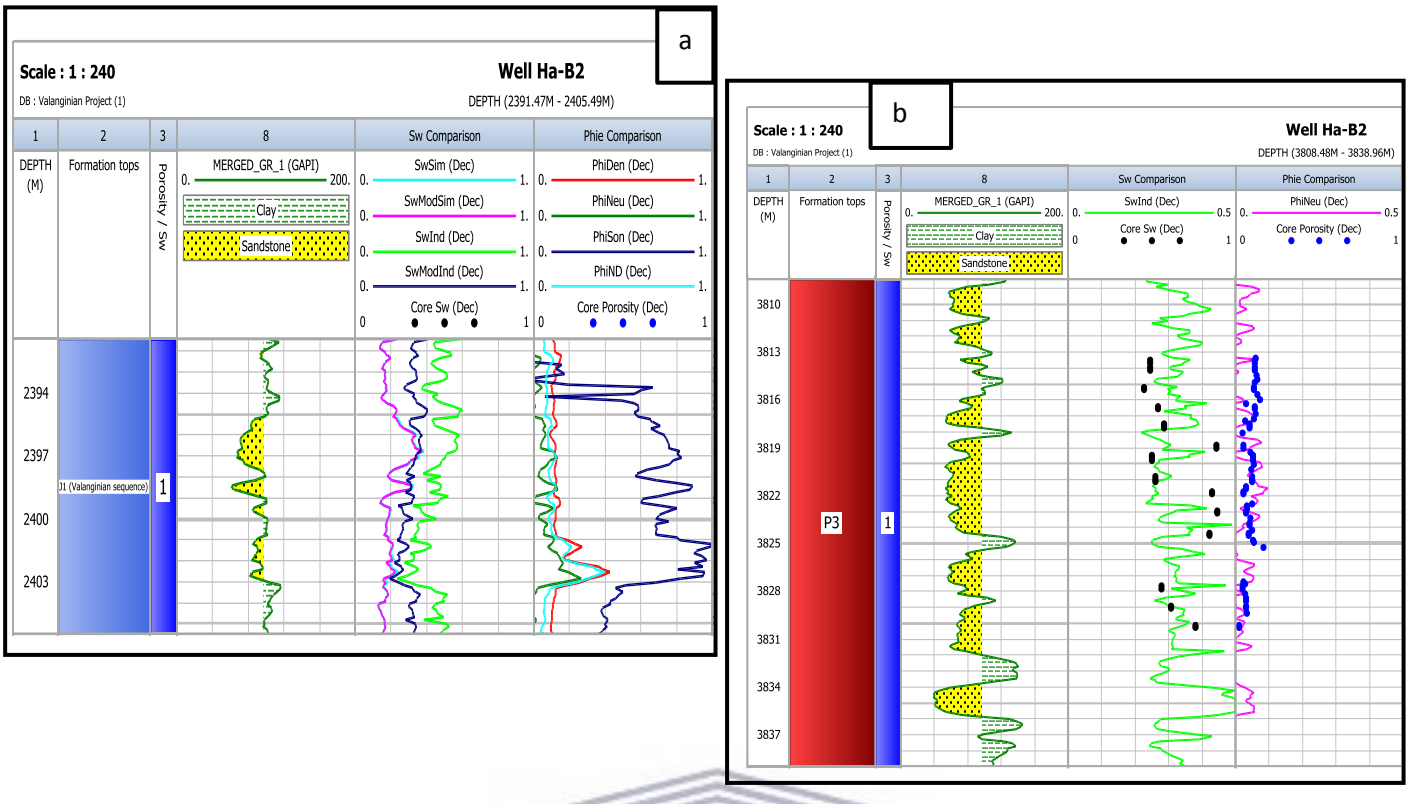

Figure 7. 17 a & b :An example of the calibrated models of effective porosity and water saturation log curves with core data and the agreed best fits model log curves of well Ha-B2.

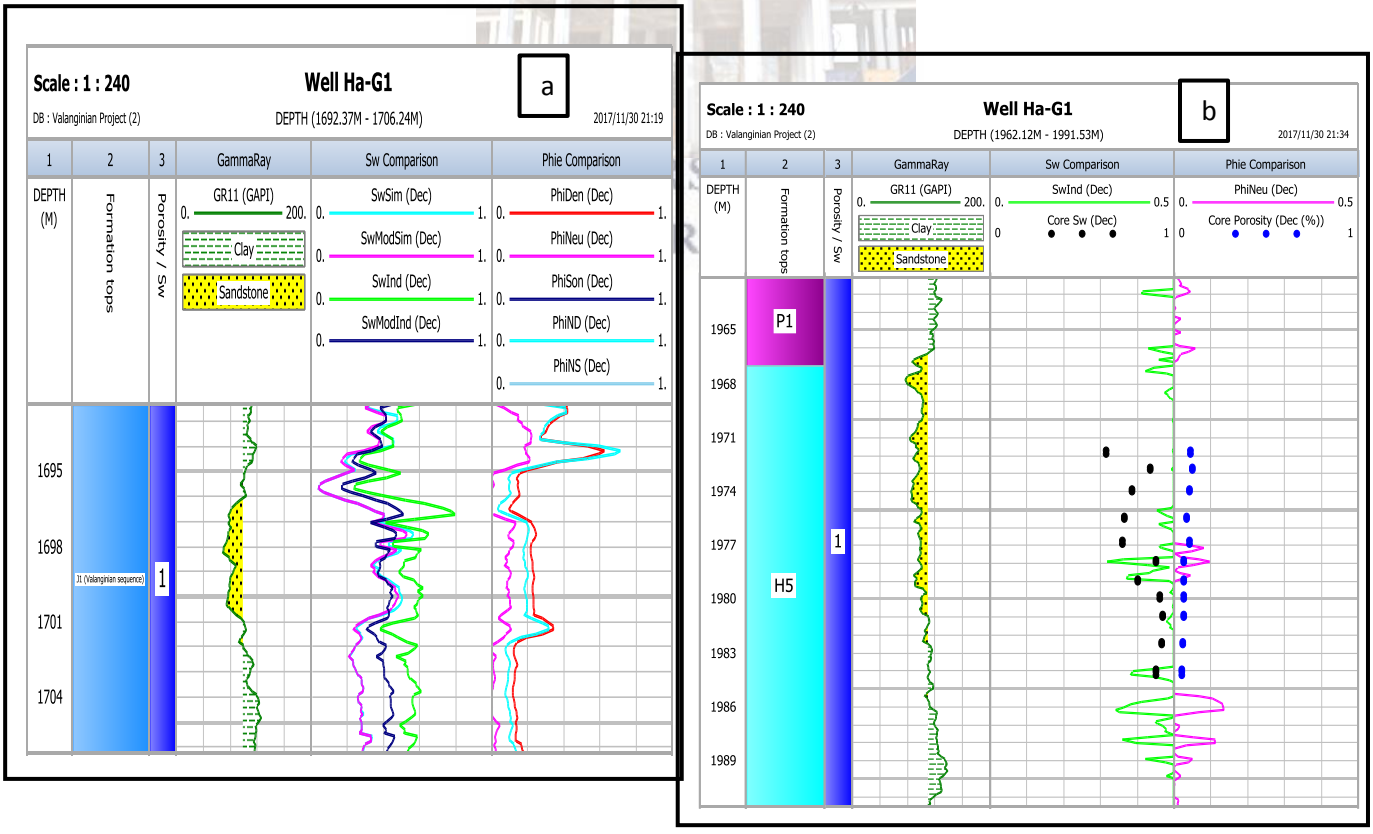

Figure 7. 18 a & b: An example of the calibrated models of effective porosity and water saturation log curves with core data and the agreed best fits model log curves of well Ha-G1.

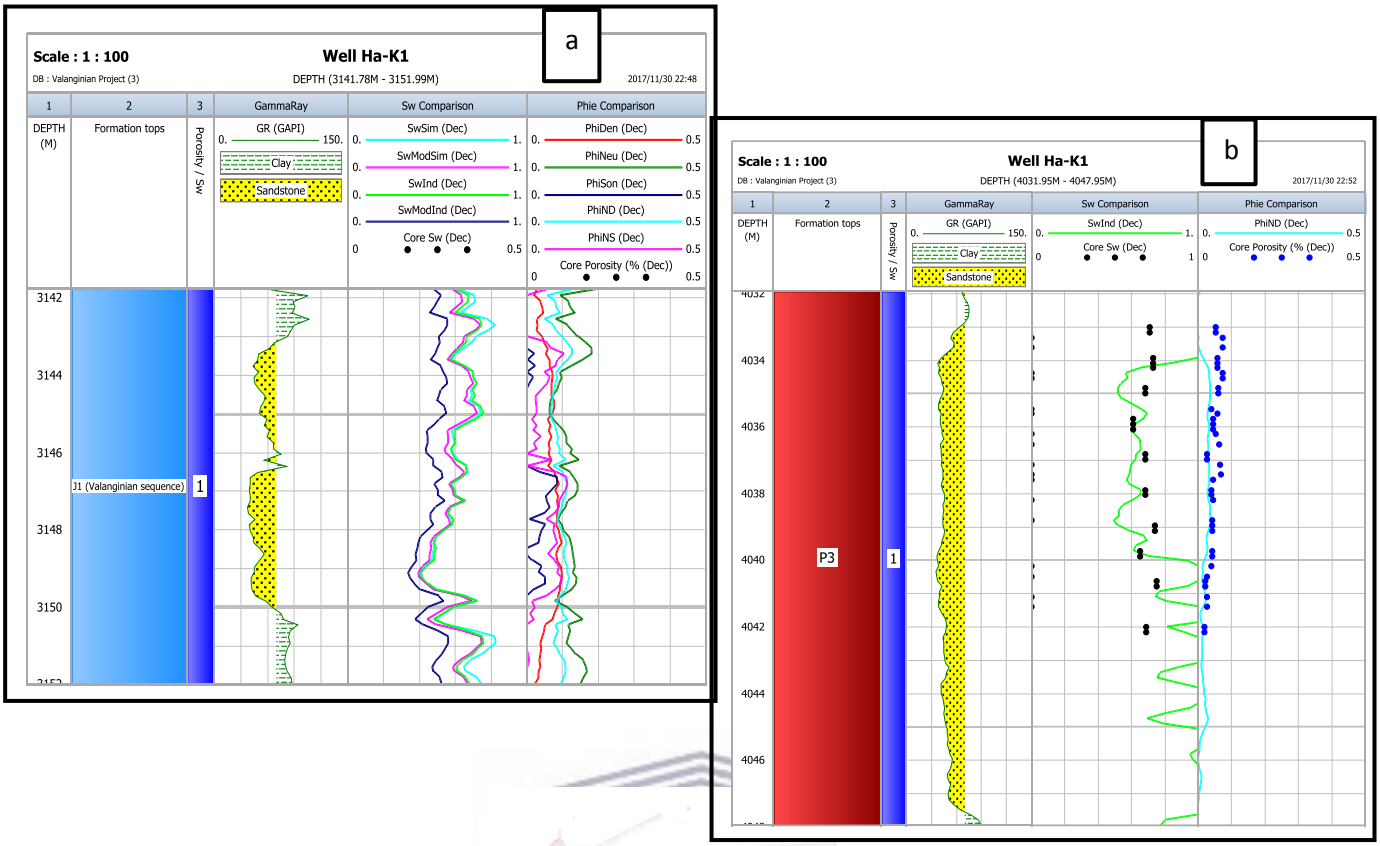

Figure 7. 19a & b: An example of the calibrated models of effective porosity and water saturation log curves with core data and the agreed best fits model log curves of well Ha-K1.

As there was no core data available for wells Ha-A1 and Ha-I1 to calibrate with the model effective porosity and water saturation, models Phie Neutron (PhiNeu) effective porosity and Sw Indonesian (SwInd) were used to calculate the porosity and water saturation for the wells. These models were considered because they have the same trend of logs curves with calculated effective porosity and volume of clay from the well data logs. Figures 7.20 and 7.21 show an example of the models' effective porosity and water saturation log curves used to calculate the porosity for wells Ha-A1 and Ha-I1.

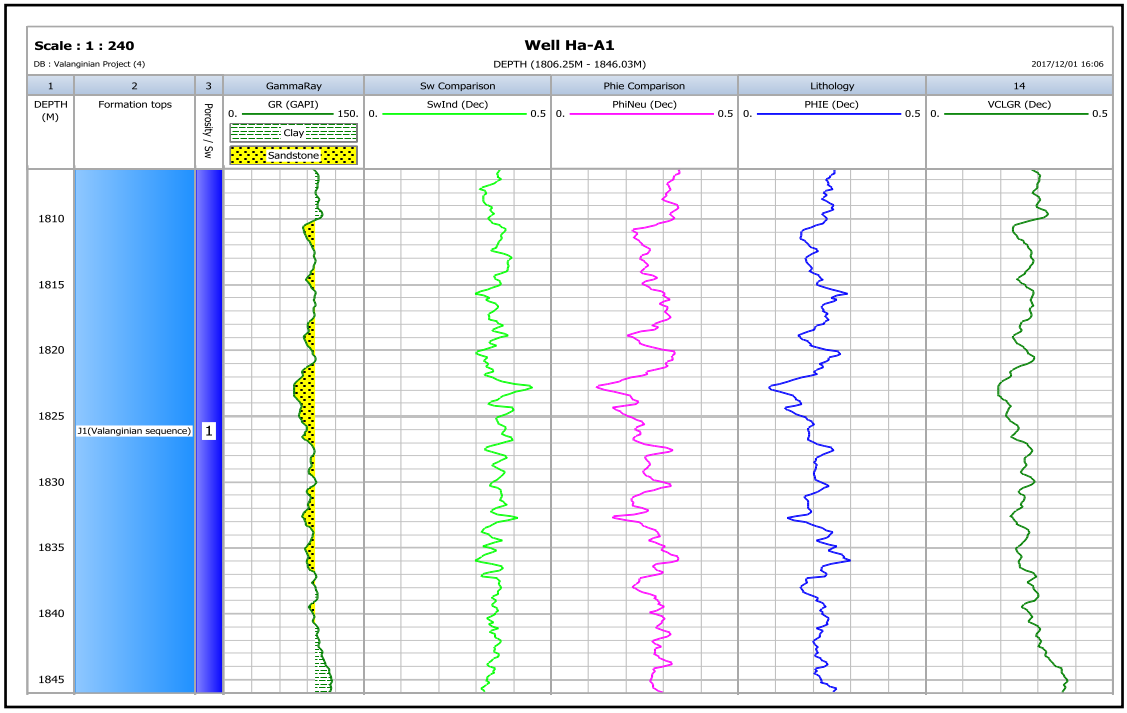

Figure 7. 20: Example of the models' effective porosity and water saturation log curves used to calculate the porosity for well Ha-A1.

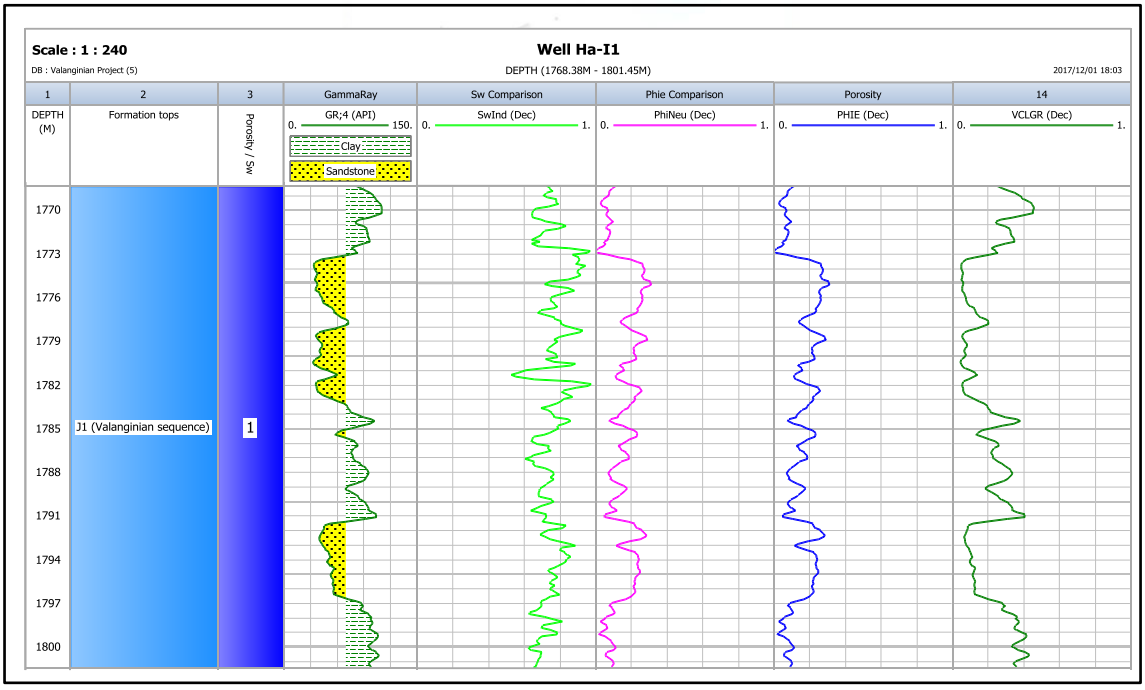

Figure 7. 21: An example of the models' effective porosity and water saturation log curves used to calculate the porosity for well Ha-I1.

The water saturation of the Valanginian reservoir from the selected wells intervals were determined from the calibration of core data with the wireline logs (log derived water saturation model). Water saturation (Sw) determination from log curves is classified into two models namely clean-sand (shale free) and shaly-sand models respectively. For this study, the

reservoir rocks intervals evaluated from the selected wells are shaly-sand reservoirs. Thus, a shaly-sand water saturation (Sw) model such as SwSimandoux (SwSim), Sw ModSimondoux (SwModSim), Sw Indonesian (SwInd) and Sw ModIndonesian (SwModInd) has been applied to determine the water saturation (Sw) of uninvaded zones of the selected reservoir intervals. For this study, Sw Indonesian (SwInd) model was best fitted after calibration with core data. The model applied effective porosity as input porosity in the water saturation model. The basic log parameters evaluated from the standalone picket plots in water bearing intervals from selected wells reservoir intervals were presented in Table 7.2. Simandoux (1963), and Indonesian formulas proposed in (1971) by Puopon and Leveaux to calculate the water saturation of shaly-sand reservoir rock are presented below.

Simandoux (1963) proposed the following relationship.

$Sw = aRw / 2\ \Phi m – Vsh / Rsh + \sqrt{}\ (Vsh / Rsh)\ 2 + 4/F * Rw * Rt$…… equation 9.

Where:

Sw = Water saturation

A = Equation Coefficient

Rw = Resistivity of the water

Rsh = Resistivity of the shale

Vsh = Volume of shale

F = Formation resistivity factors

Rt = True formation resistivity from corrected deep resistivity log.

Φ = Effective Porosity (fraction)

m = Cementation exponent

With the Indonesian formulas proposed in (1971) by Puopon and Leveaux, the relationship can be expressed as follows:

$1 / \sqrt{}Rt = \sqrt{}\Phi e^{m} / a * Rw + Vcl^{(1-Vcl/2)} / \sqrt{}Rcl) * Swn^{/2}$……equation 10.

Where:

Rt = Resistivity curve from deep log reading

Rcl = Resistivity of wet clay

Φe = Effective porosity

Sw = Water saturation

Vcl = Volume of shale (fraction)

Rw = Formation water resistivity

m = Cementation exponent

a = Tortuosity factor

n = Saturation exponent

7.4.1 Determination of initial fluid parameters

Initial fluid saturation parameters such as water saturation exponent *(n)*, cementation exponent *(m)*, tortuosity factor *(a)* and resistivity of water formation *(Rw)* were determined in a water bearing zone of the studied wells. This was determined to obtain accuracy of water saturation estimates in the interval zones studied, to avoid evading of potentially productive pay zones within the selected intervals zones of the studied wells in Valanginian section.

7.4.1.1 Water saturation exponent (n) parameter

The water saturation exponent value is described as a function of both pore system geometry and formation wettability (Bennion, *et al.*, 1996). The water saturation exponent is commonly assumed to be 2.0, but this value varies significantly from one formation to another and could result in overestimation or underestimation of water saturation (Bennion, *et al.*, 1996). The measurement of the water saturation exponent *(n)* is mostly conducted on samples from the range of permeability, porosity and lithology that could be present in the formation, because it varies in both lithology and wettability. The standard value of 2.0 is generally accepted in the oil and gas industry for evaluation of the water saturation exponent *(n)*. This study applied the standard *(n)* value of 2.0 for the water saturation exponent measured from the standalone Pickett plot for each of the wells Ha-B2, Ha-G1, Ha-K1, Ha-A1 and Ha-I1 studied, in which porosity is plotted against resistivity of the water bearing zones of the boreholes studied (Figure 7.22 – 7.26).

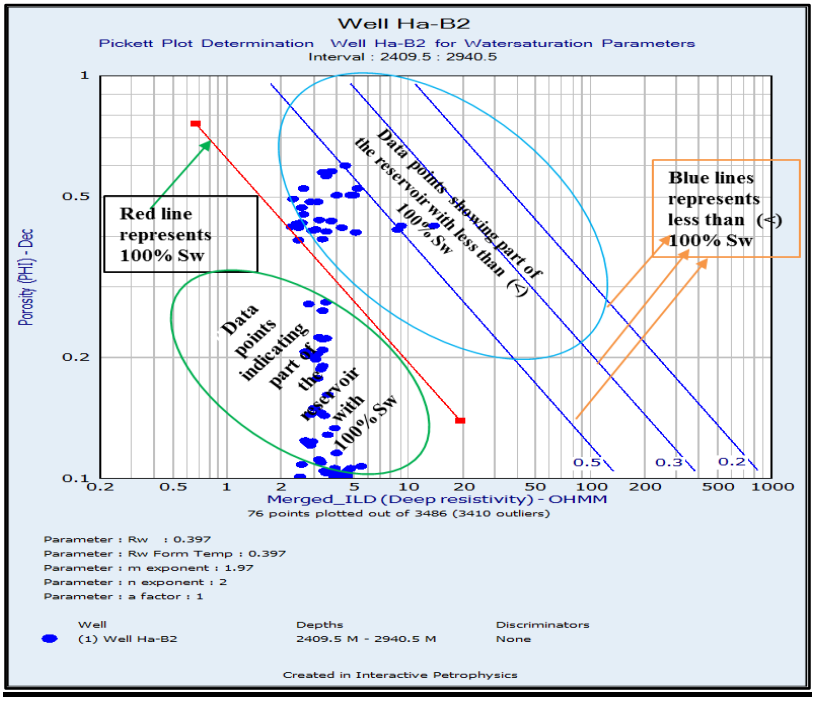

Figure 7. 22: Pickett plot of the Valanginian section in Ha-B2 well.

7.4.1.2 Tortuosity factor (a)

This fluid parameter is also known as the Archie Constant, values of which are measured experimentally for a formation and the factors are determined based on the range of porosity values for a known lithology probable to exist in a specific formation (Bennion, *et al.*, 1996). However, the degree of consolidation that controls the Archie constant value is known as the tortuosity factor *(a)*, The value of 1.0 Archie constant is applicable for compacted sands formation and may exceed 1.0 as the degree of compaction becomes severe (Bennion, *et al.*, 1996) while a value of 0.62 is appropriate for poorly consolidated sands. Therefore, a tortuosity factor *(a)* with a constant value of 1.0 was calculated for all the five wells Ha-B2, Ha-G1, Ha-K1, Ha-A1 and Ha-I1 studied from the standalone Pickett plot (Figure 7.22 - 26), this value of 1.0 indicates that the sandstone units from the wells are compacted.

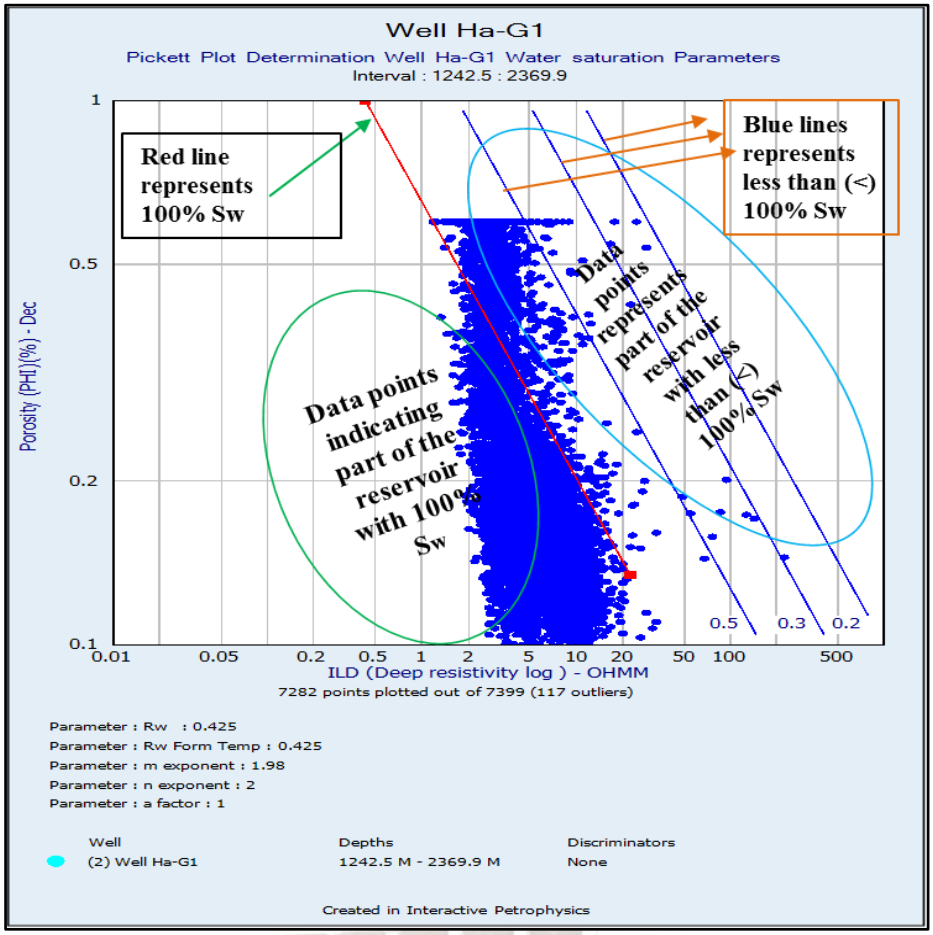

Figure 7. 23: Pickett plot of the Valanginian section in Ha-G1 well.

7.4.1.3 Cementation exponent factor (m).

The value of the cementation exponent depends on the degree and type of cementation in the pore system. It is a measure of the degree of cement and consolidation of the rock; the greater the degrees of cement, the greater the value of the porosity exponent *(m)*. A value of 2.0 is commonly applied, this value varies depending upon the level of cementation (Bennion, *et al.*, 1996). For instance, poorly cemented rocks may be less than 2.0 while in high-quality cemented or oolicastic rocks, porosity exponent *(m)* values may be as high as 3.0. However, cementation exponent factors of 1.97, 1.98, 1.97, 1.94, and 1.96 were measured from the standalone Pickett plots (Figure 7.22 -7.26), for wells Ha-B2, Ha-G1, Ha-K1, Ha-A1 and Ha-I1 respectively. This suggests that these wells are moderately cemented (consolidated < 15% porosity). Table 7.3 illustrates the lithology and cementation values by James, (2017).

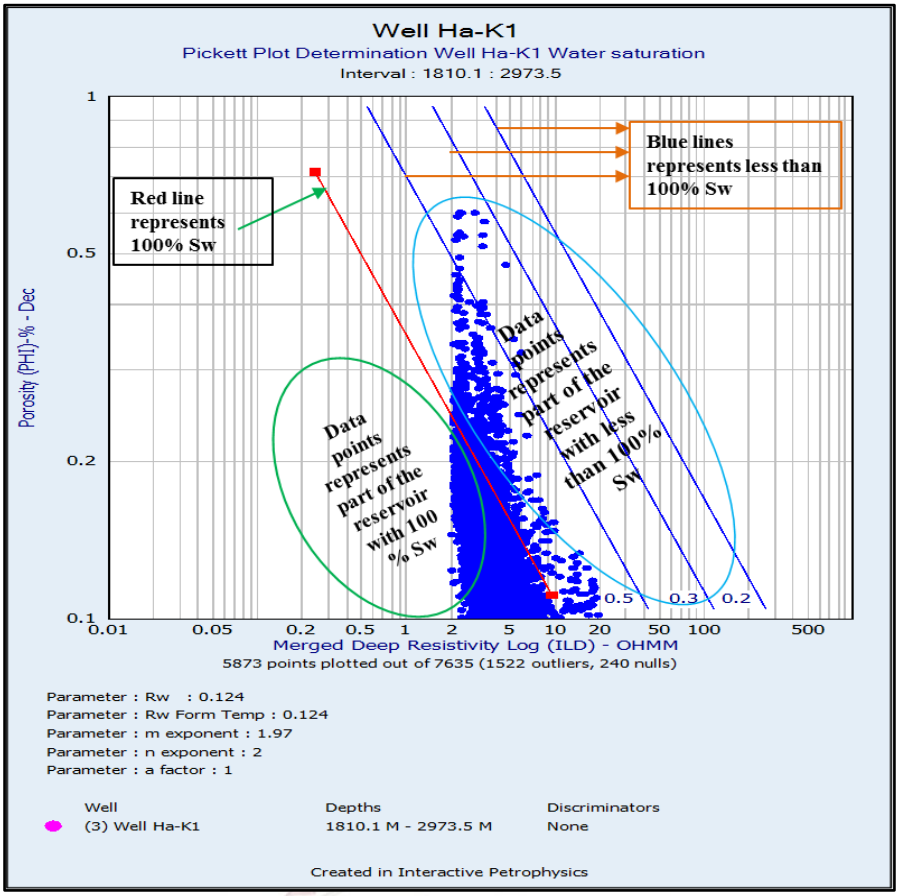

Figure 7. 24: Pickett plot of the Valanginian section in well Ha-K1.

7.4.1.4 Formation water resistivity factor (Rw).

Formation water resistivity (*Rw*) is a major factor in the calculation of initial water saturation based on the effects of the ionic composition of water on overall electrical conductivity and consequently resistivity. This factor is controlled by the nature of water present in the formation. Fresh water indicates high resistivity values while the saline brine exhibits low resistivity values with extreme electrical conductivity. Standalone Pickett plot (Figure 7.22 - 26), was used to calculate water resistivity *(Rw)* of the wells in this study and the following values 0.397, 0425, 0.124, 0.127, 0.088 were obtained for wells Ha-B2, Ha-G1, Ha-K1, Ha-A1 and Ha-I1 respectively.

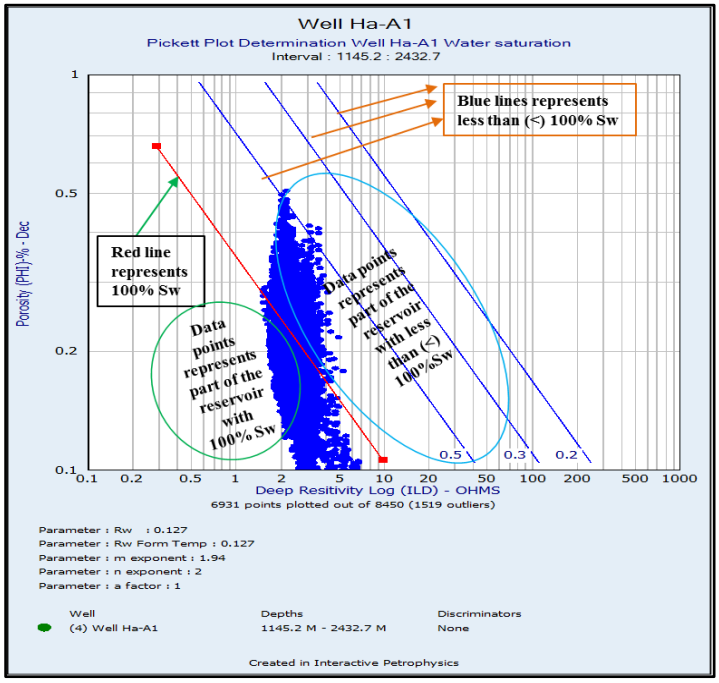

Figure 7. 25: Pickett plot of the Valanginian section in Ha-A1 well.

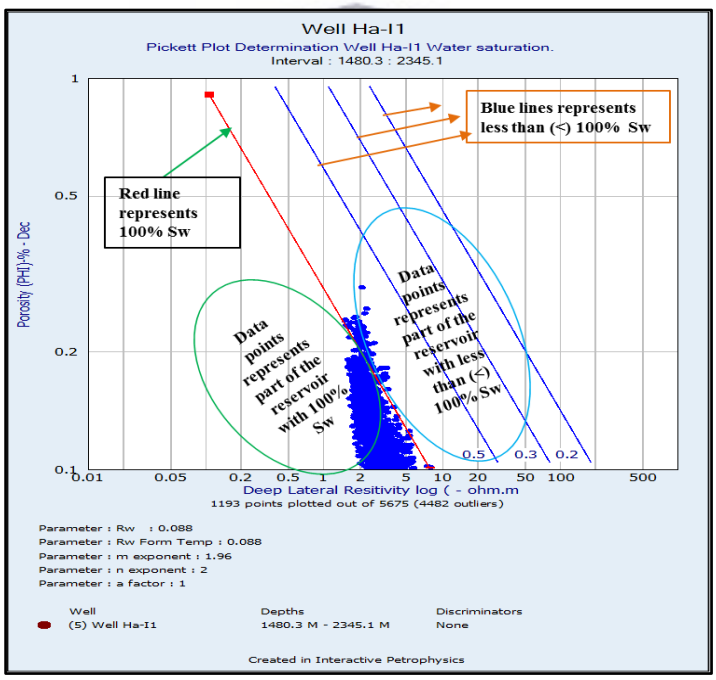

Figure 7. 26: Pickett plot of the Valanginian section in Ha-I1 well.

Table 7. 2 :The basic log analysis parameters calculated from the standalone picket plots for the fluid saturation parameters for the wells respectively.

Well name	Top depth (m)	Bottom depth (m)	Rw	m	n	a
Ha-B2	2409.5	2940.5	0.397	1.97	2	1
Ha-G1	1242.5	2369.9	0.425	1.98	2	1
Ha-K1	1810.1	2973.5	0.124	1.97	2	1
Ha-A1	1145.2	2432.7	0.127	1.94	2	1
Ha-I1	1408.3	2345.1	0.088	1.96	2	1

Table 7. 3: Lithology and cementation values. After James (2018)

Lithology	Cementation value
Unconsolidated rocks (loose sands limestones)	1.3
Very slightly cemented	1.4 – 1.5
Slightly cemented (sand with > 20% porosity)	1.6 – 1.7
Moderately to well cemented (consolidated <15% porosity)	1.8 – 1.9
Highly cemented (quartzite, limestone, dolomite)	2.0 – 2.2

7.4.1.5 Permeability Determination from well log

Permeability is the ability that allows the flow of mobile media such as gas, oil and water through the rocks pore spaces. This parameter is very vital when calculating the storage and flow capacity of reservoir fluids. However, permeability is the most difficult property to predict and determine (Mohaghegh, *et al.*, 1997). There are different methods to determine permeability, these include, Empirical model, multiple variable regressions model and Virtual measurement model. In this study, only empirical and multiple variable regression models are discussed but only the multiple variable regressions model was applied in this study to determine the permeability capacity of the Valanginian section.

The empirical models are based on the correlation between permeability, porosity, and irreducible water saturation and it consists of four models such as Tixier, Timur, Coates and Dumanoir and Coates (Mohaghegh, *et al.*, 1997). Three of these models (Tixier, Timur, and Coates) assume certain values for cementation factors *(m)* and saturation exponent *(n)* which can be utilized in a clean sand formation, provided there is residual water saturation. Coates and Dumanoir, used core and log data with the adoption of a common exponent (*w)* for both the cementation exponent *(m)* and the saturation exponent *(n),* but observed that this can only work in a heterogeneous reservoir (Mohaghegh, *et al.*, 1997).

The second method known as multiple variable regressions model was applied to predict the permeability under this study. It is an extension of the regression analysis that incorporates additional independent variables in the predictive equation. The dependent and independent variables in this study are the logarithm of permeability due to being log-normal, and provide well log data such as porosity (Φ), water saturation (S_w) and Volume of clay *(Vcl)* i.e. the clay content respectively. As no direct digital well logs were available during the time when the

well was drilled , to measure the permeability directly, for the present work permeability (calculated or predicted permeability K, mD) was estimated from the regression equation obtained from porosity versus permeability (poroperm) cross plots (Figure 7.27-7.29). The regression equations 11-13 were used to calculate the permeability of the respective cored wells Ha-B2, Ha-G1and Ha-K1. The wells Ha-A1 and Ha-I1 were not cored and therefore permeability could not be predicted. As the calculated or predicted permeability (K) mD for these wells might be of equal ranges calculated from the three cored wells Ha-B2, Ha-G1and Ha-K1, this study suggests to extrapolate the values from the three calibrated wells.

Ha-B2 = 10 ^ (-2.17677 + 11.3938 * PhiNeu)……equation 11

Ha-G1 = 10 ^ (-1.98527 + 12.5447 * PhiNeu)……equation 12

Ha-K1 = 10 ^ (-2.09203 + 8.92641 * PhiND)…… equation 13

Where; PhiNeu = Neutron-porosity model.

PhiND = Density-porosity model.

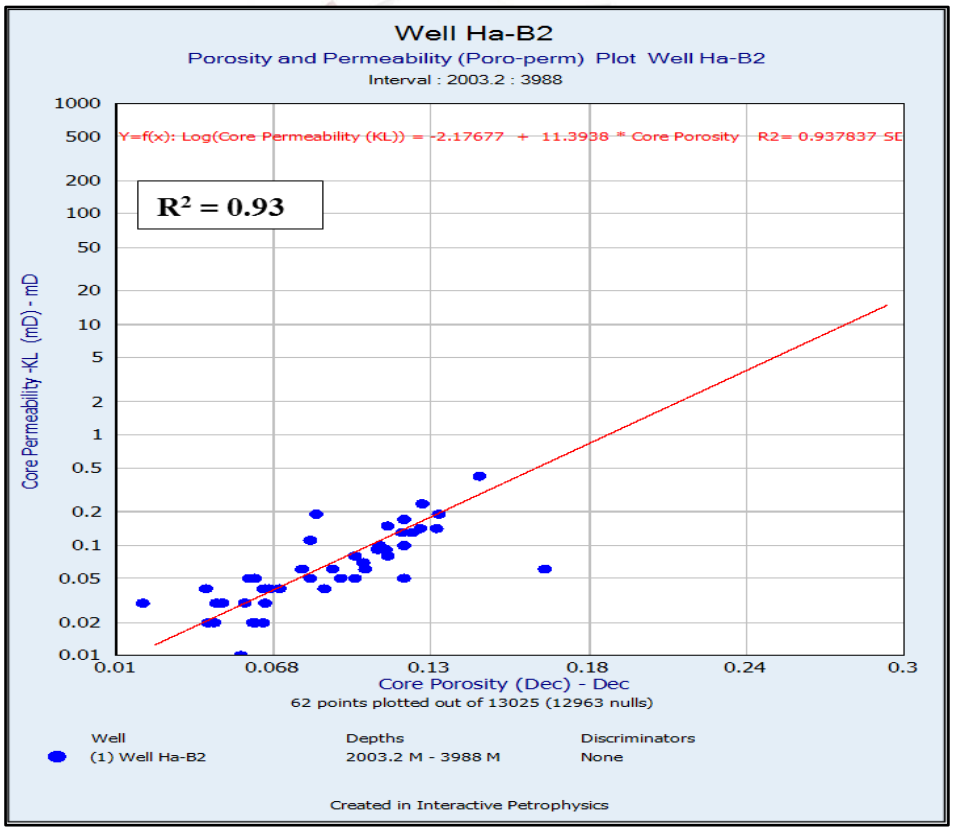

Figure 7. 27: Porosity versus permeability (poro-perm) cross plot for well Ha-B2 with the values obtained from the regression equations that were used to calculate the permeability (mD).

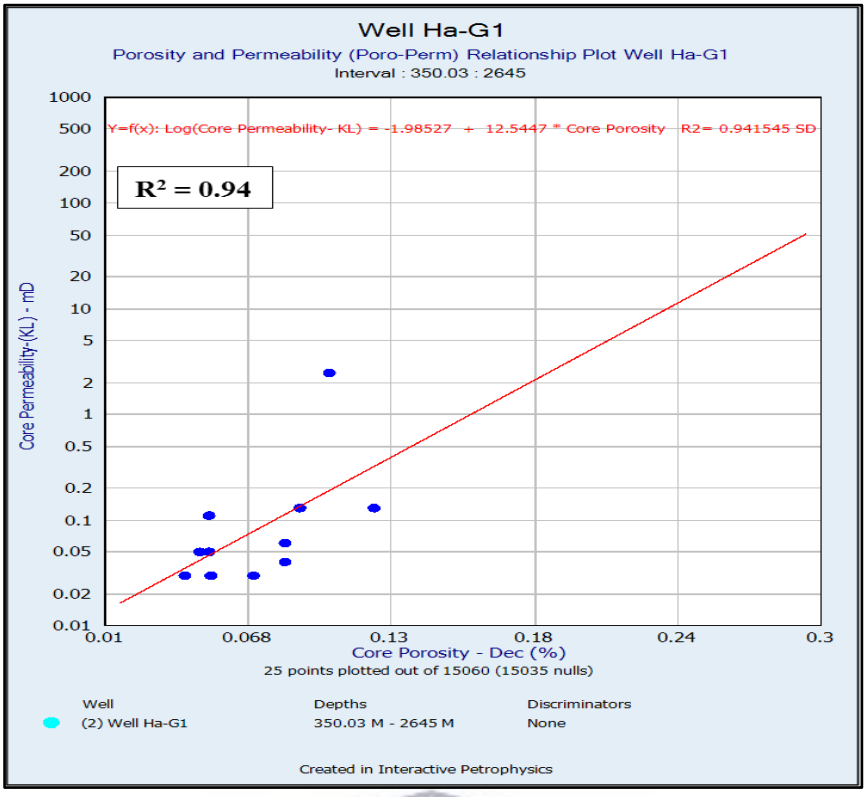

Figure 7. 28: Porosity versus Permeability (poro-perm) cross plot well Ha-G1 with the values obtained from the regression equations that were used to calculate the permeability (mD).

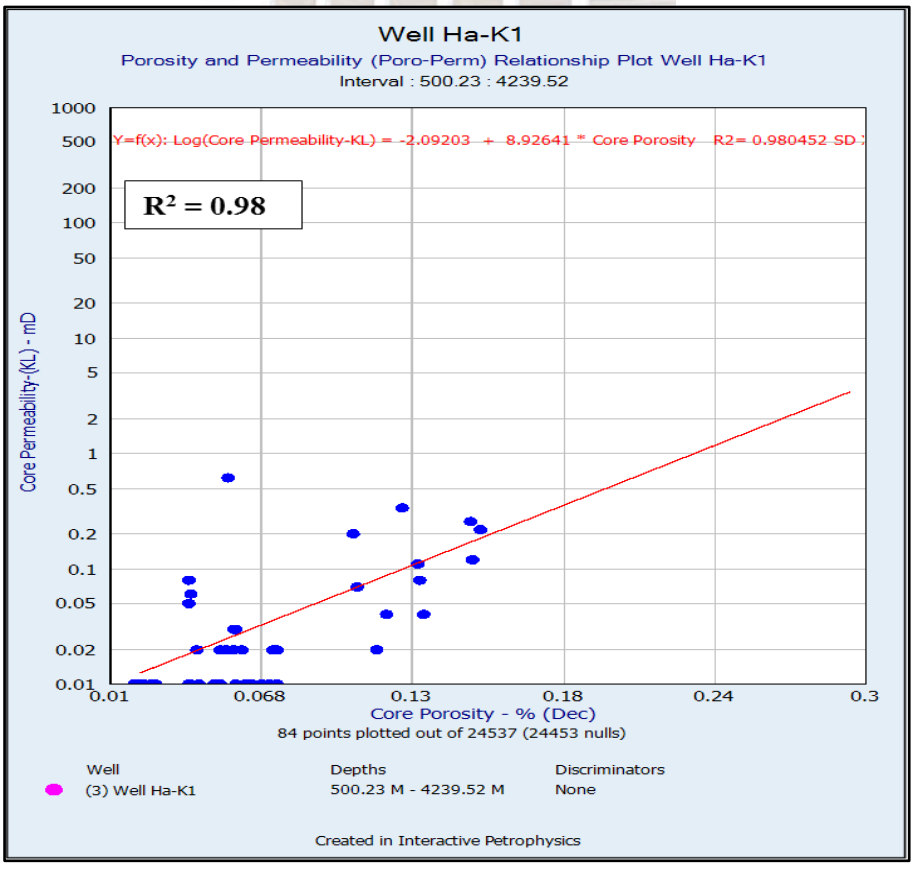

Figure 7. 29: Porosity versus Permeability (poro-perm) cross plot well Ha-K1 with the values obtained from the regression equations that were used to calculate the permeability (mD).

The calculated permeability (calculated or predicted permeability K, mD) was generated from the IP interpretation calculator as a log curve and displayed in the track to estimate the average permeability at a specific depth, based on the given scale. Figure 7.30 - 39 below indicates the calculated or predicted permeability K (mD) displayed as log curves and the histogram plots for the selected reservoirs of each wells. Table 7.4 below illustrates the permeability classification as modified after Djebbar & Donaldson, (1999), which was used to classify the average permeability (mD) of the wells studied in the Valanginian sequence.

Table 7. 4: illustrate the permeability classification. After (Djebbar & Donaldson, 1999).

Permeability values (mD)	Classification
Less than 1	Poor
Between 1 and 10	Fair
Between 10 and 50	Moderate
Between 50 and 250	Good
Between 250 and 1000	Very good
Above 1000	Exceptional

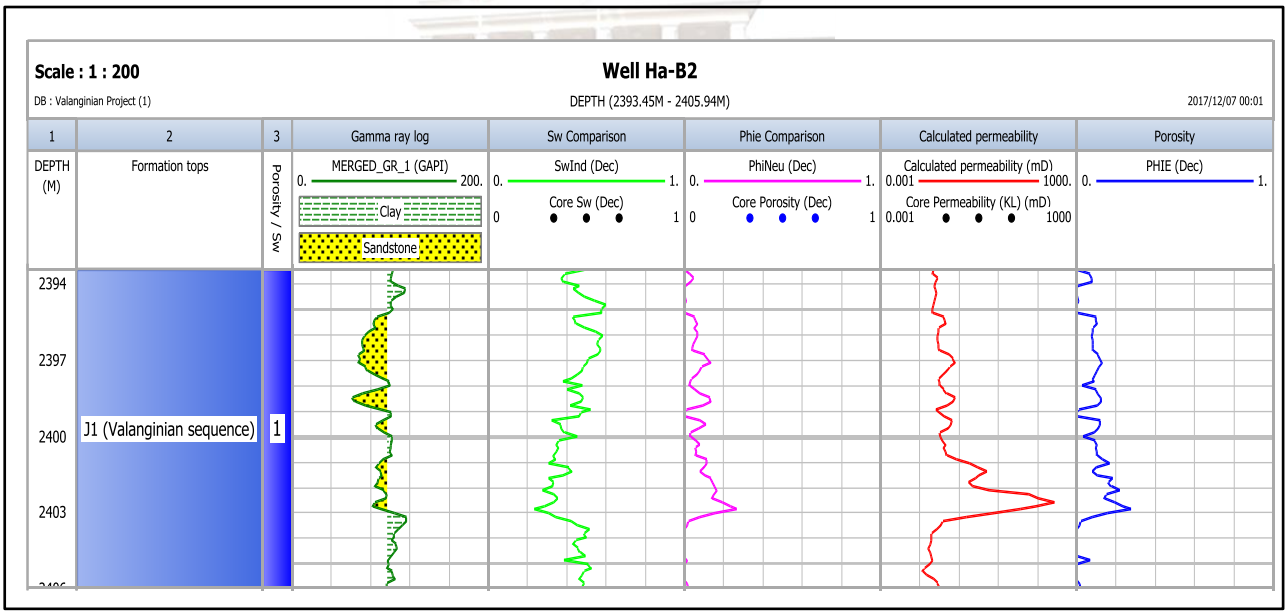

Figure 7. 30: Log curves plot displaying calculated permeability K (predicted K, mD) (track 7) for well Ha-B2, at intervals 2393.45 m – 2405.94 m depths.

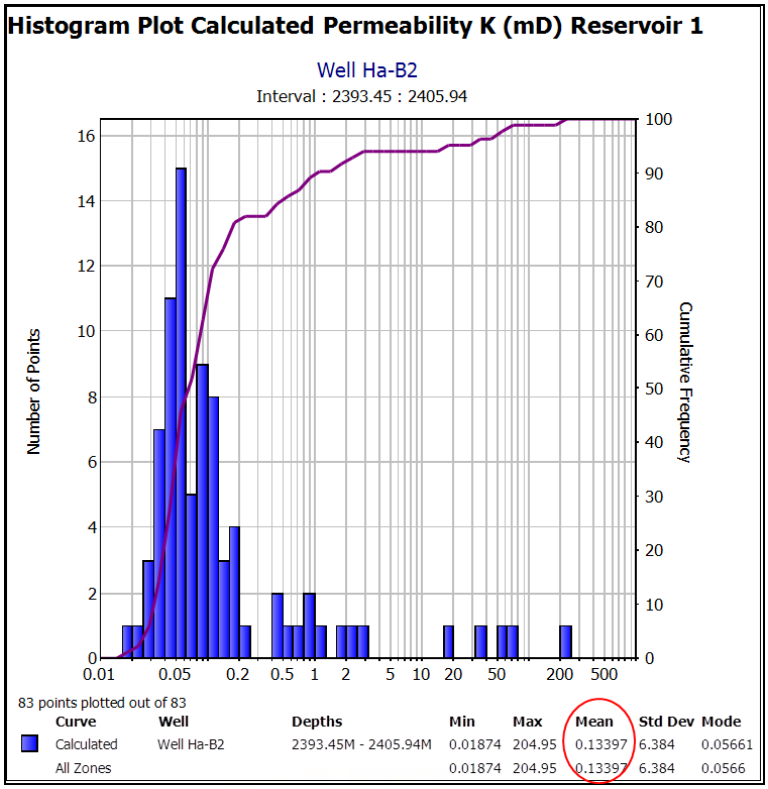

Figure 7. 31: Histogram plots illustrating calculated permeability K (predicted K, mD) interval reservoir 1, well Ha-B2, at depths 2393.45 m – 2405.94 m.

Thus, the reservoir encountered in the Valanginian section from the well Ha-B2, reveal a poor permeability of 0.133mD according to the calculated or predicted permeability histogram plot, (Figure 7.31).

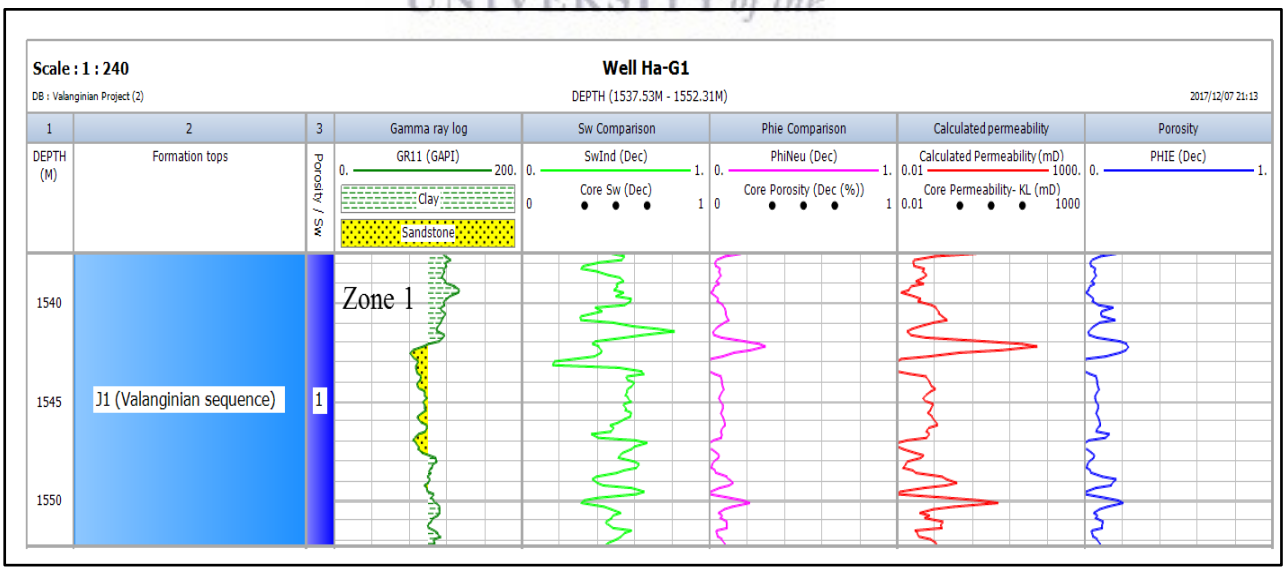

Figure 7. 32: Log curves plot displaying calculated permeability K (predicted K, mD) (track 7) of well Ha-G1 interval reservoir 1, at depths of 1537.53 m – 1552.31 m.

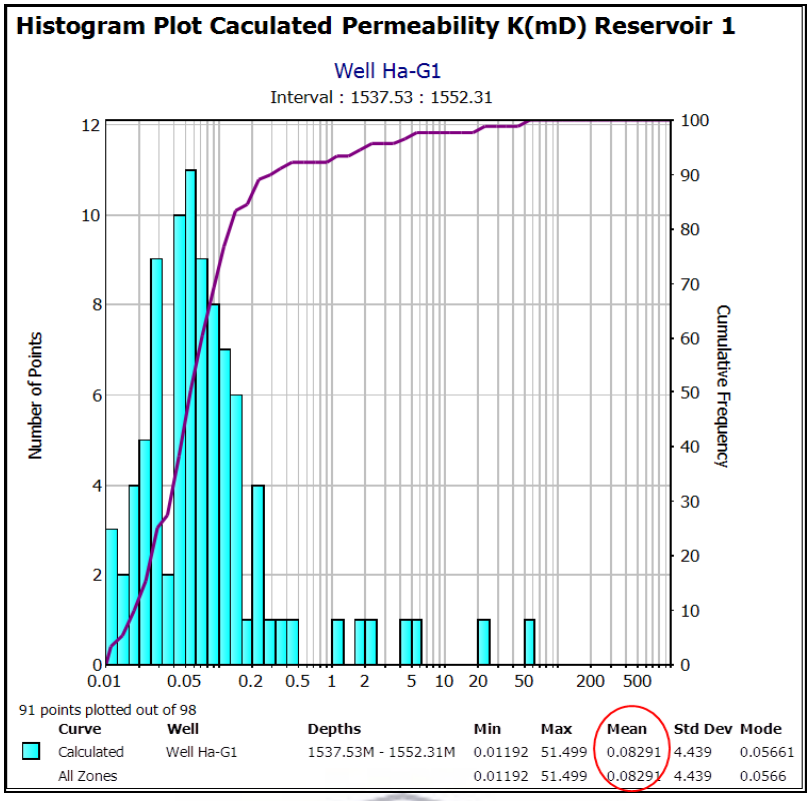

Figure 7. 33: Histogram plots illustrating calculated permeability K (predicted K, mD) of interval reservoir 1, well Ha-G1, at depths 1537.53 m – 1552.31m.

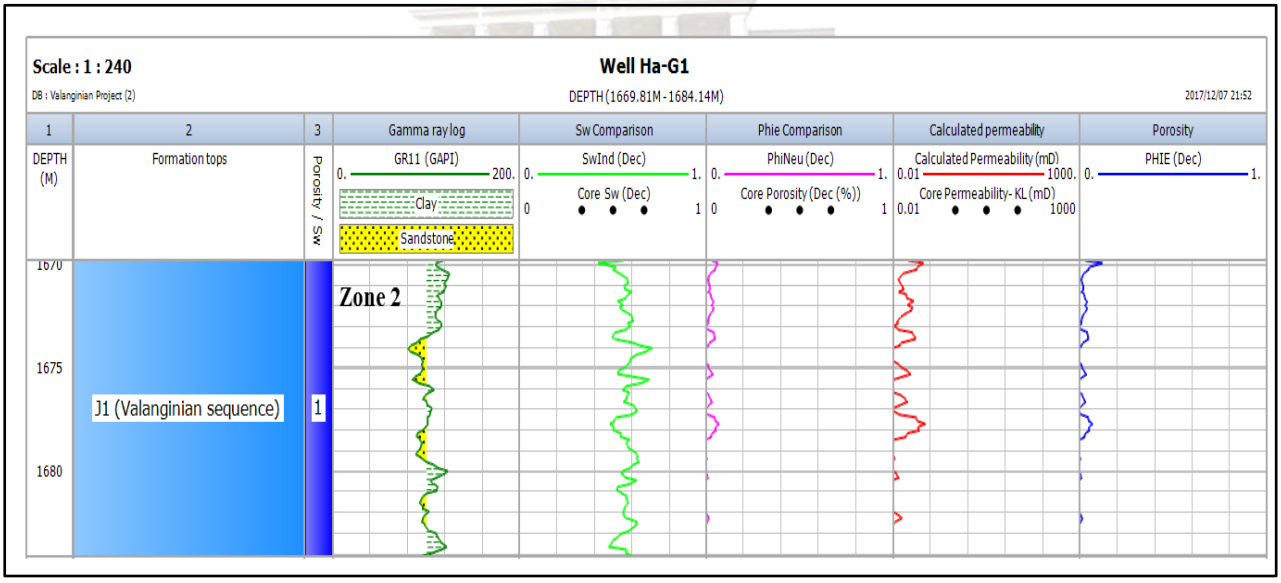

Figure 7. 34: Log curves plot displaying calculated permeability K (predicted K, mD) (track 7) of well Ha-G1 interval reservoir 2, at depths 1669.81 m – 1684.14 m.

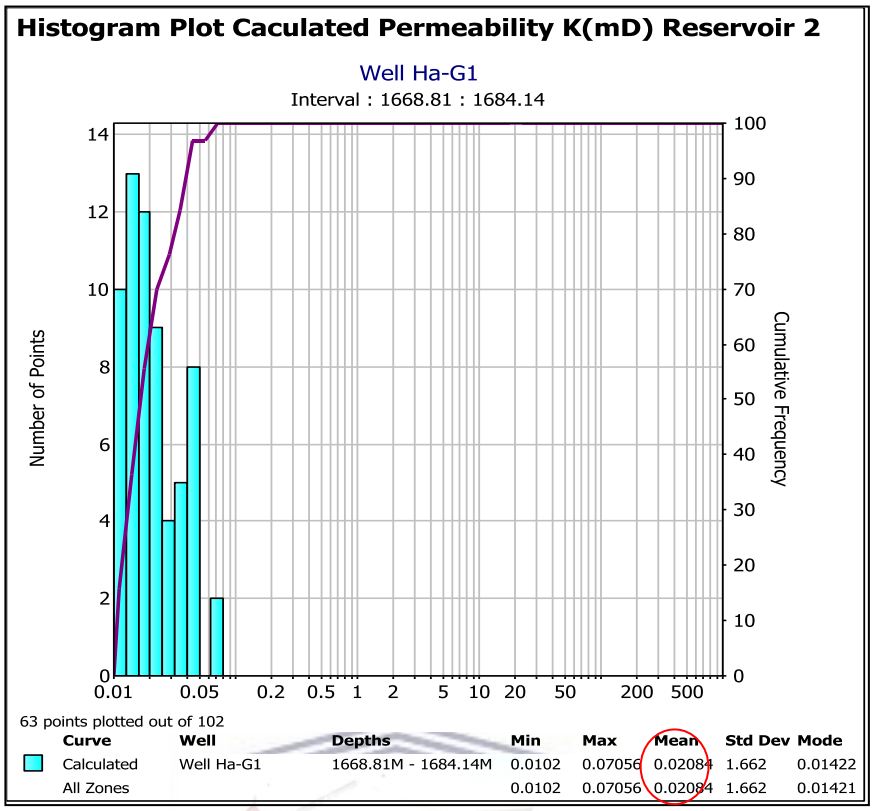

Figure 7. 35: Histogram plots illustrating calculated permeability K (predicted K, mD) interval reservoir 2, well Ha-G1, at depths 1669.81 m – 1684.14 m.

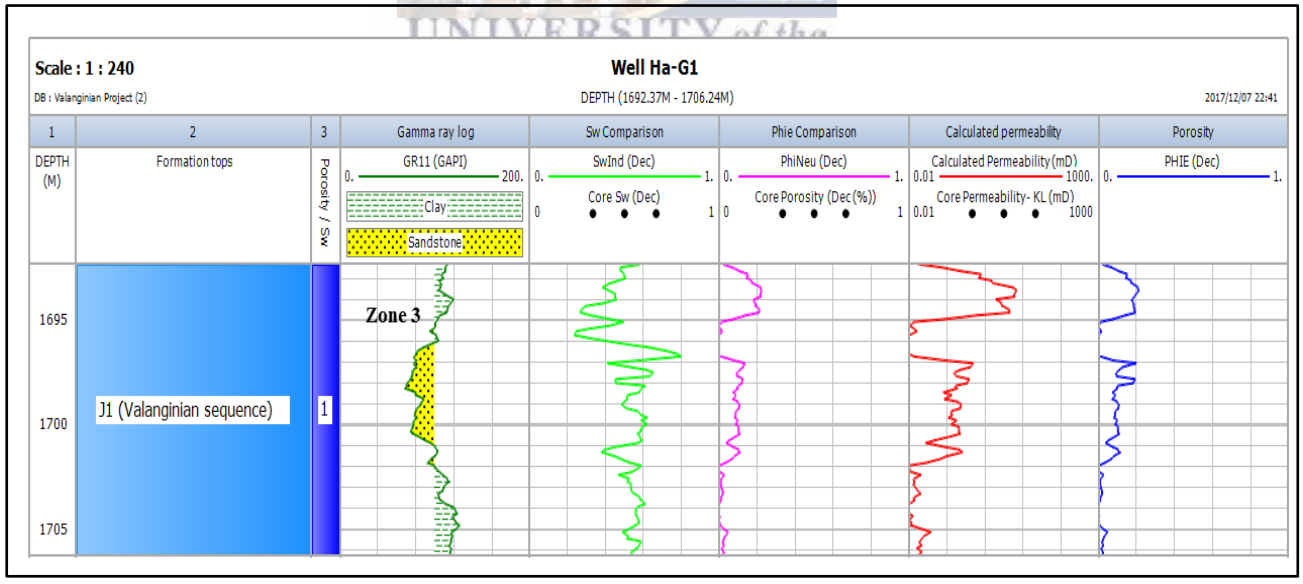

Figure 7. 36: Log curves plot displaying calculated permeability K (predicted K, mD) (track 7) interval reservoir 3, well Ha-G1, at depths 1629.37 m – 1706.24 m.

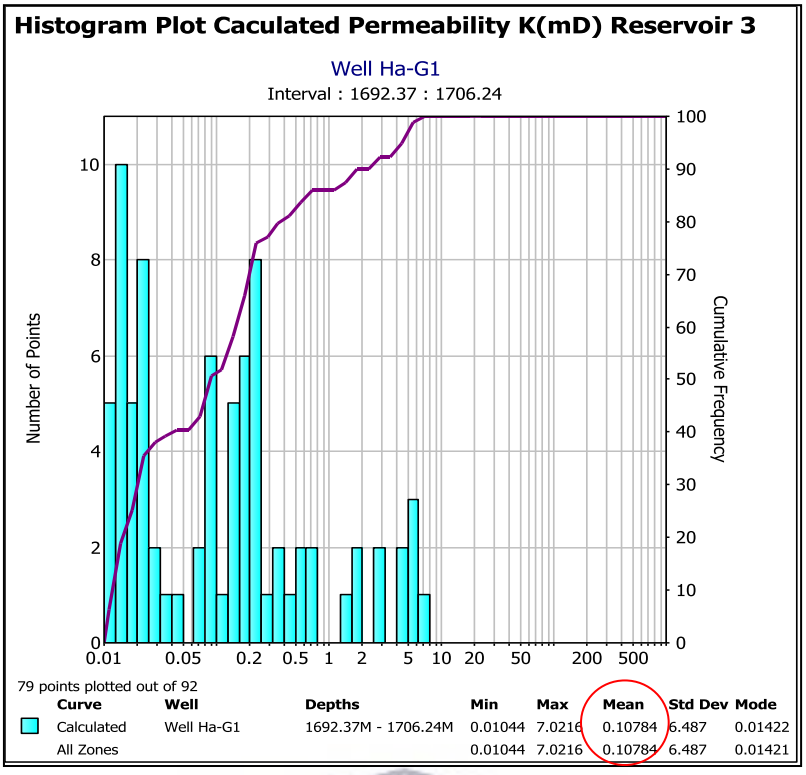

Figure 7. 37: Histogram plots illustrating calculated permeability K (predicted K, mD) interval reservoir 3, well Ha-G1, at depths 1692.37 m – 1706.24 m.

Therefore, from the histogram plot of the calculated or predicted permeability K (mD), the three reservoirs at intervals 1537.53 m – 1552.31m, 1669.81 m – 1684.14m, and 1629.37 m – 1706.24 m depths encountered within the borehole of well HA-G1 in the Valanginian section indicate a poor permeability of 0.082mD, 0.020mD, and 0.107mD respectively.

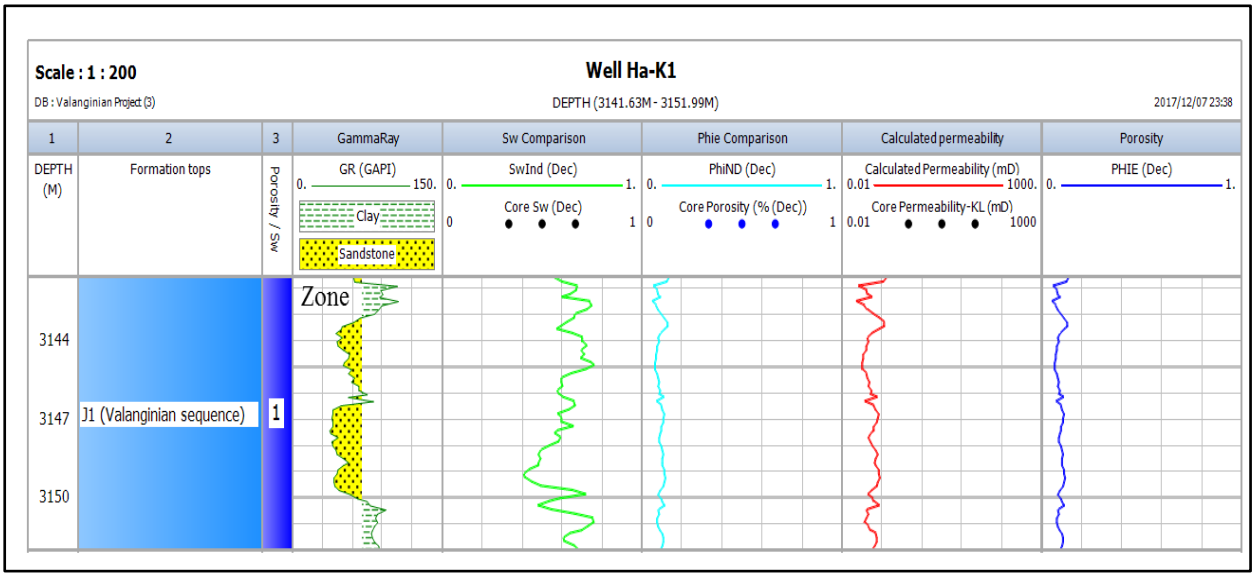

Figure 7. 38: Log curves plot displaying calculated permeability K (predicted K, mD) (track 7) interval reservoir, well at depths Ha-K1, 3141.63 m – 3151.33 m.

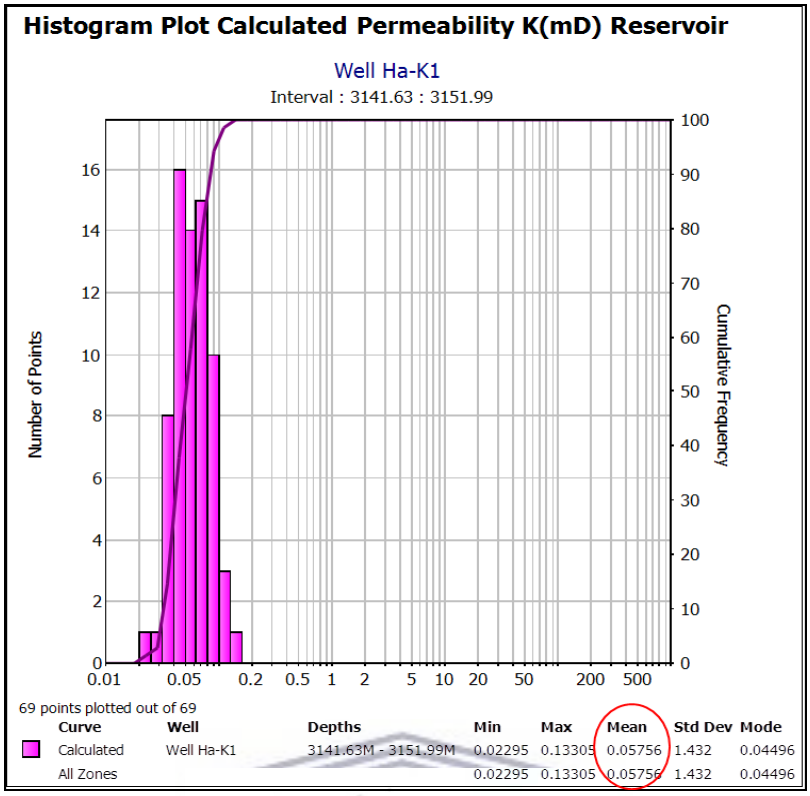

Figure 7. 39: Histogram plots illustrating calculated permeability K (predicted K, mD) interval reservoir well Ha-K1, at depths 3141.63 m – 3151.33 m.

The reservoir encountered in the within Valanginian section of wellbore Ha-K1 shows a poor permeability of 0.05mD from the calculated or predicted permeability histogram plot, (Figure 7.39).

7.5 Cut-off Determination

In the context of integrated reservoir studies, Cut-offs become the limiting values of formation parameters to define pay, thereby excluding those rock volumes that will not add significantly to the economic evaluation of the reservoir. The main primary use of cut-offs is to delineated net pay, defined mostly as the aggregate of those interval depths through which hydrocarbons are economically producible. i.e. it is the concept used to determine the effective petrophysical properties of a rock in the presence of poor reservoir zones (Worthington, 2008).

The cut-offs parameters are determined by means of identifying reference parameters that will enable one to distinguish between the intervals that have reservoir potential and those that have none. Although, cut-offs parameters have been used for several years, there is no typical method to determining and applying it (Worthington & Cosentino, 2003). Therefore, it is usually applied to a calculated result to expel poor quality or non-productive zones. However,

non-productive zones or non-reservoir rocks may contain low porosity and permeability yet still have no hydrocarbon saturation (Opuwari, 2010). The rocks with adequate permeability to allow the flow of hydrocarbons at commercially substantial rates are categorized as net reservoirs and net sandstones. But, in a situation they produce hydrocarbons at commercially satisfactory hydrocarbon to water ratios are recognized as pay reservoirs (Suzanne & Robert, 2004).

To distinguish pay sand from non-pay sand, there are typical cut-off values for formation parameters that are accepted. These include the maximum volume of shale (Vsh) to range between 0.25 and 0.40, minimum porosity to range between 0.03 and 0.16 and maximum water saturation to range between 0.30 and 0.70. These values are expressed as percentages, i.e. (25% - 40%) volume of shale, (3% - 16%) porosity, and (30% 70%) water saturation. Permeability cut-off values of 0.1mD and 1mD are generally considered for gas and oil reservoirs net pay respectively. In general, for porosity and permeability cut-off, any reservoir rocks where the pores have a porosity or permeabilty less than cut-off values are considered to be non-reservoir rocks and will not allow flow of fluids. While water saturation cutoff, defined as pores with water saturation (Sw) greater than cut-off value, will have water saturation of $1-S_h$, where S_h is the hydrocarbon saturation. For this study, the cut-off determination was applied on the intervals of Valanginian sections of the wells studied, to shale volume (Vsh), porosity (Φ), water saturation (Sw) and permeability (K) parameters respectively.

7.5.1 Porosity and Permeability Cut-off Determination

Conventionally, the permeability cut-offs of 1mD and 0.1mD are generally applied to the oil and gas reservoir respectively, these values are considered as minimum value for hydrocarbon production (Lucia, 2007). The reservoirs in this study within the Valanginian sections of Gamtoos Basin are gas bearing. Thus, permeability cut-off value of 0.1mD and porosity cut-off values of 0.117 which is equal to (11.7 %) were applied for hydrocarbon production of the potential reservoir intervals studies. The (Φc) and (Kc) on the x-axis and y-axis indicate the porosity and permeability cut-offs respectively (Figure 7.40). Based on these cut-offs, any reservoir intervals with an effective porosity of less than 0.117 (11.7%) and a permeability of less than 0.1mD are considered as a non-reservoir and any intervals with the values above the cut-offs are regarded as a potential reservoir within the Valanginian section. The permeability and porosity frequency distribution histogram plots also show the cut-offs of porosity and permeability (Figure 7.41 and 7.42). The calculated permeability values from the regression equations were presented as well in Table 7.5.

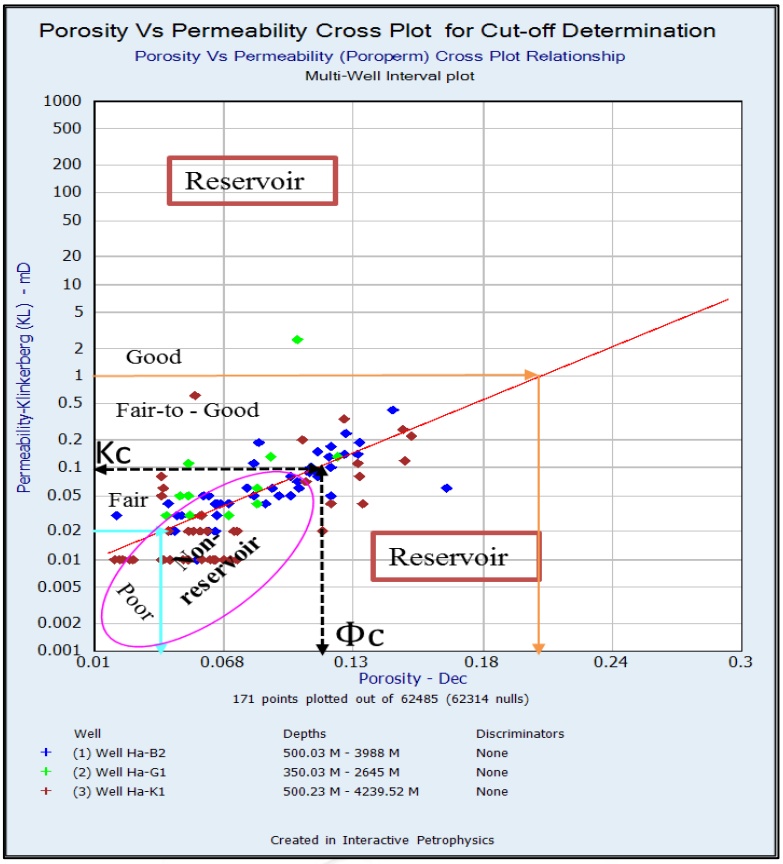

Figure 7. 40: Porosity versus permeability cross plot for cut-off determination.

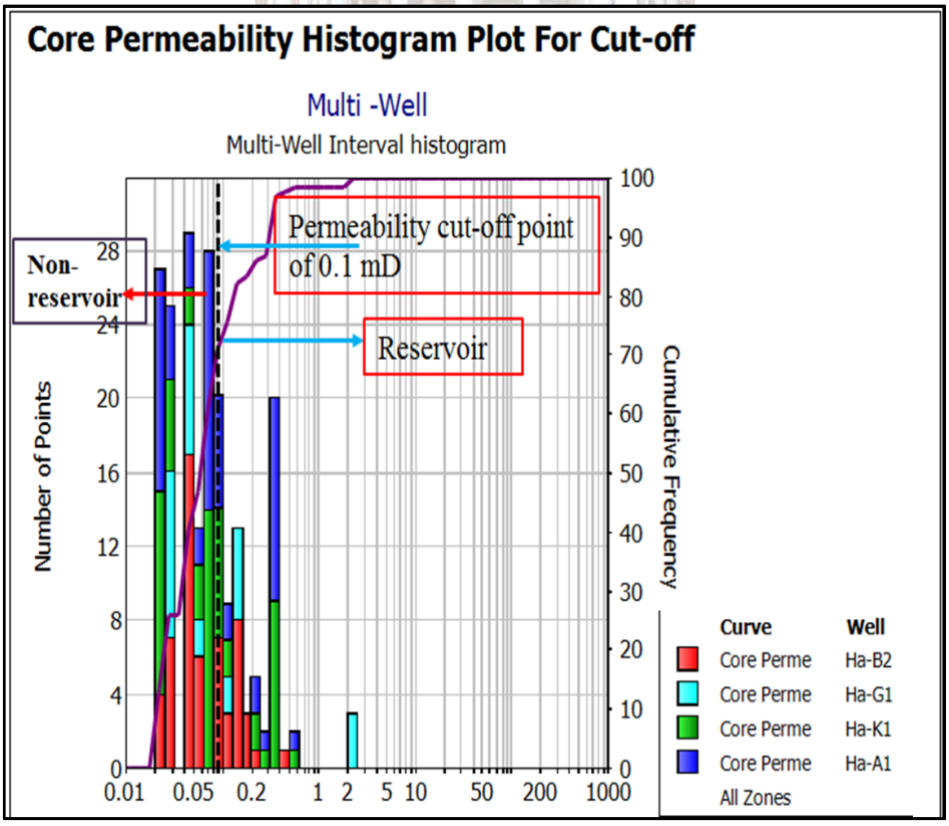

Figure 7. 41: Core permeability histogram plot for the study wells

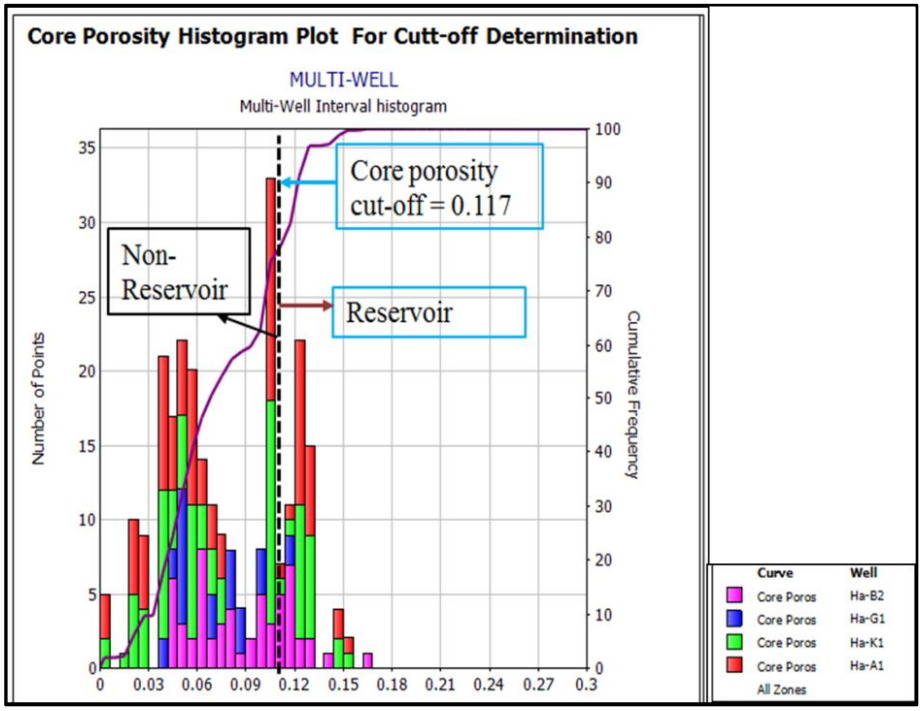

Figure 7. 42: Core porosity histogram plot for the wells studies.

Table 7. 5: Calculated permeability of the evaluated reservoirs for each of the studied wells.

Well names	Top depth (m)	Bottom depth (m)	Reservoir/Zones names	Permeability Value (mD)
Ha-B2	2393.45	2405.94	1	0.133
Ha-G1	1537.53	1552.31	1	0.082
Ha-G1	1668.81	1684.14	2	0.020
Ha-G1	1692.31	1706.24	3	0.107
Ha-K1	3141.63	3151.33	1	0.057

The permeability presented above in Table 7.5 is the calculated permeability, generated from the average reading of the permeability log curves of the cored wells Ha-B2, Ha-G1 and Ha-K1 in the Valanginian section for the selected intervals studied. It has been observed that the average permeability (mD) readings from the calculated or predicted permeability across the intervals are generally poor, ranging from 0.02 mD to 0.1mD. Based on this result it is concluded that the reservoir permeability for the Valanginian section is poor.

7.5.2 Volume of Shale Cut-off Determination

The concept of volume of shale cut-off (Vshc) is to distinguish between the reservoir interval and non-reservoir interval to find the rocks that have equal volume of shale or less than a certain value of the total reservoir volume. The multi-well volume of shale cut-off for the

reservoir and non-reservoir rock studies in the Valanginian section was defined at 0.26. For the present work , the rock with a volume of shale of 0.26 (equivalent to 26 %) or above were assumed to be shale and considered to be non-reservoir. While those rocks with a volume shale cut-off at 26% or below were classified as a reservoir rocks. The volume of shale cut-off is shown in Figure 7.43 where volume of shale is plotted against porosity and gamma ray. The average volume of shale was obtained from the volume of clay on the log curves, calculated for the wells and presented in a composite log track.

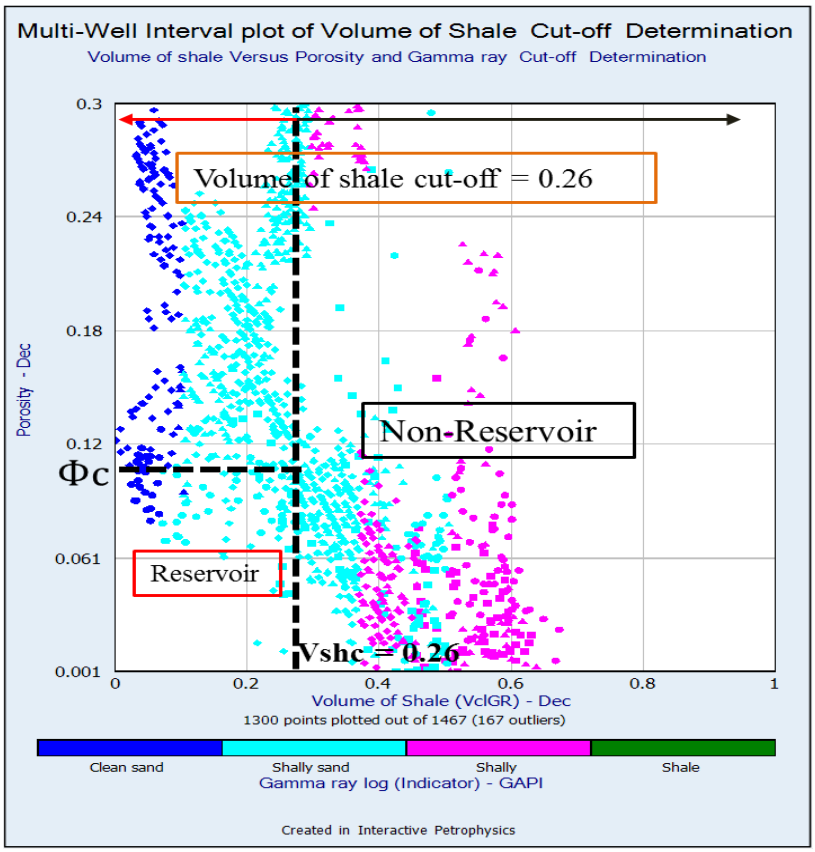

Figure 7. 43: Volume of shale (Vshc) against porosity and gamma ray plot to classfied reservor and non-reservoirs of the wells studies in Valanginian section.

7.5.3 Water saturation Cut-off Determination

The water saturation cut-off is the factor used to distinguish between the hydrocarbon bearing sandstone (pay) and water bearing (wet) interval in a formation evaluation. In this study, the water saturation cut-off was determined to be 66% and used to differentiate between the pay and wet intervals of the wells studies in Valanginian section. The intervals with water saturation of 66% or below were assumed to be hydrocarbon bearing sandstone while the intervals with more than 66% were considered as wet or non-productive intervals. The water saturation cut-off value is represented in Figure 7.44 below, where water saturation against porosity cross has been plotted.

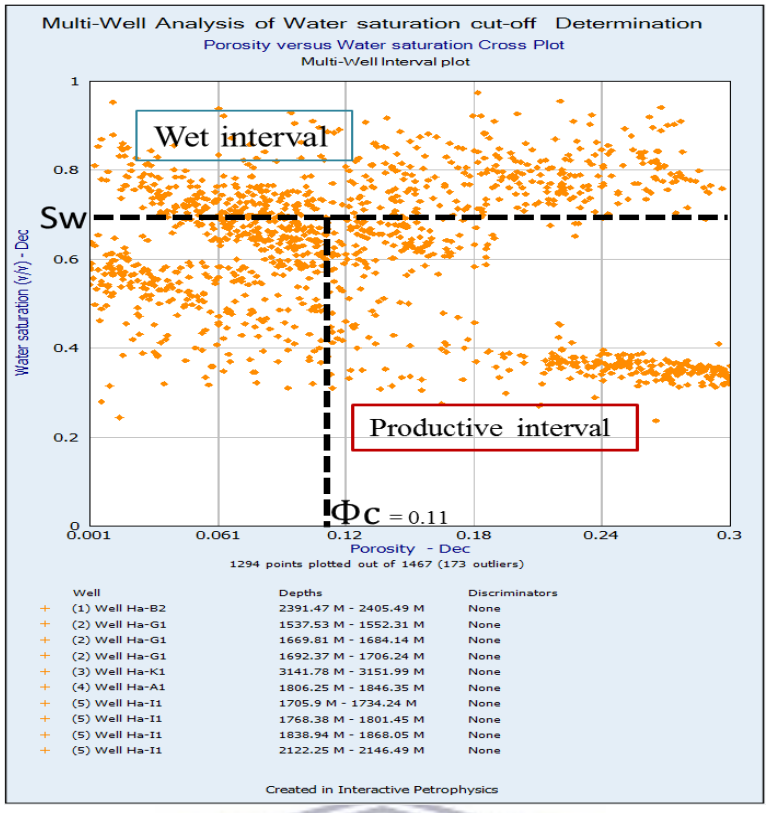

Figure 7. 44: Multi-well porosity against water saturation cross plot for cut-off determination.

7.5.4 Net-pay Determination

"Net-pay" is defined as the interval of the rock that contains a hydrocarbon/water ratio suitable to produce at commercial rates. The term "gross" is defined as the reservoir interval that contains zones where hydrocarbons can be produced and zones that do not support the production of hydrocarbons. To determine net pay, it is essential to calculate the hydrocarbon pore per feet, (F_{HCP}) at the borehole and to calculate the whole reservoir's original oil in place (OOIP) or original gas in place (OGIP) (Cobb et al., 1998). Net-to-gross ratio is the ratio of the total amount of pay footage to the total thickness of reservoir interval, assuming the well is vertical (Cobb et al., 1998). A net-to-gross ratio (N/G) of 1 suggests that the entire reservoir interval is pay footage (Cobb et al., 1998). But the interval is considered as non-pay and does not add any value to the calculation of OOIP and OGIP reserves. However, reservoir volumetric calculation was not part of the objective and scope of this study.

Thus, to differentiate between gross and net pay in the petrophysical analysis, a cut-off value must be applied. In this study a cut-off values used to identify the pay interval of the reservoirs studies are: porosity ≥ 0.117, volume of shale ≤ 0.263 and water saturation ≤ 0.663. That is the reservoir intervals with effective porosity equal to or greater than 11.7%, Shale volume less than or equal to 26.3% and water saturation equal to or less than 66.3% were considered as the

net pay intervals. With the aid of the cut-off limit, the flag curves were generated in the database, the net (pay) reservoir flag interval was computed from the volume of shale, porosity and water saturation cut-off and defined by the red colour. The gross reservoir flag interval as computed from the volume of shale and porosity cut-off is defined by the green colour. Finally the rock flag was computed from the volume of shale/clay and is defined by the yellow colour, presented in the table 7.6.

Table 7. 6: The calculated reservoir flag cut-offs.

	Flag Name	Flag shading colour	Shale Volume cut-off.	Porosity Cut-off	Water saturation Cut-off
1	Rock		yes	no	no
2	Gross reservoir		yes	yes	no
3	Net (pay) reservoir		yes	yes	yes

7.5.4.1 Well Ha-B2 Net-pay

The petrophysical reservoir average results, evaluated for the reservoir interval encountered within the borehole of well Ha-B2, in the Valanginian section is presented below in Table 7.7. The net thickness was calculated to be 0.61m with the average effective porosity of 13.1%, water saturation of 49.3%, volume of clay 20.6% and permeability of 0.133mD. The reservoir and pay flag of the interval reservoir are presented below in Figure 7.45. The consequence of these parameters will be discussed later in the chapter.

Table 7. 7: Petrophysical reservoir average report of well Ha-B2.

Top depth (m)	Bottom depth (m)	Gross (m)	Net (m)	N/G (frac)	Av phi (frac)	Av Sw (frac)	Av Vcl (frac)	Av K (mD)
2392.90	2406.60	13.70	0.61	0.044	0.131	0.493	0.206	0.133

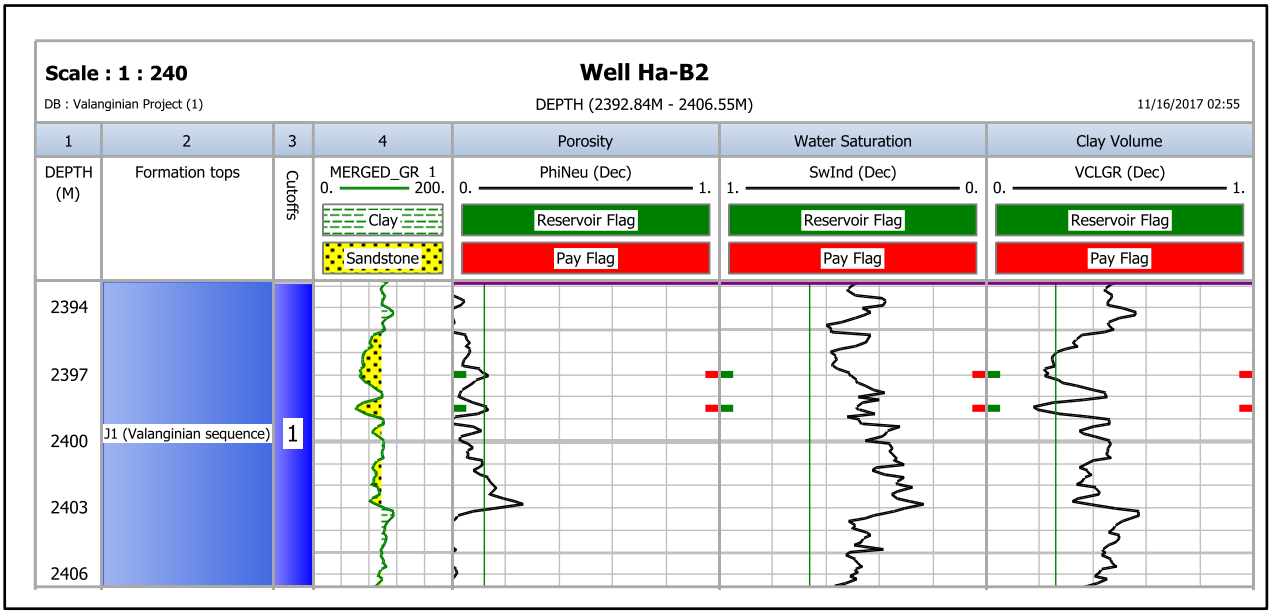

Figure 7. 45: Well Ha-B2 calculated reservoir and pay flags.

7.5.4.2 Well Ha-G1 Net-pay

In the well Ha-G1 three reservoir intervals were encountered within the Valanginian section and were evaluated; none of these reservoirs intervals indicates net pay potential, as presented in Table 7.8. In the well Ha-B2 the intervals within this section do not have the capability to produce hydrocarbons. This might be as a result of the geological heterogeneity factor such as the degree of cementation during the diagenetic process that resulted in low permeability in this formation. The net pay reservoir flags are shown in Figures 7.46 – 7.48 below.

Table 7. 8: Represent the petrophysical reservoir average report of well Ha-G1.

Reservoir/ Zone	Top depth (m)	Bottom depth (m)	Gross (m)	Net (m)	N/G (frac)	Av phi (frac)	Av Sw (frac)	Av Vcl (frac)	Av K (mD)
1	1537.53	1552.31	14.78	0.00	0.00	……	…..	…..	0.082
2	1669.81	1684.14	14.33	0.00	0.00	……	…..	…..	0.020
3	1692.37	1706.24	13.87	0.00	0.00	……	…..	…..	0.107

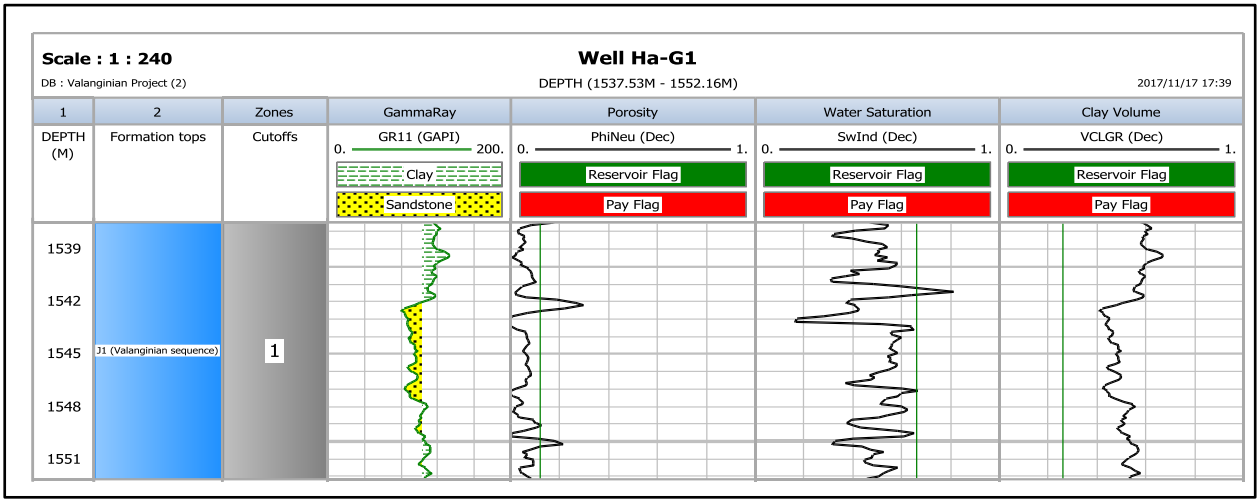

Figure 7. 46: Calculated reservoir and pay flags of reservoir (Zone 1) in Well Ha-G1.

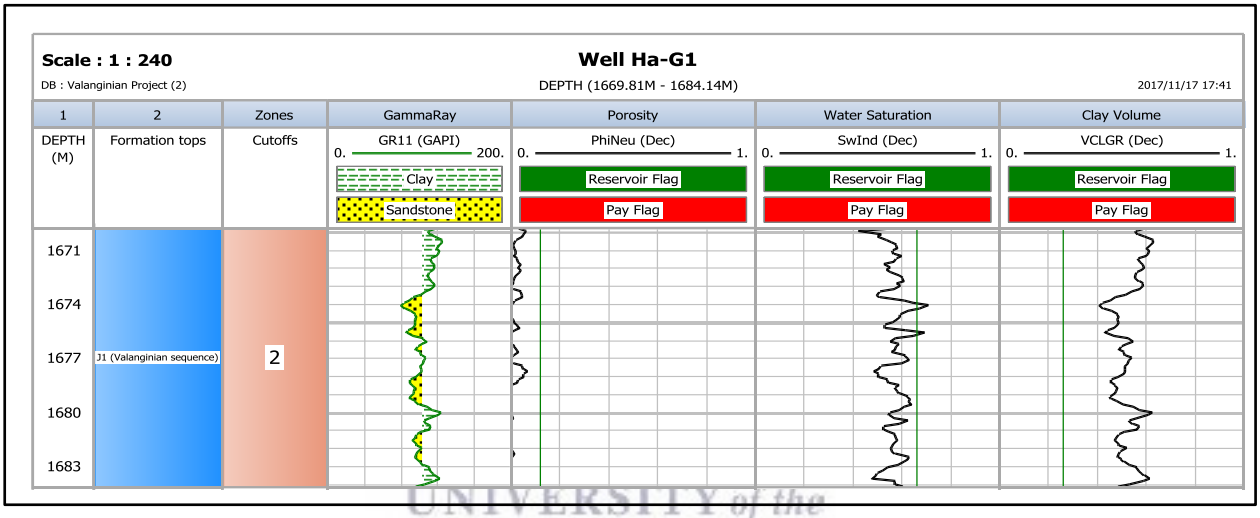

Figure 7. 47: Calculated reservoir and pay flags of reservoir (Zone 2) in Well Ha-G1.

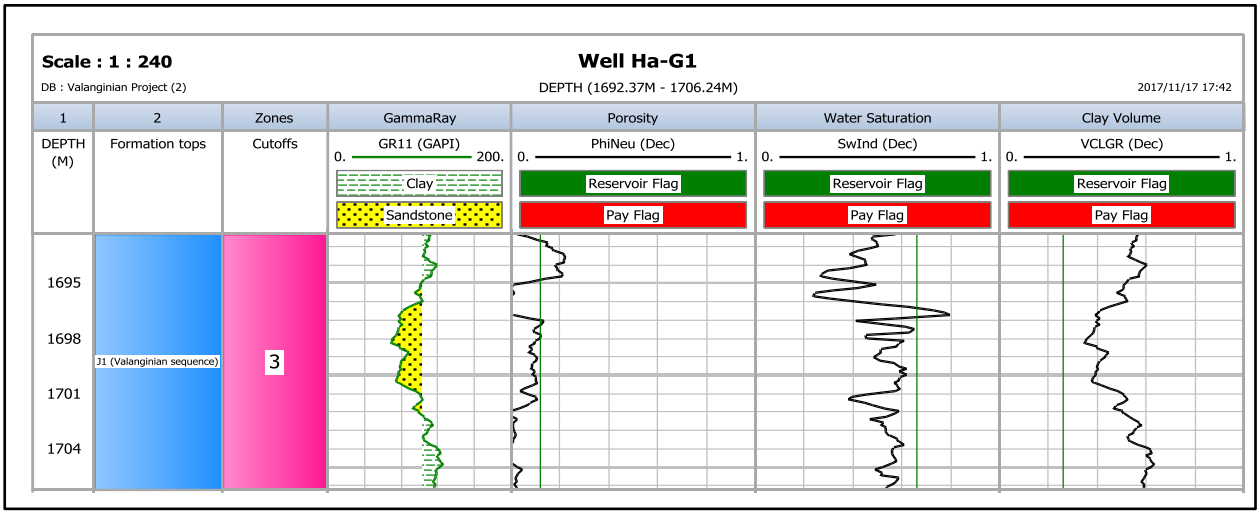

Figure 7. 48: Calculated reservoir and pay flags of reservoir (Zone 3) in Well Ha-G1.

7. 5.4.3 Well Ha-K1 Net-pay

The potential sandstone reservoir interval encountered in the borehole for well Ha-K1, in the Valanginian section was evaluated and the net pay is presented in the Table 7.9. The net thickness of the producing interval was 0.53m; average effective porosity of this interval was 12.5%, average water saturation of 55.5%, average volume of clay 10% and average permeability of 0.057mD. The net pay reservoir flags are shown in Figure 7.49 below.

Table 7. 9: Petrophysical reservoir averages report of well Ha-K1.

Top depth (m)	Bottom depth (m)	Gross (m)	Net (m)	N/G (frac)	Av phi (frac)	Av Sw (frac)	Av Vcl (frac)	Av K (mD)
3141.78	3151.99	10.21	0.53	0.052	0.125	0.555	0.010	0.057

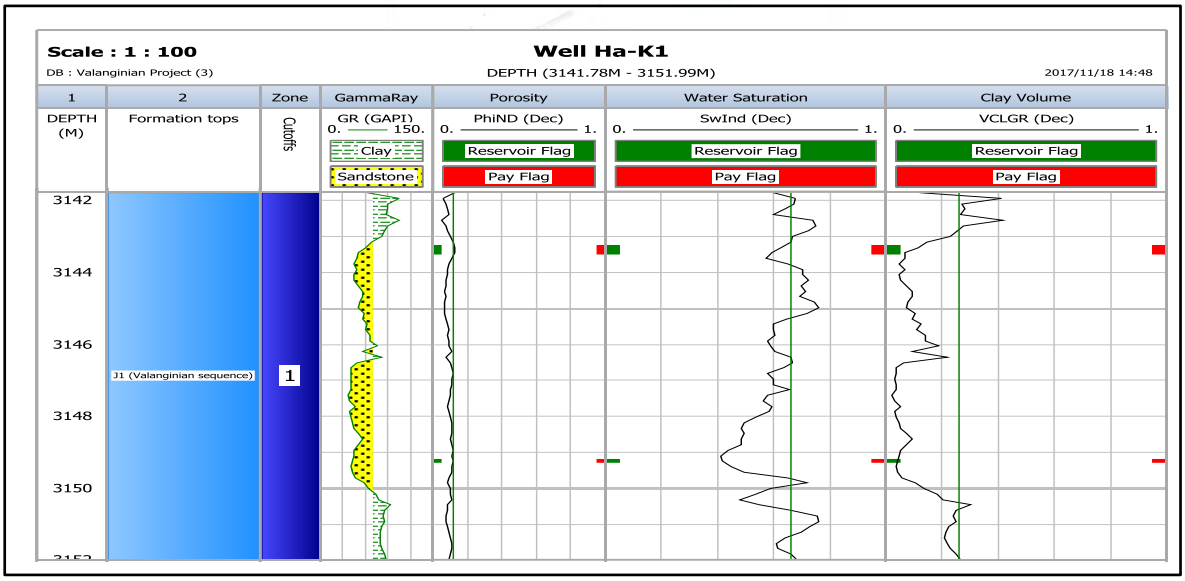

Figure 7. 49: Calculated reservoir and pay flags of reservoir in Well Ha-K1.

7.5.4.4 Well Ha-A1 Net-pay

In well Ha-A1, the evaluated sandstone reservoir potential encountered within the formation indicated a net pay potential. The net pay thickness of the producing interval was ~15.9m; average effective porosity was 16.2%, average water saturation of 35.9% and the average volume of clay was 24.0%, as presented in Table 7.10; the net pay reservoir flags are shown in Figure 7.50 below.

Table 7. 10: Petrophysical reservoir average report of well Ha-A1.

Top depth (m)	Bottom depth (m)	Gross (m)	Net (m)	N/G (frac)	Av phi (frac)	Av Sw (frac)	Av Vcl (frac)
1806.25	1846.33	40.08	15.85	0.395	0.162	0.359	0.240

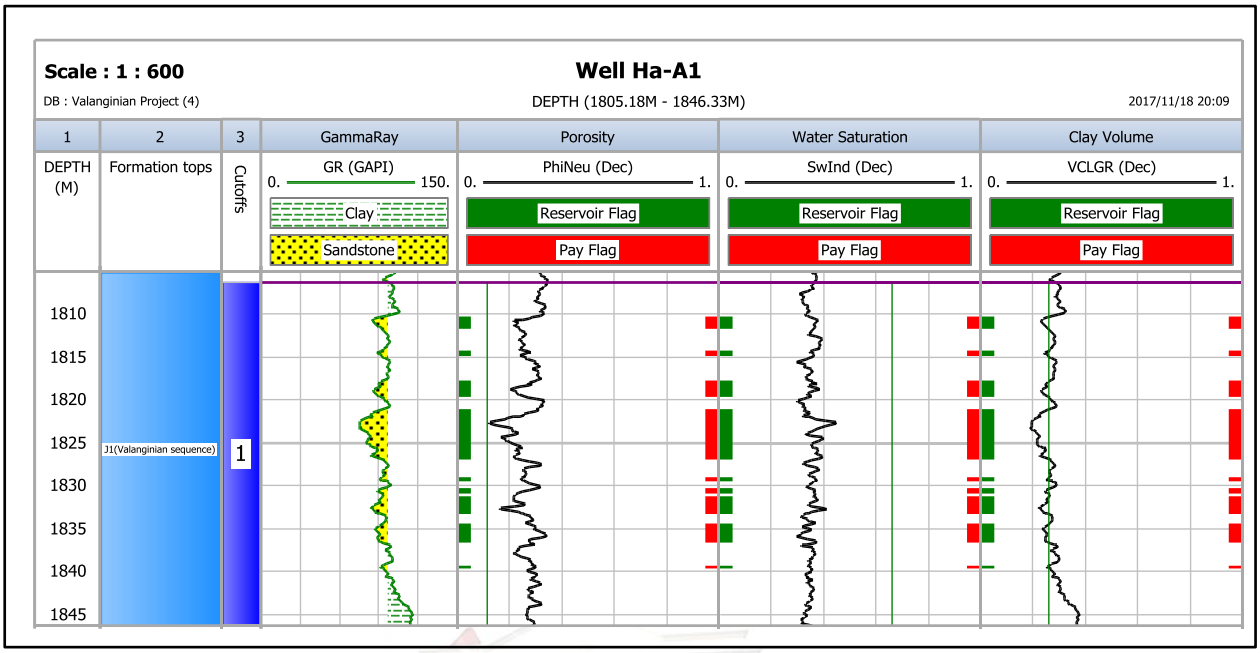

Figure 7. 50: Calculated reservoir and pay flags of reservoir in Well Ha-A1.

7.5.4.5 Well Ha-I1 Net-pay

Five sandstone reservoir intervals were evaluated in well Ha-I1; in the study, the reservoir intervals indicated pay net potential, except interval 1. The net pay thickness of producing interval ranges from 1.52m to 6.71m. The effective porosity values range from 13% to 19%, average water saturation ranges from 58% to 63% and the average volume of clay ranges from 12.9% to 18.8% as indicated in Table 7.11; reservoir pay flags are shown in Figures 7.51 to 7.55.

Table 7. 11: Petrophysical reservoir average report of well Ha-I1.

Reservoir/ Zone	Top depth (m)	Bottom depth (m)	Gross (m)	Net (m)	N/G (frac)	Av phi (frac)	Av Sw (frac)	Av Vcl (frac)
1	1705.98	1734.24	28.26	0.00	0.00	…	…	…
2	1768.38	1801.45	33.07	1.52	0.046	0.191	0.633	0.188
3	1838.94	1868.05	29.11	3.66	0.126	0.139	0.580	0.129
4	2122.04	2146.50	24.46	5.94	0.243	0.143	0.622	0.143
5	2185.20	2217.80	32.60	6.71	0.206	0.151	0.609	0.151

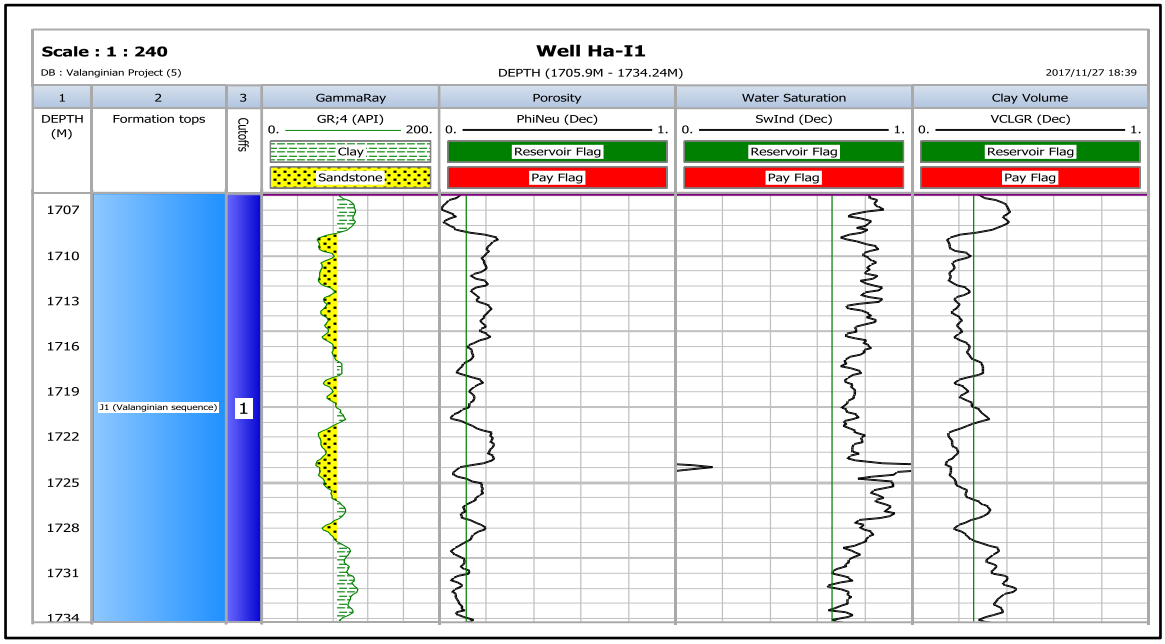

Figure 7. 51: Calculated reservoir and pay flags of reservoir (Zone 1) in Well Ha-I1.

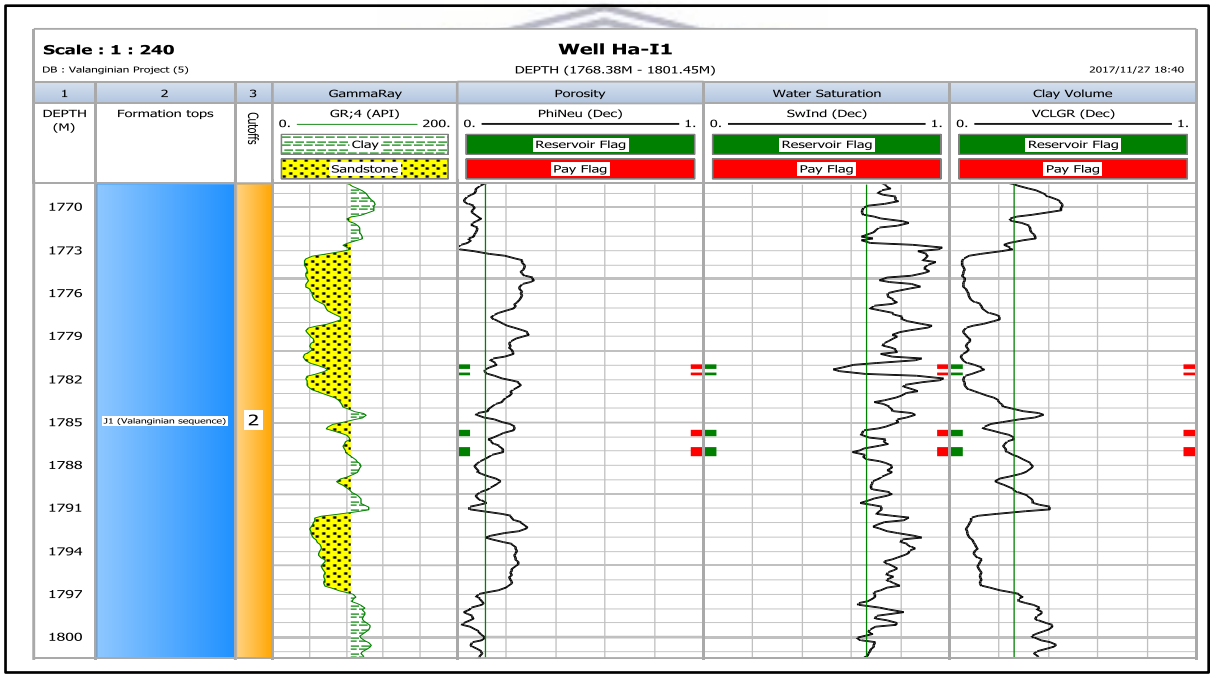

Figure 7. 52: Calculated reservoir and pay flags of reservoir (Zone 2) in Well Ha-I1.

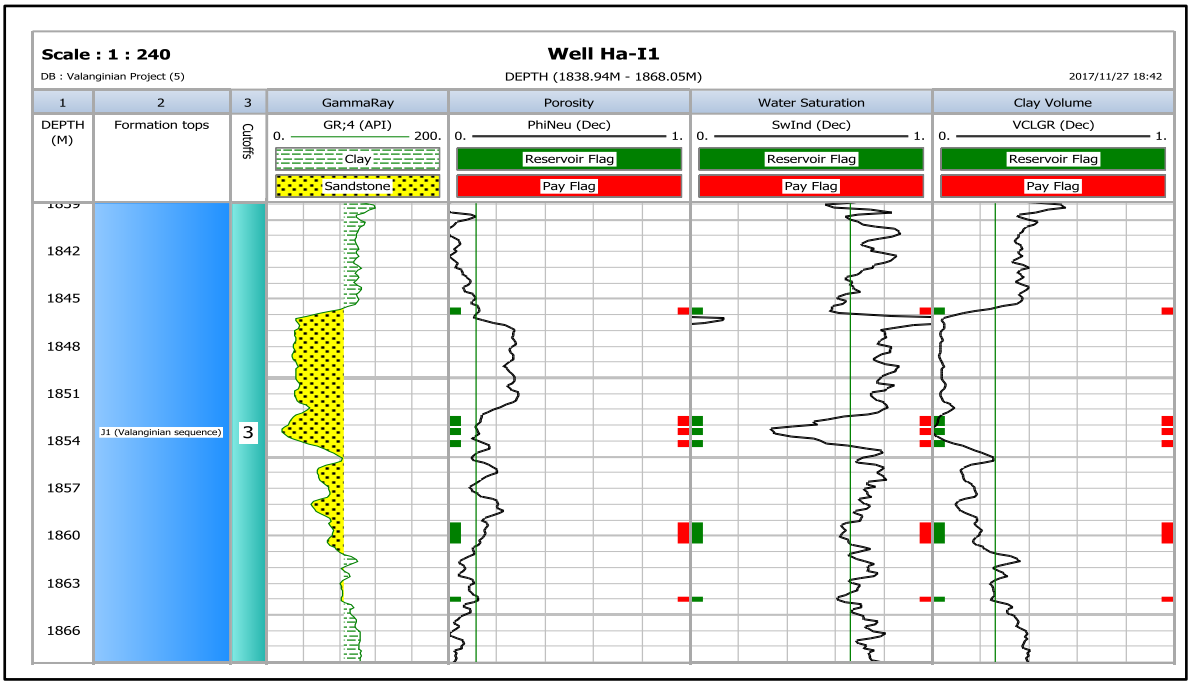

Figure 7. 53: Calculated reservoir and pay flags of reservoir (Zone 3) in Well Ha-I1.

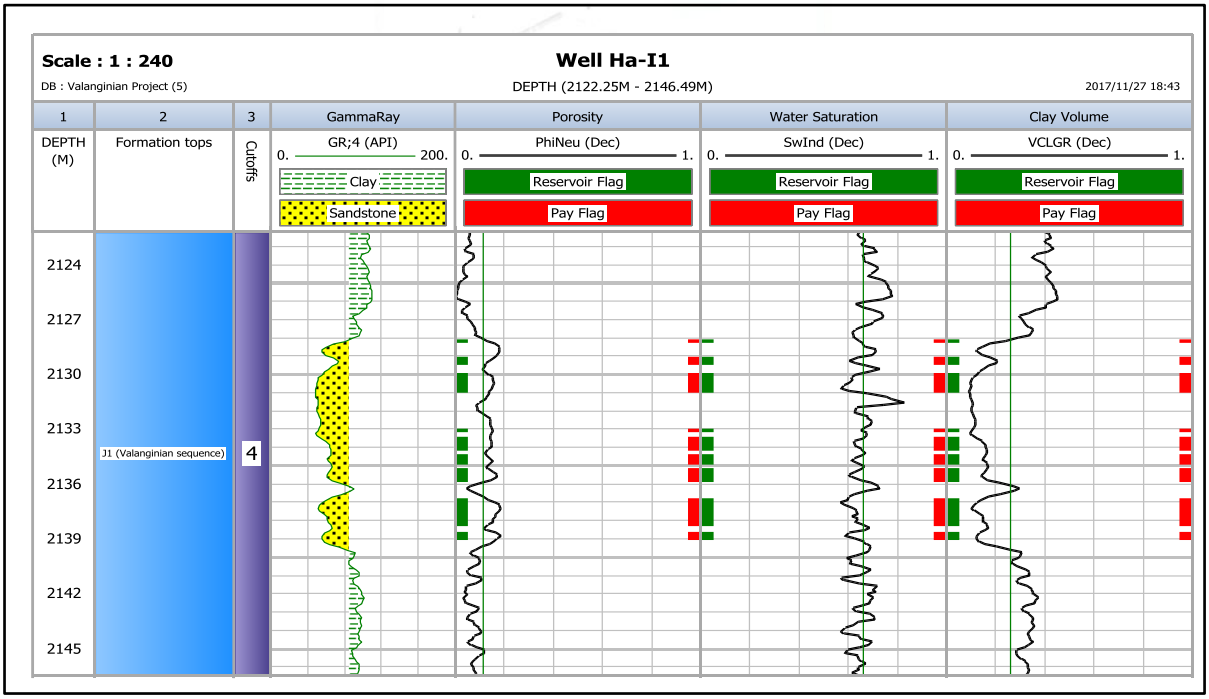

Figure 7. 54: Calculated reservoir and pay flags of reservoir (Zone 4) in Well Ha-I1.

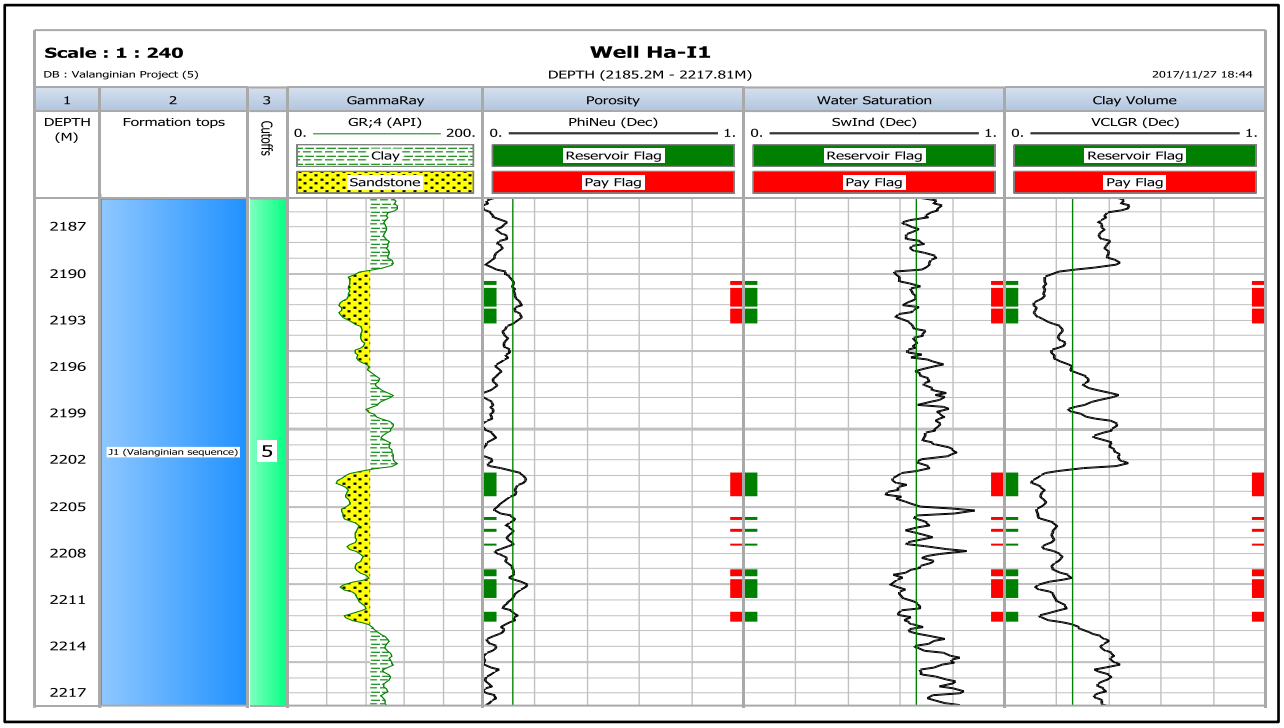

Figure 7. 55: Calculated reservoir and pay flags of reservoir (Zone 5) in Well Ha-I1.

In addition, based on the results of the pay intervals of wells studied in the Valanginian sections is summarized in Table 7.7 - 7.11 above, well Ha-A1 indicated a high average net-to-gross ratio of 39.6m and well Ha-B2 showed the lowest net-to-gross ratio of 4.4m. Wells Ha-I1 and Ha-K1 indicate net-to-gross ratio of 20.6m and 5.2m respectively, while well Ha-G1 indicated a 0m net-to-gross ratio. These values suggest that well Ha-A1 on average has the large thickness that can produce hydrocarbons as compared to the other wells in the JI formation. The average effective porosities within the pay sand of the interval studied for wells Ha-B2 and Ha-K1 are almost the same for each well (Ha-B2 =13.1% and Ha-K1 =12.5%). Well Ha-I1 has the highest effective porosity of 19.1% followed by well Ha-A1 with an effective porosity of 16.2%. In general, the effective porosity trend varies within the Valanginian section which can be classified as a poor to good porosity formation. The average water saturation within the net pay sand of the formation for well Ha-I1 is 61.4% and for well Ha-K1 it is 55.5%. These values are higher compared with well Ha-B2 of 49.3% and Ha-A1 of 35.0% respectively for lower water saturation within the formation. The average volumes of clay within the net pay sand of the intervals are, 24.0% for well Ha-A1, 20.6% for well Ha-B2, 14% for well Ha-I1, and 10% for well Ha-K1. These values validated that the evaluated reservoirs within the Valanginian section are shaly-sand reservoirs. (The volume of clay/shale between 0 and 35 suggests that the formation contains shaly-sand, (Jensen, *et al.*, 2013).

The table 7.12 below illustrates the qualitative evaluation of porosity as adapted from Rider, (1986), which was used to classify the average effective porosity of the Valanginian section.

Table 7. 12: Qualitative evaluation of porosity Adapted from Rider, (1986),

Percentage porosity %	Qualitative description
0 - 5	Negligible
5 - 10	Poor
15 – 20	Good
20 – 30	Very Good
>30	Excellent

7.6 Conclusion

The sandstone reservoir units encountered in the Valanginian sections from the five wells of the Gamtoos Basin have been evaluated in this study, within the limited amount of data available from the well logs. Due to availability of insufficient data, necessary measures involved in the petrophysical evaluation were applied during the work flow and interpretation to arrive at the presented result.

Wells Ha-B2, Ha-G1, Ha-K1, Ha-I1 and Ha-A1 are the main target in the evaluated field. The Gamma ray logs were utilized for the identification of the potential reservoirs within the drilled wells. Eleven reservoir intervals in total were identified across the five wells studied as follows; one reservoir for wells Ha-B2, Ha-K1 and Ha-A1, at 2393.45 m – 2405.94 m, 3141.78 m – 3151.99 m and 1806.25 m – 1846.33 m respectively. Three reservoirs for well Ha-G1 as follows 1537.53 m – 1552.31 m, 1669.81 m – 1684.4 m, 1692.37 m – 1706.24 m and five reservoirs for well Ha-I at 1705.9 m – 1734.24 m, 1768.38 m – 1801.45 m, 1838.94 m – 1868.05 m, and 2122.5 m – 2146.49 m respectively.

Drilled wells Ha-B2, Ha-K1and Ha-A1 of the Valanginian section contain more shaly intervals with shallow sandstone reservoir units, thus lack an extensive reservoir within the formation. Fair to good potential sandstone reservoir depths with an intercalated shale formation were encountered in drilled wells Ha-G1 and Ha-I1 of the Valanginian section in the study area.

The conventional core analysis results considered vital for calibration of the non-cored intervals for the wells Ha-G1, Ha-B2 and Ha-K1, were discussed. The conventional core data were used to calibrate with model log of porosity, water saturation and permeability in order to determine good, calculated effective porosity, as well as permeability and water saturation of

the formation. The average core porosity and permeability from the cored wells ranges from 4% to 10% with an average of 5% and 0.08 mD, 0.05mD, and 0.09mD respectively.

Based on the formation evaluation of the Valanginian section from the wireline logs analysis, most of the reservoir encountered in the wells such as Ha-B2, Ha-K1 and Ha-G1 indicates presence of gas.

The porosity, water saturation and volume of clay were calculated within the pay sand intervals of producing wells. The average effective porosity within the pay sand intervals varies within the sections such as 12.5% , 13.1%, 15.2% and 16.2% for wells HA-K1, Ha-B2,Ha-I1 and Ha-A1 respectively suggesting poor to good effective porosity for the formation as classified by Rider,(1986). The formation pore spaces have insufficient space to accommodate fluids. Well Ha-G1 shows no pay sand interval so, the well is classified as a non-producing well in the formation. The average water saturation values obtained within the pay sand interval of the wells are 49.3%, 55.5%, 35.9% and 59.2% for wells Ha-B2, Ha-K1, Ha-A1 and Ha-I1 respectively. The volumes of clay for the pay sand intervals are 20.6%, 10.0%, 24.0%, and 15.1% for wells Ha-B2, Ha-K1, Ha-A1 and Ha-I1 respectively. The calculated permeability values obtained for the intervals are less than 1mD (0.1mD), which suggests that the formation has poor permeability and cannot transmit fluids.

CHAPTER EIGHT

8. Static Reservoir Modeling of the Valanginian Depositional Sequence, Gamtoos Basin, Offshore South Africa

ABSTRACT

The understanding of uncertainties entailed in reservoir modeling is a crucial tool to support decision making in the petroleum industry. Reservoir modeling is an effective technique that plays a major role in assisting reservoir management for any decision related with development and production of hydrocarbon reserves, which must be taken into consideration with regards to the uncertainties of the formation involved. This part of the study focuses on formation evaluation of reservoir heterogeneity using 2D-seismic data objectively to generate 3D static models of the reservoir. This technique is useful for a better understanding of the spatial distribution of discrete and continuous reservoir properties such as porosity, permeability and water saturation, of Valanginian section encountered in the Gamtoos Basin, offshore South Africa. The Petrel Software 2014® work station was used to achieve this.

The methodology was built on integration of 2D-seismic data, well log data of six wells obtained from geological, geophysical and petrophysical interpretations were used to characterize and provide an accurate description of the internal architecture and visualization of the reservoir heterogeneity of the Valanginian section. These data are used to construct a 3D-view of lithofacies, porosity, permeability and water saturation model parameters that describe the reservoir, and provide effective information of the hydrocarbon heterogeneity of the reservoir rock of Valanginian section.

The lithofacies architecture is simulated using the Sequential Indicator Simulation (SIS) algorithm to control the model distribution of petrophysical properties (porosity, permeability and water saturation) of the reservoir since they are closely related. In addition, the petrophysical parameters are simulated using the Sequential Gaussian Simulation (SGS) algorithm. The reservoir structural model shows no prominent faults around the well location of the study area except small minor listric faults striking north-south.

Statistical analysis model of the porosity and permeability model for Valanginian section indicates porosity and permeability that are mainly concentrated between 0.08% - 0.19% from the north to the south i.e. in the northern and southern part the porosity distribution ranges between 0.16% - 0.19% (i.e. 16% - 19%), 0.08% - 0.12% (i.e. 8% - 12%). The permeability

ranges from 0.1mD to 1.0 mD for the entire succession. With an average porosity of 14.0%; and mean permeability of <0.1mD, a fair porosity value and poor permeability of the reservoir rock formation are evident. The water saturation strengthens between 0.30% and 0.45% (30% to 45%) which is indicative of presence of hydrocarbon. These estimation values were used to quantify the geological reserves of hydrocarbon bearing reservoir rock of the Valanginian section.

The reservoir model revealed that the Valanginian section is a hydrocarbon bearing reservoir rock with Petrophysical properties of the reservoir rock formation in the northern part showing fair-to-good porosity and poor permeability with pore spaces to be capable to accommodate fluids but with bad connectivity to transmit fluids within the formation. While in the southern part, the model indicates poor to fair porosity and poor permeability which has no substantial capacity pore space, and lacks the ability to transmit fluids.

This study has revealed the effectiveness of 3D reservoir modeling as a tool for suitable understanding of the spatial distribution of the discrete and continuous petrophysical properties in the study area. A geological model has been created to enhance the reservoir management of the formation, as well as a framework for future performance and production behaviour of the Valanginian section.

Keywords: **3D-Reservoir Modeling; Basin ; Heterogeneity; Porosity; Permeability; Water- saturation; Hydrocarbon; Petrophysical; Valanginian section.**

8.1 An Introductory to Static Reservoir Modeling

The request for oil products has placed huge pressure on the search for hydrocarbons with development of technologies to evaluate the certainty of hydrocarbons thus reducing the risks associated with it. Many countries depend on the economic value of oil and its products. Therefore, it is essential to build up a model of the reservoir as accurately as possible in order to calculate the reserves and to determine the most up-to-date way of recovering as much as possible of the petroleum economically. Moreover, it also allows 3D visualization of the subsurface that could improve understanding of reservoir heterogeneity and supports oil recovery enhancement. To build this model, an investigation into the data integrity was carried out, specifically the reservoir with its formation host rock. In order to understand the reservoir heterogeneity of the selected wells studied and to drill the target of the sequence in the Gamtoos Basin, 2D-seismic data interpretation integrated with wire log data and well data were used to build a 3D reservoir model that revealed the reservoir heterogeneity of the Valanginian section and the reliability of the data. However, reservoir volumetric calculation was not part of the objective and scope of this study.

8.2 Analysis of the Static Reservoir Modeling Approach

8.2.1 Analysis of the Reservoir Modeling

In assessing the requirements of a dynamic simulation process and to attain final well and production behaviour, it was important to build a reservoir model that characterized as closely as possible the sub-surface reality of J1 horizon on the top Valanginian Sequence which has been encountered throughout the wells. The model of the J1horizon was built by integrating relevant sub-surface data and their interpretation and is presented in the following sections. The structural interpretation from seismic data, lithological descriptions and facies interpretation, porosity, permeability and water saturation from log analyses were used to build the reservoir model. The Petrel 2014® software suite was used to build the reservoir model. The structural- and properties model of the reservoir are described as follows.

8.2.2 Structural Modeling Analysis

The structural model of the Valanginian section was based on seismic interpretation data. The input data consist of fault polygons and the interpreted fault surfaces. Fault modeling was the first steps in building the structural models in the Petrel work flow tool. This process was used to create a structural and geometrical fault interpretation within the Valanginian section and passing through a Pillar grid to generate a 3-D structural frame work. Most of the faults

mapped on seismic section data of the Valanginian sections are minor listric fault which are of no significance to the model. Making Zones was the next process in defining the vertical resolution of the 3D grid, thus each zone was created from each of the horizons mapped from the seismic data. The areal dimension of the grid cells' increment was optimized at 50m x 50 m and the 3D model contains a total number of grid cells 1034586 cells (nI x nJ x nGridLayer, 207 x 238 x 21) blocks.

8.2.3 Analysis of the Property Modeling

8.2.3.1 Facies Model Analysis

The geological facies modeling is part of the property modeling carried out for the Valanginian section of the studied area. This is an important aspect of modeling which helps to simulate the sand bodies within the formation. The Valanginian section consists of sandstone, silt and shale lithology. The lithofacies within this section were defined and calculated using Pythons® script codes; the method of "most of" was used to average the facies. The Sequential Indicator Simulation method using Kriging indicator was utilized to simulate the sand bodies in the formation. And the fraction of the sand, silt and shale content were 43.18%, 42.02% and 14.79% respectively. This is the stochastic method that combines variogram and target volume fractions, as well as an appropriate value for the smallest well data sets, when the shape of a specific facies bodies is uncertain. This enables easy modeling of a facies environment where facies volume varies vertically, laterally or both.

8.2.4 Analysis of the Petrophysical Modeling

8.2.4.1 Porosity model Analysis

The porosity is a vital property of a hydrocarbon reservoir as it determines the volume of oil present in reservoir. The porosity model of the Valanginian section was based on the effective porosity logs model (PhiNeu) generated from the Petrophysical interpretation results for well log data of the selected wells studied. The well logs were upscaled by using arithmetic averaging methods, and the porosity was distributed in the model by using a Sequential Gaussian Simulation (SGS) method. The data analysis tool by Petrel 2014® runs the variogram calculation and data transformation. This porosity attribute in the model is controlled by the distribution of the lithofacies present in the reservoir. The porosity distribution was generally concentrated between 0.08% - 0.19% populated across the Valanginian section as displayed in Figure 8.1 below.

8.2.4.2 Permeability model Analysis

Permeability is an important characteristic in Petroleum reservoir rocks. It is the property of the porous medium that measures the capacity and ability of the formation to transmit fluids. It is a significant rock property due to its ability to control the directional movement and fluid flow rate in the reservoir. The permeability model was also generated for the Valanginian section of the study area. The permeability log (K) calculated results from the Petrophysical interpretation of the selected wells data studies was exported in LAS format from the IP® software and imported and subsequently loaded in the Petrel 2014® software workstation. The Stochastic simulation algorithm method by means of the Sequential Gaussian simulation (SGS) method was geostatistically applied in assigning the specific properties. The calculated permeability log (K) was upscaled by means of the geometric mean method, as the spatial correlation in the reservoir is log normally distributed and sensitive to lower values. The permeability model for the Valanginian section mainly concentrated between 0.1000mD to 1.000mD. The permeability model of the Valanginian section is shown in Figure 8.2 below.

8.2.4.3 Water Saturation model Analysis

Saturation is defined as the fraction of oil, water and gas obtained in a given pore space and it is expressed as a volume/volume percent of saturation units. Typical saturation analysis does not indicate 100% fluid saturation because of the volume expansion and fluid loss connected with bringing out a subsurface core of typically higher temperature and pressure to the surface with lower temperature and pressure. To determine the quality of hydrocarbon accumulation in a porous rock formation, it is required to define the fluid saturation (oil, water, gas) of the rock material. Thus, the water saturation distribution model was built for the Valanginian section of the study area to identify the potential high water area across the formation. The result of well log data Sw-Indonesian (SwInd log) for the water saturation model derived from the Petrophysical interpretation of the selected studied wells' log data, was upscaled by using an arithmetic averaging method and a model using the Stochastic simulation algorithm method via the Sequential Gaussian simulation (SGS) method, on a Petrel 2014® software workstation.

8.3 Analysis and Interpretation Results of the Static Reservoir Modeling of Valanginian Section of the Gamtoos Basin

Property modeling is the technique of filling the grid cells with petrophysical properties and the geological facies. Thus, the importance of this modeling is to distribute properties between the wells such that it logically preserves the reservoir heterogeneity and matches the well data. The processes are then reliant on the geometry of the existing grid. When interpolating between data points, Petrel® software will propagate property values along the grid layers. Therefore, in this study, the geological model-facies were defined by using a 'weighted nearest neighbour' algorithm; next, the facies model was built with Sequential Indicator Simulation(SIS); we populated the geological model with petrophysical parameters and Sequential Gaussian Simulation (SGS) was used to populate grid cells with porosity, permeability and water saturation values. This method was adopted based on these properties, as continuous variables data were available.

8.3.1 Interpretation and Discussion of the Porosity Model

The formation porosity map model generated and populated for the Valanginian section of the studied area, indicated poor to good porosity distribution across the wells located within the section. It was mainly concentrated between 0.08% - 0.19% (i.e. 8% - 19%) across the section. In the northern part of the study area (Figure 8.1), the porosity distribution shows a good porosity range between 0.16% - 0.19% (i.e. 16% - 19%), within the well area (Ha-I1, Ha-G1and Ha-N1). This suggests that the pore space within this reservoir section has the capacity to accommodate fluids. However, in the Southern portion of the Valanginian section of the study area, the porosity distribution indicates a poor to fair porosity, concentrated between 0.08% - 0.12% (i.e. 8% - 12%), within the well areas (Ha-B2, Ha-K1 and Ha-A1) (Figure 8.1), suggests that reservoir rock within in this section area has no substantial capacity pore space to accumulate fluids. Conversely according to Levorsen, (1967), based on the entire average porosity value of 14% within the Valanginian section, the entire succession can be classified as a fair reservoir rock as shown in Table 8.1. Figure 8.1 illustrates the 3D view grid cells upscaled porosity model distribution across the formation of the study area.

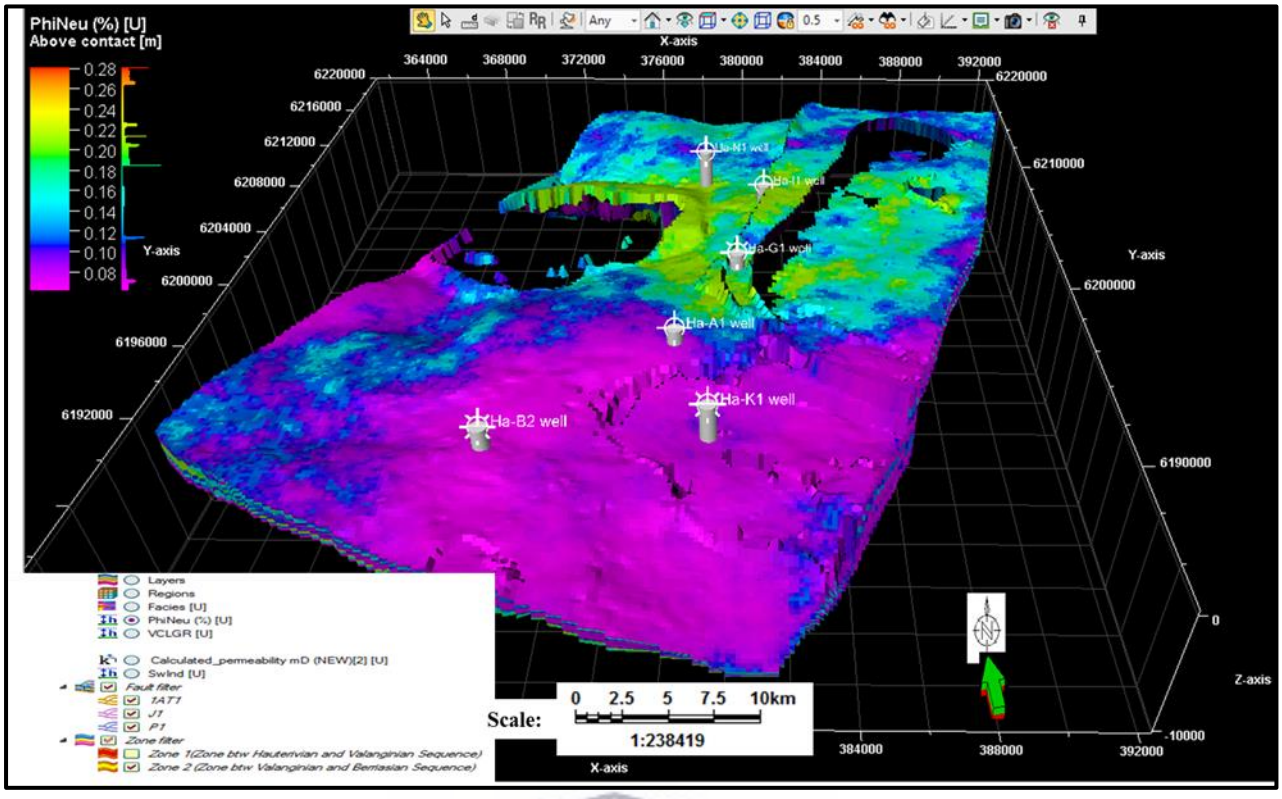

Figure 8. 1: 3D perspective view of upscale porosity model distribution in Valanginian section across the study area.

Table 8.1, Qualitative evaluation of porosity modified after Loveren, (1967)

Percentage porosity % (Effective porosity, (Φe, %)	Qualitative description
0 - 5	Negligible
5 - 10	Poor reservoir rock
10 – 15	Fair reservoir rock (general)
15 – 20	Good reservoir rock
20 – 25	Very good reservoir rock.

8.3.2 Interpretation and Discussion of the Permeability Model

The 3D perspective view of the grid cells upscaled permeability model for the Valanginian section of the study area underscores a permeability that is concentrated mainly between 0.1000 mD to 1.000 mD, as shown in Figure 8.2, within the well areas of the section. With the average of permeability less than 1.0 mD in the entire reservoir rock section, the value indicates a poor reservoir permeability which is a reflection of poor connectivity of pore space in the reservoir sand and an inability to transmit fluids within the section. According to Levorsen, (1967), this shows that based on permeability characteristic as shown in Table 8.2, the Valanginian section is a poor reservoir rock unit that cannot transmit fluids. Figure 8.2

illustrates the 3D view grid cells upscaled permeability model distribution of the entire Valanginian section of the study area.

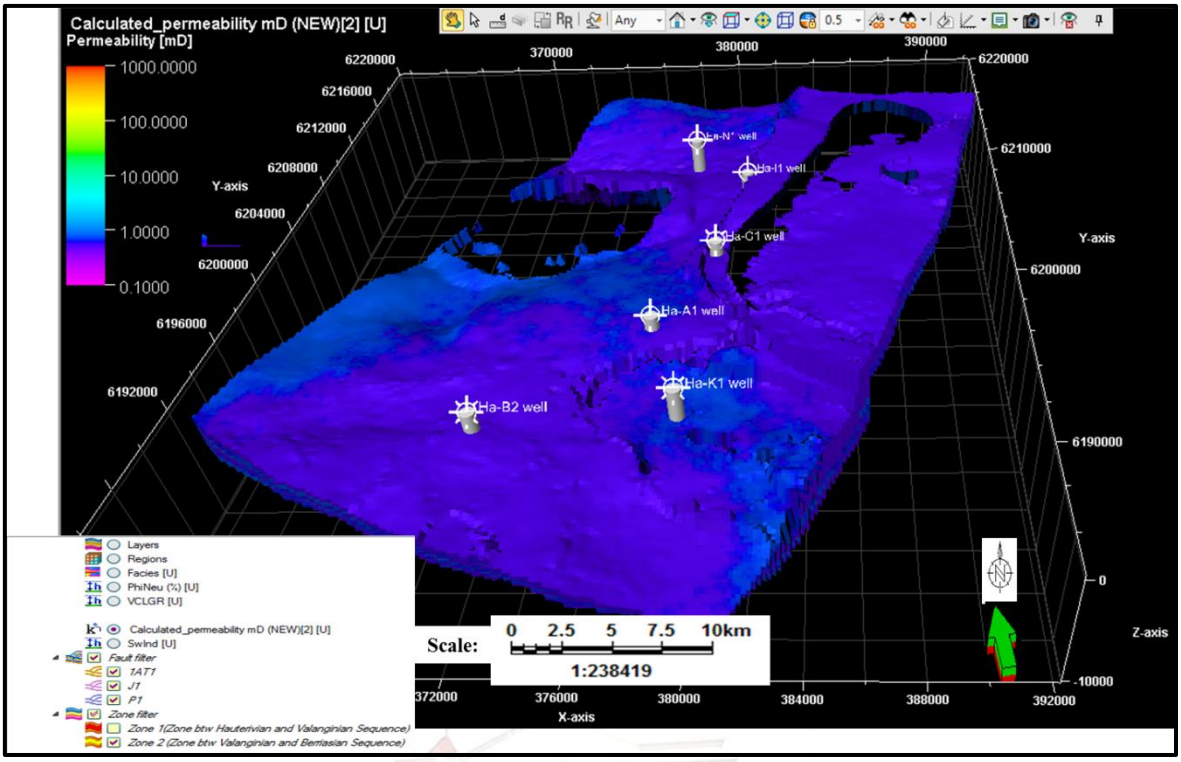

Figure 8. 2: 3D perspective view of the upscaled permeability model distribution in Valanginian section across the study area.

Table 8.2. Qualitative evaluation of permeability. Modified after Levorsen, (1967).

Permeability values (mD)	**Qualitative Description**
Less than 10.5	Poor to Fair
Between 15 and 50	Moderate
Between 50 and 250	Good
Between 250 and1000	Very good
> 1000	Excellent.

8.3.3 Interpretation and Discussion of the Water saturation model.

The water saturation cut-off results derived from the petrophysical interpretation was used to determine the hydrocarbon bearing zones (pay) and water bearing zones (wet) in the interval for the formation evaluation of the Valanginian section was 66%. The intervals with water saturation of 66% or below were believed to be hydrocarbon bearing zones while the intervals with water saturation greater than this value were considered as wet or non- productive water bearing interval (as illustrated in the previous chapter's Figure 7.44 above). The 3D perspective view of the water saturation model for the Valanginian section reveals that water saturation

distribution within the wells Ha-N1,Ha-I1, Ha-G1, Ha-A1, Ha-K1 and Ha-B2 of the entire Valanginian section from the north to the south part of the study area varies from 0.30 to 0.45 (30% to 45%) (Figure 8.3).This is indicative of a hydrocarbon bearing reservoir, suggesting that the Valanginian section is to be regarded as a hydrocarbon bearing reservoir rock.

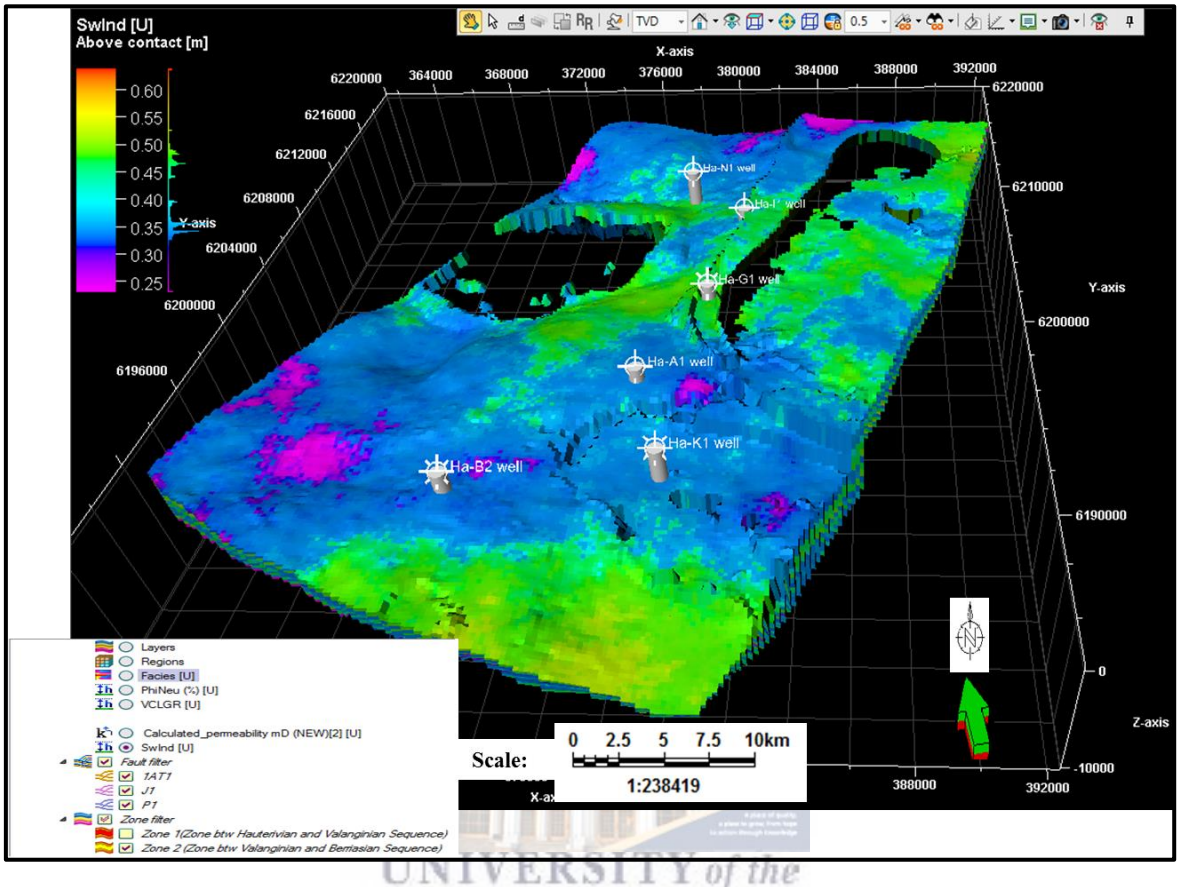

Figure 8. 3: 3D perspective view of upscaled water saturation model distribution in Valanginian section across the study area.

8.3.4 Interpretation and Discussion of the Sedimentological Lithofacies model

The 3D- facies model for the Valanginian section of the study area is shown in Figure 8.4. The model shows that the dominant facies is shale, with a small proportion of silt and even less sand facies with the presence of an erosional surface in the northern part of the Valanginian section. However, in the central part of the studied area the proportion of sand facies becomes dominant towards the east with small amounts of intercalated shale and silt facies. In the western part and towards the southern part of the section a dominant shale facies with a fraction of sand facies and minor intercalated silt facies is present. In general, the distributions of the facies model of the Valanginian section of the study area clearly indicate an abundance of shale facies compared to sand and silt. Geologically the eastern part shows a well

distributed of sand facies where a potential reservoir can be encountered within the formation. The western to the southern parts of the area are dominated by shale and sand facies; potential reservoirs with a good seal or cap rock (shale) could thus also be encountered there, which is good for any reservoir rock with hydrocarbon accumulation as it can prevent against reservoir spill points during the hydrocarbon migration in the reservoir. Figure 8.4 illustrates the 3D view upscaled Lithofacies model distribution in Valanginian section the study area.

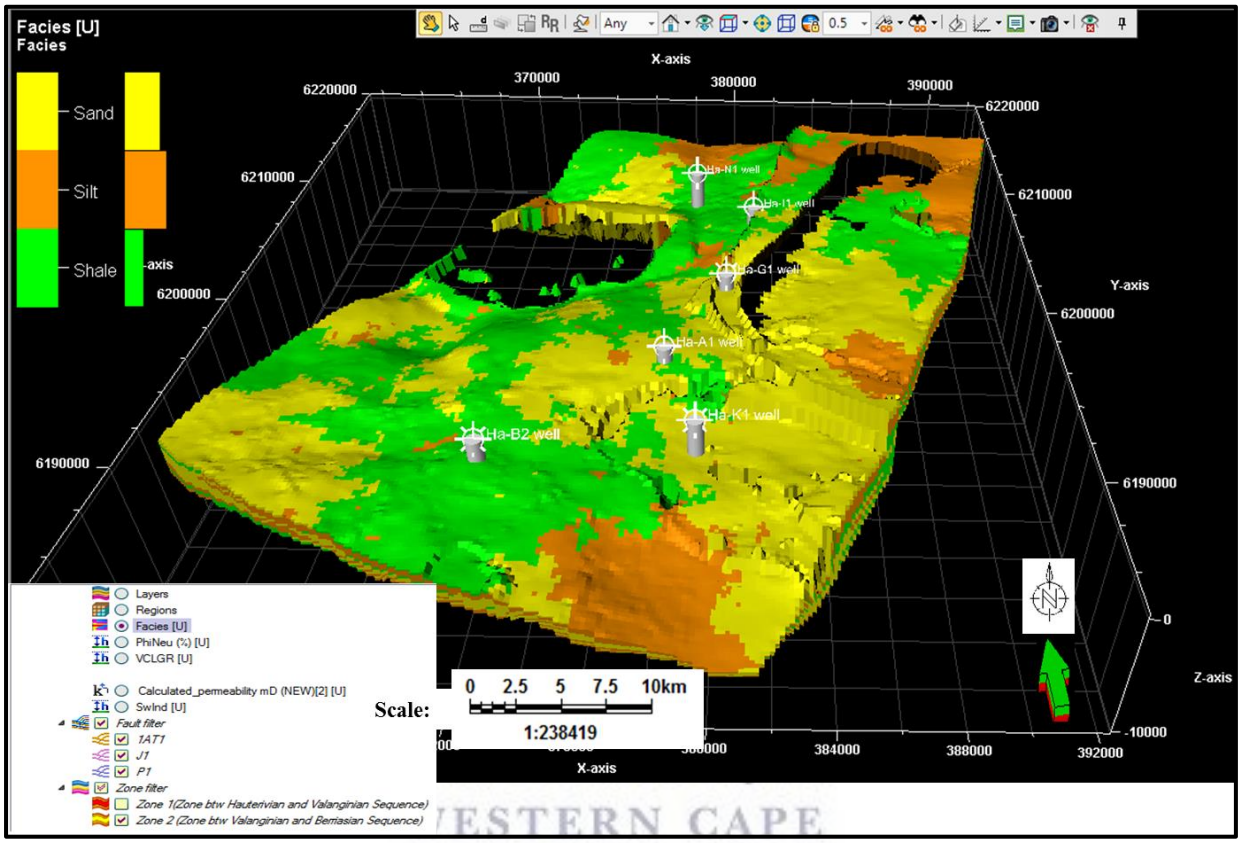

Figure 8. 4: 3D perspective view upscaled Lithofacies model distribution in Valanginian section across the study area.

Thus, in the Valanginian section of the study area, poor argillaceous facies (shale) are more dominant than the good arenaceous facies (sand). Therefore, considering potential reservoir rock within the section this shows an indication of increased shale lithology, suggesting that the Valanginian section is not a good reservoir section.

8.3.5 Structural model Interpretation

The structural model has been discussed in the depth-structure map interpretation provided in chapter five of this thesis.

8.4 Conclusion

The present research shows the usefulness of integrating seismic and well log data for reservoir modeling. The results of the comprehensive petrophysical analysis of the wells studied show the quality of the reservoirs across the wells in the succession at different depth intervals. The Valanginian reservoir shows a variation in porosity from poor to good from the south to the north respectively and poor permeability values throughout the area. The study also suggests a hydrocarbon bearing reservoir rock based on the evaluation of the water saturation. The discrete properties facilitated an understanding of the facies properties of the Valanginian section while the continuous properties gave the petrophysical characteristics of the section in terms of porosity, permeability and water saturation. This analysis will therefore assist to control the reservoir during development.

The modeling of the Valanginian reservoir has provided an improved understanding of the spatial distribution of the discrete and continuous properties in the section. The study has developed a geological model for the Valanginian section that can be updated as new data are acquired for further subsequent development. The model can also be exported for simulation to be run for future development of the reservoir.

The study area indicates the presence of hydrocarbon bearing reservoir rock. The petrophysical properties (porosity, permeability and water saturation) that control the hydrocarbon movement within the sedimentary section were modelled. The modelled results based on porosity, permeability and water saturation indicates that the southern part is an area of poor to fair porosity, while the northern area shows a good porosity. However, permeability of both the areas are poor. The entire succession indicates presence of a hydrocarbon bearing reservoir in term of water saturation evaluation. This study shows highest and lowest porosity values of 19% and 0.08% respectively, permeability values of 0.1mD (< 1.0 mD) and highest and lowest water saturation values of 0.30 to 0.45 (30% to 45%).

CHAPTER NINE

9. Conclusion and Recommendation

9.1 Introduction

The Early Cretaceous Valanginian reservoir section of the Gamtoos Basin, offshore South Africa was investigated from the study of six exploratory wells using integrated approach comprising of seismic evidences (stratigraphy based on seismic sequence and seismic facies), formation evaluation (Petrophysics), static modeling and biostratigraphy. The present work interprets the detailed results obtained from 2D-seismic data and its integration with well log data and information from foraminiferal biostratigraphy for a better understanding of the evolution of the reservoir sequence, depositional environment and assessment of geologic time, as well hydrocarbon potential for the Valanginian reservoir succession. It is concluded that the integration of these methods has proven to be suitable to meet the aim of this study as stated above.

9.2 Conclusion

The seismic stratigraphy based on seismic sequence and seismic facies analysis studies in the area under Gamtoos Basin from the north to the south revealed four major seismic reflection termination patterns namely downlap, onlap, toplap and erosional truncation within the Valanginian sequence. The overall depositional environments were concluded to range between fluvial, channel-fill, shallow marine, submarine canyon to deep marine parts of the continental shelf, submarine fan lobe and basin floor to deep marine environments.

The seismic facies analysis used four seismic reflection attributes namely amplitude, continuity, frequency and the external geometry reflection. A wide range of reflection patterns has been encountered: moderate-to-low, low-to-moderate, high-to-moderate, disrupted-to-discontinuous, continuous-to-discontinuous, continuous-to-semicontinuous, subparallel-hummocky clinoform, parallel-to-subparallel-to-hummocky clinoform, wedge-like-to-mounded geometry, wedge-like form, sheet-to-wedge geometry, medium-to-high frequency reflection, low frequency and high-to-low frequency reflection respectively. The depositional environments range between delta, submarine fan, shallow to deep marine, basin floor fan, basin floor shelf delta respectively.

The integrated calibrated well log signatures interpretations from Gamma Ray also indicate a wide variety of depositional environments such as: channel-fill, submarine canyon–fill, braided

fluvial and deltaic, fluvial flooding plain, storm dominated shelf and distal deep marine slope environments. These all are different areas of a shallow marine to deep marine depositional environment in the northern part of the study area. While in the southern part of the study area the study has demonstrated the presence of fluvial point bar, tidal point bar, deep tidal channel-fill, shallow marine, submarine channel to deep marine depositional environments, which all together indicate a transgressive system tract.

The depositional system pattern indicates aggradational stacking, aggradational & progradational-retrograding stacking patterns in the study area. Litho-facies modelling indicates the presence of a turbidity channel depositional environment within the study area, with marine flooding of high energy density turbidites from northeast to southeast. This led to massive sandstone-dominant deposits with intermittent siltstone and minor intercalated shale deposits. In the Northwest to Southern parts, massive silt-dominant and shale deposits of low energy with intermittent sandstone lithofacies turbidites channel depositional environments have been encountered.

The biostratigraphic analysis of the study area was carried out on unwashed cutting sample from the two representative wells namely; Ha-G1 and Ha-I1 from the north to the south respectively. The studied depth intervals for the two wells are 1265.0 – 1670.0m and 1410.0 – 2380.0m respectively for which samples were available. The lithology of the wells comprises mainly of grey shales and siltstones with intermittent sandstone bands. The biostratigraphic work reveals a close similarity in foraminiferal composition of the two wells in the Valanginian succession. This was compared with the biostratigraphic information available from nearby areas, DSDP / OSD data and information available from other areas across the globe for Valanginian stage. The benthic assemblage confirms Valanginian age for the studied sections. Paleo-ecological studies of benthic foraminifera suggest that the sediments were deposited in deep marine areas (uppermost bathyal to upper bathyal conditions) with a bathymetry fluctuating between 300m to 500m during this period.

The well log signatures from the selected five wells were studied to understand the heterogeneity of reservoir belonging to the Valanginian section. The log signatures indicate good borehole conditions. The wireline log interpretation based on gamma ray, resistivity, density, caliper log and neutron-porosity spikes and shapes gives a clear indication of the reservoir zone and thick shale layers within the shallow-to deep marine sandstone. The porosity and permeability cut-off determination was applied on the eleven sandstone reservoir intervals studied from the wells to differentiate between the pay and non-pay interval sand. By means of

poro-perm plots based on conventional value of 0.1mD for the gas reservoir sandstone, based on input from conventional core analysis data (poro-perm data) indicate gas reservoir. The result shows presence of tight heterogeneous reservoir with seven of the sandstone intervals which are proved to be hydrocarbon producing with lower water saturation of fair-to-good effective porosity and a formation of poor permeability that has no ability to transmit fluids.

The 3D static reservoir model created for the understanding of the lithofacies and spatial distributions of the discrete and continuous petrophysical properties revealed the effectiveness of the reservoir modeling technology as a tool for understanding any uncertainties affecting decision making in the petroleum industry. The lithofacies architecture simulated using the Sequential Indicator Simulation (SIS) algorithm to control the model distribution of petrophysical properties: porosity, permeability and water saturation were simulated using the Sequential Gaussian Simulation (SGS) algorithm.

Statistics revealed that effective porosity and permeability of the reservoir in Valanginian section mainly concentrated between 0.08% - 0.19% and permeability ranges from 0.1mD to 1.0 mD (an average porosity of 14.0%; and mean permeability of < 0.1mD) from the north to the south across the study area. The water saturation ranges between 0.30% and 0.45% (30% to 45%) indicative of hydrocarbon bearing intervals based on cut-off value for the study area.

In the northern part of the area the sand reservoirs within the Valanginian section, the model indicates fair-to-good effective porosity and poor permeability that has pore spaces and capable to accommodate fluids but with poor connectivity to transmit fluids. While in the southern part it has been shown to have poor to fair porosity and poor permeability which has no substantial capacity pore spaces, not enough space to accumulate fluids and a lack of ability to transmit fluids.

The 2D-seismic reflection profile interpretation reveals faulted Valanginian shallow marine sandstones beneath the drift-onset 1At1 and J1 unconformities. The evolution of the Valanginian sequence is controlled by extensional events due to a series of interpreted listric normal faults and rifting created graben possibly by the opening of the Atlantic during the breakup of Gondwana in the late Jurassic/early Cretaceous. The Valanginian sequence shares some characteristics with volcanic arc sequences and erosional surfaces. This comprises in situ hemipelagic clastic sediments that are supplied from the continent transporting along the channel by turbidity current. The Valanginian sequence is well-defined structurally at the level of the regional drift-onset unconformity 1At1 and J1 with a structural trap classification for most of the interpreted profiles.

9.3 Main Scientific Contributions of the Thesis

The paucity of the knowledge and information about the Valanginian succession particularly regarding the depositional environment, geological age as well as the nature of the heterogeneity of the reservoir sandstone within the Gamtoos Basin necessitated the integration of seismic sequence and seismic facies, biostratigraphic analysis , petrophysical evaluation and static modeling techniques. No scholarly work has been carried out or published till date on this basin based on these integrated studies. This dissertation makes a scientific contribution that addresses this gap, information and knowledge about the depositional environments and the reservoir potential and quality within the Valanginian sequence.

This thesis has demonstrated detailed information about seismic stratigraphy based on seismic sequence and seismic facies and its dependability in deducing depositional environments. It also provided least geologic observation based on biostratigraphic studies by means of micro faunas fossils groups in the basin to infer the geologic age and time and possible depositional environments. It also revealed the quality of reservoirs heterogeneity of the Valanginian sequence for its hydrocarbon potential based on fair-to-good effective porosity and poor permeability. This suggests that the interval reservoirs have well developed porosity which accommodate fluids but, with poor connectivity that lacks capacity to transmit fluids. From the study it is possible to ascertain that it is a hydrocarbon bearing succession. The application of the static reservoir modeling in this basin based on stochastic methods illustrates recent techniques are useful for better understanding the heterogeneity of reservoir management in hydrocarbon production capacities. It thus gives a clear observation and spatial distribution of the petrophysical and lithofacies properties of the reservoir characterization of the Valanginian sequence in Gamtoos Basin.

The economic significance of this dissertation has been established based on the prospective potential for hydrocarbon capacity production in the study area, given crucial attentions to the highlighted points in this dissertation. This will enable the concerned oil and gas companies to design suitable production platform or methods for optimum oil and gas recovery that will enhance the economic growth of the region and the environs globally.

9.4 Recommendations

This study recommends that deep-water reservoirs and regional petrophysical evaluation of Lower Cretaceous (Berriasian) sequences should be studied and targeted for hydrocarbon exploration in the Gamtoos Basin to delineate oil and gas plays in the study area, because potential reservoirs zones encountered in this sequence are more pronounced based on the conventional electric well log such as gamma-ray, resistivity, neutron and density logs across the sequence.

Therefore, I strongly recommend that the diagenetic effect and its impact on the reservoir quality of the Valanginian sequence should be studied in detail as a result of its poor permeability encountered in the sequence based on the petrophysical evaluation studied in this work. To, ascertain the presence of clay minerals in the pore space and related diagenetic changes that effected reservoir quality within the Valanginian sequence in the study area.

This study also recommends that image log should be utilized in future wells to optimize interpretation not only depositional environments interpretation but also for structural analysis. This includes fracture analysis that can aid in improving understanding of the conventional reservoir in terms of planning an effective hydraulic fracturing, as well necessary for maximising the modeling reservoirs producibility.

Recommendation of 3D seismic acquisition in the entire study area of Gamtoos Basin is appropriate to enhance adequate clarity in understanding the difficulties and different deceptive structures during the 2D interpretation. Also enhancing the reservoir modeling for both structural and prospect play interpretation for hydrocarbon exploration.

I also recommend that the geological 3D perspective view of the spatial distribution of the discrete and continuous petrophysical properties and facies models built for the Valanginian sequence should be updated, as and when new data are acquired for the area developments. These models could be reassigned to reservoir engineers for better characterization during simulation that will enhance the reservoirs productions encountered in the sequence in futures. In addition, horizontal wells should be drilled in the study area to enhance optimization of the reservoirs in the Valanginian sequence.

9.5 Conference Contributions Presentation Authored From the PhD. Study

Ayodele, O.L, Chatterjee, T.K, van Bever Donker, J.M., (2018). Seismic Sequence and Seismic Facies Analysis of the Early Cretaceous (Valanginian) depositional sequence Gamtoos Basin, offshore South Africa. National Association of Black Geoscientist (NABG), 37th Annual Conference, Houston, Texas, USA, September, 2018.

Ayodele, O.L, Chatterjee, T.K, van Bever Donker, J.M., (2018). Static Reservoir Modeling of the Valanginian Depositional Sequence of Gamtoos Basin, offshore South Africa. AAPG International Conference and Exhibition, Cape Town, South Africa, November, 2018.

Publish; Search and Discovery Article #11180, January 14 (2019) ** AAPG Data pages, Inc. http://www.searchanddiscovery.com/pdfz/documents/2019/11180ayodele/ndx_ayodele.pdf.html

References

Abrahamsen, P., Omre, H. and Lia, O., 1991, January. Stochastic models for seismic depth conversion of geological horizons. In Offshore Europe. Society of Petroleum Engineers. (SPE 23138).

Adeoti, L., Onyekachi, N., Olatinsu, O., Fatoba, J. and Bello, M., 2014. Static reservoir modeling using well log and 3-D seismic data in a KN field, offshore Niger Delta, Nigeria. International Journal of Geosciences, 5(01), p.93.

Alasm, D., 2012. Stratigraphy based on the fossil occurrence: Linked. [Online] Available at: https://www.slideshare.net/daengaslam/biostratigraphy-geologist [Accessed 18 July 2016].

Allen, G. P. & Posamentier, H. W., 1993. Sequence stratigraphy and facies model of an incised valley fill:The Gironde estuary, France. Journal of Sedimentary Petrology, 63 (3), pp. 378 - 391.

AlRuwaili, S.B. and AlWaheed, H.H., 2004, January. Improved petrophysical methods and techniques for shaly sands evaluation. In SPE Annual Technical Conference and Exhibition. Society of Petroleum Engineers.

Andreoli, M.A.G., Doucoure, M., Van Bever Donker, J., Brandt. D. and Andersen. N.J.B., 1996. Neotectonics of Southern Africa –a review. Africa Geoscience Review, 3(1), pp. 1-16.

Asquith, G.B., Krygowski, D. and Gibson, C.R., 2004. Basic well log analysis 16. Tulsa: American Association of Petroleum Geologists.

Atlas, D., 1979. Log Interpretation Charts: Houston, Texas, Dresser Industries.

Aveili, J.Q., 2016. Sarvak Formation Reservoir Modeling, in Oilfield Kuhmond (Southwestern Iran). Open Journal of Geology, 6(11), p.1361.

Badley, M.E., 1985. Practical seismic interpretation.

Bartenstein, H., 1974. Upper Jurassic-Lower Cretaceous primitive arenaceous foraminifera from DSDP sites 259 and 261, eastern Indian Ocean. Initial Reports of the Deep Sea Drilling Project, 27, pp.683-695. Washington D.C., US Government Printing Office.

Bassiouni, Z., 1994. Theory, measurement, and interpretation of well logs (Vol. 4). Henry L. Doherty Memorial Fund of AIME, Society of Petroleum Engineers.

Bateman, R.M., 1985. Openhole log analysis and formation analysis.

Ben-Avraham, Z., Hartnady, C.J.H. and Malan, J.A., 1993. Early tectonic extension between the Agulhas Bank and the Falkland Plateau due to the rotation of the Lafonia microplate. Earth and Planetary Science Letters, 117(1-2), pp.43-58.

Bohling, G., 2005. Stochstic Simulation and Reservation Modeling Workflow In: Deutsch, C.V. 2002, Geostatistical Reservoir Modeling. Kansas, Oxford University Press.

Broad, D.S., 1989. Petroleum geology and hydrocarbon potential of the Gamtoos Basin, Soekor Report, pp 56. (Unpublished).

Broad, D. S., 1990. Petroleum geology of Gamtoos and Algoa Basins.Geological Society of South Africa., pp. 60- 63.

Broad, D.S., 2000. Petroleum exploration Offshore South Africa; Journal of Africa Earth Science, 31(1), 50 -51.

Broad, D., 2004. South Africa activities and opportunities. An unpublished power point presentation to PetroChina.

Broad, D.S., Jungslager, E.H.A., McLachlan, I.R. and Roux, J., 2006. Offshore Mesozoic Basins. The Geology of South Africa. Geological Society of South Africa, Johannesburg/Council for Geoscience, Pretoria, 553, pp.571.

Broad, D.S., and Mills, S.R., 1993. South Africa offshore exploration potential in variety of basins. Oil and Gas, 91 (49), pp.38 -44.

Brown, A.A., 1967. January. New methods of characterizing reservoir rocks by well logging. In Mexico 7th World Petroleum Congress.

Brown, L. F. (ed)., 1995. Sequence stratigratigraphy in Offshore South African Divergent Basins. An atlas on Exploration for Cretaceous Lowstand Traps by Soekor Ltd, AAPG Studies in Geology., 41, pp. 83 -137.

Bueno, J.F., Drummond, R.D., Vidal, A.C., Leite, E.P. and Sancevero, S.S., 2011. Constraining uncertainty in static reservoir modeling: A case study from Namorado Field, Brazil. AAPG Search and Discovery. Article #40755.

Catuneanu, O. W. et al., 2009. Towards the standardization of sequence stratigraphy.. [Online] Available at: https://www.sciencedirect.com/science/article/pii/S0012825208001104 [Accessed 12 July 2018].

Connolly, E.T., 1965, January. Resume and current status of the use of logs in production. In SPWLA 6th Annual Logging Symposium (Volume I). Society of Petrophysicists and Well-Log Analysts.

Cosentino, L., 2001. Integrated reservoir studies. Edition Technip.

Cosentino , L., 2003. Static Reservoir Study; Oil field characteristic and relevant studies. [Online] Available at: http://www.treccani.it/export/sites/default/Portale/sito/altre_aree/Tecnologia_e_Scienze_applicate/enciclopedia/inglese/inglese_vol_1/pag553-574ing3.pdf.
[Accessed 4th April 2018].

Dalziel, I.W., Mosher, S. and Gahagan, L.M., 2000. Laurentia-Kalahari collision and the assembly of Rodinia. The Journal of Geology, 108 (5), pp.499-513.

David, S.O., Rodolfo, S.B., Jonathan, S.O., Pasquel, O. and Arteaga, D., 2015, November. A universal equation to calculate shale volume for Shaly-sands and carbonate reservoirs. In SPE Latin American and Caribbean Petroleum Engineering Conference. Society of Petroleum Engineers.

Djebbar, T. & Donaldson, E. C., 1999. Theory and practice of measuring reservoir rock and fluid transport properties, USA: Butterworth- Heimann.

Doyen, P.M., Psaila, D.E. and Strandenes, S., 1994, January. Bayesian sequential indicator simulation of channel sands from 3-D seismic data in the Oseberg Field, Norwegian North Sea. In SPE Annual Technical Conference and Exhibition. Society of Petroleum Engineers (SPE 28382).

Dullien, F., 1979. Porous media fluid transport and pore structure, Burlington: Elsevier Science.

Duros, P., Fontanier, C., De Stigter, H.C., Cesbron, F., Metzger, E. and Jorissen, F.J., 2012. Live and dead benthic foraminiferal faunas from Whittard Canyon (NE Atlantic): Focus on taphonomic processes and paleo-environmental applications. Marine Micropaleontology, 94,

Egeland, T., Georgsen, F., Knarud, R. and Omre, H., 1993, January. Multifacies modelling of fluvial reservoirs. In SPE Annual Technical Conference and Exhibition. Society of Petroleum Engineers. pp. 863 -872.

El-Gawad, E.A., 2007. The use of well logs to determine the reservoir characteristics of Miocene rocks at the Bahar Northeast field, Gulf of Suez, Egypt. Journal of Petroleum Geology, 30(2), pp.175-188.

Emery, D. & Myers , K. J., 1996. Sequence Stratigraphy. In:.Blackwell, Oxford, p. 297.

Feng, C., Sun, M., Pu, R., Zhang, M. and Li, D., 2017. 3D Reservoir Modeling of Triassic Yanchang Formation Chang 8 Layer in Honghe36 well area, Ordos Basin, China. The Open Petroleum Engineering Journal, 10 (1), pp. 239 -250.

Fens, T. W., 2000. Petrophysical prpoperties from small rock samples using image analysis techniques, Stevinweg, Netherlands: Delft University Press.

Frewin, J., Grobbler, N. and Feddersen, J., 2000. The Oribi and Oryx oil fields: geological characterisation of a deep-marine channel-lobe system, Block 9, Bredasdorp Basin, offshore South Africa. Journalof Africa Earth Sciences, 31(1), pp.22.

Galloway, W.E., 1989. Genetic stratigraphic sequences in basin analysis I: architecture and genesis of flooding-surface bounded depositional units. AAPG bulletin, 73(2), pp.125-142.

Gingras, M.K., Baniak, G., Gordon, J., Hovikoski, J., Konhauser, K.O., La Croix, A., Lemiski, R., Mendoza, C., Pemberton, S.G., Polo, C. and Zonneveld, J.P., 2012. Porosity and permeability in bioturbated sediments. In Developments in Sedimentology (Vol. 64, pp. 837-868). Elsevier.

Giwa, G.O., Oyede, A.C. and Okosun, E.A., 2006. Advances in the application of biostratigraphy to petroleum exploration and production. Search and Discovery Article, 50029, pp.11-14.

Godwill, P.A. and Waburoko, J., 2016. Application of 3D reservoir modeling on Zao 21 oil block of zilaitun oil field. J Pet Environ Biotechnol, 7(1), p.8.

Granberry, R.J., Jenkins, R.E. and Bush, D.C., 1968, January. Grain Density Values of Cores from Some Gulf Coast Formations and Their Importance in Formation Evaluations. In SPWLA 9th Annual Logging Symposium. Society of Petrophysicists and Well-Log Analysts, pp.1-18.

Graven, G., 1986. The role of regional fuid flow in Genesis of the pine point deposit, Western Canada Sedimentary Basin.. Economic Geology , Vol 81 (4), p. 1015.

Gray, D.R., Foster, D.A., Meert, J.G., Goscombe, B.D., Armstrong, R., Trouw, R.A.J. and Passchier, C.W., 2008. A Damara orogen perspective on the assembly of southwestern Gondwana. Geological Society, London, Special Publications, 294(1), pp.257-278.

Guasti, E., Speijer, R.P., Brinkhuis, H., Smit, J. and Steurbaut, E., 2006. Paleoenvironmental change at the Danian–Selandian transition in Tunisia: Foraminifera, organic-walled dinoflagellate cyst and calcareous nannofossil records. Marine Micropaleontology, 59(3-4), pp.210-229.

Guest, K., 1990. The use of core derived quantitative mineralogical data to improve formation evaluation. In Advances in core evaluation, accuracy, and precision in reserves estimation [Reviewed proceedings of the first Society of Core Analysts European core analysis symposium, May 21-23, London, UK]: Gordon and Breach Science Publishers, New York (pp. 187-209).

Haldorsen, H.H. and Damsleth, E., 1990. Stochastic Modeling (includes associated papers 21255 and 21299). Journal of Petroleum Technology, 42(04), pp.404-412.

Hamada, G.M., 1996. An integrated approach to determine shale volume and hydrocarbon potential in shaly sand. In SCA Int. Symposium (pp. 2093-107).

Harrison , B. and Jing, X. D., 2001. Saturation height method and their impact on Volumetric Hydrocarbon in Place Estimates. New Orleans Louisiana, Socity of Petroleum Engineers SPE 71326.

Herron, S.L. and Herron, M.M., 2000, January. Application of nuclear spectroscopy logs to the derivation of formation matrix density. In SPWLA 41st Annual Logging Symposium. Society of Petrophysicists and Well-Log Analysts.

Holbourn, A.E. and Kaminski, M.A., 1995. Lower Cretaceous benthic foraminifera from DSDP Site 263: micropalaeontological constraints for the early evolution of the Indian Ocean. Marine Micropaleontology, 26 (1-4), pp.425-460.

Holden, L., Madsen, R., Skorstad, A., Jakobsen, K.A., Tjolsen, C.B. and Vik, S., 1995, January. Use of well test data in stochastic reservoir modelling. In SPE Annual Technical Conference and Exhibition. Society of Petroleum Engineers.

Hudson, M. R., 1998. Structural geology of French peak accommodation zone, Nevada. Geological Society of America Bulletin , 104, pp. 581 - 594.

Hughes, B., 2002. Introduction to wireline log analysis. Baker Atlas.

Hunt, D. and Tucker, M.E., 1992. Stranded parasequences and the forced regressive wedge systems tract: deposition during base-level fall. Sedimentary Geology, 81(1-2), pp.1-9.

Hurst, A., 1987. Problems of reservoir characterization in some North Sea sandstone reservoirs solved by the application of microscale geological data. North Sea Oil and Gas reservoirs, Graham and Trotman, 153- 167.

Jahaz, I., 1990. Core Analysis-Opportunity and Challenges in the 1990. Europe Core Analysis Symposium, 1-15pp.

James , G. S., 2018. Formular and Calculations for Drilling Operations. Second Edition ed. Hoboken, New Jersey: John Wiley (Scrivener Publishing).

Jarvis, K., 2006. Integrating well and Seismic data for Reservoir Characterization: Risks and rewards. Australia, Australia Earth Sciences Convention (ASEG) Extended Abstracts, July, 2006(1), Geological Society of Australia. pp.1-4.

Jensen, J. L., Ayers, W. B. & Blasingane, T. A., 2013. introduction to shally sand analysis, Texas: Department of Petroleum Engineering Texas A and M University .

Jones, R.W. and Wonders, A.A.H., 1992. Benthic foraminifers and Paleobathymetry of Barrow Group (Berriasian-Valanginian) deltaic sequences, sites 762 and 763, Northwest Shelf, Australia, Proceedings of Ocean Drilling Program, Scientific Results, 122, pp.557-568.

King, G.R., Costa, R., Minck, R., Leggett, E., Carleton, B., Laidlaw, C. and Domingos, F., 1998, January. Reservoir characterization, geological modeling, and reservoir simulation of the N'Sano field, Upper Pinda reservoir. In SPE Asia Pacific Conference on Integrated Modelling for Asset Management. Society of Petroleum Engineers.

Koning , M. & Jokat, W., 2006. The Mesozoic breakup of the Weddell Sea. Journal of Geophysical Research, Vol. 111; pp. 1 -29:, B12102, doi:10.1029/2005JB004035.

LeRoy , D. O., 1977. Economic Microbiostratigraphy. In: L.W. LeRoy, D.O.LeRoy and J.W.Raese . Subsurface Geology-Petroleum -Mining-Construction. pp. 212 -233.

Lob, C. and Mutterlose, J., 2012. The onset of anoxic condition in the early Barremian of the Boreal Realm evidenced by benthic foraminiferal. Revue de micropaleontology, 55(3), pp.113 – 126.

Loeblich, Alfred R., Tappan, Helen. 1988. Foraminiferal Genera and Their Classification, vol. (I –IV), Springer Science, New York, pp.1-970.

Loveren , A., 1967. Geology of Petroleum. Second Edition ed. American Association of Petroleum Geologist (AAPG) Foundation.

Lucia, F.J., 2007. Carbonate reservoir characterization: An integrated approach. Springer Science & Business Media.

Luton, L.C. and Prieto, C., 2000. Accurate Depth Conversions Reduce Risk. Gulf Coast. Association of Geological Societies Transactions, Vol L, pp. 343 - 246.

Malan , J. A., 1993. Geology, potential of Algoa, Gamtoos Basins of South Africa. Oil and Gas Journal; (United State), 91(46).pp1-4.

Malan, J. A., Martin, A. K. & Cartwright, J. A., 1990. The structural and stratigraphic development of the Gamtoos and Algoa Basins, offshore South Africa. Abstract, Geocongress. Gological Society of South Africa.,Vol. 90, pp. 328 - 331.

Malan, J.A., Viljoen, J.H.A. and Minter, W.E.L., 1990. Mesozoic and Cenozoic geology of the Cape South coast. Geological Society of South Africa.

McHardy, W.J., Wilson, M.J. and Tait, M., 1982. Electron microscope and X-ray diffraction studies of filamentous illitic clay from sandstones of the Magnus Field. Clay Minerals, 17(1), pp.23-40.

McLachlan, I.R., and McMillan, I. K., 1979. Microfaunal biostratigraphy, chronostraigraphy and history of Mesozoic and Cenozoic deposits on the coastal margin of South Africa.In: Anderson, A. M. and Van Biljon, W.J. (Eds.),Some Sedimentary Basins and Associated Ore Deposits of South Africa. Geological Society of South Africa Special Publication., 6, pp. 161 - 181.

McLachlan, I.R., Wickens, H.D., and 1990. The stratigraphy and sedimentology of the reservoir interval of the Kudu 9A-2 and 9A-3 boreholes. Geological Survey of Namibia Communications, 6, pp.9-23.

McMillan, I.K., 1990. Foraminiferal biostratigraphy of the Barremian to Miocene rocks of the Kudu 9A-1, 9A-2 and 9A-3 boreholes. Communications of the Geological Survey of Namibia, 6, pp.23-29.

McMillan, I.K., 2003. Foraminiferally defined biostratigraphic episodes and sedimentation pattern of the Cretaceous drift succession (Early Barremian to Late Maastrichtian) in seven basins on the South African and southern Namibian continental margin. South African Journal of Science, 99(11-12), pp.537-576.

McMillan, I.K., Brink, G.I., Broad, D.S. and Maier, J.J., 1997. Late Mesozoic sedimentary basins off the south coast of South Africa. In Sedimentary Basins of the World. 3, pp. 319-376. Elsevier.

Meert, J.G. and Van Der Voo, R., 1996. Paleomagnetic and 40Ar/39Ar study of the Sinyai dolerite, Kenya: implications for Gondwana assembly. The Journal of Geology, 104(2), pp.131-142.

Mirzaee,N., 2015. Linkedin. [Online] Available at: https://www.linkedin.com/pulse/applied-wettability-concept-estimation-i-basics-nabi-mirzaee
[Accessed 17 July 2017].

Mirzajani, A., Yousefzade, A., Sayyad Rahim, M. & Abbdolmaleki, S. H., 2002. Study of miofauna and bed features in the Caspian Sea (Gilan water). IranianScientifically Journal of Fisheries , Vol. 11, pp. 199 - 132.

Mitchum Jr, R. M., Vail, P. R. & Sangree, J. B., 1977a. Seismic stratigraph and global changes of sea level, Part 6: Stratigraphy interpretation of seismic reflection paterns in depositional sequences. In: Payton, C.E.,(Ed), Seismic Stratigraphy-Applications to Hydrocarbon Exploration.. American Association of Petroleum Geologists (AAPG), Volume Memoir 26., p. 516.

Mitchum Jr, R. M., Vail, P. R. & Thompson III, S., 1977. Seismic stratigraphy and global changes of sea-level, part 2: the depositional sequence as a basic unit for stratigraphic analysis. In: Payton, C.E (Ed), Seismic Stratigraphy - Applications to Hydrocarbon Exploration.. America Association of Petroleum Geologists, Volume Memoir, 26, pp. 53 - 62.

Mitchum, R. J., 1977. Glossary of Seismic Stratigraphy. American Association of Petroleum Geologists, (AAPG) 26, pp. 41 - 54.

Moghaddasi, B. et al., 2009a. Abundance and Distribution of Bethic Foraminifera in the Northern Oman Sea (Iranian Side) Continental Shelf Sediments. Research Journal of Environmental Science, Academic Journals Inc, Volume 3 (2), pp. 210 -217.

Mulroy's,P.[Online]
Available at: http://www.rowan.k12.ky.us/userfiles/994/Classes/1493/Index%20Fossil%20Characteristics%20and%20Correlation.pdf
[Accessed 20 July 2017].

Mudaly, K., Turner, J., Escorcia, F. & Higgs, R., 2009. F-O gas field, Offshore South Africa from integrated approach to field development.. Cape Town South Africa., American Association of Petroleum Geologist (AAPG) Search and Discovery article #20070.

Murgese, D.S. and De Deckker, P., 2005. The distribution of deep-sea benthic foraminifera in core tops from the eastern Indian Ocean. Marine Micropaleontology, 56 (1-2), pp.25-49.

Murray, J.W., 2001. The niche of benthic foraminifera, critical thresholds and proxies. Marine Micropaleontology, 41(1-2), pp.1-7.

Nagy, J., 1992. Environmental significance of foraminiferal morphogroups in Jurassic North Sea deltas. Palaeogeography, Palaeoclimatology, Palaeoecology, 95 (1-2), pp.111-134.

Nagy, J., Reolid, M. and Rodríguez-Tovar, F.J., 2009. Foraminiferal morphogroups in dysoxic shelf deposits from the Jurassic of Spitsbergen. Polar Research, 28(2), pp.214-221.

Niranja, N.C., 2016. Seismic data interpretation and evaluation for hydrocarbon exploration and production: A practitioner's guide. Switzerland: Springer International Publishing.

Ofwona, C., 2010. Introduction to Geophysical Well Logging and Flow Testing, Exploration for Geothermal Resources. Kenya, UNU-GTP, GDC KenGen.

Ogg, J. G., Huang, C.,and Himnov, L., 2014. Triassic timescale status: a brief oview. Albertiana 41, pp. 3 - 30.

Olney, M., 2002. Foraminifera Microfossil Image Recovery and Circulation for Learning and Education (MIRACLE), London: University Colleg London (UCL), Micropalaeontology Unit.

Omre, H., 1991. "Stochastic Model for Reservoir Characterization" In: Recent Advances in Improved Oil Recovery Methods for North Sea Oil Sandstone Reservoirs, eds J. Kleppe and S. M Skjaeveland,. Norwegian Petroleum Directorate.

Opuwari, M., 2010. Petrophysical evaluation of the Albian age gas bearing sandstone reservoir of the O-M field, Orange Basin, South Africa,PhD.Thesis, South Africa: University of the Western Cape.

Pallatt, N., Wilson, J. and McHardy, B., 1984. The relationship between permeability and the morphology of diagenetic illite in reservoir rocks. Journal of Petroleum Technology, 36(12), pp.2-225.

Penney , R. K. & Looi, S. Y., 1996. Understanding effective and total porosity:the key to optimising Mineralogical evaluation. Australian Petroleum Production and Exploration (APPEA), Vol 36 (1), pp. 284 - 292.

Pirson, S. J., 1958. Oil Reservoir Engineer. 2nd Edition, ed. New York, McGraw-Hill; 735

Petroleum Agency of South Africa, 2004/2005. Petroleum exploration information and opportunities, Cape Town : Petroleum Agency SA Brochure.

Poupon, A. Leveaux, J. 1971. Evaluation of water saturation in shaly formations. In: SPWLA 12th Annual Logging Symposium, pp 1-2.

Reolid, M., Nagy.J, Rodriguez-Tovar, F.J., and Oloriz, F., 2008. Foraminiferal assemblages as paleoenvironmental bioindicators in Late Jurassic epicontinental platforms: relation with tropic conditions. Acta Paleontologica Polonica, Vol.53, No.4, pp.705-722.

Rider, M.H., 1986. The Geological Interpretation of Well Logs. Gulf Publishing, pp. 151 - 165.

Rider, M.H., 1990. Gamma-ray log shape used as a facies indicator: critical analysis of an oversimplified methodology. Geological Society, London, Special Publications, 48(1), pp.27-37.

Rider, M. H., 1996. The geological interpretation of well logs. 3rd Revised edition ed. New York: Petroleum Exploration consultant Rider-French consultant Ltd Cambridge and Sutherland. Halsted press, a division of John Wiley and Sons.

Robein , E., 2003. Velocity, Time-Imaging, and Depth-Imaging in Reflection Seismics: Principles and Methods. Houten, Netherlands.

Roksandic, M. M., 1978. Seismic Facies Analysis Concepts. Geeophysical Prospecting, 26(2), pp. 383 - 398.

Roux, J., 1997. Potential outlined in southern Outeniqua Basin off S. Africa. Oil and Gas Journal, 95(29), pp.87 -91.

Sangree, J.B. and Widmier, J.M., 1974. Interpretation of depositional facies from seismic data: Continuing Education Symposium. Geophysical Society of Houston.

Sangree, J.B. and Widmier, J.M., 1979. Interpretation of depositional facies from seismic data. Geophysics, 44(2), pp.131-160.

Sangree, J. B. and Widmier, J. M., 1977. Seismic Stratigraphy and global changes of sea level , Part 9: Seismic interpretation of clasic depositional facies,. See Payton 1977, pp. 165 - 84.

Saputra, I., 2008. Shale Volume Calculation. HRS Jakarta.

Schlumberger, 1979. The Interpretation of Gamma ray Log , Houston: Dresser Atlas .

Schlumber, 1974. Log interpretation manual: vol.II (application), New York: Schlumberger Limited.

Schlumberger, 1989. Log Interpretation Principles/Applications. New York.

Schlumberger, 2007. Introduction Software book.

Schlumberger, 2000. Log intepretation principle and application Logging while drilling. Oilfield review, Volume (1) 1, pp. 1 - 14.

Schmoker, J.W., Krystinik, K.B. and Halley, R.B., 1985. Selected characteristics of limestone and dolomite reservoirs in the United States. AAPG Bulletin, 69(5), pp.733-741.

Schtjens , P. M., 1991. Intergranular pressure solution in halite aggregates and quartz sands; an experimental investigation, Netherlands: PhD Thesis, University of Utrecht.

Serra , O. & Abbott, H. T., 1982. The contribution of logging data to sedimentology and stratigraphy. Society of Petroleum Engineers. AIME, Special paper journal , pp. 117 - 131.

Serra, O., 1984. Fundamentals of well-log intepretation: the acquisition of logging data. Elsevier, Volume 1, pp. 1 - 6.

Serra, O., 1985. Sedimentary environments from wireline logs. Schlumberger Limited.

Sheriff , R. E., 1975. Inferring stratigraphy from seismic data. Offshore Technology Conference, Preprint II, 253 -263.

Sinclair, G.G. and Duguid, S.J., 1990. Laboratory Induced Damage-A Review of the Problem. In Advances in Core Evaluation: Accuracy and Precision in Reserves Estimation:

Reviewed Proceedings of the First Society of Core Analysts European Core Analysis Symposium, London, UK, 21-23 May 1990 (Vol. 1, p. 95). Taylor & Francis.

Singh, A., 2008. Micropaleontology in Petroleum Exploration. Hyderabad, India, 7th International Conference and Exposition on Petroleum Geophysics., pp. 1 - 8.

Simandoux, P., 1963. Dielectric measurements on porous media, application to the measurements of water saturation: study of behaviour of argillaceous formations. Revue de l'Institut Francais du Petrol, 18 (supplementary issue), pp.93-215.

Simm, R., Bacon, M., and Bacon, M., 2014. Seismic Amplitude: An interpreter's handbook. Cambridge University Press.

Soto Becerra, R., Arteaga, D., Hidalgo, C.M. and Rodriguez, F., 2010, January. The correct shale-volume characterization increases hydrocarbon reserves: case study of cretaceous formation, Lake of Maracaibo, Venezuela. In SPE Latin American and Caribbean Petroleum Engineering Conference. Society of Petroleum Engineers.

Suzanne, G. C. & Robert, M. C., 2004. Petrophysics of the Lance Sandstone Reservoir in Jonah Field, Sublette County, Wyoming. American Association of Petroleum Geologists (AAPG) Studies in Geology and Rocky Mountain Association of Geologist 2004, Volume Guidebook, pp. 226 - 227.

Szydło, A., 2005. Benthic foraminiferal morphogroups and taphonomy of the Cieszyn beds (Tithonian-Neocomian, Polish Outer Carpathians). Studia Geologica Polonica, 124, pp.199-214.

Thomson, K., 1999. Role of continental break-up, mantle plume development and fault reactivation in the evolution of the Gamtoos Basin, South Africa. Marine and Petroleum Geology, 16(5), pp.409-429.

Torsaeter, O., and Hendraningrat, L., Li, S., 2013. July. Enhancing oil recovery of low-permeability berea sandstone through optimised nanofluids concentration. In SPE Enhanced Oil Recovery Conference. Texa, Society of Petroleum Engineers.

Turner, J.R., Grobbler, N. and Sontundu, S., 2000. Geological modelling of the Aptian and Albian sequences within Block 9, Bredasdorp Basin, offshore South Africa. Journal of African Earth Sciences, 31(1), pp.80.

Vail, P. R., Mitchum, R. M. & Thompson III, S., 1977. Seismic stratigraphy and global changes of sea level, part 3: relative changes of sea level from coastal onlap, In: C.W. Payton, (Ed)., Seismic stratigraphy applications to hydrocarbon exploration: American Association of Petroleum Geologist (AAPG) Memoir, Volume 26, pp. 63 - 97.

Valicenti, V.H. and Stephens, J.M., 1984. Ostracods from the Upper Valanginian and Upper Hauterivian of the Sundays River Formation, Algoa Basin, South Africa.

Van Wagoner, J. C., Mitchum, R. M., Campion, K. M. & Rahmanian, V. D., 1990. Siliciclastic sequence stratigraphy in well logs, cores, and outcrops: conept for high-resolution

correlation of time and facies:. American Association of Petroleum Geologists (APPG) Methods in Exploration, Volume 7, p. 55.

Weigi Ma & Quanhou Li, 2015. Review on the Modeling of oil and gas reservoir. International organization of Scientific Research Journal of Enginering (IOSRJEN),Vol. 05, pp. 14 - 16.

White, R.E. and Simm, R., 2003. Tutorial: Good practice in well ties. First Break, 21(10). pp. 75 - 83.

Williamson, M.A. and Stam, B., 1988. Jurassic/Cretaceous Epistominidae from Canada and Europe. Micropaleontology, pp.136-158.

Winter, H.de la R., 1973. Geology of the Algoa Basin, South Africa. In Sedimentary Basins of the African Coasts, 2nd Part: South and East Coasts, ed. G. Blant. Assoc. Afr. Geology Society South Africa, 77, pp.247-252.

Wise, S.W. and Wind, F.H., 1983. Mesozoic and Cenozoic calcareous nannofossils recovered by DSDP Leg 71 in the Falkland Plateau region, Southwest Atlantic Ocean. Initial Reports of the Deep Sea Drilling Project, 71, pp.481-550.

Worthington, P.F., 2008. The application of cutoffs in integrated reservoir studies. SPE Reservoir Evaluation & Engineering, 11(06), pp.968-975.

Worthington, P.F. and Cosentino, L., 2005. The role of cut-offs in integrated reservoir studies. SPE Reservoir Evaluation & Engineering, 8(04), pp.276-290.

Yu, X. & Li, X., 2012. The Application of Sequential Indicator Simulation and Sequental Gaussian Simulation in Modeling a Case in Jilin Oilfield, Qingdao, China: Exploration and Development Institute Jilin oilfield Company .

Zeng, H., 2010. Geologic significance of anomalous instantaneous frequency. Geophysics, 75 (3), pp. 23 - 30

Zeng, H., Jackson, J. A. and Jackson, K. G., 2010. Thin-Bed Detection and Correlation with Instantaneous Frequency. In SEG Technical Program Expanded Abstracts 2010 (pp. 1292-1296). Society of Exploration Geophysicists.